STUDY OF THERMO-ACOUSTIC BEHAVIOUR OF BENZOIC ACID DERIVATIVES IN AQUEOUS SOLUTIONS OF CARBOXYLIC ACIDS

Thesis Submitted for the Award of the Degree of

DOCTOR OF PHILOSOPHY

in

Physics

By

Ashpinder Kaur Gill

Registration Number: 12224372

Supervised by

Dr. Kailash Chandra Juglan (11468)

Professor, Department of Physics

LPU, Phagwara

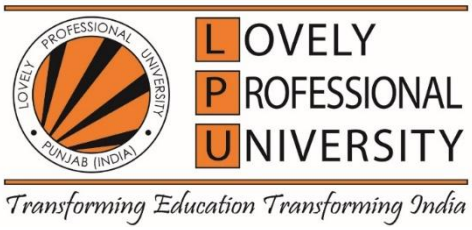

LOVELY PROFESSIONAL UNIVERSITY, PUNJAB

2026

DECLARATION

I, hereby declare that the presented work in the thesis entitled "**Study of thermo-acoustic behaviour of benzoic acid derivatives in aqueous solutions of carboxylic acids**" in fulfillment of the degree of **Doctor of Philosophy (Ph. D.)** is the outcome of research work carried out by me under the supervision of Dr. Kailash Chandra Juglan, working as Professor, in the Department of Physics of Lovely Professional University, Punjab, India. In keeping with the general practice of reporting scientific observations, due acknowledgments have been made whenever the work described here has been based on the findings of other investigators. This work has not been submitted in part or in full to any other University or Institute for the award of any degree.

(Signature of Scholar)

Ashpinder Kaur Gill

Registration No.: 12224372

School of Chemical Engineering and Physical Sciences

Lovely Professional University,

Punjab, India

CERTIFICATE

This is to certify that the work reported in the Ph. D. thesis entitled "**Study of thermo-acoustic behaviour of benzoic acid derivatives in aqueous solutions of carboxylic acids**" submitted in fulfillment of the requirement for the award of degree of **Doctor of Philosophy (Ph.D.)** in the Department of Physics, is a research work carried out by Ashpinder Kaur Gill, 12224372, is a bonafide record of her original work carried out under my supervision and that no part of thesis has been submitted for any other degree, diploma or equivalent course.

(Signature of Supervisor)

Dr. Kailash Chandra Juglan
Professor, Department of Physics
School of Chemical Engineering and Physical Sciences
Lovely Professional University, Phagwara, Punjab

ABSTRACT

Ultrasonic techniques have emerged as an indispensable tool in diverse scientific disciplines, particularly in the investigation of thermo-acoustic properties of liquid systems. The propagation of ultrasonic waves through a medium provides valuable information regarding the molecular organization, structural dynamics, and intermolecular interactions at the molecular level. By analyzing variations in ultrasonic velocity and density, it becomes possible to correlate the physicochemical behavior of molecules with their interactional patterns in solution. Owing to its non-invasive and highly precise nature, ultrasonic methodology is extensively employed for the characterization of liquids, as it effectively reveals the strength of intermolecular forces and the degree of association between solute and solvent species. Furthermore, the application of this approach to systems comprising benzoic acid derivatives- such as sodium benzoate, potassium benzoate, and sodium methyl para-hydroxybenzoate together with carboxylic acids at varying concentrations and temperatures, enables a deeper understanding of their acoustic and volumetric behavior. These insights hold significant relevance not only for fundamental studies of solution chemistry but also for practical applications in the pharmaceutical, cosmetic, and food industries. Each system was scrutinized at a fixed 0.1 MPa pressure with the temperature varied systematically between 288.15 K and 318.15 K. The studies were performed for different molalities and concentrations of carboxylic acids and benzoic acid derivatives. Measurements of densities and sound speeds were conducted with high precision by means of the (Anton-Paar) “DSA 5000 M” an advanced density and sound velocity meter specifically designed for the accurate determination of physicochemical properties of liquid systems.

In **Section I, Problem 1** investigates the thermodynamic behavior of glycolic and lactobionic acid in aqueous sodium benzoate mixtures. The study was conducted at four different concentrations of sodium benzoate (0.04, 0.05, 0.06) $mol \cdot kg^{-1}$ and at varied temperatures. The investigational measurements of densities and sound velocities for the ternary systems (water + sodium benzoate + glycolic/lactobionic acid) were obtained using the DSA 5000 M. From the measured densities, a series of volumetric parameters was evaluated, including the apparent molar volume, the limiting partial molar volume, and the partial molar volume of transfer. Acoustic measurements were employed to determine the apparent molar and limiting partial isentropic compression, and transfer of partial molar isentropic compression. Furthermore, the partial molar

expansibility, its temperature derivative, and higher-order interaction parameters were also computed. Particular emphasis is placed on elucidating the structure-forming or disrupting tendencies of carboxylic acid molecules in the presence of sodium benzoate. The outcomes emphasize the type and strength of inter-molecular interactions that govern the stability and organization of these ternary systems. **Problem 2** in this section dealt with the investigation of liquid mixtures containing alpha-hydroxy acids, specifically glycolic and lactic acids in sodium methyl p-hydroxy benzoate solution. The objective of this work was to investigate the density and ultrasonic speed of these systems at four varied temperatures and at three concentrations of sodium methyl p-hydroxy benzoate in water. The experimental measurements served as the basis for the evaluation of density and sound speed-related parameters, along with the determination of apparent molar, partial molar, and transfer properties of volume and isentropic compression, expressed as V_ϕ, V_ϕ^0, ΔV_ϕ^0, $K_{\phi,s}$, $K_{\phi,s}^0$, and $\Delta K_{\phi,s}^0$. From the values of ΔV_ϕ^0 and $\Delta K_{\phi,s}^0$, the interaction coefficients (V_{AB}, V_{ABB}, K_{AB} *and* K_{ABB}) were calculated. In addition, the limiting apparent molar expansibilities, their temperature derivatives, and certain empirical parameters were obtained. The outcomes of this study were interpreted to provide insights into molecular interactions and the structural effects that govern the behavior of the investigated liquid systems.

In **Section II, Problem 3** presents a comprehensive investigation of the volumetrical and acoustical properties of ternary solutions composed of water, potassium benzoate, and alpha-hydroxy acids (glycolic acid/malic acid). The investigations of density and ultrasonic velocity were conducted at four distinct temperatures and a constant 0.1 MPa pressure. Based on these measurements, a systematic evaluation of ultrasonic and volumetric characteristics was performed across different concentrations of the mixture. The experimental data facilitated the determination of a wide range of thermodynamic properties, including apparent molar volumes, partial molar volumes, expansibilities, and interaction parameters, which provide valuable insights into the interactions inside the ternary mixtures. The analysis revealed that hydrophilic interactions prevailed in the studied systems, while hydrogen-bonding effects were also inferred. Overall, physicochemical investigations of such ternary liquid systems remain essential for developing a profound understanding of the nature of interactions in intricate mixtures. **Problem 4** deals with the ternary system that consists of water, sodium benzoate, lactic acid, and malic acid. The data of density (ρ) and velocity of

sound (c) were recorded as a function of composition at 0.1 MPa pressure. These results were employed to analyze acoustic and volumetric parameters. On the basis of ρ and c data, apparent, partial, and transfer properties were determined. The analysis further incorporated the evaluation of expansibilities and their first-order temperature derivative. In addition, theoretical expressions based on the McMillan-Mayer concept were applied to the system. The calculated parameters provided information about the physicochemical characteristics among co-solute and solvent species present in the mixtures under study. The results were interpreted with reference to the processes of structural assembly and disintegration in ternary liquid mixtures. According to the co-sphere model, the derived parameters served as an indicator of the types of interactions occurring inside the system, thereby facilitating the characterization of the observed behavior.

In **Section III, Problem 5** addresses the interactional behavior of water-soluble solutions of potassium benzoate in the composition variation of 0.01 to 0.03 mol·kg^{-1} with butyric and lactic acids over the temperature interval 288.15-318.15 K. Densities and sound speeds values were determined with the aid of an "Anton-Paar DSA 5000 M" instrument. The measured data served as the basis for the computation of a range of thermo-acoustical properties. From the density results, apparent and partial molar quantities, transfer partial molar volumes, and expansibility parameters were calculated. Simultaneously, sound velocity data provided access to apparent and partial molar isentropic compressions as well as transfer of partial molar isentropic compressibilities. Furthermore, interaction coefficients and empirical constants were derived to evaluate solute-solvent and solute-solute interactions. A comparative assessment between butyric and lactic acid systems revealed a marked variation in the intensity and nature of molecular interactions, which reflects the influence of organic acid chain length on the structural organization of the ternary mixtures. **Problem 6** emphasizes the need to understand intermolecular interactions in ternary liquid mixtures involving sodium methyl p-hydroxybenzoate (SMP) with organic acids such as malic and tartaric acids. The effectiveness of SMP as a preservative in food, pharmaceutical, and cosmetic formulations is highly dependent on its molecular-level interactions in aqueous media. To evaluate these interactions, precise measurements of density and sound speed were performed over a concentration series of (0.00, 0.02, 0.04, and 0.06) mol·kg^{-1} and varied ranges of temperatures. From these experimental data, significant thermodynamic characteristics were derived, such as apparent molar

volume, isentropic compressibilities, expansibility coefficients, and interaction parameters. This problem particularly addresses how changes in temperature and concentration influence hydration effects, hydrogen bonding, and dipole interactions within the mixtures. The outcomes not only enhance the understanding of SMP behavior in aqueous media but also support its effective application in designing stable and functional preservative formulations.

In **Section IV, Problem 7** examines the thermophysical behavior of potassium benzoate (a preservative) in aqueous mixtures with tartaric acid (α-hydroxy acid) and lactobionic acid (polyhydroxy acid), an area of significance in nutritional science. Densities and sound velocities were measured with a DSA 5000 M for ternary systems at potassium benzoate concentrations of 0.000-0.035 mol·kg^{-1} over the studied temperature variety. From these measurements, apparent and limiting molar volumes (V_ϕ and V_ϕ^0), isentropic compressions ($K_{\phi,s}, K_{\phi,s}^0$), and their transfer functions (ΔV_ϕ^0 and $\Delta K_{\phi,s}^0$) were derived. The interaction constants were calculated in accordance with McMillan-Mayer theory. The results revealed a dominant solute-solvent with prevailing hydrophilic interactions. Collectively, the findings highlight the interaction dynamics and structural effects of potassium benzoate in organic acids-water systems.

Problem 8 investigates the physicochemical behavior of butyric and tartaric acids in water and in aqueous sodium benzoate mixed solvent systems over a wide range of four separate temperatures. Experimental determinations of density and ultrasonic velocity were conducted for different compositions of the mixtures. From these fundamental measurements, several derived thermodynamic parameters were computed, including apparent molar volume and isentropic compressions at infinite dilution (V_ϕ^0,$K_{\phi,S}^0$). In addition, transfer properties (ΔV_ϕ^0 and $\Delta K_{\phi,s}^0$) along with pair and triplet interaction constants (V_{AB}, V_{ABB}; K_{AB} *and* K_{ABB}) were evaluated. The temperature derivatives of the apparent molar volumes were employed as a criterion to assess the structure maker or disruptor tendencies of the solutes. The systematic analysis of these parameters provides insight into the nature of solutes as well as solvent interactions, thereby elucidating their contribution to the structural organization and physicochemical characteristics of the studied mixtures.

ACKNOWLEDGMENT

First and foremost, I would like to express my deepest gratitude to the **Almighty God** for his divine blessings, strength, and guidance throughout this journey. His grace has been my source of inspiration, providing me with the perseverance and courage needed to overcome challenges and complete this work. I owe every success and accomplishment to His endless support and unwavering presence in my life.

I extend my sincere appreciation to my supervisor, **Dr. Kailash Chandra Juglan**, Professor in the Department of Physics, Lovely Professional University, Phagwara, for his invaluable guidance, continuous support, and motivation throughout my research. His expertise and encouragement have been crucial in shaping this work, and I feel privileged to have the opportunity to learn under his mentorship. His profound knowledge, critical insights, and constructive feedback provided me with a strong academic foundation and helped me overcome various challenges encountered during the course of my study.

I am also sincerely thankful to **Dr. Nabaparna Chakraborty**, whose constant support and assistance have been instrumental in completing this research. Her patience, suggestions, thoughtful advice, insightful discussions, and selfless help at every stage of my work have provided immense value and positivity throughout my research journey. Her ability to listen, understand, and guide me through both academic and personal challenges has been truly inspiring. I will always remain grateful for her invaluable contributions to this work. I gratefully acknowledge the respected panel members- **Dr. Mukesh Kumar**, **Dr. Sandeep Kumar,** and **Dr. Harjit Singh Ghotra** for their invaluable guidance, constant encouragement, and for shaping my research objectives through their valuable suggestions.

I am also profoundly thankful to the laboratory staff and research scholars of the **Guru Nanak Dev University, Amritsar** and **DAV College, Chandigarh**, whose cooperation and technical support greatly facilitated the experimental aspects of this work. Their valuable assistance in handling the instruments, careful execution of experimental procedures, and contributions to data acquisition proved essential in ensuring the accuracy and reliability of my results. The collaborative environment played a significant role in the smooth progress and successful completion of this research study.

I would like to acknowledge my seniors, **Dr. Harsimran Kaur** and **Dr. Manisha Lamba,** for their guidance and encouragement throughout the course of my research work. Their constant support and willingness to share their expertise have been a

continuous source of inspiration and have played a pivotal role in shaping my research journey. A special note of thanks goes to my beloved mother, **Mrs. Sukhdeep Kaur**, for her unconditional love and unwavering belief in my abilities. Her constant support and blessings have been the foundation upon which I built my determination and dedication. Lastly, I wish to extend my heartfelt gratitude to my fiancé, **Mr**. **Taranpreet Singh**, for his endless encouragement, understanding, and unwavering support. His faith in me has been a continuous source of immense strength and motivation throughout this journey. This accomplishment would not have been possible without his continued support and best wishes.

Ashpinder Kaur Gill

TABLE OF CONTENTS

S. No.	Title	Page No.
1	Declaration	ii
2	Certificate	iii
3	Abstract	iv-vii
4	Acknowledgement	viii-ix
5	Table of contents	x-xii
6	List of Tables	xiii-xix
7	List of Figures	xx-xxv
8	List of Abbreviations	xxvi-xxvii
CHAPTER 1		
INTRODUCTION		1-13
1.1	Ultrasonic Research	
1.2	Ultrasonic Testing	
1.3	Ultrasonic Evaluation of Liquids	
1.4	Density and Sound Velocity Meter	
1.5	Benzoic Acid Derivatives	
	1.5.1 Sodium Benzoate	
	1.5.2 Potassium Benzoate	
	1.5.3 Sodium methyl Para-Hydroxy Benzoate	
1.6	Carboxylic Acids	
	1.6.1 Lactobionic Acid	
	1.6.2 Glycolic Acid	
	1.6.3 Tartaric Acid	
	1.6.4 Lactic Acid	
	1.6.5 Malic Acid	
	1.6.6 Butyric Acid	
References		9-13
CHAPTER 2		
REVIEW OF LITERATURE		14-44
References		38-44
RESEARCH GAP		44

CHAPTER 3		
OBJECTIVES AND EXPERIMENTAL PROCEDURES		45-59
3.1	Objectives of the research	
3.2	Experimental procedure	
3.3	Chemical structures	
3.4	Specifications of the Chemicals used	
3.5	Methods and preparations	
3.6	Experimental Methods	
	3.6.1 Density and Sound Velocity Analyzer (DSA) 5000M	
3.7	Apparent and Partial molar properties	
	3.7.1 Apparent molar volume	
	3.7.2 Partial molar volume	
	3.7.3 Partial molar volume of transfer	
	3.7.4 Temperature dependent partial molar volume	
	3.7.5 Apparent molar isentropic compression	
	3.7.6 Partial molar isentropic compression	
	3.7.7 Partial molar isentropic compression of Transfer	
	3.7.8 Interaction coefficients	
CHAPTER 4		
RESULTS AND DISCUSSION		60-321
Section I		
Problem 1	Study of glycolic and lactobionic acids in water-soluble sodium benzoate solutions: an acoustic and thermodynamic approaches	60-90
Problem 2	Analysis of Molecular Interactions of an Aqueous Benzoates with Glycolic and Lactic Acid: Spectroscopic, Acoustic, and Volumetric Approach	91-120
References		121-123
Section II		
Problem 3	Volumetric and ultrasonic investigation of glycolic and malic acids with water-soluble potassium benzoate solutions at different temperatures	124-156

Problem 4	Investigating Interactions of Alpha-Hydroxy Acids with Sodium Benzoate for Advanced Formulation and Translational Applications: An Ultrasonic Approach	157-186
References		187-190
Section III		
Problem 5	Molecular Interactions of Butyric and L(+)-lactic Acids in Water-Soluble Potassium Benzoate Solutions: An Acoustic and Thermodynamic Study	191-221
Problem 6	Acoustic and volumetric analysis of malic and tartaric acids in aqueous medium of sodium methyl p-hydroxybenzoate from 288.15 K to 318.15 K	222-255
References		256-259
Section IV		
Problem 7	Thermodynamic Analysis of Tartaric and Lactobionic Acids with Aqueous Potassium Benzoate Mixtures through Volumetric and Acoustic Methods	260-288
Problem 8	Exploration of Intermolecular Interactions of Butyric and Tartaric Acids with Sodium Benzoate in Aqueous Medium	289-319
References		320-321
Summary and Conclusions		322-326
Future Scope of the Work		327
List of publications		328-329
List of Communicated papers		330
List of conferences		331

LIST OF TABLES

Table No.	Caption of Tables
CHAPTER 3	
Objectives and Experimental Procedures	
Table 3.1	Investigation of different problems during the research.
Table 3.2	List of chemicals used and their structures.
Table 3.3	Detailed description of the chemicals used in this investigation.
CHAPTER 4	
Results and Discussion	
Section I	
Problem 1	
Table 4.1	Data of densities 'ρ', and apparent molar volume 'V_ϕ' were found in the liquid system of sodium benzoate solution with glycolic and lactobionic acids.
Table 4.2	Values of partial molar volume, $'V_\Phi^{0\prime}$, and experimental slope, $'S_V^{*\prime}$ were obtained for sodium benzoate in aqueous glycolic and lactobionic acids.
Table 4.3	Transfer parameter $\Delta_{tr}V_\emptyset^0$ of sodium benzoate in aqueous glycolic and lactobionic acids solution at several temperatures.
Table 4.4	Empirical constants, a^*, b^*, c^* of sodium benzoate solutions with glycolic and lactobionic acids were calculated using equation (4.4) to describe their relationship with molality.
Table 4.5	Expansibility coefficient '$E_{\Phi,p}^0$' and its derivative values were obtained of sodium benzoate in glycolic and lactobionic acids mixtures.
Table 4.6	Sound velocity 'c' and apparent molar isentropic compressibility '$K_{\phi,S}$' values of glycolic and lactobionic acids in sodium benzoate solutions.
Table 4.7	Obtained values of $K_{\phi,s}^0$ and S_K^* of the combination (sodium benzoate + water + glycolic and lactobionic acids).
Table 4.8	Values of transfer parameter $\Delta_{tr}K_{\emptyset,S}^0$ of sodium benzoate in aqueous glycolic and lactobionic acids at several temperatures.

Table 4.9	Interaction coefficients for the ternary liquid combination comprising sodium benzoate solutions with glycolic and lactobionic acids.
Problem 2	
Table 4.10	Densities 'ρ', and sound velocity 's' in the liquid mixture of aqueous Sodium Methyl Para-hydroxy Benzoate with Glycolic Acid/Lactic Acid at several temperatures.
Table 4.11	Computed data of V_ϕ for glycolic and lactic acids in aqueous sodium methyl para-hydroxybenzoate at several temperatures and concentrations.
Table 4.12	Values of $K_{\phi,s}$ were calculated for glycolic and lactic acids in aqueous Sodium methyl parahydroxybenzoate solutions at several temperatures and concentrations.
Table 4.13	Values of $'V_\Phi^{0\prime}$, and , $'S_V^{*\prime}$ values of SMP in an aqueous Glycolic Acid and Lactic Acid solutions with their standard errors.
Table 4.14	Obtained data of $K_{\Phi,S}^0$, and S_K^*, of the liquid system (SMP +water+GA/LA).
Table 4.15	Transfer parameters ΔV_Φ^0 and $\Delta K_{\Phi,S}^0$ of SMP in Glycolic Acid/Lactic Acid aqueous solution.
Table 4.16	Calculation of empirical coefficients, a^*, b^*, c^* of SMP solutions with GA and LA along with ARD (Average relative deviations).
Table 4.17	Partial molar expansibilities 'E_Φ^0' values of Sodium methyl p-hydroxybenzoate in aqueous solutions with GA and LA.
Table 4.18	Interaction Coefficients (V_{AB}, K_{AB} ,V_{ABB} and K_{ABB}) for SMP solutions with Glycolic and Lactic Acid.
Section II	
Problem 3	
Table 4.19	Densities 'ρ' were investigated in the ternary combination of potassium benzoate in water-soluble glycolic and malic acids at four varying temperatures.
Table 4.20	Apparent molar volumes 'V_ϕ' investigated in the liquid system of soluble glycolic and malic acids in potassium benzoate at varying temperatures.

Table 4.21	Values of $'V_{\phi}^{0}'$, and $'S_{V}^{*}'$ for potassium benzoate in water-soluble glycolic and malic acids at numerous temperatures.
Table 4.22	Transfer property $\Delta_{tr}V_{\emptyset}^{0}$, of PB in water-soluble with glycolic and malic acids were determined at several temperatures.
Table 4.23	Computed data of constants, a^{*}, b^{*}, c^{*} of potassium benzoate in water-soluble glycolic and malic acids.
Table 4.24	Data of expansibilities 'E_{ϕ}^{0}' for PB in water-soluble glycolic and malic acids at several temperatures.
Table 4.25	Sound velocity 'c' of alpha-hydroxy acids (glycolic and malic acids) were determined in water-soluble potassium benzoate solution at several temperatures.
Table 4.26	Data of '$K_{\phi,S}$' were obtained in the water-soluble mixtures of PB with glycolic and malic acids at numerous temperatures.
Table 4.27	Data of $K_{\phi,S}^{0}$, and S_{K}^{*}, of the ternary system of potassium benzoate in glycolic and malic acids at several temperatures.
Table 4.28	Data of transfer parameter $\Delta_{tr}K_{\emptyset,S}^{0}$, of water-soluble solutions of PB with glycolic and malic acids at several temperatures.
Table 4.29	Calculated pair and triplet parameters of glycolic and malic acids in water-soluble PB solutions at numerous temperatures.
	Problem 4
Table 4.30	Values of densities 'ρ' were determined in the combination of sodium benzoate solutions with lactic and malic acids at four different temperatures.
Table 4.31	Values of 'V_{ϕ}' were determined in the combination of sodium benzoate solutions with lactic and malic acids at four different temperatures.
Table 4.32	Values of 'V_{ϕ}^{0}' and 'S_{V}^{*}' of sodium benzoate with lactic and malic acids solutions along with their standard errors.
Table 4.33	Values of transfer, ΔV_{ϕ}^{0}, of the combination of Sodium Benzoate in water-based lactic and malic acids solutions at several temperatures.
Table 4.34	Calculation of empirical constants of sodium benzoate in aqueous

	lactic and malic acids solutions.
Table 4.35	Coefficient of expansibilities 'E_{Φ}^{0}' for sodium benzoate in aqueous solutions with lactic and malic acids.
Table 4.36	Values of sound velocity 's' were determined in the combination of sodium benzoate with lactic and malic acids mixtures at several temperatures.
Table 4.37	Data of '$K_{\phi,s}$' of alpha-hydroxy acids (lactic and malic acids) in sodium benzoate aqueous solution.
Table 4.38	Calculated $K_{\phi,s}^{0}$ and S_{K}^{*}, of alpha-hydroxy acids (lactic and malic acids) in sodium benzoate aqueous solution.
Table 4.39	Values of transfer $\Delta K_{\phi,S}^{0}$, of alpha-hydroxy acids (lactic and malic acids) in aqueous sodium benzoate solution at several temperatures.
Table 4.40	Interaction coefficients for the ternary liquid combination of aqueous sodium benzoate solutions with lactic and malic acids.
Section III	
Problem 5	
Table 4.41	Densities 'ρ' and apparent molar volumes 'V_{ϕ}' were determined in the combination of potassium benzoate in L(+)-lactic and butyric acids at four different temperatures.
Table 4.42	Data of $'V_{\Phi}^{0}'$, and $'S_{V}^{*}'$ values of Potassium Benzoate in L(+)-lactic and butyric acids solutions with their standard errors.
Table 4.43	Transfer, ΔV_{Φ}^{0} values of the combination of potassium benzoate in L(+)-lactic and butyric acids solutions at various temperatures.
Table 4.44	Calculation of empirical constants of potassium benzoate in aqueous solutions with L(+)-lactic and butyric acids.
Table 4.45	Values of expansibilities 'E_{Φ}^{0}' potassium benzoate in L(+)-lactic and butyric acids at various temperatures.
Table 4.46	Values of 's' and '$K_{\phi,s}$' for L(+)-lactic and butyric acids in aqueous potassium benzoate solution at several temperatures.

Table 4.47	Calculated $K^0_{\phi,S}$ and S^*_K, of the potassium benzoate in L(+)-lactic and butyric acids solutions at various temperatures.
Table 4.48	Values of $\Delta K^0_{\phi,S}$, of the ternary system of potassium benzoate in aqueous L(+)-lactic and butyric acids mixtures at various temperatures.
Table 4.49	Interaction coefficients for the liquid system of potassium benzoate solutions with L(+)-lactic and butyric acids at different temperatures.
	Problem 6
Table 4.50	Densities 'ρ' were determined in the ternary system of sodium methyl 4-hydroxybenzoate (SMP) in water-containing solutions with malic acid (MA) and tartaric acid (TA).
Table 4.51	Apparent molar volumes 'V_ϕ' were determined in the ternary system of sodium methyl para-hydroxy benzoate in water-based solutions with malic acid (MA) and tartaric acid (TA).
Table 4.52	$V^{0\prime}_\Phi$, and $'S^{*\prime}_V$ values of sodium methyl para-hydroxy benzoate (SMP) in water-soluble solutions with malic acid (MA) and tartaric acid (TA) with their standard errors.
Table 4.53	Transfer property 'ΔV^0_Φ' of sodium methyl para-hydroxy benzoate (SMP) in water-soluble solutions with malic acid (MA) and tartaric acid (TA) at various temperatures and concentrations
Table 4.54	Calculated empirical parameters of sodium methyl para-hydroxy benzoate (SMP) in water-soluble malic acid (MA) and tartaric acid (TA).
Table 4.55	Data of partial molar expansibilities 'E^0_Φ' sodium methyl para-hydroxy benzoate (SMP) in water-soluble solutions with malic acid (MA) and tartaric acid (TA) at various temperatures.
Table 4.56	Sound velocity 's' values of sodium methyl para-hydroxy benzoate (SMP) in water-soluble solutions with malic acid (MA) and tartaric acid (TA) at different temperatures.
Table 4.57	Values of '$K_{\phi,s}$' for sodium methyl para-hydroxy benzoate in water-soluble solutions with malic acid (MA) and tartaric acid (TA) at different temperatures.

Table 4.58	Evaluated $K^0_{\phi,S}$ and S^*_K, for sodium methyl para-hydroxybenzoate (SMP) in water-soluble solutions with malic acid (MA) and tartaric acid (TA) at various temperatures.
Table 4.59	Values of transfer parameter, $\Delta K^0_{\phi,S}$, of sodium methyl para-hydroxy benzoate (SMP) in water-soluble solutions with malic acid (MA) and tartaric acid (TA).
Table 4.60	Calculated coefficients of interaction for (MA/TA) in water-soluble SMP solutions at numerous temperatures.
Section IV	
Problem 7	
Table 4.61	Measured data of densities 'ρ' and sound velocity 'c' were investigated for potassium benzoate in tartaric and lactobionic acids at several temperatures.
Table 4.62	Apparent molar volumes 'V_ϕ' were obtained in the liquid system of potassium benzoate in water-based solutions with tartaric acid (TA) and lactobionic acid (LBA).
Table 4.63	Data of '$K_{\phi,s}$' for potassium benzoate with tartaric acid (TA) and lactobionic acid (LBA) mixtures at different temperatures.
Table 4.64	Values of $'V^0_\Phi'$ and $'S^*_V'$ of potassium benzoate (PB) in water-soluble solutions with tartaric acid (TA) and lactobionic acid (LBA) with their standard errors.
Table 4.65	Evaluated $K^0_{\phi,S}$, and S^*_K, for potassium benzoate (PB) with aqueous tartaric acid (TA) and lactobionic acid (LBA) mixtures at several temperatures.
Table 4.66	Transfer property of '$\Delta_{tr}V^0_\emptyset$' for potassium benzoate (PB) with tartaric acid (TA) and lactobionic acid (LBA) solutions at several temperatures.
Table 4.67	Data of transfer parameter, $\Delta_{tr}K^0_{\emptyset,S}$, of the ternary system of potassium benzoate (PB) in water-soluble tartaric acid (TA) and lactobionic acid (LBA) at several temperatures.
Table 4.68	Examined empirical parameters of potassium benzoate (PB) in water-soluble tartaric acid (TA) and lactobionic acid (LBA).

Table 4.69	Data of partial molar expansibilities 'E_{Φ}^{0}' potassium benzoate (PB) in water-soluble solutions with tartaric acid (TA) and lactobionic acid (LBA) at various temperatures.
Table 4.70	Calculated Pair and triplet coefficients of (TA/LBA) with potassium benzoate solutions at numerous temperatures.
Problem 8	
Table 4.71	Data of 'ρ' and 'c' were investigated for sodium benzoate in aqueous butyric and tartaric acids mixtures at several temperatures.
Table 4.72	Apparent molar volumes 'V_{ϕ}' were determined for sodium benzoate in aqueous butyric and tartaric acids mixtures at several temperatures.
Table 4.73	Values of '$K_{\phi,s}$' of sodium benzoate in water-soluble solutions with tartaric acid (TA) and butyric acid (BA) at different temperatures.
Table 4.74	Values of $'V_{\Phi}^{0}'$, and $'S_{V}^{*}'$ of sodium benzoate (SB) in water-soluble solutions with tartaric acid (TA) and butyric acid (BA) with their standard errors.
Table 4.75	Evaluated $K_{\phi,S}^{0}$, and S_{K}^{*} values of the combination of sodium benzoate (SB) in water-soluble solutions with tartaric acid (TA) and butyric acid (BA) at several temperatures.
Table 4.76	Transfer property of 'ΔV_{Φ}^{0}' of sodium benzoate (SB) in aqueous tartaric acid (TA) and butyric acid (BA) mixtures at several temperatures.
Table 4.77	Values of $\Delta K_{\phi,S}^{0}$, of the combinations of sodium benzoate (SB) in water-soluble solutions with tartaric acid (TA) and butyric acid (BA) at several temperatures.
Table 4.78	Calculated empirical parameters of sodium benzoate (SB) in water-soluble tartaric acid (TA) and butyric acid (BA) at several concentrations.
Table 4.79	Data of partial molar expansibilities 'E_{Φ}^{0}' sodium benzoate (SB) in water-soluble solutions with tartaric acid (TA) and butyric acid (BA) at various temperatures
Table 4.80	Calculated Pair (V_{AB}, K_{AB}) and triplet (V_{ABB}, K_{ABB}) coefficients of (TA/BA) in water-soluble mixtures of sodium benzoate.

LIST OF FIGURES

Figure No.	Caption of Figures
CHAPTER 3	
Objectives and Experimental Procedures	
Figure 1.1	Frequency ranges of sound waves
Figure 1.2	Block Diagram of Anton Paar DSA 5000M
Figure 3.1	Sartorius (Model CPA225D) analytical balance and prepared solutions in airtight borosilicate glass vials
Figure 3.2	Density and Sound Velocity Meter
Figure 3.3	Density and sound speed cell of DSA-5000 M
Figure 3.4	Five key features for precise measurement of the density and sound velocity
CHAPTER 4	
Results and Discussion	
Section I	
Problem 1	
Figure 4.1	The density of aqueous sodium benzoate was presented at several temperatures using experimental and literature results [1-3].
Figure 4.2	Molecular interactions between ternary liquid systems.
Figure 4.3	Changes in the $V_{\emptyset}$ (apparent molar volume) through three-dimensional plots for sodium benzoate (SB) concentrations of (a) 0.0; (b) 0.1; (c) 0.4; (d) 0.7 mol·kg^{-1} for molality of glycolic acid [cube: blue] and lactobionic acid [sphere: red] at several temperatures.
Figure 4.4	The plot illustrates the changes in ($V_{\emptyset}^{0}$) for glycolic acid [Blue] and lactobionic acid [Red] in aqueous sodium benzoate solution.
Figure 4.5	The sound velocity of aqueous sodium benzoate was evaluated at several temperatures using experimental and literature results [2,3]
Figure 4.6	Variations in $K_{\phi,s}$ of glycolic acid in (a) 0.0 sodium benzoate, (b) 0.1 sodium benzoate, (c) 0.4 sodium benzoate and (d) 0.7 sodium benzoate for molality of aqueous glycolic acid solutions

Figure 4.7	Variations in $K_{\phi,s}$ of lactobionic acid in (a) 0.0 sodium benzoate, (b) 0.1 sodium benzoate, (c) 0.4 sodium benzoate and (d) 0.7 sodium benzoate for molality of aqueous lactobionic acid solutions
Figure 4.8	Changes in $K_{\emptyset,s}^{0}$ for (a) glycolic acid and (b) lactobionic acid in aqueous sodium benzoate (SB) at several temperatures
Problem 2	
Figure 4.9	The density of a binary combination of an aqueous SMP was shown at different temperatures utilizing literature as well as experimental data [42].
Figure 4.10	Ultrasonic speed of a binary liquid combination (SMP + Water) was shown at different temperatures utilizing literature as well as experimental data [42].
Figure 4.11	GA/LA and Sodium methyl para-hydroxy benzoate molecular interactions.
Figure 4.12	Three-dimensional Plots illustrate the variations in $(V_{\emptyset})$ of (a) 0.000 SMP; (b) 0.015 SMP; (c) 0.025 SMP;(d) 0.035 SMP for molality of glycolic acid (blue; cube) and lactic acid (red; sphere) at varying temperatures
Figure 4.13	Changes of $K_{\phi,s}$ of Glycolic acid (GA) in (a) 0.000 SMP, (b) 0.015 SMP, (c) 0.025 SMP and (d) 0.035 SMP for molality of glycolic acid aqueous solutions [288.15 K: Square (Black); 298.15K: Circle (Red); 308.15K: Upward triangle (Blue); 318.15 K: Downward triangle (Green)]
Figure 4.14	Changes of $K_{\phi,s}$ of Lactic Acid (LA) in (a) 0.000 SMP, (b) 0.015 SMP, (c) 0.025 SMP and (d) 0.035 SMP for molality of lactic acid aqueous solutions [288.15 K: Square (Black); 298.15K: Circle (Red); 308.15K: Upward triangle (Blue); 318.15 K: Downward triangle (Green)]
Figure 4.15	The scatter plot represents the variations in $V_{\emptyset}^{0}$ for Glycolic Acid (Red) and Lactic Acid (Green) within a SMP aqueous solution at several temperatures
Figure 4.16	Plots of variations of $K_{\emptyset,s}^{0}$ for (a) glycolic acid and (b) lactic acid in aqueous SMP solution at varying temperatures

Section II	
Problem 3	
Figure 4.17	The density of malic acid with water was presented at several temperatures applying measured and literature results [1,2].
Figure 4.18	Glycolic and Malic Acids with Potassium Benzoate interactions
Figure 4.19	Plots demonstrate the changes in $(V_{\emptyset})$ of (a) 0.00 PB; (b) 0.04 PB; (c) 0.05 PB; (d) 0.06 PB with the molality of glycolic acid at varying temperatures
Figure 4.20	Plots demonstrate the changes in $(V_{\emptyset})$ of (a) 0.00 PB; (b) 0.04 PB; (c) 0.05 PB; (d) 0.06 PB with the molality of malic acid at varying temperatures
Figure 4.21	Plots representing the variations in $V_{\emptyset}^{0}$ for (a) glycolic acid, (b) malic acid inside a PB water-soluble solution at numerous temperatures
Figure 4.22	Variations in $K_{\phi,s}$ of glycolic acid in (a) 0.00 PB, (b) 0.04 PB, (c) 0.05 PB and (d) 0.06 PB at several temperatures
Figure 4.23	Variations in $K_{\phi,s}$ of malic acid in (a) 0.00 PB, (b) 0.04 PB, (c) 0.05 PB and (d) 0.06 PB at several temperatures
Figure 4.24	Changes of $K_{\emptyset,s}^{0}$ for (a) glycolic acid (b) malic acid in PB solutions at numerous temperatures
Problem 4	
Figure 4.25	Three-dimensional plots illustrate the variations in $(V_{\emptyset})$ of (a) 0.00 SB; (b) 0.01 SB; (c) 0.02 SB;(d) 0.03 SB for molality of lactic acid (blue; tetrahedron) and malic acid (red; cube) at varying temperatures
Figure 4.26	The plots represent the variations in $V_{\emptyset}^{0}$ for (a) Lactic and Malic Acid within a Sodium Benzoate aqueous solution at several temperatures
Figure 4.27	Changes of $K_{\phi,s}$ of Lactic Acid (LA) in (a) 0.00 SB; (b) 0.01 SB; (c) 0.02 SB; (d) 0.03 SB for molality of lactic acid aqueous solutions at several temperatures.
Figure 4.28	Changes of $K_{\phi,s}$, of Malic Acid (MA) in (a) 0.00 SB; (b) 0.01 SB; (c) 0.02 SB; (d) 0.03 SB for molality of malic acid aqueous solutions at several temperatures.
Figure 4.29	Plots of variations of $K_{\emptyset,s}^{0}$ for (a) lactic acid and (b) malic acid in

	aqueous sodium benzoate solution at varying temperatures.
Section III	
Problem 5	
Figure 4.30	The density of a binary combination of aqueous butyric acid was shown at different temperatures utilizing experimental as well as literature data [1-6]**.**
Figure 4.31	The density of a binary combination of an aqueous L(+)-lactic acid was shown at different temperatures utilizing experimental as well as literature data [7,8].
Figure 4.32	Lactic Acid/ Butyric Acid and Potassium Benzoate interactions
Figure 4.33	Three-dimensional plots illustrate the variations in $(V_{\emptyset})$ of (a) 0.00 PB; (b) 0.01 PB; (c) 0.02 PB;(d) 0.03 PB for molality of lactic acid (blue; sphere) and butyric acid (red; cube) at varying temperatures.
Figure 4.34	The plot represents the variations in $V_{\emptyset}^{0}$ for lactic acid (red; dot) and butyric acid (blue; cube) within a potassium benzoate aqueous solution at several temperatures
Figure 4.35	Ultrasonic speed of a binary combination of an aqueous L(+)-lactic acid was shown at different temperatures utilizing experimental as well as literature data [7].
Figure 4.36	Changes of $K_{\phi,s}$, of (a) butyric acid (BA) and(b) L(+)-lactic acid (LA) in potassium benzoate solutions at several concentrations (0.00 PB, orange; 0.01 PB, blue; 0.02 PB, purple; and 0.03 PB, pink) [square: 288.15 K; circle: 298.15 K; upward triangle: 308.15 K; downward triangle: 318.15 K].
Figure 4.37	Plots of variations of $K_{\emptyset,s}^{0}$ for (a) butyric acid and (b) lactic acid in aqueous potassium benzoate solution at varying temperatures
Problem 6	
Figure 4.38	Variation of densities for tartaric acid + water between measured and literature values at different concentrations and temperatures [53-55].
Figure 4.39	Interactions of malic or tartaric acids with sodium methyl p-hydroxybenzoate solutions.
Figure 4.40	Plots demonstrate the changes in $(V_{\emptyset})$ of (a) 0.00 SMP; (b) 0.02 SMP; (c) 0.04 SMP; (d) 0.06 SMP with the molality of malic acid at varying

	temperatures
Figure 4.41	Plots demonstrate the changes in ($V_{\emptyset}$) of (a) 0.00 SMP; (b) 0.02 SMP; (c) 0.04 SMP; (d) 0.06 SMP mol·kg^{-1} with the molality of tartaric acid at varying temperatures
Figure 4.42	Plots representing the variations in $V_{\emptyset}^{0}$ for (a) malic acid, (b) tartaric acid inside an SMP water-soluble solution at numerous temperatures
Figure 4.43	Variation of sound speed for tartaric acid + water between measured and literature values at different concentrations and temperatures [53].
Figure 4.44	Changes of $K_{\phi,s}$ of Malic Acid (MA) in (a) 0.00 SMP; (b) 0.02 SMP; (c) 0.04 SMP; (d) 0.06 SMP for molality of malic acid aqueous solutions
Figure 4.45	Changes of $K_{\phi,s}$ for Tartaric Acid (TA) in (a) 0.00 SMP; (b) 0.02 SMP; (c) 0.04 SMP; (d) 0.06 SMP for molality of tartaric acid aqueous solutions.
Figure 4.46	Plots representing $K_{\emptyset,s}^{0}$ for (a) malic acid and (b) tartaric acid in water-soluble sodium methyl p-hydroxybenzoate solution at varying temperatures
Section IV	
Problem 7	
Figure 4.47	Tartaric Acid/ Lactobionic Acid and Potassium Benzoate interactions.
Figure 4.48	Comparative three-dimensional plots demonstrate the variations in $V_{\emptyset}$ of (a) 0.000 PB; (b) 0.015 PB; (c) 0.025 PB;(d) 0.035 PB for molalities of tartaric acid (green; sphere) and lactobionic acid (pink; cube) at several temperatures
Figure 4.49	Changes of apparent molar isentropic compression, $K_{\phi,s}$, of tartaric acid (TA) in water-soluble potassium benzoate at varying concentrations.
Figure 4.50	Changes of apparent molar isentropic compression, $K_{\phi,s}$, of lactobionic acid (LBA) in water-soluble potassium benzoate at varying concentrations.
Figure 4.51	The comparative plot presents the variations in $V_{\emptyset}^{0}$ for tartaric acid (red; star) and lactobionic acid (pink; tetrahedron) within a potassium benzoate aqueous solution at several temperatures

Figure 4.52	Plots of distinctions of $K_{\emptyset,s}^{0}$ for (a) tartaric acid and (b) lactobionic acid in water-soluble potassium benzoate solution at several temperatures
Problem 8	
Figure 4.53	Tartaric Acid/ Butyric Acid and Sodium Benzoate interactions.
Figure 4.54	Plots demonstrate the variations in $(V_{\emptyset})$ of (a) 0.00 SB; (b) 0.05 SB; (c) 0.07 SB; (d) 0.09 SB for molality of tartaric acid at varying temperatures
Figure 4.55	Plots demonstrate the variations in $(V_{\emptyset})$ of (a) 0.00 SB; (b) 0.05 SB; (c) 0.07 S.B; (d) 0.09 SB for molality of butyric acid at varying temperatures.
Figure 4.56	Variations of $K_{\phi,s}$ of tartaric acid (TA) in water-soluble sodium benzoate at varying concentrations.
Figure 4.57	Variations of $K_{\phi,s}$ of butyric acid (BA) in water-soluble sodium benzoate at varying concentrations.
Figure 4.58	The comparative plot presents the changes in $V_{\emptyset}^{0}$ for tartaric acid and butyric acid within a sodium benzoate aqueous solution at several temperatures.
Figure 4.59	Plots of distinctions of $K_{\emptyset,s}^{0}$ for (a) tartaric acid and (b) butyric acid in water-soluble sodium benzoate solution at several temperatures.

List of the Symbols and Abbreviations

c	Sound speed
ρ	Density of the solution
K	Kelvin (Temperature)
ρ_0	Density of the solvent
M	Molar mass of the solute (carboxylic acids)
m_A	Molality of the solute (carboxylic acids)
H_2O	Water
T	Temperature
V_ϕ	Apparent molar volume
S_V^*	Experimental slope coefficient for volume
V_ϕ^0	Partial molar volume
ΔV_ϕ^0	Partial molar volume of transfer
$K_{\phi,S}$	Apparent molar isentropic compression
k_S	Isentropic compressibility
T_{ref}	Reference temperature
p	Pressure
MPa	Mega Pascal
$k_{S,0}$	Isentropic compressibility of solvent
$K_{\phi,S}^0$	Partial molar isentropic compression
S_K^*	Experimental slope coefficient for isentropic compression
a, b, c	Empirical Constants
σ	Average relative deviation (ARD)
E_ϕ^0	Partial molar expansibility
$\Delta K_{\phi,S}^0$	Partial molar isentropic compression of transfer

m_B	Molal concentration of cosolute (Benzoic Acid Derivatives)
V_{AB}	Pair interaction coefficient for volume
K_{AB}	Pair interaction coefficient for isentropic compression
V_{ABB}	Triplet interaction coefficient for volume
K_{ABB}	Triplet interaction coefficient for isentropic compression
LBA	Lactobionic Acid
GA	Glycolic Acid
TA	Tartaric Acid
LA	Lactic Acid
MA	Malic Acid
BA	Butyric Acid
SB	Sodium Benzoate
PB	Potassium Benzoate
SMP	Sodium Methyl Parahydroxybenzoate

CHAPTER 1

INTRODUCTION

1.1 Ultrasonic Research

Acoustics is the branch of physics that investigates the properties and behavior of sound waves in various media. It encompasses audible sound, infrasound, and ultrasound, each defined by its frequency range. Ultrasonics, a significant subdivision, deals with waves exceeding 20 kHz, which lie beyond the upper range of human hearing. These waves extend up to several gigahertz in modern instrumentation and act as mechanical vibrations that require a medium for propagation [1,2]. The classification of sound waves based on their frequency ranges is illustrated in **Figure 1.1**. Ultrasonics has become a powerful tool in scientific research because the velocity of ultrasonic waves through liquids and mixtures provides insight into their structural and molecular behavior. It has gained prominence as a versatile non-destructive testing (NDT) method as it enables the examination of materials without altering their structure [3–6].

Figure 1.1 Frequency ranges of sound waves

1.2 Ultrasonic Testing

Ultrasonic testing represents a widely applied non-destructive technique that relies on the transmission and reception of high-frequency sound waves to investigate the internal features of a material [7]. The method generally employs two approaches: the pulse-echo technique, in which reflected waves are analyzed after encountering a boundary within the material, and the through-transmission technique, where waves pass through the specimen and are received on the opposite side. Among these, the pulse-echo method is more advantageous, as it requires access from only one side of the specimen and provides detailed information on internal discontinuities [8,9]. Frequencies commonly employed in ultrasonic testing range from 500 kHz to 20 MHz, which allows precise detection of defects, variations in thickness, and other

hidden irregularities. When ultrasonic waves encounter an interface, partial reflection occurs, and the resulting patterns of reflected signals offer valuable insights into the dimensions, structure, and integrity of the test material [10–15].

1.3 Ultrasonic Evaluation of Liquids

The study of ultrasonic waves in pure liquids and liquid mixtures holds fundamental importance for evaluating intermolecular interactions among constituent molecules. Investigations based on ultrasonic techniques provide direct insight into structural features, bonding patterns, and molecular processes in complex systems. Molecular association as well as dissociation can be represented with greater accuracy through this approach, which makes it highly valuable for analyzing the thermo-acoustical and physico-chemical behavior of liquid systems [16,17]. The magnitude and character of molecular interactions in binary or ternary mixtures become clearer when examined through ultrasonic data. Each category of liquid mixture exhibits distinct properties that generate significant scientific interest. The study of the physicochemical behavior of fluids under varied conditions of temperature, pressure, or concentration is essential for improving the performance of materials in liquid form, which explains its relevance in multiple industrial domains [18–20].

Ultrasonic methods are significant in the development of theoretical models and their translation into engineering and industrial practice. Physics and chemistry both benefit from such investigations, since they reveal the influence of solutes on solvents and demonstrate the distortions created by molecular shape and interaction. Evidence for molecular interactions appears when acoustical parameters show deviation from linear variation with concentration in liquid mixtures [21–23]. The determination of thermodynamic properties of liquid systems that include organic solvents, electrolytes, polymers, or molecular compounds becomes possible because ultrasonic waves respond sensitively to molecular structure and interparticle forces [24,25]. Several scientific disciplines have employed ultrasonic investigations to characterize acoustic and thermodynamic behavior in binary and ternary systems. Research in this field has expanded due to its wide scope and adaptability [26,27]. The study of deviations in thermodynamic and acoustic parameters from ideal values provides a descriptive and analytical understanding of solute-solvent interactions in liquid mixtures. Accurate evaluation of these parameters from experimental density and sound velocity data yields valuable information about the strength and nature of molecular forces [28-31]. Acoustic and volumetric properties of mixtures are indispensable for identifying the effects of mixing in different chemical systems

[32–34].

Recent years have witnessed progress in applying ultrasonic techniques to diverse areas such as chemistry, materials technology, and agriculture [35,36]. Thermodynamic parameters derived from ultrasonic measurements reveal the occurrence of hydrogen bonding, dipole-dipole and ion-dipole associations in solutions. These contributions have advanced the knowledge of nanoscale and macroscale properties of liquid systems [37–39]. Research on acoustic and volumetric behavior of ternary mixtures at different temperatures has also provided information relevant to the oil and gas sector, particularly in processes such as enhanced extraction [40,41]. Despite extensive investigations, several fundamental aspects of this technique remain insufficiently clarified. Pure liquids and multicomponent mixtures require a systematic study of their physicochemical and transfer properties, which can clarify the fundamental forces that govern the liquid behavior. Such investigations not only improve theoretical understanding but also support industrial processes where liquids play a crucial role [42,43].

Numerous investigations have been carried out on thermophysical and acoustic properties of liquid mixtures using parameters such as density, ultrasonic velocity, apparent molar volume, and isentropic compressibility to understand intermolecular interactions in solution systems. These studies have provided valuable information regarding solute–solvent interactions and structural effects in binary and ternary liquid mixtures. However, many earlier investigations were mainly restricted to limited temperature ranges or specific binary systems, and comparatively fewer systematic studies have focused on ternary systems involving benzoic acid derivatives in aqueous carboxylic acid solutions. Furthermore, detailed interpretation of thermo-acoustic behavior through combined volumetric and acoustic parameters remains relatively limited for such systems. Therefore, further systematic investigation is required to understand the molecular interactions and structural behavior of these complex liquid mixtures. In view of these considerations, the present work focuses on investigating the thermo-acoustic behavior of benzoic acid derivatives in aqueous solutions of selected carboxylic acids over a range of concentrations and temperatures to obtain deeper insight into intermolecular interactions in ternary liquid systems.

1.4 Density and Sound Velocity Meter

1.4.1 Instrumentation

The measurements of densities and sound speeds were performed in a single cycle of sample analysis with a Density and Sound Speed Analyzer, Model “DSA 5000M”, manufactured by

Anton-Paar. The advanced measuring principle reduces the uncertainty associated with the estimation of concentrations in binary liquid mixtures, which ensures high precision in experimental observations. In addition to these primary functions, the instrument plays a vital role in various applications such as quality control during manufacturing processes, accurate preparation of solutions and reliable assessment of concentration levels in ternary liquid systems. A schematic diagram of the density and ultrasonic velocity measurement system is shown in **Figure 1.2**. The versatility of the device which is coupled with superior accuracy, establishes it as a highly effective tool for thermodynamic, acoustic and volumetric investigations.

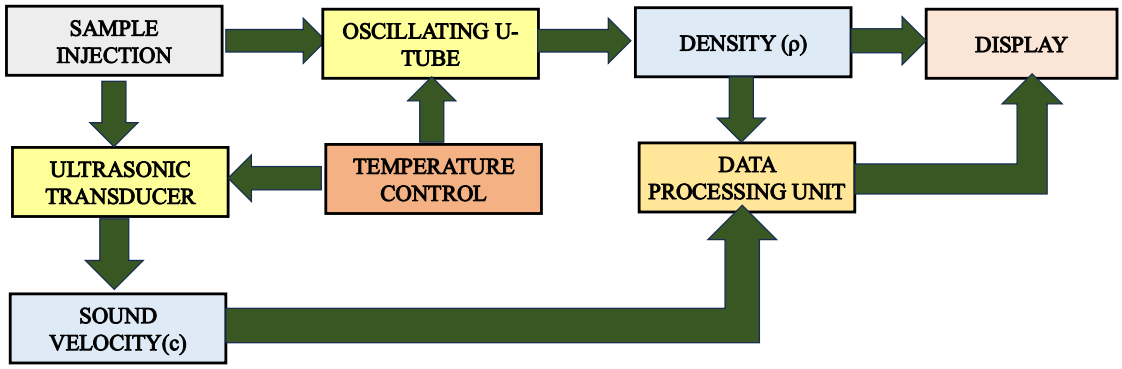

Figure 1.2 Block Diagram of Anton Paar DSA 5000M

1.4.2 Special Features of DSA 5000M

The DSA 5000M incorporates several advanced features that enhance the accuracy and reliability of the measurements:

- **High precision**: repeatability of results is ensured up to the seventh decimal place.
- **Dual-parameter capability**: density and sound velocity measured in a single operation.
- **Filling Check system**: automatic detection of filling irregularities such as air bubbles or particles.
- **U-View imaging**: high-resolution visual monitoring of the filled U-tube with images stored alongside measurement data.
- **Automatic calibration**: performed with certified reference standards to ensure consistency.
- **Thermo Balance system**: correction of errors arising from temperature-related fluctuations.
- **Rapid analysis**: measurement time per sample limited to a few minutes, enabling

analysis of up to 30 samples per hour.

1.5 Benzoic Acid Derivatives

Benzoic acid derivatives are organic compounds that are structurally related to benzoic acid, which is an aromatic compound. They play a significant role in various fields due to their diverse properties and applications. These compounds are commonly utilized in the pharmaceutical industry as they often exhibit antimicrobial, antifungal, and anti-inflammatory properties [44–46]. Their versatility and functional groups make them valuable tools in chemical and industrial processes, which contribute to advancements in technology and the improvement in the quality of various consumer goods [17,31,47]. Compounds like sodium benzoate, potassium benzoate, and sodium methyl p-hydroxybenzoate are all derivatives of benzoic acid.

1.5.1 Sodium Benzoate

Sodium Benzoate (C_6H_5COONa) is the sodium salt of benzoic acid and appears as a white, crystalline and odorless solid. It dissolves readily in water and produces benzoic acid under acidic conditions. In the food sector, sodium benzoate serves as a preservative under the code E211 [48–50]. It prevents the growth of bacteria, yeasts, and molds in acidic food products such as fruit juices, carbonated beverages, pickles, sauces, and jams. Its effectiveness remains limited to acidic environments, as neutral or alkaline media reduce its antimicrobial potential [51]. The pharmaceutical field employs sodium benzoate as a component of syrups, oral medicines, and topical solutions [52,53]. In cosmetics, it functions as a preservative in products such as creams, shampoos, and lotions, where it ensures stability and longer shelf life [54,55]. Sodium benzoate represents a key derivative of benzoic acid with broad applications in food preservation, pharmaceuticals, and cosmetics. Its role in product safety and stability makes it a compound of significant practical value.

1.5.2 Potassium Benzoate

Potassium Benzoate (C_6H_5COOK) is the potassium salt of benzoic acid. It occurs as a white, crystalline, odorless solid that dissolves easily in water. The compound remains stable, tasteless, and highly soluble which makes it suitable for industrial and commercial purposes. In the food industry, potassium benzoate functions as a preservative under the code E212 [56,57]. It inhibits the development of bacteria, yeasts, and molds in acidic food

products such as soft drinks, jams, pickles, and fruit juices. The pharmaceutical sector makes use of potassium benzoate in liquid medicines and syrups, where it preserves formulations and ensures stability. It also finds utility in cosmetic products where it acts as a preservative to extend shelf life and maintain product quality [33]. Its high solubility, preservative efficiency, and broad range of applications in food, pharmaceutical, cosmetic, and industrial fields highlight its significance in product stability and safety [58-60].

1.5.3 Sodium Methyl Parahydroxybenzoate

Sodium methyl p-hydroxybenzoate ($C_6H_4(OH)COOCH_3.Na$) is a derivative of benzoic acid in which a hydroxyl group occupies the para position of the aromatic ring and the carboxyl group undergoes esterification with methanol, followed by conversion into its sodium salt. This structural modification imparts greater solubility in water and enhances its suitability for use in a wide range of formulations. The compound appears as a white crystalline solid with a mild odor and demonstrates stability under normal storage conditions. The compound possesses notable antimicrobial efficiency against both bacteria and fungi [61–63]. Its effectiveness depends strongly on pH with maximum activity observed in slightly acidic to neutral media. Due to this property, sodium methyl p-hydroxybenzoate has found broad acceptance in food preservation, where it prevents spoilage and extends the shelf life of sauces, processed foods, and beverages [58,64]. The cosmetic field also employs sodium methyl p-hydroxybenzoate for safeguarding creams, shampoos, lotions, and similar personal care products [65].

1.6 Carboxylic Acids

Carboxylic acids are a versatile class of organic compounds that play a crucial role in various biological, industrial, and chemical processes. Their significant contribution to enhancing the shelf life of various products underscores their importance in ensuring the quality, safety, and longevity of consumer goods. These acids exhibit unique properties due to the presence of both a hydroxyl and a carbonyl group in the same molecule. Biologically, carboxylic acids are essential components of amino acids, the building blocks of proteins, and fatty acids. They also participate in metabolic pathways, which act as intermediates in processes like the citric acid cycle [66]. In the industrial realm, carboxylic acids are used in the production of plastics, solvents, and pharmaceuticals. In pharmaceuticals, carboxylic acids are found in drugs that treat pain, inflammation, and cholesterol issues. Additionally, these acids contribute to food preservation (as preservatives) and flavor enhancement (as

flavoring agents) in the food industry [67–69].

1.6.1 Lactobionic Acid

Lactobionic acid belongs to the group of polyhydroxy acids, which contain multiple hydroxyl groups along with a carboxyl group. The structure of lactobionic acid arises from the oxidation of lactose, where galactose connects with gluconic acid through a glycosidic bond [70,71]. It is often used in skincare products due to its unique properties. In skincare, lactobionic acid is primarily known for its exfoliating and moisturizing effects. It works by gently exfoliating the top layer of dead skin cells, promotes cell turnover and gives fresher and brighter skin. The abundance of hydroxyl groups gives the compound high water solubility, a strong hydrophilic nature and excellent capacity for moisture retention. Its larger molecular size compared to other exfoliants like alpha-hydroxy acids makes it suitable for individuals with sensitive skin as it is less likely to cause irritation [72–74].

1.6.2 Glycolic Acid

Glycolic acid is the simplest alpha-hydroxy acid which consists of one hydroxyl group and one carboxyl group. Its small molecular size allows rapid penetration into biological tissues which enhances its effectiveness compared to larger hydroxy acids. It is derived from sugarcane and has small molecules that allow it to penetrate the skin deeply. The presence of both hydroxyl and carboxyl groups gives glycolic acid the ability to interact with other molecules through hydrogen bonding [75,76]. In cosmetic and pharmaceutical applications, it functions as an exfoliant by breaking connections between dead skin cells which promotes renewal and improved texture. Its acidity, combined with controlled use contributes to treatments for acne, hyperpigmentation, and signs of aging. It is used in products like cleansers, toners, and serums to help improve skin texture, reduce fine lines, and promote a more even skin tone [77–79].

1.6.3 Tartaric Acid

Tartaric acid is a naturally occurring dicarboxylic acid that contains two carboxyl groups and two hydroxyl groups attached to adjacent carbon atoms. This configuration provides strong optical activity and allows the existence of stereoisomers, including meso and enantiomeric forms [80–82]. It is widely distributed in grapes, tamarinds, and other fruits, which contribute to their sour taste. The acid exhibits strong chelating ability with metal ions and plays an important role in stabilizing color and flavor. In addition, tartaric acid serves as an acidulant in food, a stabilizer in pharmaceuticals, and a raw material in the

preparation of effervescent salts and other chemical derivatives [83–85].

1.6.4 Lactic Acid

Lactic acid is an alpha-hydroxy acid that consists of a hydroxyl group adjacent to a carboxyl group on a three-carbon backbone. It exists in two stereoisomeric forms with the L-form being predominant in biological systems. It is a type of organic acid that forms in the body as a result of anaerobic metabolism, where glucose is broken down without the presence of sufficient oxygen. It can accumulate in muscles during intense exercise which leads to the sensation of muscle fatigue and soreness. Lactic acid finds various applications across different industries [86–88]. Lactic acid appears naturally in sour milk and other fermented products as a result of carbohydrate metabolism [89]. In cosmetics, it is utilized for exfoliation and moisturizing properties. The pharmaceutical sector employs it for its chiral properties in drug synthesis [90].

1.6.5 Malic Acid

Malic acid is a dicarboxylic acid with one hydroxyl group and two carboxyl groups, which occurs widely in fruits such as apples and cherries, where it contributes to the characteristic tart taste. Its strong acidulant property leads to extensive use in the food and beverage sector for flavor enhancement and preservation [91,92]. Malic acid helps to control the acidity level in some processed foods. Malic acid is also used in oral care products, such as toothpaste, for its potential teeth whitening effects. Malic acid is used as an ingredient in skin care products and chemical peels. It is known for its exfoliating effects that help to remove dead skin cells, promote skin renewal, and improve the appearance of skin [93,94].

1.6.6 Butyric Acid

Butyric acid is a short-chain fatty acid with four carbon atoms and a terminal carboxyl group. It occurs naturally in dairy products such as butter and cheese [95,96]. Industrially, butyric acid finds application in the production of esters for flavor and fragrance in pharmaceuticals and as a precursor for biofuel development. In addition to its culinary and biological roles, butyric acid has various applications in industries such as food manufacturing, pharmaceuticals, and cosmetics [97]. It is used as a flavoring agent in the production of plasticizers, perfumes, and even in some medicines due to its potential therapeutic effects on certain gastrointestinal disorders [98].

References

1. J.D. Pye and W.R. Langbauer, in Anim. Acoust. Commun. 221-25- (1998).
2. F. Duck and T. Leighton, J. Acoust. Soc. Am. 144, 2490 (2018).
3. R.B. Thompson and D.O. Thompson, Proc. IEEE 73, 1716 (1985).
4. R. Panda, S. Panda, and S.K. Biswal, CMIC 11, 2 (2024).
5. F. Honarvar and A. Varvani-Farahani, Ultrason. 108, 106227 (2020).
6. M. Gupta, M.A. Khan, R. Butola, and R.M. Singari, Adv. Mater. Process. Technol. 8, 2286 (2022).
7. J. Jodhani, A. Handa, A. Gautam, Ashwni, and R. Rana, Mater. Today Proc. 78, 627 (2023).
8. A. Ahmad and L.J. Bond, in Nondestruct. Eval. Mater. 169-183 (2018).
9. J. Krautkrämer and H. Krautkrämer, Ultrason. Test. Mater. 193–264 (1983).
10. B. Venkatraman and B. Raj, Non-Destruct. Eval. Corros. Crack. 1–55 (2019).
11. N.H.M.M. Shrifan, M.F. Akbar, and N.A.M. Isa, IEEE Access **7**, 110628 (2019).
12. N. Das, M. Kumar Praharaj, and S. Panda, J. Mol. Liq. 403, 124841 (2024).
13. I. Alqurashi, N. Alver, U. Bagci, and F.N. Catbas, J. Nondestruct. Eval. 44, 53 (2025).
14. M.D. Stanciu, M. Cosnita, C.N. Cretu, H.D. Teodorescu, and M. Trandafir, Materials 15, 5192 (2022).
15. B. Wang, S. Zhong, T.-L. Lee, K.S. Fancey, and J. Mi, Adv. Mech. Eng. 12, 168781402091376 (2020).
16. E. Maeva, I. Severina, S. Bondarenko, G. Chapman, B. O'Neill, F. Severin, and R.Gr. Maev, Can. J. Phys. 82, 981 (2004).
17. A.K. Gill, N. Chakraborty, and K.C. Juglan, *Adv. Med. Diagn. Treat. Care*. 450–459 (2023).
18. P. Kaur, N. Chakraborty, K.C. Juglan, H. Kumar, and M. Singla, J. Mol. Liq. 339, 116810 (2021).
19. N. Chakraborty, K.C. Juglan, and H. Kumar, J. Chem. Thermodyn. 154, 106326 (2021).
20. M. Lamba, N. Chakraborty, K.C. Juglan, R. Sharma, and M. Singla, J. Chem. Eng. Data 69, 171 (2024).
21. J. Tomasi and M. Persico, Chem. Rev. 94, 2027 (1994).
22. A. Ali, S. Hyder, and A.K. Nain, J. Mol. Liq. 79, 89 (1999).
23. T. Chen, X. Feng, Y. Yin, and Y. Xu, J. Solution Chem. 49, 1402 (2020).
24. E. Hendriks, G.M. Kontogeorgis, R. Dohrn, J.-C. De Hemptinne, I.G. Economou, L.F. Žilnik, and V. Vesovic, Ind. Eng. Chem. Res. 49, 11131 (2010).

25. Z. Lei, B. Chen, C. Li, and H. Liu, Chem. Rev. 108, 1419 (2008).
26. I. Saxena, V. Kumar, and A. Gupta, J. Solution Chem. 53, 182 (2024).
27. N. Das, M.K. Praharaj, and S. Panda, CAC 21, 276 (2025).
28. X. Xue, H. Wu, Q. Cai, M. Chen, S. Moon, Z. Huang, T. Kim, C. Peng, W. Feng, N. Sharma, and X. Jiang, IEEE Trans. Ultrason., Ferroelect., Freq. Contr. 71, 786 (2024).
29. A.B. Singh, C. Khandelwal, and G.S. Dangayach, Polym. Plast. Technol. Mater. 63, 1608 (2024).
30. Ashima, K.C. Juglan, and H. Kumar, J. Chem. Thermodyn. 140, 105916 (2020).
31. A.K. Gill, N. Chakraborty, and K.C. Juglan, Chem. Phys. Imp. 10, 100843 (2025).
32. K. Kaur, K.C. Juglan, and H. Kumar, J. Mol. Liq. 268, 700 (2018).
33. A.K. Gill, N. Chakraborty, and K.C. Juglan, J. Chem. Eng. Data 70 2260-2276 (2025).
34. K. Dhal, S. Singh, and M. Talukdar, Journal of Molecular Liquids 368, 120761 (2022).
35. K.S. Suslick and G.J. Price, Annu. Rev. Mater. Sci. 29, 295 (1999).
36. M.A. Sattar and D.S. Laila, Front. Plant Sci. 16, 1620868 (2025).
37. S. Rana, R.C. Thakur, and H.S. Dosanjh, AIP. Conf. Proc. 020094 (2023).
38. N. Chakraborty, K.C. Juglan, and H. Kumar, J. Chem. Thermodyn. 163, 106584 (2021).
39. M. Sethu Raman, M. Kesavan, K. Senthilkumar, and V. Ponnuswamy, J. Mol. Liq. 202, 115 (2015).
40. P.M. Junaid, A.H. Dar, K.K. Dash, T. Ghosh, R. Shams, S.A. Khan, A. Singh, V.K. Pandey, G.A. Nayik, and G.V.S. Bhagya Raj, J. Food Process Eng. 46, e14192 (2023).
41. J. Mierez, M.J. AlTammar, K.M. Alruwaili, and R.T. Alfaraj, Ultrason. Sonochem. 103, 106767 (2024).
42. M. Lucas, A. Gachagan, and A. Cardoni, J. Mech. Eng. Sci. 223, 2949 (2009).
43. J.A. Gallego-Juarez, Phys. Procedia. 3, 35 (2010).
44. A. Madani, Z. Esfandiari, and Y. Fakhri, Iran. J. Public Health. 54, 1204-1215 (2025).
45. M. Bešter-Rogač, J. Chem. Eng. Data 56, 4965 (2011).
46. A. Del Olmo, J. Calzada, and M. Nuñez, Crit. Rev. Food Sci. Nutr. 57, 3084 (2017).
47. W. Johnson, W.F. Bergfeld, D.V. Belsito, R.A. Hill, C.D. Klaassen, D.C. Liebler, J.G. Marks, R.C. Shank, T.J. Slaga, P.W. Snyder, and F.A. Andersen, Int. J. Toxicol. 36, 5S (2017).
48. M. Silva and F. Lidon, Emir. J. Food Agric. 28, 366 (2016).
49. B. Nair, Int. J. Toxicol. 20, 23-50 (2001).
50. C. Novais, A.K. Molina, R.M.V. Abreu, C. Santo-Buelga, I.C.F.R. Ferreira, C. Pereira, and L. Barros, J. Agric. Food Chem. 70, 2789 (2022).

51. R. Sehrawat, K.A. Khan, M.R. Goyal, and P.K. Paul, Technol. Interv. Process. Fruits Veg. (2018).
52. D. Mohammed and H. Issa, ChemRxiv. (2024).
53. M.-C. Husson, M. Schiff, A. Fouilhoux, A. Cano, D. Dobbelaere, A. Brassier, K. Mention, J.-B. Arnoux, F. Feillet, B. Chabrol, N. Guffon, C. Elie, and P. De Lonlay, Orphanet J. Rare Dis. 11, 127 (2016).
54. P. Poddębniak and U. Kalinowska-Lis, Appl. Sci. 14, 1581 (2024).
55. S.A. Raji, A.P.I. Popoola, and O.L. Akanji, J. Mol. Struc. 1312, 138414 (2024).
56. P. Piper, Bev. 4, 33 (2018).
57. N. Zengin, D. Yüzbaşıoğlu, F. Ünal, S. Yılmaz, and H. Aksoy, Food Chem. Toxicol. 49, 763 (2011).
58. C. Butterhof, T. Martin, W. Milius, and J. Breu, Zeitschrift Anorg. Allg. Chem. 639, 2816 (2013).
59. N. Karunagaran and P. Ramasamy, AIP Conf. Proc. 1536, 887–888 (2013).
60. A.K. Gill, N. Chakraborty, and K.C. Juglan, Phys. Scr. 99, 115009 (2024).
61. Ashima, K.C. Juglan, and H. Kumar, J. Chem. Thermodyn. 140, 105916 (2020).
62. G. Zavišić, S. Ristić, S. Petričević, D. Janković, and B. Petković, Foods 13, 2487 (2024).
63. A. Thakur, K.C. Juglan, and H. Kumar, J. Phys.: Conf. Ser. 1531, 012018 (2020).
64. R.J. Yu and E.J. Van Scott, J. Cosmet. Dermatol. 3, 76 (2004).
65. M. Braga, P.M. Ferreira, and J.R.M. Almeida, Biofuels Bioprod. Bioref. 15, 231 (2021).
66. M. Ghai, N. Agnihotri, V. Kumar, R. Agnihotri, A. Kumar, and K. Sahu, Phys. Sci. Rev. 9, 3097 (2024).
67. J. Wang, M. Lin, M. Xu, and S.-T. Yang, Anaerobes Biotechnol. 323–361 (2016).
68. K. Bhakri, M. Lamba, K.C. Juglan, and N. Chakraborty, J. Mol. Liq. 406, 125117 (2024).
69. T. Cardoso, C. Marques, J.L.A. Dagostin, and M.L. Masson, J. Food Sci. 84, 1672 (2019).
70. S. Alonso, M. Rendueles, and M. Díaz, Biotechnol. Adv. 31, 1275 (2013).
71. J. Cao, H. Fu, L. Gao, and Y. Zheng, Folia Microbiol. 64, 899 (2019).
72. S. Sáez-Orviz, I. Marcet, M. Rendueles, and M. Díaz, J. Sci. Food Agric. 102, 3495 (2022).
73. L.-F. Gutiérrez, S. Hamoudi, and K. Belkacemi, Int. Dairy J. 26, 103 (2012).
74. K. Kantikosum, Y. Chongpison, N. Chottawornsak, and P. Asawanonda, CCID 12, 151

(2019).
75. S.V. Portnova, N.S. Kuzmina, Y.F. Yamshchikova, and E.L. Krasnykh, J. Chem. Eng. Data 67, 2323 (2022).
76. E. Moghimipour, A. Gorji, R. Yaghoobi, A. Salimi, M. Latifi, M. Aghakouchakzadeh, and S. Handali, J. Drug Target. 32, 74 (2024).
77. T.-Y. Liu, P.-Y. Xu, Dan Huang, B. Lu, Z.-C. Zhen, W.-Z. Zheng, Y.-C. Dong, X. Li, G.-X. Wang, and J.-H. Ji, J. Hazar. Mater. 446, 130670 (2023).
78. S.-J. Kim, J.-H. Park, D.-H. Kim, Y.-H. Won, and H.I. Maibach, Dermatol. Surg. 24, 1054 (1998).
79. S.K. Sharma and A. Thakur, J. Mol. Liq. 322, 114527 (2021).
80. T. Chen, Q. Zhang, Z. Li, X. Yin, and F. Hu, Spectrochim. Acta A Mol. Biomol. Spectrosc. 205, 312 (2018).
81. M. Castaldi, G. D'Errico, L. Paduano, and V. Vitagliano, J. Chem. Eng. Data 44, 672 (1999).
82. M. Li, J. Su, H. Yang, L. Feng, M. Wang, G. Xu, J. Shao, and C. Ma, Hortic. 9, 1173 (2023).
83. A.K. Gill, N. Chakraborty, and K.C. Juglan, Chem. Thermodyn. Therm. Anal. 100216 (2025).
84. X. Li, M. Liu, W. Li, X. Wang, S. Wang, H. Yin, N. Yan, X. Jin, and C. Yang, Chem. Rec. 24, e202400099 (2024).
85. H.-C. Huang, I.J. Lee, C. Huang, and T.-M. Chang, Curr. Pharm. Biotechnol. 21, 566 (2020).
86. B. Algiert-Zielińska, P. Mucha, and H. Rotsztejn, Int. J. Dermatol. 58, 374 (2019).
87. P.E. Di Prampero and G. Ferretti, Respir. Physiol. 118, 103 (1999).
88. N.C. Spurway, Br. Med. Bull. 48, 569 (1992).
89. B.A. Green, R.J. Yu, and E.J. Van Scott, Clin. Dermatol. 27, 495 (2009).
90. M. Yadav, N. Sehrawat, S. Kumar, A.K. Sharma, M. Singh, and A. Kumar, Phys. Sci. Rev. 9, 187 (2024).
91. T.-H. Lee, H. Yu, M. Forrester, T. Wang, L. Shen, H. Liu, J. Li, W. Li, G. Kraus, and E. Cochran, ACS Sustainable Chem. Eng. 10, 2624 (2022).
92. R. Khandelwal, P. Srivastava, and V.S. Bisaria, World J. Microbiol. Biotechnol. 39, 217 (2023).
93. C. Marques, A.R. Sotiles, F.O. Farias, G. Oliveira, M.L. Mitterer-Daltoé, and M.L. Masson, Arab. J. Chem. 13, 9118 (2020).

94. T.S.D. Oliveira, A. Ghosh, and P. Chaudhuri, J. Phys. Chem. A 127, 3551 (2023).
95. M. Wang, S. Wichienchot, X. He, X. Fu, Q. Huang, and B. Zhang, Trends in Food Sci. Technol. 88, 1 (2019).
96. V. Biswas, A. Praveen, A.L. Marisetti, A. Sharma, V. Kumar, S.K. Sahu, and D. Tewari, Dietetics 1, 182 (2022).
97. M. Dwidar, J.-Y. Park, R.J. Mitchell, and B.-I. Sang, Sci. World J. 2012, 1 (2012).
98. M.T. El-Saadony, M. Umar, F. Hassan, M. Alagawany, M. Arif, A.E. Taha, S.S. Elnesr, K.A. El-Tarabily, and M.E. Abd El-Hack, Anim. Health. Res. Rev. 23, 136 (2022).

CHAPTER 2

REVIEW OF LITERATURE

Urick (1947) [1] proposed a method to determine the adiabatic compressibility of finely divided substances by utilizing sound velocity and density data of their suspensions in liquids. The principle of this approach rests on the assumption that the velocity of sound in a suspension is equivalent to that in an ideal solution composed of the same constituents. Experimental verification was carried out through velocity measurements in kaolin-water systems and xylene-water emulsions. The procedure was further applied to evaluate the compressibility of oil droplets within emulsions and blood corpuscles in horse blood. The method provided reliable values, particularly for materials whose compressibility did not deviate significantly from that of the suspending medium.

Koodriavtsev (1956) [2] derived an equation that expressed sound velocity in terms of internal energy and physical constants for pure liquids and binary mixtures. Calculated sound velocities for organic liquid mixtures agreed with experimental data and the variation with concentration was explained. The equation applied to aqueous electrolyte solutions produced velocities consistent with measurements and allowed the determination of adiabatic compressibility. The study demonstrated the use of acoustic data to evaluate physicochemical properties of electrolyte solutions.

Hammes et al. (1966) [3] studied ultrasonic absorption in water-dioxane mixtures at 10 ºC and 25 ºC over the full composition range. The data revealed relaxation processes associated with the formation of hydrogen-bonded complexes. Analysis of relaxation amplitudes and times allowed the determination of aggregate stoichiometry and thermodynamic constants. The small standard volume and enthalpy changes reflected the stability of the aggregates and the formation of hydrophobic water clusters around the dioxane hydrocarbon moiety.

Desnoyers et al. (1973) [4] examined sodium benzoate and its ortho, meta, and para hydroxy derivatives in aqueous medium at 25 ºC through measurements of density, heat capacity, viscosity, osmotic properties, and conductivity. The introduction of substituents had little influence on molar volume and viscosity but caused a strong reduction in heat capacity, attributed to solute-solvent hydrogen bonding. The ortho isomer showed distinct behavior due to intramolecular hydrogen bonding and displayed specific interactions at higher

concentrations, while the meta and para isomers revealed cation-anion attractions. Both sodium and potassium benzoates demonstrated signs of association at concentrations above 1 m.

Prasad et al. (1978) [5] investigated adiabatic compressibility, molar volume, intermolecular free length, available and free volume from density and sound speed in three ternary liquid mixtures with p-xylene as the common component system: system I (p-xylene-acetone-carbon tetrachloride), system II (p-xylene-acetone-cyclohexane), and system III (p-xylene-benzene-cyclohexane) at 23 ºC. Ultrasonic speeds were measured with the Debye-Sears light diffraction method and densities were determined with a double-walled pycnometer. Molecular interaction reached a maximum at the mole fraction of acetone 0.5 in system I and 0.6 in system II, while in system III the values remained nearly constant which indicates negligible interaction. Excess properties were also reported and used to explain the observed interactions.

Zaghloul et al. (1980) [6] determined the dissociation behavior of tartaric, maleic, and phthalic acids in water-ethanol mixtures at six temperatures using the EMF method. From the dissociation constants, the thermodynamical parameters, namely, Gibbs free energy, enthalpy, and entropy, were calculated for both the first and second ionization processes. The results demonstrated that the extent of ionization decreased with increasing ethanol content due to the lower dielectric constant of the medium, which reduces the stabilization of ions. Comparison with other dicarboxylic acids highlighted the influence of molecular structure and solvent composition on solute-solvent interactions.

Wakabayashi et al. (1982) [7] studied aqueous solutions of butyl and phenyl groups over 1-55 ºC to determine apparent and partial molar volumes and expansibilities. Substituting butyl groups with phenyl groups reduced cation hydrophobicity as reflected in smaller viscosity-B coefficients and weaker temperature-dependent volume and expansibility variations. However, low-temperature extrema persisted which indicates that phenyl groups have a limited effect on butyl cospheres and cation interactions.

Apelblat (1986) [8] examined the enthalpies of solution for several organic acids in water at 298.15 K using an LKB calorimeter. Both anhydrous and hydrated forms of acids, such as oxalic acid, citric acid, and several dicarboxylic acids like succinic, adipic, malic, and tartaric acids were studied and the data were extrapolated to infinite dilution to obtain molar enthalpies of solution and hydration. The findings revealed clear differences between anhydrous and

hydrated acids, showing that hydration water within the crystal lattice significantly affects the dissolution process.

Simeer et al. (1987) [9] investigated the complexation of β-cyclodextrin with benzoic acid and sodium benzoate in aqueous solution at 30 ºC and 50 ºC by means of a heat conduction microcalorimeter (LKB 2277) with a flow-mix cell. Thermodynamic parameters, including the dissociation constant, enthalpy and entropy change were obtained. The dissociation constant exhibited a wide range of values, which indicated that the carboxyl group of benzoic acid and the carboxylate ion of sodium benzoate occupy the cavity of β-cyclodextrin preferentially. The study demonstrated that direct calorimetric methods provide a reliable determination of both thermodynamic parameters of complex formation and the dissociation constant.

Juni and Nakano (1987) [10] analyzed the application of polyhydroxy acids in drug delivery systems. The study focused on lactic acid and glycolic acid homo- and co-polymers, poly-beta-hydroxybutyric acid and polycaprolactone. They examined the physicochemical properties of these polymers, including their biodegradability and biocompatibility. In addition, the study evaluated the performance of various dosage forms prepared from these polymers through in vitro and in vivo experiments. The results highlighted the potential of these polymers to serve as effective carriers for controlled drug release and biocompatible delivery systems.

Rao et al. (1990) [11] investigated the acoustic behavior of polyvinyl pyrrolidone (PVP) in N, N-dimethylformamide (DMF) solutions. Density values were obtained using a pycnometer, while viscosity was measured with an Ostwald viscometer. Analysis of refractive index, viscosity, and ultrasonic velocity indicated significant solute-solvent interactions in the PVP-DMF system.

Aminabhavi et al. (1994) [12] examined the densities, refractive indices, and viscosities of diethylene glycol and dimethyl ether in mixtures with esters such as ethyl acetate, diethyl succinate, methyl and ethyl benzoate. The experimental data were applied to calculate several thermodynamic and volumetric parameters. The results indicated the presence of substantial intermolecular associations between the components in the mixtures, reflecting solute-solvent affinity and structural organization within the solution.

Magazu et al. (1997) [13] conducted a study on aqueous solutions of α-α-trehalose using

ultrasonic measurements to obtain density and sound velocity values. The results revealed significant deficiencies in the solution preparation procedure, which may affect the reproducibility and accuracy of the measurements. Evaluation of excess compressibility as a solute concentration demonstrated that α-α-trehalose molecules formed intramolecular H_2 bonds at higher concentrations.

Yun et al. (1999) [14] examined 1:1 complexes of lanthanide ions with para-substituted benzoic acid derivatives (4-amino, 4-hydroxy, 4-nitro) in aqueous medium at 25 ºC and 0.1 M $NaClO_4$. Potentiometric and calorimetric analyses revealed that the stability of the complexes depended on the electronic nature of the substituents. Charge distribution calculations showed that greater negative shifts at the carboxylate group correspond to higher stability constants, which reflected the influence of substituent effects on lanthanide-benzoate interactions.

Ali et al. (1999) [15] investigated pure solvents such as ethanol, 1-hexanol, 1-octanol, N, N-dimethylformamide, and acetonitrile at 303.15 K using density, viscosity and sound speed measurements. From these data, excess adiabatic compressibility, free length and volume, viscosity and acoustic impedance were calculated to assess molecular association. Results highlighted the role of determining the intermolecular forces in the mixtures.

Matos et al. (2001) [16] reported densities and kinematic viscosities for the binary mixtures such as methyl butanoate with n-heptane and n-octane at 283.15-313.15 K. Binary excess volumes showed negative values for n-heptane + methyl butanoate and positive values for n-heptane + n-octane, which indicates strong solute-solvent interactions. Derived parameters, including isobaric thermal expansion coefficients and pressure coefficients of molar excess enthalpy, varied systematically with composition. Ternary excess volumes and viscosity deviations aligned with predictions based on binary data, confirming model reliability for multicomponent systems.

Chitra et al. (2001) [17] studied hydrogen-bond formation in mixtures of methyl benzoate and N-methylaniline in benzene using dielectric methods. Computational analysis identified the stable structure of the complex; comparison of calculated and experimental dipole moments supported the proposed interaction model. This work highlighted the complementary role of experimental and theoretical approaches in understanding hydrogen-bonded systems.

Garcia et al. (2002) [18] investigated the refractive indices, density, and viscosity for binary combinations of methyl benzoate with n-alkanes by ultrasonic methods. The experimental values permitted the evaluation of thermophysical parameters and excess molar volumes, while the intercept method provided the partial molar volumetric property of both components. The Peng-Robinson and Soave-Redlich-Kwong cubic equations of state were applied to process the excess properties. The results indicated that molecular interactions and structural effects governed the behavior of the mixtures and the theoretical models showed satisfactory agreement with the experimental data.

Steele et al. (2002) [19] determined the ideal-gas and liquid-phase enthalpies of formation of six organic compounds (methyl benzoate, ethyl benzoate, R-(+)-limonene, trans-crotonaldehyde, tert-amyl methyl ether, and diethylene glycol using combustion calorimetry. Vapor pressures, densities, and heat capacities were measured with ebulliometric and calorimetric methods over wide temperature ranges. Critical constants and related thermophysical properties were derived through experimental data and a fitting procedure. Wagner-type vapor-pressure equations were proposed and the results were validated against literature values. Recommended critical parameters and group-additivity values were also reported.

Vartiainen et al. (2003) [20] examined the incorporation of food preservatives into plastics for antimicrobial packaging. Sodium nitrite in plaques suppressed Aspergillus niger and Bacillus subtilis, while sodium benzoate and potassium sorbate acted only on B. subtilis. Strongest inhibition appeared in PS (potassium sorbate) and PET (polyethylene terephthalate). Further tests on LDPE films with sodium benzoate and sodium nitrite showed negligible effect on permeability, excessive migration, and no antimicrobial activity.

Li et al. (2003) [21] studied o-, m-, and p-sodium methylbenzoate in DMF-water mixtures at 298.15 K using oscillating-tube densimetry. Apparent and partial molar volumes were determined and transfer volumes from water to DMF-water mixtures were analyzed. The findings reveal the effects of substituents and solvent composition on interactions.

Xie et al. (2004) [22] investigated the volumes and apparent molar heat capacities of aqueous tartaric acid, two buffer systems, and disodium tartrate across the temperature range 283.15-328.15 K at 1 MPa. Apparent molar volumes of $H_2Tar(aq)$ and $Na_2Tar(aq)$ were also

determined between 377.15 and 529.15 K at 10.4 MPa. The experimental data were represented using a model that accounted for both molality and temperature dependence. Extrapolation to infinite dilution provided standard partial molar heat capacities and volumes for $H_2Tar(aq)$, $HTar^-(aq)$, and $Tar^{2-}(aq)$. The variation of volume with temperature for $Na_2Tar(aq)$ agreed with the behavior of typical aqueous electrolytes, while $H_2Tar(aq)$ displayed unusual characteristics since its values did not shift toward more positive magnitudes with increasing temperature.

Yan et al. (2004) [23] studied alpha-amino acids in calcium chloride by measuring densities and viscosities at different temperatures. Apparent molar volumes, viscosity coefficients, hydration numbers, and activation parameters were derived from the data. The results suggested linear trends with chain length which highlights hydration effects and structural influence of amino acids in solution.

Resa et al. (2005) [24] investigated mixtures of ethanol, water, and sucrose to study the conversion of water and sucrose into carbon dioxide and ethanol. They measured thermoacoustic properties such as density and ultrasonic velocity for these systems. The experimental results were compared with predictions from the Urick, Natta-Baccaredda, and Nomoto relations. The comparison revealed the presence of hydrogen-bond interactions in the mixture.

Sengwa et al. (2006) [25] studied binary mixtures of monoalkyl ethers of ethylene glycol with various polar solvents using dielectric measurements at 1 MHz and 25 ºC. Excess dielectric constants and Kirkwood correlation factors were derived to assess solvent-cosolvent interactions. Results showed that interaction strength depended on ether chain length and solvent type with clear differences between hydroxyl- and non-hydroxyl-containing solvents.

Minofar et al. (2007) [26] studied aliphatic and aromatic carboxylates and phenolate groups of humic acid in aqueous solutions near the surface. Sodium formate followed classical electrolyte surface behavior, while sodium benzoate, sodium acetate, and sodium phenolate showed hydrotropic character with surface-active anions. Molecular dynamics results confirmed their strong orientation at the solution-vapor interface.

Widegren and Magee (2007) [27] examined the dynamic viscosity and density of the binary system of 1-hexyl-3-methylimidazolium bisamide. Their results demonstrated that

hydrophobic ionic interactions governed the structural and transport behavior of the system.

Rehman et al. (2008) [28] studied density, viscosity, and electrical conductivity of the water + ethanol + lithium chloride system over a wide temperature and composition range. Excess molar volumes and thermal expansion coefficients showed no major structural changes with temperature. Viscosity and conductivity analyses revealed composition-dependent activation energies and conductivity maxima with sharper effects in ethanol-rich mixtures.

Green et al. (2009) [29] reported that polyhydroxy acids had major applications in cosmetic and therapeutic formulations. They served as anti-ageing, peels, moisturizers, and remedies for hyperpigmentation. Antioxidant, chelation, and barrier-strengthening effects were also noted. Bionic acids delayed the ageing process by suppressing matrix metalloproteinase activity.

Rathnam et al. (2009) [30] reported refractive index, density, and kinematic viscosity data for binary mixtures of isoamyl acetate or methyl benzoate with ortho-, meta-, and para-xylene. Measurements were performed using a pycnometer, a Ubbelohde viscometer, and a thermostated Abbe refractometer. Viscosity deviations and molar refraction deviations were evaluated from the investigated data. The R-K formula was applied and the binary coefficients along with standard deviations were obtained.

Kostov et al. (2010) [31] conducted a comparative study on lactobionic and glycolic acids with respect to efficacy and irritation potential in gel and emulsion carriers. The results demonstrated that LBA-based formulations produced superior skin tolerance, with reduced irritation and less barrier damage. Both LBA and GA exhibited greater activity in vehicles that contained a novel APG emulsifier. The findings established the importance of the carrier system in the effectiveness of topical agents.

Kornhauser et al. (2010) [32] examined the applications, classification, mechanisms, and photoactivity of hydroxy acids. The study confirmed their use in cosmetic formulations and in dermatology for the treatment of acne, photo-ageing, rosacea, ichthyosis, and pigmentation disorders.

Kharat (2010) [33] investigated ultrasonic velocity and density of aqueous maleic acid and tartaric acid at 298.15 and 308.15 K over a wide molality range under atmospheric pressure.

The data were fitted with polynomial relations, and several volumetric and ultrasonic parameters were derived from the experimental results. Analysis of these values revealed the nature of interactions, the structure-maker or breaker tendencies of the acids and their relation to taste perception in aqueous medium.

Rathnam et al. (2010) [34] reported viscosity, density, and ultrasonic velocity data for mixtures of methyl benzoate with n-hexane, octane, cyclohexane, and heptane. Measurements were performed with a DMA 35 Anton Paar digital density meter and an interferometer at different temperatures. Excess thermodynamic parameters were derived from the investigational results and the R-K equation was applied for further evaluation. The analysis indicated that the McAllister and Auslander models provided more reliable representations of viscosities for the binary liquid mixtures under the investigated conditions.

Przybyla et al. (2011) [35] studied mixtures of dichloromethane and heptane over the temperature series of 288.15- 318.15 K and evaluated properties such as molar isobaric expansion and thermodynamic excess volume. Their results indicated the occurrence of dipole-dipole bonds in the binary system.

Madhuri et al. (2011) [36] assessed density and viscosity data for binary mixtures of benzyl benzoate with acetonitrile or benzonitrile at several temperatures obtained through an interferometer. From these results, thermodynamic parameters such as adiabatic compressibility, internal pressure, enthalpy, activation energy, and ultrasonic velocity were derived. The results indicated a strong molecular association between the components.

Davila et al. (2011) [37] determined the densities of methyl benzoate with cyclohexane and 1-hexanol within the temperature variation of 278.15 K to 350.15 K. The Triden-10 parameter equation was employed to correlate the data with temperature and pressure. Isothermal compressibility, internal pressure, and isobaric expansivity were evaluated on this basis. The analysis revealed a significant influence of both temperature and pressure on interactions between molecules.

Suarez et al. (2011) [38] examined dilute aqueous solutions of propanoic, butanoic, pentanoic, and hexanoic acids at 293.15-308.15 K through densities and surface tension investigations. Excess molar and limiting partial molar volumes, and group contributions of methylene and

carboxyl groups were evaluated. The results showed that the temperature influences through a balance of hydrophilic and hydrophobic interactions.

Mohan et al. (2011) [39] examined the thermodynamic, dielectric, and conformational behavior of Hydrogen-bonded mixtures of propan-1-ol with methyl and ethyl benzoates. Measurements were carried out with an LF impedance analyzer, the plunger technique, and an Abbe's refractometer. Thermodynamic parameters like relaxation time, excess inverse relaxation time, and Kirkwood's correction factors were derived. FT-IR spectra confirmed the presence of hydrogen bonds amid the O-H cluster of propan-1-ol and the CH groups of the benzoates.

Kornhauser et al. (2012) [40] explored the effect of cosmetic formulations containing hydroxyacids and related compounds on skin exposed to sunlight. Their work placed particular emphasis on the safety and protective aspects of these formulations, especially when used over extended periods. The study pointed out the potential risks of long-term application and discussed the protective strategies that can reduce the harmful effects of solar exposure. An important outcome of their investigation was the clarification that the effects of medicated hydroxyacids are not confined to their keratolytic property. Instead, they exert broader biological actions on skin, which have significant implications for their safe and effective use in dermatological and cosmetic applications.

Parveen et al. (2012) [41] studied aniline-acetic acid and aniline-propionic acid mixtures at 293.15 to 313.15 K. They evaluated thermodynamic and acoustic parameters, including specific heat ratio, pseudo-Gruenisen parameter, non-linearity parameter and Debye temperature. Deviations in compressibilities and other thermodynamical parameters were calculated and fitted with the Redlich-Kister equation. Experimental densities were compared with HBT and Rackett models and the refractive indices were analyzed using several mixing rules.

Rathnam et al. (2012) [42] reported densities and viscosities for binary mixtures of methyl benzoate at varying temperatures with a portable density meter, Ubbelohde viscometer, and ultrasonic interferometer. Excess thermodynamic parameters derived through the R-K polynomial equation revealed negative deviations in isentropic compressibility, which confirmed strong intermolecular associations in the mixture.

Pathak et al. (2012) [43] carried out a systematic investigation on epoxy resin solutions to understand their thermophysical and acoustic behavior. They measured viscosity, density, and ultrasonic velocity of solvents such as tetrahydrofuran, chloroform, and 1,4-dioxane at a fixed temperature. These experimental results were further applied to calculate a range of thermodynamic parameters that provided insight into the molecular interactions present in the solutions. Such an approach highlighted the role of ultrasonic and volumetric measurements in evaluating solute-solvent interactions in polymer-solvent systems.

Papari et al. (2013) [44] determined densities and sound velocities for binary systems of 2-phenylethanol with alcohols (1-, 2-, and 2-methyl-1-butanol) at six temperatures by a vibrating-tube densimeter. The calculated excess molar volumes, deviations in compressibility, and excess expansion coefficients were all negative. These results confirmed the dominance of attractive solute-solvent interactions.

Nagarjun et al. (2013) [45] determined densities and sound velocities for binary mixtures of ethyl benzoate at various temperatures using a 25 ml specific gravity bottle and interferometer method. The calculated excess thermodynamic parameters revealed significant deviations from ideal behavior, which indicated the existence of strong solute-solvent interactions. These interactions were concentration and temperature-dependent, and the trends were successfully pronounced by the R-K equation.

Pal et al. (2013) [46] evaluated binary mixes of dipropylene glycol dimethyl ether with methyl, ethyl, and n-butyl acetates. Measurements of sound speed and density allowed the evaluation of excess molar volumes and deviations in isentropic compressibility. The results suggested strong interactions between dissimilar molecules, which reflect structural rearrangements in the mixtures due to molecular size and polarity differences.

Nain et al. (2013) [47] investigated l-threonine in aqueous sucrose solutions across various temperatures. Derived parameters such as expansivity, compressibility, apparent molar volumes, and hydration number indicated that interactions strengthened with increasing sucrose concentration. The findings highlighted enhanced molecular association and structural ordering in the mixtures.

Rathnam et al. (2013) [48] measured sound velocity and viscosity for methyl benzoate with

ethers by the ultrasonic approach. The analysis of deviations in viscosity and isentropic compressibility, along with their excess values, indicated pronounced interactions between methyl benzoate and ether molecules. The interaction strength varied with composition, and the R-K equation provided a reliable correlation of the observed deviations.

Sreehari Sastry et al. (2013) [49] measured viscosities, densities, and sound velocity for ethyl benzoate with alkanols using a viscometer, a specific-gravity bottle, and an interferometer. The excess thermodynamic parameters were negative for all mixtures, which demonstrated strong attractive interactions between the components. These results confirmed consistent intermolecular associations across compositions and temperatures. The Redlich-Kister polynomial equation provided an accurate correlation of the experimental trends.

Vijayalakshmi et al. (2014) [50] examined mixtures of ethyl benzoate with ortho-, meta-, and para-chlorotoluenes + toluene and determined their viscosities and densities using a Ubbelohde viscometer together with a Rudolph Research Analytical densimeter across different temperatures. From the obtained data, they derived isentropic compressibility, isobaric thermal expansion coefficient, molar heat capacity, and the deviations in both viscosities and acoustic impedance. The study highlighted the occurrence of notable molecular interactions and the observed behavior of the mixtures was attributed mainly to dipole-dipole type associations between unlike components.

Bahadur et al. (2014) [51] investigated mixtures of butanoic, pentanoic, and heptanoic acids using volumetric, acoustic, and refractive index methods at several temperatures. Excess molar volumes, isentropic compressibilities, excess isentropic compressibilities, and refractive index deviations were derived and fitted with the Redlich-Kister equation. The results highlighted the presence of molecular interactions and confirmed the suitability of the mixing rules for predicting the sound velocity as well as the application of the Lorentz-Lorenz relation for estimating density from refractive index and vice-versa.

Sastry et al. (2014) [52] reported measurements of velocities and viscosities for the binary combinations of methyl benzoate or ethyl benzoate with 2-propanol at several temperatures by means of an Ostwald viscometer and an ultrasonic interferometer operated a 2 MHz. The experimental results were applied to the R-K polynomial equation to evaluate thermodynamic and acoustic parameters. The observed variations in these parameters indicate the possible

creation of H-bonding within the constituent molecules.

Bahadur et al. (2014) [53] measured density, sound velocity, and refractive index for the binary combinations of butyric and hexanoic acids across the full composition range at 293.15-313.15 K in 5 K intervals. The R-K equation was applied to fit the excess and deviation properties, while the Lorentz-Lorenz relation was used to correlate density and refractive index. Among the four sound velocity mixing rules, the Berryman rule provided the best prediction. The results explained the role of intermolecular interactions in the mixtures.

Chauhan et al. (2015) [54] reported measurements of densities and sound velocities for selected saccharides in glycine mixtures at various temperatures. From these data, isentropic compressibilities, apparent molar volumes and isentropic compressions, and their transfer values are evaluated. The results demonstrated strong solute-solvent interactions that were attributed to hydrogen bonding between saccharides and glycine molecules.

Lalikoglu et al. (2015) [55] prepared layered double hydroxide (LDH) by the coprecipitation method to study the separation of lactic acid. Characterization was carried out using FTIR, XRD, and molecular size analyses. The maximal removal of 66.49% was obtained with 1 g of LDH at 298 K. Adsorption data followed the Langmuir model with R^2 values of 0.9894, 0.9972, and 0.9998 at 298, 308, and 318 K, respectively. Separation strongly depended on initial lactic acid concentration and thermodynamic analysis indicated variations in ΔG^o, ΔH^o, and ΔS^o, which confirmed the feasibility of the process.

Choudhary et al. (2015) [56] presented thermodynamic and ultrasonic studies of 5-chloro-2-hydroxy-3-nitroacetophenone in N, N-dimethylformamide over a range of temperatures. The work included the determination of acoustic impedance, adiabatic compressibility, free length, and analysis of viscosity data with the Jones-Dole relation. Examination of parameter variations with concentration and temperature revealed the occurrence of significant interactions, which suggests structural modification in the solution medium.

Singh et al. (2015) [57] carried out experimental determinations of densities and sound velocities for solutions of sucrose with ammonium-based protic ionic liquids. From these measurements, various acoustical and volumetric properties were obtained. The results indicated strong ionic liquid-sucrose interactions, where the hydrogen bonding and electrostatic effects contributed to enhanced solute hydration and structural organization in the

solutions.

Haghani et al. (2016) [58] investigated the density and viscosities of selected amino- acids in sodium benzoate mixtures using a Ubbelohde viscometer and an oscillating U-tube density meter. Several parameters were derived from the density results. The results indicated significant interactions between the amino acids and sodium benzoate.

Kulkarni and Khadke (2016) [59] measured density, ultrasonic velocity, and viscosity of PVF in acetone and DMF at 300 K using a specific gravity bottle, ultrasonic interferometer, and Ostwald viscometer. From these measurements, adiabatic compressibility, ultrasonic attenuation, and relaxation time were calculated. The study revealed molecular interactions amongst the solutes and solvents in the liquid systems.

Bhattacharya et al. (2016) [60] employed density and ultrasonic measurements to assess the apparent molar volumes and isentropic compressions of the amphiphilic drugs amantadine hydrochloride and semicarbazide hydrochloride in aqueous solutions. For the binary drug solutions, critical micelle concentration along with thermodynamic functions such as free energy, enthalpy, and micellization parameters were obtained. The variation of these properties with temperature reflected the presence of solute-solute as well as drug-water interactions.

Pal et al. (2016) [61] investigated volumetric and ultrasonic characteristics of ionic liquids with 1,2-propanediol. From density and sound speed results, excess molar volumes and deviations in isentropic compressions were derived. The Redlich-Kister relation was employed for the representation of excess functions. Molecular interactions, particularly those involving hydroxyl groups in the mixtures, were further examined through Fourier transform infrared spectroscopy.

Marczyk et al. (2016) [62] assessed the lipid barrier of skin in patients with acne vulgaris after treatment with lactobionic acid, corundum microdermabrasion and their combined application. The results demonstrated a marked decrease in sebum secretion across all treatments. The most pronounced effect was observed for lactobionic acid, which acted as an exfoliant and showed structural features analogous to alpha-hydroxy acids.

Nayeem et al. (2016) [63] evaluated density and ultrasonic speed data for the mixture of benzyl

benzoate with ethyl acetate. A pycnometer and an interferometer operated at 2 MHz were employed for the measurements. Several thermodynamic parameters such as excess acoustic impedance, compressibilities, Lennard-Jones potential and relative association, were derived from the experimental results. The analysis of these properties revealed the type of significant intermolecular interactions (dipole-dipole) within the system.

Dhondge et al. (2017) [64] reported densities and viscosities measurements for dilute systems of sodium L-ascorbates, thiamine and pyridoxine hydrochloride, and at three different temperatures. From density data, apparent molar volumes, expansivities, and thermal expansion coefficients were obtained. Viscosity results were analyzed with the Jones-Dole relation to derive coefficients and hydration numbers. Free energy, entropy, and enthalpy of activation were also determined through the B-coefficient. The variations in these parameters highlighted the occurrence of molecular interactions amid solute and solvent molecules.

Mehrdad et al. (2017) [65] studied the role of ionic liquids in modifying the thermo-dynamic and transport characteristics of L(+)-lactic acid in polyethylene glycol media. They determined the density, sound velocity, and viscosity of L(+)-lactic acid in polyethylene glycol with 1-octyl-3-methylimidazolium bromide over the temperature ranges. Using these experimental measurements, they calculated apparent molar volumes, transfer molar volumes, apparent molar isentropic compressions, and viscosity B-coefficients. The interpretation of these parameters provided insight into the interactions. The study concluded that the presence of ionic liquids weakened solute-solvent interactions and this weakening effect became more pronounced with greater ionic liquid concentration, longer alkyl chain length and higher temperature.

Banipal et al. (2017) [66] evaluated standard partial molar volumes for a range of sugars, and sugar alcohols in thiamine hydrochloride and pyridoxine hydrochloride solutions at diverse concentrations and temperatures. Transfer volumes, expansibilities, apparent molar properties were also calculated to interpret solvation behavior and taste responses. Complementary UV-Vis absorption studies were carried out in the same solutions and compared with previous results on L-ascorbic acid. The influence of stereochemistry on hydration patterns was emphasized.

Hnedkovsky et al. (2017) [67] measured densities of sodium benzoate and acetate at 323.15-

573.15 K and 10 MPa using vibrating tube densimetry. Apparent molar volumes showed a steep decrease at high temperatures with acetate ions smaller than benzoate which reflects ion hydrophobicity. Volume changes for neutralization reactions were similar for both salts and varied with temperature which expands the high-temperature volumetric database.

Kumar et al. (2017) [68] studied densities, sound speeds, and viscosities of L-alanine and L-phenylalanine in citric acid medium. Using the obtained data, parameters such as molar volumes, compressibilities, and intermolecular free lengths were derived. The findings demonstrated notable solute-solvent interactions, which suggest the role of both hydrophilic and hydrophobic groups in governing molecular association in thee studied systems.

Prabhu and Venis (2018) [69] examined density, viscosity and ultrasonic speed data for systems of methyl benzoate with chlorobenzene and benzaldehyde. The specific gravity bottle method and a viscometer were used for the measurements. Deviations in free length, impedance, and intermolecular free volume were derived from the investigated data. Excess thermodynamic functions were fitted to the R-K relation to attain interaction parameters. The results pointed to dipole-dipole type associations, particularly between methyl benzoate and benzaldehyde.

Kaur et al. (2018) [70] examined polyethylene glycols in aqueous solutions through density and sound speed determinations. From these measurements, thermo-acoustical parameters along with expansibilities and their derivatives were obtained. The outcomes suggested the occurrence of strong solute-solvent associations due to H_2 bonds among the OH groups of glycols and water molecules.

Khatun et al. (2018) [71] investigated aqueous solutions of urea and thiourea in the temperature variation of 298.15 K-323.15 K using volumetric and ultrasonic velocity techniques. Apparent molar volumes and adiabatic compressibilities were obtained along with limiting values. The analysis revealed distinct differences between urea and thiourea which exhibited stronger solute-solvent interactions and a greater tendency to disrupt the structural order of water.

Nagarjuna and Babu (2018) [72] studied mixtures of benzyl benzoate with 1-butanol at numerous temperatures using the interferometer method at 2 MHz, Ostwald viscometer, and specific gravity bottle. Thermoacoustic quantities, including excess molar volume, free length,

Gibbs free energy, and isentropic compressions were calculated from the measured results. The excess molar volumes were fitted to the R-K relation to provide interaction parameters. The results indicated a significant association between unlike molecules through dipolar and dispersive forces.

Olivieri et al. (2018) [73] assessed lactobionic acid as an additive for artificial tears through in vitro and in vivo models. The study showed that lactobionic acid, either alone or in combination with hyaluronic acid, exhibited protective effects in the WH test. In rabbit corneas, the addition of 4 % lactobionic acid with 0.15 % hyaluronic acid reduced the rise of MMP-9 and TGF-β in tears and corneal tissue. Furthermore, 4% lactobionic acid slows down the growth of bacterial isolates in culture which confirms its therapeutic potential.

Jyothirmai et al. (2018) [74] measured density and sound speed for systems of methyl benzoate with dimethyl carbonate at atmospheric pressure using a pycnometer and an interferometer. Lennard-Jones potential and relative association values were obtained from the results. The data were compared with predictions from Peng-Robinson and Soave-Redlich-Kwong equations of state as well as topological models. Thermodynamic potential derivatives were also calculated. The findings confirmed close agreement between experimental and theoretical values, supporting the reliability of the derived interaction parameters.

Kaur et al. (2018) [75] determined densities and sound speeds for EG, DEG, and TEG glycols in glycerol aqueous media. From density data, volumetric properties were obtained and from ultrasonic results, acoustical parameters were evaluated. The study revealed stronger solute-solvent interactions and highlighted the influence of hydroxyl groups on hydration patterns.

Kantikosum et al. (2019) [76] evaluated the efficacy of cosmeceutical products containing glycolic and salicylic acids in patients with mild-to-moderate acne vulgaris. Lactic acid, licochalcone A, and gluconolactone were applied as adjuncts to adapalene therapy. The study showed that combining cosmeceuticals with adapalene did not improve therapeutic outcomes compared to adapalene alone, but also reduced adverse effects.

Tyczyńska et al. (2019) [77] investigated a binary mixture of N, N-dimethylformamide with 1-propanol across the entire composition range. The experimental work included the determination of density, sound velocity, and specific heat capacity at different compositions.

Several derived thermodynamic and acoustic properties were evaluated from the measured data. The analysis suggested distinct deviations in physicochemical parameters, which indicated strong solute-solvent interactions. The results suggested that hydrogen bonding and dipole-dipole forces contributed to structural rearrangements within the mixture.

Cardoso et al. (2019) [78] reviewed the production methods, patents, regulatory aspects, and applications of lactobionic acid in the food sector. The analysis highlighted challenges in integrating LBA into food products and identified potential areas for future research.

Rajbanshi et al. (2019) [79] examined inter-molecular interactions of sodium benzoate and salicylate in solutions containing benzyl triethylammonium chloride or benzyl trimethylammonium chloride. The study revealed that these preservatives act synergistically, enhance antibacterial and antifungal activity and reduce the potential harmful effects of excessive preservative intake.

Arsule et al. (2019) [80] examined the density and ultrasonic velocity of acetylsalicylic acid solutions at fixed temperatures and concentrations in relation to varying amino acid levels. Thermo-acoustic parameters were derived. The results indicated that acetylsalicylic acid significantly influenced the hydration and interaction of amino acids. These findings confirm that solute composition strongly affects amino acid solvation and molecular arrangement.

Chen et al. (2020) [81] evaluated the density, viscosity, sound speed, and refractive index of methyl benzoate with 1-propanol, 1-butanol, and ethanol. Excess parameters and isentropic compressibilities revealed moderate molecular interactions between the ester and alcohol molecules. The study indicates that intermolecular forces play a key role in determining mixture properties.

Ashima et al. (2020) [82] studied ethylene and propylene glycol interactions with sodium ethylparaben at various temperatures. Partial molar volumes and compressibilities were calculated, which demonstrates the tendency of solutes to modify solution structure. These results highlight the impact of solute addition on structural behavior and molecular packing.

Ashima et al. (2020) [83] investigated PEG-200 and 600 in sodium methyl p-hydroxybenzoate at 25 ºC. Acoustic impedance, adiabatic compressibility, intermolecular free length and

attenuation were derived. Results indicated that PEG chain length affected molecular packing and solution rigidity. The observations show that polymer size influences both structural stability and acoustic properties.

Nagarjuna et al. (2020) [84] measured the density and sound speed of ethyl 4-hydroxybenzoate solutions between 303 K and 313 K. Thermodynamic and acoustical properties calculated via the R-K equation, alongside IR and FT-IR data, confirmed hydrogen-bond formation and structural ordering. This study demonstrates that hydrogen bonding governs structural arrangements in these solutions.

Venkatesan et al. (2020) [85] determined viscosities and densities of diisopropyl ether with methyl/ethyl benzoates and benzyl acetate using a bicapillary pycnometer and an Ostwald viscometer. Excess parameters and R-K coefficients showed significant solute-solvent interaction, especially at higher concentrations. This indicates that molecular interactions increase with concentration and influence the mixture properties.

Thakur et al. (2020) [86] measured sound velocities and densities of EG and PG in methanolic mixtures of propyl P-hydroxybenzoate at varied temperatures and constant pressure. Apparent and partial molar parameters were inferred and the analysis of ternary mixtures at different compositions and temperatures provided insights into intermolecular interactions.

Kaur et al. (2021) [87] measured the ρ and c of saccharides in cefadroxil solutions at various temperatures. Molecular docking analysis suggested specific stereochemical OH group interactions that altered solute hydration and transfer properties. These findings confirm that stereochemistry strongly affects solvation and solution behavior.

Brinzei et al. (2021) [88] provided experimental evidence on the density and viscosity of L-serine and valine in sodium chloride systems. The study covered a variety of temperatures and concentrations of the electrolyte. Analysis of the experimental data allowed the determination of derived thermodynamic and transport parameters, which served as indicators of interactions inside the mixtures. The outcomes demonstrated the ability of the mixtures to promote either structure formation and disruption.

Amirchand et al. (2021) [89] investigated saccharides in aqueous calcium salt solutions at two

temperatures. Volumetric analysis revealed predominant hydrophobic interactions and evidence of hydrophobic-ionic association via NMR. The study demonstrates that hydrophobic interactions govern structural arrangement in these systems.

Richu et al. (2021) [90] studied thiamine hydrochloride and L-ascorbic acid in binary and ionic liquid media at six temperature ranges. Cosphere overlap analysis highlighted solute-solvent structuring and stabilizing interactions. The results indicate that ionic environments strongly influence molecular arrangement and interactions.

Chakraborty et al. (2021) [91] examined Vitamin B3, water, and polyethylene glycol ternary solutions. Various thermo-acoustical parameters, along with empirical constants, were evaluated which indicate enhanced solvation and molecular interactions. The data confirm that ternary mixtures promote structured solvation and complex molecular interactions.

Bandral et al. (2022) [92] studied glycine and glycylglycine in aqueous betaine hydrochloride. Derived volumetric, compressibility, and rheological parameters demonstrated solute-solvent interactions and altered hydration numbers. The observations indicate that zwitterionic interactions play a significant role in solution structure.

Rajput et al. (2022) [93] carried out a study on nucleosides in aqueous ascorbic acid under different thermal conditions using DSA 5000 M with a rolling ball viscometer. The investigation yielded values of apparent and partial molar properties, transfer parameters, relative viscosity, and hydration number. Viscosity coefficients were also evaluated and the analysis clarified the solvation behavior as well as the dominant intermolecular interactions in the solutions.

Dhal et al. (2022) [94] evaluated the viscosity and density of glutamic acid in water with sodium benzoate and potassium glutamate at various concentrations and temperatures. Densities and viscosities were used to determine volumetric parameters and interaction coefficients. FTIR spectra were also scrutinized to evaluate OH-stretch behavior. Results suggested that solute combinations lead to the disruption of intermolecular structures and alter hydration patterns.

Masilo et al. (2022) [95] investigated binary systems of acetophenone with the acids (acetic and propionic) by measuring density, sound speed, refractive index, and surface tension over

293.15-333.15 K and 0.1 MPa. Thermodynamic parameters derived from these measurements, as a function of acetophenone mole fraction, revealed strong molecular interactions dominated by hydrogen bonding and dipole-dipole forces within the mixtures.

Galvao et al. (2022) [96] analyzed kinematic viscosity in aqueous binary systems containing malonic, maleic, malic, tartaric, and citric acids across 303.2-363.2 K and concentrations up to 3.0 $mol.kg^{-1}$. They applied the Eyring equation with the UNIFAC model to evaluate thermodynamic parameters and predict transport behavior. The results showed that viscosity arises with solute size and solution molar mass, which confirmed strong molecular interaction effects. The proposed model reproduced the experimental data with good accuracy, which demonstrated its suitability for property correlation in such systems.

Sharma et al. (2022) [97] investigated the properties of D-maltose and D-lactose in trisodium citrate within the temperature range from 293.15 to 313.15 K. The study involved the determination of apparent molar volumes and isentropic compressions from investigational results of densities and sound velocities. The findings indicated notable variations in intermolecular interactions within the ternary systems and the evaluation of Hepler's constant established the structure-breaking tendency of the solutes.

Dhal et al. (2022) [98] reported the sound velocity, density, specific conductance and viscosity of glutamic acid in solutions containing sodium benzoate. Using these measurements, volumetric (apparent and partial molar volume), acoustic impedance, internal pressure, and relative association were determined. The study revealed strong ionic-hydrophilic interactions, which confirms that carboxylate ions significantly influence molecular association.

Amirchand et al. (2023) [99] conducted a comprehensive physicochemical analysis to explore the interactional behavior of L-ascorbic acid in aqueous L-histidine solutions. The study revealed the existence of strong hydrophilic-ionic interactions, which suggested that ascorbic acid molecules establish significant associations with the ionizable groups of L-histidine. Such interactions indicate an enhanced solvation tendency of ascorbic acid in the studied medium. The findings provide deeper insights into the solvation dynamics of ascorbic acid, which contributes to a better understanding of its stability, compatibility, and functional role in food formulations where amino acids and vitamins coexist.

Dhal et al. (2023) [100] carried out an investigation on the densities, velocities, and viscosities of aspartic (AA) acid in combination with sodium benzoate and ammonium acetates under constant temperature conditions. The experimental data were further utilized to derive several acoustic and thermodynamic properties, such as acoustic impedance, surface tension, and both isothermal and isentropic compressibilities, which provide valuable insights into the nature of intermolecular interactions present in the system.

Kaur et al. (2023) [101] carried out an analysis of the ρ and of chloroxylenol-methanol systems in glycols at several temperatures and concentrations. From the collected data, several properties were derived to assess the inter-molecular interactions within the structure. The outcomes demonstrated noticeable variations in these properties with changes in temperature and pressure, which indicates strong molecular associations and structural modifications in the medium. The results confirmed that glycols exhibit significant interaction with chloroxylenol-methanol mixtures, thereby influencing the overall solution behavior and stability.

Nagarjuna et al. (2023) [102] conducted a study on para-methoxy benzoic acid with different amides by determining sound velocity, viscosity, and density through interferometer, specific gravity bottle, and viscometer techniques at 2 MHz frequency. From the experimental data, several thermoacoustic parameters such as surface tension, acoustic impedance, partial molar volumes, and excess functions were obtained. The results showed marked variations in these parameters, which reflected significant interactions in the mixtures.

Chinnarao et al. (2023) [103] examined sonic velocities of binary mixes of benzyl benzoate and geranyl acetate at 2 MHz frequency to explore molecular interactions in the liquid state. The R-K polynomial equation was applied to the experimental results to evaluate acoustical and thermodynamic properties, which deviated from ideal mixing behavior. The study also confirmed antibacterial activity of both the pure compounds and their mixtures, thus providing additional practical importance of the work.

Lamba et al. (2024) [104] used the “Density meter” to obtain densities and sound speeds of PEG 200/400 in tetrasodium EDTA solutions. Resulting parameters, including apparent and partial molar properties, transfer values, compressibilities, and expansibilities revealed strong solute-solvent interactions, dipole-dipole, hydrophilic and ionic-hydrophilic forces. The results also showed that molecular association became more pronounced with temperature rise and higher

solute molality.

Sirohi et al. (2024) [105] applied Flory's statistical theory (FST) to estimate ultrasonic speed, density, and other thermophysical parameters from the investigated results for eight binary mixtures of ionic liquids with water between 288.15 and 308.15 K. The predicted values of measured statistics matched well with literature findings, which confirmed the validity of FST. A comparison of internal pressure values obtained through FST and the standard thermodynamic approach showed close agreement. The variation of parameters with concentration and temperature revealed dominant A-A type interactions in water-rich regions, which demonstrated the strength of solute-solvent association.

Singh et al. (2024) [106] examined the thermophysical behavior of dimethyl sulfoxide (DMSO), dimethylacetamide (DMA), and dimethylformamide (DMF), along with their binary mixtures across 298-318 K at 1 atm. Measurements of density, ultrasonic velocity, and viscosity allowed the derivation of parameters such as relaxation time, acoustic impedance, enthalpy, Gibbs free energy, internal pressure, Rao's and Wada's constants. Incorporation of DMA and DMF into DMSO caused structural modification through variations in hydrogen bonding, free volume, and relaxation time. Increased constants indicated denser molecular packing, while reduced internal pressure reflected weaker intermolecular forces and enhanced thermodynamic stability.

Kaur et al. (2024) [107] investigated the physicochemical behavior of 2-methoxy/ethoxyethanol dissolved in aqueous inositol over a range of concentrations and numerous temperatures. Measurement of density, velocity, and spectroscopic features were performed at four temperatures between 288.15 and 318.15 K. Apparent and partial molar quantities as well as expansibilities and its thermal derivatives were evaluated to understand interactions from these data. Additional FTIR spectra of inositol-water systems revealed the presence of hydrophilic-hydrophilic interactions.

Bhakri et al. (2024) [108] studied aqueous mixtures of PEG-200 and 400 with lactobionic acid at a range of concentrations and temperatures. Measurements of ρ and c were utilized to determine apparent and partial molar volumes, transfer characteristics, interaction coefficients along with isentropic compressibilities. Spectroscopic analysis further identified bond types and structural features in the mixtures. The outcomes highlighted strong interactions and

concentration-dependent structural changes in the liquid systems.

Pradhan et al. (2024) [109] investigated interactions between L-glutamic acid and arabinose or D-xylose using ultrasonic speed measurements and FTIR spectroscopy. The study revealed strong ion-solvent interactions indicated by acoustic parameters and extensive intermolecular hydrogen bonding confirmed by the FTIR spectra. These findings provide insights into solvation dynamics and hydrogen bonding with implications for biochemistry, pharmacology, food chemistry, and molecular interactions in aqueous systems.

Kumar et al. (2024) [110] analyzed the interaction of the antidiabetic drug metformin hydrochloride with water and aqueous dulcitol solutions by volumetric, ultrasonic, conductometric, and spectroscopic methods. Density, molar conductance, and sound velocity were measured at four temperatures to calculate partial molar volumes, adiabatic compressibility, transfer volumes, Walden's product, and other thermodynamic parameters. The results showed strong MF-MF and MF-solvent associations, and Walden's product confirmed the structure-forming character of MF in the systems. UV-visible spectra further supported these results through higher intensity and shifted absorption maxima that indicate drug-solvent association.

Das et al. (2024) [111] synthesized protic ionic liquids with triethylenetetramine as cation and carboxylic acids as anions. Structural characterization and purity confirmation were carried out through ^{1}H and ^{13}C NMR together with ESI-MS analysis. Density, viscosity, refractive indices, and sound speed were measured from 293.15-333.15 K, along with thermal stability and water content. From these data, parameters such as expansion coefficient, standard entropy, molar volume, lattice potential energy, activation energy, and free volume were derived. Refractive index measurements enabled the evaluation of electronic polarizability and free volume, while COSMO-RS calculations provided further interpretation of the structure-property relationship of the synthesized PILs.

Wang et al. (2025) [112] investigated the thermodynamic properties and intermolecular hydrogen transfer behavior in binary mixtures of 1,2-propanediol and diethylenetriamine. Experimental determinations of density, sound velocity, and viscosity demonstrated pronounced bonds within the hydroxyl groups of 1,2-PD and the amino groups of DETA, which resulted in non-ideal mixing patterns. Analysis of excess and apparent molar volumes

and viscosity deviations substantiated the presence of intermolecular hydrogen linkages. DFT analyses characterized optimized structures and possible pathways that established a concerted hydrogen transfer mechanism. These outcomes contributed to a deeper understanding of hydrogen transfer between alcohols and amines and supplied useful information for the rational design of materials with tailored physicochemical properties for industrial and scientific purposes.

Nain et al. (2025) [113] studied binary mixtures of PEG 200 with methyl and ethyl methacrylate through density and sound speed measurements at 293.15-323.15 K and 100 kPa. Derived excess and partial molar properties indicated stronger PEG-methacrylate interactions for methyl than ethyl. Scaled particle theory and FTIR results supported the experimental observations.

Sharma et al. (2025) [114] reported thermophysical properties of binary systems of 1,8-cineole with glycol ethers at 293.15-323.15 K and 0.1 MPa. Excess molar volume, isentropic compressibility deviation, acoustic impedance deviation, viscosity deviation, and excess Gibbs free energy of activation were derived and correlated with the Redlich-Kister equation. Negative V_mE for DEGMBE and positive values for DEGMEE and TEGMME indicated stronger specific interactions in DEGMBE and weaker forces in the other systems. These factors emphasized structural effects, confirmed the hydrogen bonding and supported the volumetric results. The findings hold significance for extraction processes, pharmaceutical formulations, and fuel combustion simulations.

Shahvarpour et al. (2025) [115] investigated acetophenone mixtures with chlorinated ethanes and ethenes. Density, sound velocity, and refractive index were measured, and excess molar volume and refractive index functions were derived and correlated with the Werblan relation. The results indicated that excess molar volumes were negative except for acetophenone + 1,2-dichloroethane, which showed positive values, whereas acetophenone with tetrachloroethene showed sign inversion. These outcomes suggested a shift in intermolecular interactions.

Gandikota et al. (2025) [116] reported that volumetric, acoustic, and computational analyses of GABA in aqueous medium at numerous concentration levels and temperatures confirmed significant hydrogen bond interactions. Quantum chemical calculations under PCM and IEEPCM models were performed to evaluate the hydrogen bond strength and dipole moment.

Temperature and concentration influenced the extent of molecular interaction. These findings offered insight into the structural and thermodynamic behavior of GABA in water.

From the above studies, it is evident that previous research can be broadly classified into three main themes: (i) fundamental investigations on ultrasonic velocity, density, and thermodynamic properties of liquid systems; (ii) volumetric and acoustic studies of binary and ternary liquid mixtures to understand intermolecular interactions; and (iii) investigations on benzoate derivatives, hydroxy acids, and their physicochemical as well as practical applications. These studies provide an important foundation for understanding molecular interactions in aqueous systems and support the present investigation.

References

1. R.J. Urick, J. Appl. Phys. 18, 983 (1947).
2. B.B. Koodriavtsev, J. Acoust. Soc. Am. 28, 771 (1956).
3. G.G. Hammes and W. Knoche, J. Chem. Phys. 45, 4041 (1966).
4. J.E. Desnoyers, R. Pagé, G. Perron, J.-L. Fortier, P.-A. Leduc, and R.F. Platford, Can. J. Chem. 51, 2129 (1973).
5. N. Prasad, O. Prakash, S. Singh, and S. Prakash, Ultrasonics. 16, 77 (1978).
6. A. Zaghloul, Talanta 45, 189 (1997).
7. T. Wakabayashi and K. Takaizumi, J. Solution Chem. 11, 565 (1982).
8. A. Apelblat, J. Chem. Thermodyn. 18, 351 (1986).
9. E. Siimer, M. Kurvits, and A. Köstner, Thermochim. Acta 116, 249 (1987).
10. K. Juni and M. Nakano, Crit. Rev. Ther. Drug Carrier Syst. 3, 209 (1987).
11. K. Chowdoji Rao, S. Venkata Naidu, and A. Varada Rajulu, Eur. Polym. J. 26, 657 (1990).
12. T.M. Aminabhavi, H.T.S. Phayde, R.S. Khinnavar, B. Gopalakrishna, and K.C. Hansen, J. Chem. Eng. Data 39, 251 (1994).
13. S. Magazù, P. Migliardo, A.M. Musolino, and M.T. Sciortino, J. Phys. Chem. B 101, 2348 (1997).
14. A. Ali, S. Hyder, and A.K. Nain, J. Mol. Liq. 79, 89 (1999).

15. S.J. Yun, S.K. Kang, and S.S. Yun, Thermochim. Acta 331, 13 (1999).

16. J.S. Matos, J.L. Trenzado, E. González, and R. Alcalde, Fluid Ph. Equilib. 186, 207 (2001).

17. M. Chitra, B. Subramanyam, and V.R.K. Murthy, Mol. Phys. 99, 1569 (2001).

18. B. García, R. Alcalde, S. Aparicio, and J.M. Leal, Ind. Eng. Chem. Res. 41, 4399 (2002).

19. W.V. Steele, R.D. Chirico, A.B. Cowell, S.E. Knipmeyer, and A. Nguyen, J. Chem. Eng. Data 47, 667 (2002).

20. J. Vartiainen, E. Skytta, J. Enqvist, and R. Ahvenainen, Packag. Technol. Sci. 16, 223 (2003).

21. S. Li, J. Yu, and R. Lin, J. Solution Chem. 32, 1065 (2003).

22. W. Xie, L. Trevani, and P.R. Tremaine, J. Chem. Thermodyn. 36, 127 (2004).

23. Z. Yan, J. Wang, W. Kong, and J. Lu, Fluid Ph. Equilib. 215, 143 (2004).

24. P. Resa, L. Elvira, F. Montero De Espinosa, and Y. Gómez-Ullate, Ultrasonics. 43, 247 (2005).

25. R.J. Sengwa, Madhvi, and S. Sankhla, Phys. Chem. Liq. 44, 637 (2006).

26. B. Minofar, P. Jungwirth, M.R. Das, W. Kunz, and S. Mahiuddin, J. Phys. Chem. C 111, 8242 (2007).

27. J.A. Widegren and J.W. Magee, J. Chem. Eng. Data 52, 2331 (2007).

28. Hafiz-ur-Rehman and M. Shahid Ansari, J. Chem. Eng. Data 53, 2072 (2008).

29. B.A. Green, R.J. Yu, and E.J. Van Scott, Clin. Dermatol. 27, 495 (2009).

30. M.V. Rathnam, S. Mohite, and M.S. Kumar, J. Chem. Eng. Data 54, 305 (2009).

31. M. Tasic-Kostov, S. Savic, M. Lukic, S. Tamburic, M. Pavlovic, and G. Vuleta, J. Cosmet. Dermatol. 9, 3 (2010).

32. A. Kornhauser, CCID 135 (2010).

33. S.J. Kharat, Int. J. Thermophys. 31, 585 (2010).

34. M.V. Rathnam, S. Mankumare, and M.S.S. Kumar, J. Chem. Eng. Data 55, 1354 (2010).

35. A. Przybyła, M. Chorążewski, E. Zorębski, and W. Marczak, Int. J. Thermophys. 32, 852 (2011).

36. N.J. Madhuri, P.S. Naidu, J. Glory, and K.R. Prasad, J. Chem. 8, 457 (2011).

37. M.J. Dávila, R. Alcalde, and S. Aparicio, J. Chem. Thermodyn. 43, 1017 (2011).

38. F. Suárez and C.M. Romero, J. Chem. Eng. Data 56, 1778 (2011).

39. T.M. Mohan, S.S. Sastry, and V.R.K. Murthy, J. Solution Chem. 40, 131 (2011).

40. A. Kornhauser, S.G. Coelho, and V.J. Hearing, Dermatol. Res. Pract. 2012, 1 (2012).

41. S. Parveen, S. Singh, D. Shukla, M. Yasmin, M. Gupta, and J.P. Shukla, J. Solution Chem. 41, 156 (2012).

42. M.V. Rathnam, R.T. Sayed, K.R. Bhanushali, and M.S.S. Kumar, J. Mol. Liq. 166, 9 (2012).

43. U.G. Pathak, J.V. Patel, and P.H. Parsania, J. Solution Chem. 41, 755 (2012).

44. M.M. Papari, H. Ghodrati, F. Fadaei, R. Sadeghi, S. Behrouz, M.N.S. Rad, and J. Moghadasi, J. Mol. Liq. 180, 121 (2013).

45. B. Nagarjun, A.V. Sarma, G.V.R. Rao, and C. Rambabu, J. Thermodyn. 2013, 1 (2013).

46. A. Pal, H. Kumar, R. Maan, and H.K. Sharma, J. Solution Chem. 42, 1988 (2013).

47. A.K. Nain, R. Pal, and Neetu, J. Chem. Thermodyn. 64, 172 (2013).

48. M.V. Rathnam, D.R. Ambavadekar, and M. Nandini, J. Thermodyn. 2013, 1 (2013).

49. S. Sreehari Sastry, S. Babu, T. Vishwam, K. Parvateesam, and Ha. Sie Tiong, Phys. Rev. B. Condens. Matter. 420, 40 (2013).

50. D. Vijayalakshmi, C. Narasimha Rao, M. Gowrisankar, K. Sivakumar, and P. Venkateswarlu, J. Mol. Liq. 197, 272 (2014).

51. I. Bahadur, S. Singh, N. Deenadayalu, P. Naidoo, and D. Ramjugernath, Thermochim. Acta 590, 151 (2014).

52. S.S. Sastry, S. Babu, T. Vishwam, and H.S. Tiong, J. Therm. Anal. Calorim. 116, 923 (2014).

53. I. Bahadur, N. Deenadayalu, P. Naidoo, and D. Ramjugernath, J. Solution Chem. 43, 787 (2014).

54. S. Chauhan, L. Pathania, K. Sharma, and G. Kumar, J. Mol. Liq. 212, 656 (2015).

55. M. Lalikoğlu, A. Gök, M.K. Gök, and Y.S. Aşçı, J. Chem. Eng. Data 60, 3159 (2015).

56. D.S. Choudhary, C.A. Ladole, and A.S. Aswar, Proc. Natl. Acad. Sci., India, Sect. A Phys. Sci. 85, 221 (2015).

57. V. Singh, P.K. Chhotaray, and R.L. Gardas, J. Chem. Thermodyn. 89, 60 (2015).

58. A. Haghani, H. Iloukhani, and M.M. Hoffmann, J. Chem. Eng. Data 61, 2960 (2016).

59. S.S. Kulkarni and U.V. Khadke, Indian J. Materi. Sci. 2016, 1 (2016).

60. D.M. Bhattacharya, U.R. Pratap, A.V. Wankhade, and S.P. Zodape, J. Mol. Liq. 214, 117 (2016).

61. A. Pal, M. Saini, and B. Kumar, Fluid Ph. Equilib. 411, 66 (2016).

62. B. Marczyk, P. Mucha, H. Rotsztejn, and E. Budzisz, JCDSA 06, 156 (2016).

63. Sk.M. Nayeem, Sk. Nyamathulla, I. Khan, and D.K. Rao, J. Mol. Liq. 218, 676 (2016).

64. S.S. Dhondge, P.N. Dahasahasra, L.J. Paliwal, Vijay.M. Tangde, and D.W. Deshmukh, J. Chem. Thermodyn. 107, 189 (2017).

65. A. Mehrdad, H. Shekaari, and N. Noorani, Fluid Ph. Equilib. 440, 77 (2017).

66. P.K. Banipal, M. Sharma, and T.S. Banipal, Food Chem. 237, 181 (2017).

67. L. Hnedkovsky, P.M. May, and G. Hefter, J. Chem. Thermodyn. 109, 100 (2017).

68. D. Kumar, S.K. Lomesh, and V. Nathan, J. Mol. Liq. 247, 75 (2017).

69. P. Prabhu and A.R. Venis, Asian J. Chem. 30, 1759 (2018).

70. K. Kaur, K.C. Juglan, and H. Kumar, J. Chem. Thermodyn. 127, 8 (2018).

71. R. Khatun, R. Sultana, and R. K. Nath, Orient. J. Chem. 34, 1755 (2018).

72. A. Nagarjuna and Shaik. Babu, Mater. Today Proc. 5, 26322 (2018).

73. M. Olivieri, M. Cristaldi, S. Pezzino, G. Lupo, C.D. Anfuso, C. Gagliano, C. Genovese, and D. Rusciano, Cornea 37, 1058 (2018).

74. G. Jyothirmai, Sk.Md. Nayeem, I. Khan, and Ch. Anjaneyulu, J. Therm. Anal. Calorim. 132, 693 (2018).

75. K. Kaur, I. Behal, K.C. Juglan, and H. Kumar, J. Chem. Thermodyn. 125, 93 (2018).

76. K. Kantikosum, Y. Chongpison, N. Chottawornsak, and P. Asawanonda, CCID Volume 12, 151 (2019).

77. M. Tyczyńska, M. Jóźwiak, M. Komudzińska, and T. Majak, J. Mol. Liq. 290, 111124 (2019).

78. T. Cardoso, C. Marques, J.L.A. Dagostin, and M.L. Masson, J. Food Sci. 84, 1672 (2019).

79. B. Rajbanshi, K. Das, K. Lepcha, S. Das, D. Roy, M. Kundu, and M.N. Roy, J. Mol. Liq. 282, 415 (2019).

80. A.D. Arsule, R.T. Sawale, and S.D. Deosarkar, J. Mol. Liq. 275, 478 (2019).

81. T. Chen, X. Feng, Y. Yin, and Y. Xu, J. Solution Chem. 49, 1402 (2020).

82. Ashima, K.C. Juglan, and H. Kumar, Res. Chem. 2, 100049 (2020).

83. A. Thakur, K.C. Juglan, and H. Kumar, J. Phys.: Conf. Ser. 1531, 012018 (2020).

84. A. Nagarjuna and S. Babu, Chem. Data Coll. 26, 100347 (2020).

85. D. Venkatesan, D.J. Amarnath, and K. Saravanakumar, Russ. J. Phys. Chem. 94, 1573 (2020).

86. A. Thakur, K.C. Juglan, H. Kumar, and K. Kaur, Phys. Chem. Liq. 58, 803 (2020).

87. K. Kaur, S. Arti, T.K. Ghosh, T.S. Banipal, and P.K. Banipal, J. Chem. Thermodyn. 159, 106477 (2021).

88. M. Brinzei and O. Ciocirlan, J. Chem. Thermodyn. 154, 106335 (2021).

89. K.D. Amirchand, S. Kaur, T.S. Banipal, and V. Singh, J. Mol. Liq. 334, 116077 (2021).

90. Richu and A. Kumar, J. Chem. Eng. Data 66, 3859 (2021).

91. N. Chakraborty, M. Lamba, K.C. Juglan, and H. Kumar, J. Phys.: Conf. Ser. 2267, 012134 (2022).

92. A. Bandral, Richu, and A. Kumar, J. Mol. Liq. 348, 118081 (2022).

93. P. Rajput, H. Singh, and A. Kumar, J. Chem. Thermodyn. 171, 106805 (2022).

94. K. Dhal, S. Singh, and M. Talukdar, J. Mol. Liq. 361, 119578 (2022).

95. K. Masilo and I. Bahadur, J. Chem. Thermodyn. 166, 106667 (2022).

96. A.C. Galvão, A.L.L. Savoldi, P.F. Arce, and W.D.S. Robazza, J. Chem. Eng. Data 67, 2052 (2022).

97. P. Sharma, S. Sharma, and M. Sharma, Chem. Thermodyn. Therm. Analy. 6, 100051 (2022).

98. K. Dhal, S. Singh, and M. Talukdar, J. Mol. Liq. 368, 120761 (2022).

99. K. Deepika Amirchand, T.S. Banipal, Y.-L. Yang, and V. Singh, J. Mol. Liq. 370, 120839 (2023).

100. K. Dhal, P. Das, S. Singh, and M. Talukdar, J. Mol. Liq. 376, 121413 (2023).

101. P. Kaur, K.C. Juglan, H. Kumar, and M. Singla, Braz. J. Chem. Eng. 40, 1213 (2023).

102. A. Nagarjuna, S. Babu, and M. Gowrisankar, Int. J. Amb. Ener. 43, 1974 (2022).

103. D. Chinnarao, C.V. Padmarao, C. Beena, M. Srilatha, M.V.V. Ramanjaneyulu, P. Choppara, N. Murali, and B.V. Rao, J. Indian Chem. Soc. 100, 100969 (2023).

104. M. Lamba, N. Chakraborty, K.C. Juglan, R. Sharma, and M. Singla, J. Chem. Eng. Data 69, 171 (2024).

105. A. Sirohi, A. Upmanyu, P. Kumar, M. Dhiman, K.C. Juglan, D.P. Singh, K.K. Saxena, A. Bhadauria, and M.I. Haque Siddiqui, ACS Omega 9, 19363 (2024).

106. P. Singh, Veneeta, and K. Kaur, J. Mol. Liq. 415, 126286 (2024).

107. H. Kaur, N. Chakraborty, and K.C. Juglan, J. Chem. Eng. Data 69, 2461 (2024).

108. K. Bhakri, M. Lamba, K.C. Juglan, and N. Chakraborty, J. Mol. Liq. 406, 125117 (2024).

109. R.K. Pradhan and S. Singh, J. Mol. Liq. 412, 125790 (2024).

110. I. Kumar, S.K. Lomesh, D. Singh, P. Kumar, P. Ahir, and S. Kumar, J. Mol. Liq. 396, 124089 (2024).

111. I. Das, K. Rama Swami, and R.L. Gardas, J. Chem. Thermodyn. 194, 107288 (2024).

112. Y. Wang, J. Zhang, H. Zhang, X. Zheng, X. Zhang, X. Zhao, and L. Zhang, J. Mol. Liq. 432, 127846 (2025).

113. A. Kumar Nain, Nidhi, and N. Chaudhary, J. Chem. Thermodyn. 200, 107358 (2025).

114. C. Sharma, U. Syal, A. Bakshi, and M. Sharma, J. Chem. Eng. Data 70, 694 (2025).

115. S. Shahvarpour, H. Iloukhani, and K. Khanlarzadeh, J. Solution Chem. 54, 141 (2025).

116. R. Gandikota and T. Vishwam, J. Chem. Thermodyn. 201, 107404 (2025).

Research Gap

After the thorough review of the literature on ultrasonic techniques, numerous studies on the physicochemical properties of Benzoic acid derivatives with esters, ethers, glycols, alpha-amino acids, etc., in various combinations at various temperatures has been conducted. However, no studies specifically focusing on the physicochemical properties of combinations of benzoic acid derivatives with carboxylic acids by ultrasonic methods have been reported. There is a research gap in understanding how carboxylic acids interact with solvents and affect their volumetric and acoustic properties. Studying the behaviour of carboxylic acids and benzoic acid derivatives, and their impact on the volumetric and acoustic properties of solutions will contribute to our understanding of the physicochemical behaviour of pharmaceuticals, cosmetics and food systems, aid in the development of pharmaceutical formulations, and have potential implications and product quality. Carboxylic acids are organic compounds containing the carboxyl functional group. Low molecular weight carboxylic acids are generally soluble in water due to hydrogen bonding with water molecules, whereas the solubility decreases with increasing hydrocarbon chain length. They are used as intermediates in chemical synthesis, components in the production of pharmaceuticals, flavors, and fragrances, as well as in the manufacture of polymers, plastics, and textiles. On the other hand, selected Benzoic acid derivatives are extremely soluble in water. Benzoic acid is a white crystalline compound. Its derivatives and salts are often used in industries such as food additives, cosmetics, and pharmaceuticals. Some common applications include their use as preservatives in food and cosmetics, as intermediates in the production of dyes and pigments, and as components in pharmaceuticals and personal care products. Additionally, they can be used as plasticizers, perfumery compounds, and in the synthesis of other chemicals. Sodium Benzoate, Potassium Benzoate, and Sodium methyl parahydroxy benzoate are examples of Benzoic acid derivatives. Benzoic acid derivatives and carboxylic acids can enhance the preservative effect while also adjusting the pH and solubility of the formulation. This combination helps extend the shelf life of products and maintain their quality.

CHAPTER 3

OBJECTIVES AND EXPERIMENTAL PROCEDURES

3.1 Objectives of the research

The selection of benzoic acid derivatives and carboxylic acids as the solvent–solute systems is based on their ability to exhibit significant intermolecular interactions such as hydrogen bonding and ion–dipole interactions in aqueous media. Investigation of these systems over a range of temperatures enables the study of temperature dependence of thermo-acoustic parameters and provides valuable insight into solute–solvent interactions. In order to systematically investigate these aspects, the following objectives were formulated for the present research.

I. To find the density, ultrasonic velocity of mixtures of benzoic acid derivatives with carboxylic acids at different temperatures and concentrations.
II. To calculate various thermodynamical and acoustical parameters such as apparent molar isentropic compression, temperature dependent partial molar volume, partial molar isentropic compression, apparent molar volume, pair and triplet interaction coefficient, partial molar volume of transfer, partial molar volume from the experimental values of density and speed of sound.
III. To study the molecular interactions by analysing thermo-acoustic parameters in liquid solution of carboxylic acids in benzoic acid derivatives.

3.2 Experimental Procedure

The densities and ultrasonic velocities of mixtures of water-soluble benzoic acid derivatives with carboxylic acids at different concentrations and temperatures were measured using an Anton Paar DSA 5000 M density and sound velocity analyzer.

3.2.1 Chemicals

The investigational work utilized three benzoic acid derivatives, namely sodium benzoate, potassium benzoate, and sodium methyl para-hydroxybenzoate, in addition to a series of organic acids, including lactobionic acid, glycolic acid, tartaric acid, lactic acid, malic acid, and butyric acid. The molecular weights of the selected compounds were as follows: (benzoic acid derivatives) [144.11, 160.21, and 174.13] $g \cdot mol^{-1}$,

(organic acids) [358.296, 76.05, 150.087, 90.08, 134.09, and 88.11] $g \cdot mol^{-1}$. Solutions of benzoic acid derivatives were prepared in triple-distilled water to obtain the required solvent systems. Prior to experimentation, all samples were purified through vacuum drying and stored in desiccators containing P_2O_5 for 48 hours to ensure stability.

3.2.2 Measurements

The densities and sound velocities of the ternary systems were determined via "Anton-Paar DSA 5000 M" instrument under controlled conditions. Measurements were performed at an applied frequency of 3 MHz and an ambient pressure of 0.1 MPa. The apparatus is equipped with a highly precise thermostat capable of regulating the temperature within $\pm$0.001 K. Experiments were carried out over the temperature range 288.15 K to 318.15 K. Prior to each measurement cycle, the apparatus was calibrated, followed by the manufacturer's recommendations with dry air, deionized water, and double-distilled water as standards. After calibration, the system ensures highly reliable determinations of solution properties. Samples were carefully introduced into the measuring cell with a syringe to avoid contamination or bubble formation. Solutions of required molalities were prepared with a Sartorius CPA 225 D balance, accurate to $\pm$0.00001 g. After the consideration of the purity of the chemicals used, the relative uncertainty in molality was estimated as $u_r(m) = 0.01$. From these experimental observations, the variation in physicochemical properties with temperature was analyzed which provides insights into solute-solvent interactions within the mixtures. For this study, different compositions that contain benzoic acid derivatives and organic acids were systematically prepared and examined to evaluate their behavior upon mixing. The details of the experimental systems investigated are summarized in **Table 3.1**.

Table 3.1 Investigation of different problems during the research.

Section -I	
Problem-1	
Study of glycolic and lactobionic acids in water-soluble sodium benzoate solutions: an acoustic and thermodynamic approaches	
Solvent	**Solutes**

Water + Sodium Benzoate +	Glycolic Acid (GA) Lactobionic Acid (LBA)
Problem-2	
Analysis of molecular interactions of an aqueous benzoates with glycolic and lactic acid: spectroscopic, acoustic and volumetric approach	
Solvent	**Solutes**
Water + Sodium methyl para-hydroxybenzoate +	Glycolic Acid (GA) Lactic Acid (LA)
Section -II	
Problem-3	
Volumetric and ultrasonic investigation of glycolic and malic acids with water-soluble potassium benzoate solutions at different temperatures	
Solvent	**Solutes**
Water + Potassium Benzoate +	Glycolic Acid (GA) Malic Acid (MA)
Problem-4	
Investigating interactions of alpha-hydroxy acids with sodium benzoate for advanced formulation and translational applications: An ultrasonic approach	
Solvent	**Solutes**
Water + Sodium Benzoate +	Lactic Acid (LA) Malic Acid (MA)
Section-III	
Problem-5	
Molecular interactions of butyric and L (+)- lactic acids in water-soluble potassium benzoate solutions: An acoustic and thermodynamic study	
Solvent	**Solutes**
Water + Potassium Benzoate +	Butyric Acid(BA) Lactic Acid (LA)
Problem-6	
Acoustic and volumetric analysis of malic and tartaric acids in aqueous medium of sodium methyl p-hydroxybenzoate from 288.15 K to 318.15	

Solvent	Solutes
Water + Sodium methyl para-hydroxybenzoate +	Malic Acid(MA) Tartaric Acid (TA)
Section-IV	
Problem-7	
Thermodynamic analysis of tartaric and lactobionic acids with aqueous potassium benzoate mixtures through volumetric and acoustic methods	
Solvent	**Solutes**
Water + Potassium Benzoate +	Tartaric Acid (TA) Lactobionic Acid (LBA)
Problem-8	
Exploration of intermolecular interactions of butyric and tartaric acids with sodium benzoate in aqueous medium	
Solvent	**Solutes**
Water + Sodium Benzoate +	Butyric Acid (BA) Tartaric Acid (TA)

3.3 Chemical structures

The structural specifications of the compounds utilized in the research are summarized in the following table.

Table 3.2 List of chemicals used and their structures.

Sodium Benzoate	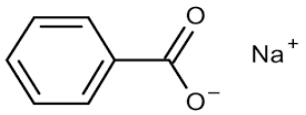
Potassium Benzoate	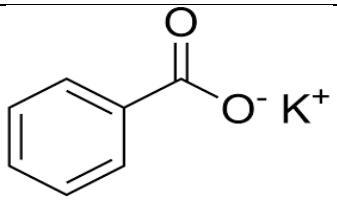

Sodium Methyl Para-Hydroxy Benzoate	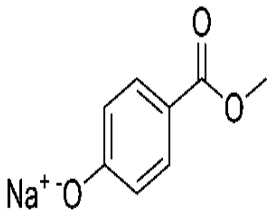
Lactobionic Acid	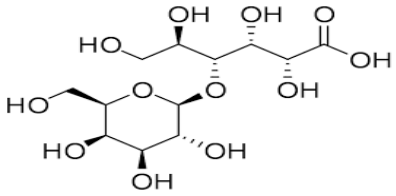
Glycolic Acid	
Tartaric Acid	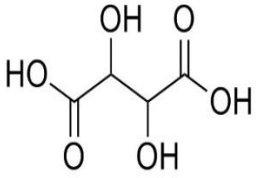
Lactic Acid	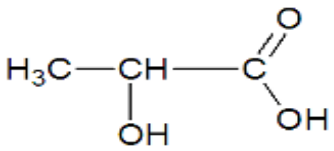
Malic Acid	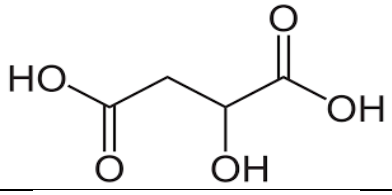
Butyric Acid	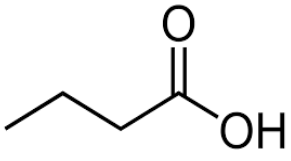

3.4 Specifications of the Chemicals used

The following table outlines the details of the compounds incorporated in the present research.

Table 3.3 Detailed description of the compounds used in this investigation.

S.No.	Compound	CAS Number	Molar mass ($g \cdot mol^{-1}$)	Source	Purification method	Mass fraction purity(supplier)	Appearance
1.	Sodium Benzoate	532-32-1	144.11	Central Drug House (P) Ltd.	Vacuum dried	≥ 0.99	White crystalline powder
2.	Potassium Benzoate	582-25-2	160.21	Central Drug House (P) Ltd.	Vacuum dried	≥0.99	White crystalline powder
3.	Sodium Methyl Para-Hydroxy Benzoate	5026-62-0	174.13	Central Drug House (P) Ltd.	Vacuum dried	≥ 0.99	White crystalline powder
4.	Lactobionic Acid	96-82-2	358.296	Tokyo Chemical Industry Co. Ltd.	Vacuum dried	≥0.99	White crystalline powder

5.	Glycolic Acid	79-14-1	76.05	Central Drug House (P) Ltd.	Vacuum dried	≥0.99	Pale yellow, clear liquid
6.	Tartaric Acid	87-69-4	150.087	Loba Chemie Pvt. Ltd. India	Vacuum dried	≥0.99	White crystalline powder
7.	Lactic Acid	50-21-5	90.08	Central Drug House (P) Ltd.	Vacuum dried	≥0.99	Colorless liquid
8.	Malic Acid	6915-15-7	134.09	Central Drug House (P) . Ltd.	Vacuum dried	≥0.99	White crystalline powder
9.	Butyric Acid	107-92-6	88.11	Central Drug House (P) Ltd.	Vacuum dried	≥0.99	Colorless (viscous) liquid

3.5 Experimental methods and preparations

The problems addressed in the research are summarized in **Table 3.1**. The chemicals selected for the present investigation are summarized in **Table 3.2** which illustrates their molecular structures, while detailed specifications including CAS registry number, physical appearance and purity as reported by the supplier are provided in **Table 3.3**. All experimental solutions were made using freshly attained triply-distilled, degassed water with a 10^{-6} $S \cdot cm^{-1}$ of specific conductance. Accurate measuring of the samples was carried out on a Sartorius "CPA 225D" analytical balance (exactness ± 0.00001 g), as shown in **Figure 3.1**. The solutions were carefully kept in sealed borosilicate glass vials to prevent external contaminants and moisture absorption. The freshly prepared samples were introduced directly into the measuring apparatus using a syringe to minimize the effect of storage time and ensure reproducibility and reliability of the experimental measurements.

Figure 3.1 Sartorius (Model CPA225D) analytical balance and prepared solutions in airtight borosilicate glass vials.

3.5.1. Density and Sound Velocity Analyzer (DSA) 5000M

The determination of densities and sound speeds was performed using the "DSA 5000 M" for aqueous solutions of Benzoic Acid Derivatives, specifically sodium benzoate, potassium benzoate, and sodium methyl para-hydroxybenzoate. In addition, measurements were performed for their mixtures with a range of the organic acids, including lactobionic acid (LBA), glycolic acid (GA), tartaric acid (TA), lactic acid (LA), malic acid (MA), and butyric acid (BA). For each measurement, approximately 3 ml of the prepared solution was

carefully transferred from the storage vial into the borosilicate U-tube of the instrument using a syringe. The loading of the sample could be visually monitored on the display panel of the Density and sound velocity analyzer, as illustrated in **Figure 3.2**.

Figure 3.2 Density and Sound Velocity Meter

The instrument automatically records the density and velocity of sound of the solution and retains the data in its memory. The analyzer comprises measurement cells, such as a U-tube cell for density determination, a pulse-echo arrangement for ultrasonic velocity measurement, and an integrated Pt 100 thermometer, as shown in **Figure 3.3**. Together, these components allow the simultaneous estimation of the two independent variables-density and sound velocity using a single experimental sample.

3.5.2 Working Principle

❖ **Density measurement**

The instrument operates on Anton Paar's oscillating U-tube principle for the determination of density. A borosilicate glass U-tube serves as the fundamental element for density determination. Electrical excitation induces oscillations in the U-tube, where the frequency is a function of the sample's density. Once oscillation is stabilized, excitation is halted and the natural decay of oscillation is recorded. This Pulsed Excitation Method enables correction for

viscosity effects, identification of entrapped air bubbles or particles.

- **Sound velocity measurement**

  Sound velocity is obtained using a pair of piezoelectric transducers: one functions as a transmitter and the other as a receiver, positioned across a fixed-length measuring chamber. One transducer emits ultrasonic pulses at a 3 MHz frequency, while the second transducer detects the transmitted pulses and records the travel time. The sound velocity is then calculated directly from the relation between distance and time which ensures reliable and reproducible values.

- **Temperature regulation**

  Both the density and sound velocity measuring cells are equipped with a precisely built-in Peltier thermostat. The Peltier-based regulation system ensures identical temperatures in both measuring cells which eliminates errors caused by thermal fluctuations.

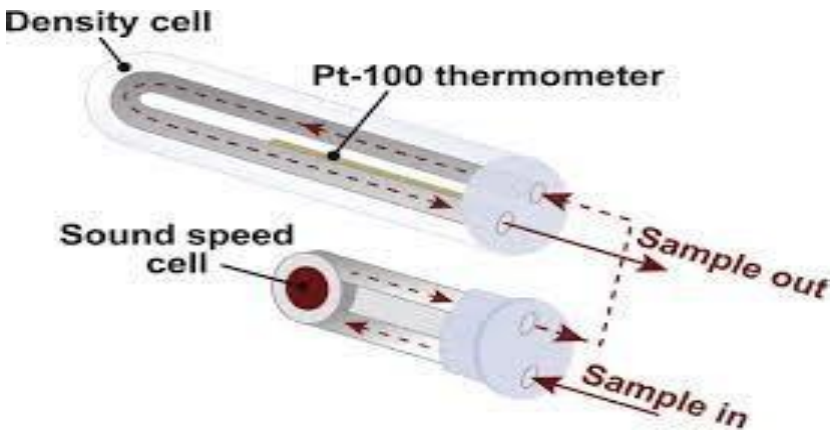

Figure 3.3 Density and sound speed cell of DSA 5000 M

This instrument ensures highly accurate measurements through its advanced temperature regulation system. Both measuring cells, constructed from stainless steel are equipped with an integrated thermostat that maintains thermal stability during operation. Temperature is monitored by two Pt 100 Platinum resistance thermometers in combination with Peltier elements, achieving a control precision of ±0.001 K. The DSA is equipped with two distinct cells for the determination

of density and sound speed. The instrument operates on the principle of the oscillating U-tube, where the solution is injected into a U-shaped borosilicate cell that resonates at a natural frequency; the frequency shift, dependent on the sample's density which is mathematically converted into a density value. Sound velocity is measured with an ultrasonic transducer, in which a transmitter sends waves through the sample and a receiver detects the travel time which enables precise sound velocity calculation.

3.6 Reliability of Measurements and Significance of the Study

The measured densities and sound velocities of water obtained during calibration were in excellent agreement with previously reported standard values, which further validates the reliability and precision of the instrument for experimental studies. The calibration, cleaning and sample insertion processes follow a standardized five-step protocol, as depicted in **Figure 3.4**. Prior to each measurement cycle, a daily water check was performed and if unsuccessful, an air/water adjustment was applied after cleaning. Calibration of the equipment was performed with double-distilled, as well as air at varying temperatures to avoid bubbles which ensures accuracy and reproducibility. After every experiment, the measuring cells were thoroughly rinsed with distilled water followed by acetone to ensure accuracy and prevent contamination, while the integrated pump was used to expel any residual liquid from the U-tube. The analyzer is capable of detecting variations in pressure from 0 to 0.3 MPa, measures sound velocities within 1000 to 2000 $m \cdot s^{-1}$, and determines densities from 0 to 3 $g \cdot cm^{-3}$.

Such studies provide valuable physicochemical data for interpreting molecular interactions and are useful in designing stable formulations in pharmaceutical, food, and cosmetic industries.

The present study is expected to provide a detailed understanding of the thermo-acoustic behaviour of benzoic acid derivatives in aqueous solutions of carboxylic acids. Through the systematic evaluation of density and ultrasonic velocity data, various volumetric and acoustical parameters are anticipated to reveal the nature and strength of solute–solvent interactions in the investigated ternary systems. The study is also expected to identify the dominant interaction mechanisms such as hydrogen bonding, ion–hydrophilic, and dipole–dipole interactions governing the structural organization of the solutions. Furthermore, the findings are expected to contribute valuable physicochemical data that may support the design and optimization of stable formulations in pharmaceutical, cosmetic, and food preservation applications.

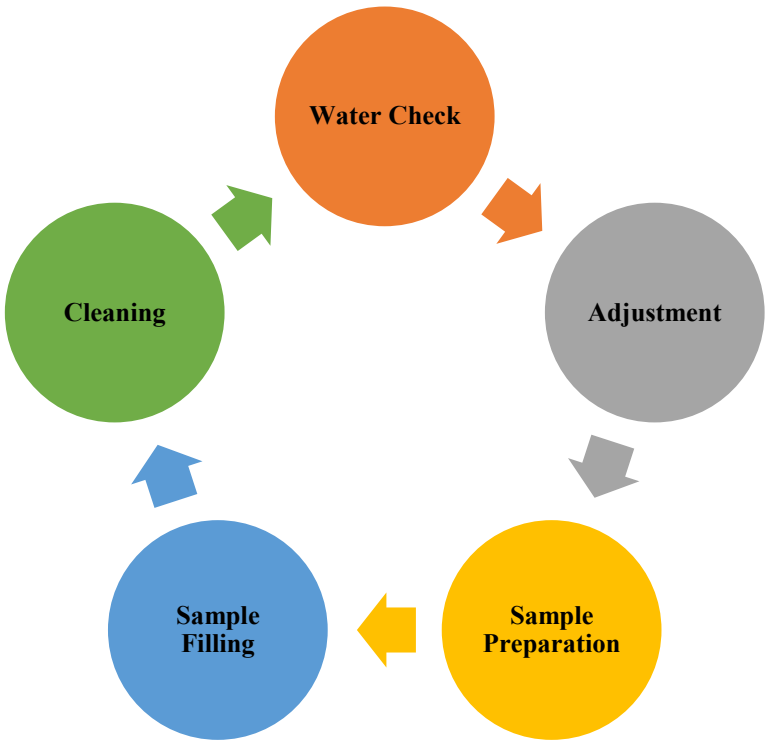

Figure 3.4 Five key features for precise measurement of the density and sound velocity.

3.7 Apparent molar and Partial molar parameters

3.7.1 Apparent molar volume (AMV)

The concept of **AMV** is employed to describe the volumetric contribution of a solute when dissolved in a solvent. It represents the differences between the molar volume of the pure solvent and that of the solution containing one mole of solute. This parameter reflects the variations in the physical characteristics of the medium upon solute addition and, therefore, is regarded as a characteristic property of the solution rather than the pure solvent. The AMV is quantitatively evaluated with the following relation:

$$V_\phi = M/\rho - (\rho - \rho_0)/m_A\rho\rho_0 \qquad (7)$$

3.7.2 Partial molar volume (PMV)

The **PMV** is a fundamental thermodynamical property that quantifies the change in the total volume of a solution when an infinitesimal amount of a solute is added, while maintained a constant temperature, pressure, and overall composition of the system. In other words, it represents the contribution of a

single mole of a component to the total volume of the solution. Owing to its sensitivity to solute and solvent interactions, PMV serves as a key parameter for understanding the structural and interactional behavior of liquid mixtures. To determine the V_ϕ^0, the experimental data of V_ϕ were analyzed using the least-squares fitting procedure.

$$V_\phi = V_\phi^0 + S_V^* m_A \quad (8)$$

3.7.3 Partial molar volume of transfer

This concept serves as a key thermodynamic parameter for examining solute-solvent interactions within a mixture. It provides insight into how the solute's partial molar volume changes when the solvent composition is altered, such as transitioning from a pure solvent to a mixed solvent system, while minimizing the influence of solute-solute interactions. This approach enables both qualitative and quantitative evaluation of solvation effects. For organic acids, the determination of transfer characteristics of partial molar volumes at infinite dilution from water to Benzoic acid derivatives solutions can be achieved with the relation:

$$\Delta V_\phi^0 = V_\phi^0(\text{in aqueous benzoic Acid Derivatives}) - V_\phi^0(\text{water}) \quad (9)$$

3.7.4 Effect of temperature on partial molar volume

This parameter of a solute offers a quantitative indication of how its molar volumes varies with temperature. This parameter is of considerable significance, as it governs the extent to which solute-solvent interactions are altered under thermal conditions. Consequently, it provides a crucial insight into the compressibility of the solution, the dynamics of solvation, and the overall structural organization of the liquid mixture.

$$V_\phi^0 = a + b(T - T_{ref}) + c(T - T_{ref})^2 \quad (10)$$

3.7.5 Apparent molar isentropic compressibility

When a solute is introduced into a solvent, its influence on the compressibility of the medium under adiabatic conditions is described by this parameter. This thermodynamic quantity offers an understanding of how the solute influences

the compressibility of the solution, which reflects the nature and strength of interactions. The term isentropic refers to processes that occur at constant entropy, which implies the absence of heat exchange with the surroundings.

$$K_{\phi,S} = (Mk_S/\rho) - \{(k_{S,0}\rho - k_S\rho_0)/m_A\rho\rho_0\} \quad (11)$$

In this context, "Isentropic compressibility" is a fundamental thermodynamic characteristic that describes the response of a system to pressure variations under conditions of constant entropy. It can be evaluated through the application of the following mathematical expression:

$$k_S = 1/c^2\rho \quad (12)$$

3.7.6 Partial molar isentropic compressibility

The concept of "**partial molar isentropic compression**" refers to the individual contribution of a solute or solvent component to the overall isentropic compressibility of a multicomponent system under constant entropy conditions. This parameter is particularly significant as it offers a quantifiable measure of the specific role played by each constituent in determining the compressional behavior of the solution. Moreover, it serves as an important indicator for understanding the elastic nature of the solution and enables a deeper knowledge of solute-solvent associations on a molecular basis.

$$K_{\phi,s} = K^0_{\phi,S} + S^*_K m_A \quad (13)$$

3.7.7 Partial molar isentropic compression of transfer

This transfer property of organic acids with the aqueous medium of the investigated preservative system were evaluated at infinite dilution. The calculations were performed using the standard thermodynamic relation, which enables the assessment of solute contributions to the solution's compressibility under isentropic conditions.

$\Delta K^0_{\phi,S}$= $K^0_{\phi,S}$(in aqueous benzoic Acid Derivatives)- $K^0_{\phi,S}$(in water) (14)

3.7.8 Interaction coefficients

The **transfer properties** (ΔV_{ϕ}^{0},ΔK_{ϕ}^{0}) from water to aqueous Benzoic Acid Derivatives (BAD) solutions were evaluated using the following relations:

$$\Delta V_{\phi}^{0}(\text{water to aqueous chemical sample solution}) = 2V_{AB}m_B + 3V_{ABB}{m_B}^2 \quad (15)$$

$$\Delta K_{\phi}^{0}(\text{water to aqueous chemical sample solution}) = 2K_{AB}m_B + 3K_{ABB}{m_B}^2 \quad (16)$$

Here, component A represents the organic acids (solutes), while component B corresponds to the benzoic acid derivatives. The term m_B denotes the molality of the aqueous derivatives of the benzoic acid solution. The coefficients V_{AB} and K_{AB} signify the **pairwise interaction parameters** for volume and isentropic compression, respectively, whereas V_{ABB} and K_{ABB} account for the corresponding **triplet interaction parameters**.

CHAPTER 4
RESULTS AND DISCUSSION
Section I
Problem 1

4.1 Title: "Study of glycolic and lactobionic acids in water-soluble sodium benzoate solutions: an acoustic and thermodynamic approaches"

In this section, the experimental determination of density and sound speed was conducted for glycolic acid (GA) and lactobionic acid (LBA) in aqueous sodium benzoate at (0.1, 0.4, and 0.7) mol·kg^{-1}.

4.1.1 Measurement of Densities

The calculation process involved density measurements to derive several volumetric properties. The densities of glycolic and lactobionic acids in sodium benzoate solution were tested at four distinct temperatures: (288.15K to 318.15K). The densities of sodium benzoate in water closely align with the literature as shown in **Figure 4.1** [1-3]**.** The obtained readings demonstrate that the density values surge as the molality of carboxylic acids in the aqueous sodium benzoate solution rises and decreases as the temperature escalates, which has been included in **Table 4.1**. The rise in the molecular weight of the solution primarily causes the escalation in the density data as the molality of GA/LBA increases. It is abundantly clear upon analysis of the graph that the density values are consistently in coherence with the reported data and exhibit the same pattern across various temperatures along with concentrations of sodium benzoate.

4.1.2 Apparent molar volume

The densities of (GA/LBA+ water + SB) are experimentally tested at four different temperatures employed in this research.

To ascertain the ($V_{\emptyset}$), the density results may be utilized by applying the equation as follows:

$$V_{\phi} = \left\{\left(\frac{M}{\rho}\right) - \left[\frac{(\rho-\rho_0)}{(m_A \rho \rho_0)}\right]\right\} \quad (4.1)$$

where the variable 'M' implies the molecular mass of the solutes, ρ_0, and ρ indicates the densities of the pure solvent and the solution, and 'm_A' denotes the molality of the glycolic acid/lactobionic acid per kg sodium benzoate, indicating the total amount of carboxylic acids (GA/LBA) per kg of (SB+water) solvent. The V_{ϕ} of glycolic acid/lactobionic acid in (sodium benzoate + water) has been determined at a variety of

temperatures. The information shown in **Table 4.1** suggests that when the concentration of sodium benzoate (SB) increases, there is a corresponding rise in V_ϕ with the escalation in temperature along with the molality of carboxylic acids, suggesting stronger associations within the molecules of the solute-solvent. This trend becomes more evident as the molecular mass upsurges from glycolic acid to lactobionic acid, suggesting enhanced molecular associations, as illustrated in **Figure 4.2. Figure 4.3** vividly illustrates the graphical representation of the liquid system. Moreover, the V_ϕ values that are positive suggest more intense solute-solvent interactions, which elevate from glycolic acid to lactobionic acid at different temperatures. As concentration rises, solute and solvent interactions diminish water molecule's electrostriction, leading to an upsurge in apparent molar volume [4,5] .

Table 4.1 Data of densities 'ρ', and apparent molar volume 'V_ϕ' were found in the liquid system of sodium benzoate solution with glycolic and lactobionic acids.

Molality m_A/ (mol·kg^{-1})	$\rho \times 10^{-3}$/(kg·m^{-3})				$V_\phi \times 10^{6}$/(m^3·mol^{-1})			
	288.15K	298.15K	308.15 K	318.15 K	288.15K	298.15K	308.15K	318.15 K
			0.0 (mol·kg^{-1}) Sodium Benzoate + Glycolic Acid					
0.00000	0.99926	0.99705	0.99404	0.99036				
0.10004	1.00126	0.99896	0.99588	0.99214	55.96	56.98	57.83	58.57
0.19904	1.00308	1.00069	0.99754	0.99374	56.69	57.67	58.49	59.26
0.30994	1.00485	1.00242	0.99919	0.99533	57.71	58.54	59.38	60.14
0.40849	1.00629	1.00380	1.00050	0.99662	58.46	59.26	60.11	60.77
0.50487	1.00755	1.00495	1.00165	0.99771	59.18	60.05	60.79	61.49
			0.1 (mol·kg^{-1}) Sodium Benzoate + Glycolic Acid					
0.00000	1.00517	1.00237	0.99877	0.99517				
0.10105	1.00707	1.00418	1.00051	0.99684	56.95	57.98	58.81	59.62
0.20499	1.00882	1.00585	1.00212	0.99840	57.83	58.76	59.58	60.31
0.29155	1.01014	1.00710	1.00331	0.99954	58.51	59.44	60.26	61.03
0.39865	1.01158	1.00848	1.00462	1.00082	59.37	60.26	61.07	61.75
0.50379	1.01282	1.00965	1.00579	1.00191	60.18	61.05	61.75	62.48
			0.4 (mol·kg^{-1}) Sodium Benzoate + Glycolic Acid					
0.00000	1.02212	1.01893	1.01481	1.01097				
0.10100	1.02386	1.02059	1.01638	1.01248	57.85	58.69	59.73	60.53
0.20918	1.02550	1.02214	1.01789	1.01393	58.74	59.68	60.46	61.22
0.29944	1.02672	1.02329	1.01898	1.01493	59.42	60.34	61.16	62.05
0.40174	1.02786	1.02437	1.02002	1.01598	60.38	61.27	62.02	62.71
0.49998	1.02885	1.02528	1.02094	1.01680	61.11	62.01	62.65	63.45
			0.7 (mol·kg^{-1}) Sodium Benzoate + Glycolic Acid					
0.00000	1.03815	1.03401	1.02962	1.02516				
0.10835	1.03982	1.03561	1.03112	1.02660	58.82	59.65	60.69	61.47

0.20196	1.04107	1.03678	1.03226	1.02767	59.68	60.55	61.38	62.19
0.30857	1.04230	1.03795	1.03334	1.02869	60.53	61.37	62.25	63.08
0.39608	1.04313	1.03871	1.03410	1.02943	61.29	62.16	62.93	63.65
0.50753	1.04405	1.03953	1.03491	1.03014	62.11	63.04	63.71	64.54
0.0 (mol·kg^{-1}) Sodium Benzoate + Lactobionic Acid								
0.00000	0.99926	0.99705	0.99404	0.99036				
0.09680	1.01228	1.00972	1.00646	1.00263	220.98	224.81	227.72	229.66
0.19782	1.02498	1.02206	1.01857	1.01462	222.62	226.51	229.31	231.09
0.29589	1.03645	1.03321	1.02958	1.02549	224.35	228.15	230.65	232.47
0.39959	1.04772	1.04413	1.04043	1.03616	226.13	229.97	232.11	234.11
0.49383	1.05719	1.05332	1.04953	1.04529	227.87	231.66	233.67	235.32
0.1 (mol·kg^{-1}) Sodium Benzoate + Lactobionic Acid								
0.00000	1.00517	1.00237	0.99877	0.99517				
0.10419	1.01888	1.01576	1.01186	1.00809	223.14	226.51	229.83	231.82
0.19155	1.02954	1.02617	1.02206	1.01815	225.09	228.35	231.45	233.49
0.29453	1.04123	1.03755	1.03319	1.02911	227.12	230.47	233.53	235.64
0.39723	1.05193	1.04809	1.04353	1.03923	229.28	232.29	235.24	237.53
0.49377	1.06117	1.05714	1.05240	1.04788	231.31	234.26	237.12	239.56
0.4 (mol·kg^{-1}) Sodium Benzoate + Lactobionic Acid								
0.00000	1.02212	1.01893	1.01481	1.01097				
0.10162	1.03519	1.03170	1.02733	1.02332	224.56	227.72	230.55	232.69
0.19582	1.04640	1.04264	1.03807	1.03390	226.47	229.65	232.38	234.52
0.29255	1.05701	1.05304	1.04830	1.04393	228.58	231.58	234.19	236.45
0.39458	1.06730	1.06307	1.05822	1.05364	230.75	233.76	236.14	238.54
0.49139	1.07629	1.07178	1.06673	1.06218	232.69	235.81	238.27	240.28
0.7 (mol·kg^{-1}) Sodium Benzoate + Lactobionic Acid								
0.00000	1.03815	1.03401	1.02962	1.02516				
0.10275	1.05108	1.04668	1.04203	1.03741	225.59	228.42	231.23	233.25
0.19691	1.06193	1.05734	1.05248	1.04777	227.84	230.51	233.32	235.07
0.29223	1.07204	1.06731	1.06226	1.05737	230.02	232.44	235.19	237.16

0.39881	1.08237	1.07754	1.07220	1.06724	232.34	234.55	237.46	239.29
0.50361	1.09162	1.08662	1.08111	1.07606	234.53	236.75	239.56	241.34

m_A denotes the molality of the glycolic and lactobionic acids in sodium benzoate solution: standard uncertainties are $u_r(m)$ = 0.01; $u(\rho)$=0.00095(g·cm^{-3}); $u(T)$=0.001 K; $u\ (V_\phi)$ = 0.59 × 10^6/(m^3·mol^{-1}).

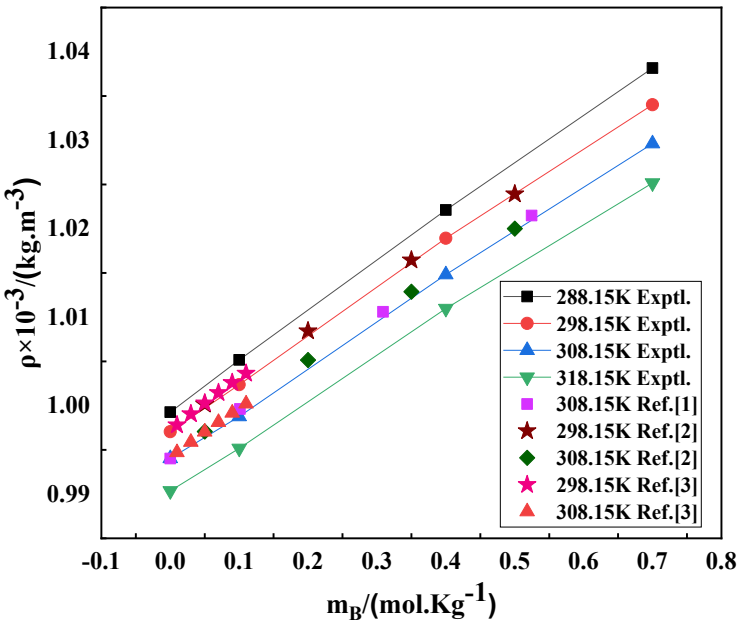

Figure 4.1 The density of aqueous sodium benzoate was presented at several temperatures using experimental and literature results [1–3].

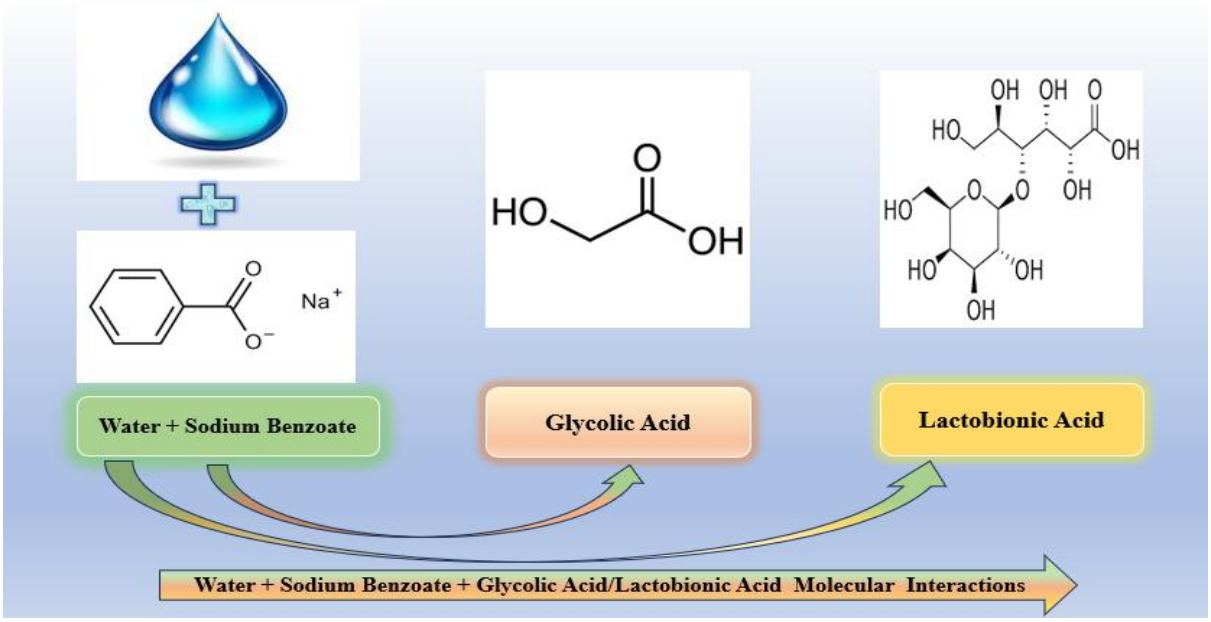

Figure 4.2 Molecular interactions between ternary liquid systems.

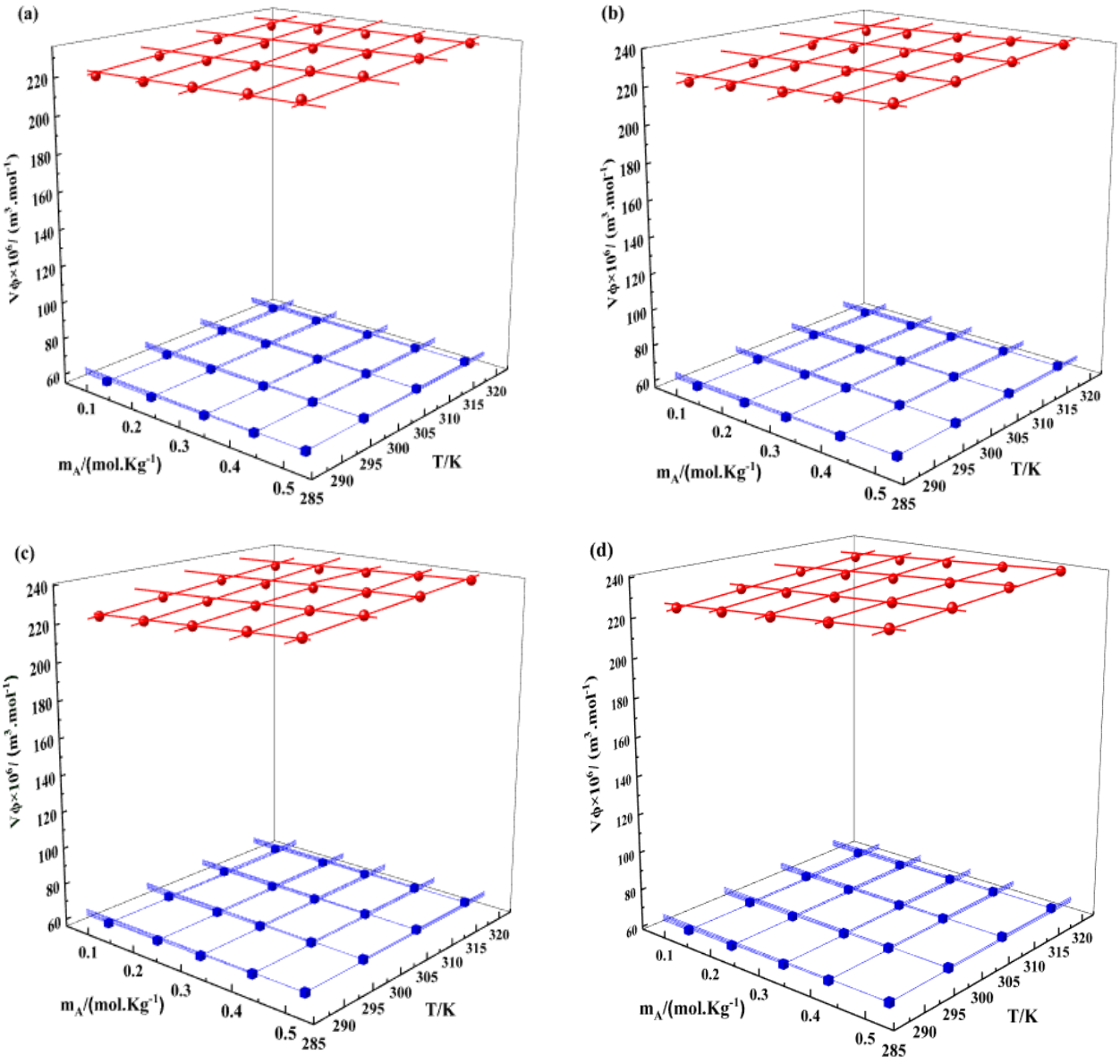

Figure 4.3 Changes in the $V_{\emptyset}$ (apparent molar volume) through three-dimensional plots for (a) 0.0; (b) 0.1; (c) 0.4; (d) 0.7 mol·kg^{-1} for molality of glycolic acid [cube: blue] and lactobionic acid [sphere: red] at several temperatures.

4.1.3 Partial molar volumes

The resulting formula has been utilized to acquire the PMV based on the apparent molar volume ($V_{\emptyset}$):

$$V_{\phi} = V_{\phi}^{0} + S_{V}^{*} m_{A} \quad (4.2)$$

the symbol S_{V}^{*} represents the experimentally derived slope of data, m_{A} represents the molality of GA/LBA. The obtained findings for the partial molar volume ($V_{\emptyset}^{0}$) which are stated in **Table 4.2** with the corresponding standard deviation data (S_{V}^{*}) and associated standard errors.

At all working temperatures for sodium benzoate, the magnitude of S_{V}^{*} has constantly shown a positive value. Consequently, this indicates that the liquid combination that is the focus of the investigation contains a significant presence of solute and solute associations. The absence of consistent trends in S_{V}^{*} data signify that additional factors influence the solute's interactions. This result implies that solute-solvent interactions have a stronger impact on the interactions amongst solute molecules in a solution than solute-solute interactions [6,7].

The $V_{\emptyset}^{0}$ is consistently positive and rises for higher concentrations of sodium benzoate for varying temperatures. This can be ascribed to the extensive solute and solvent interaction, as demonstrated in **Figure 4.4**. Standard partial molar properties, which are temperature-dependent, are employed to ascertain information about the interactions among solvent molecules, as the solute-solute interaction is minimal. In all ternary systems, the solvent molecules encompass and indefinitely separate each solute molecule from the other solute molecules. Accurately determining the limiting partial molar volume is vital for understanding several interactions, namely solute as well as solvent, ion-ion, and ion-solvent [8]. The model of cosphere overlap suggests that the interaction between two groups of ions involves overlapping hydration spheres, leading to a reduction in bulk volume. Additionally, interactions between hydrophobic groups contribute to volume expansion. The positive $V_{\emptyset}^{0}$ value arises owing to the supremacy of ion and hydrophilic interactions, which outweigh the effects of associations within ions and hydrophobic groups [9,10].

Table 4.2 Values of partial molar volume, $'V_{\phi}^{0}'$, and experimental slope, $'S_V^*'$ of sodium benzoate in aqueous glycolic and lactobionic acids.

Molality m_B/ (mol·kg^{-1})	$V_{\phi}^{0} \times 10^{6}$/(m^3·mol^{-1})				$S_V^* \times 10^{6}$ /(m^3·kg·mol^{-2})			
	288.15K	**298.15K**	**308.15K**	**318.15K**	**288.15K**	**298.15K**	**308.15K**	**318.15 K**
				Glycolic Acid				
0.0	55.15(±0.06)	56.19(±0.03)	57.07(±0.03)	57.85(±0.04)	8.06(±0.17)	7.58(±0.10)	7.40(±0.11)	7.21 (±0.11)
0.1	56.17(±0.02)	57.20(±0.01)	58.08(±0.04)	58.89(±0.04)	8.01 (±0.07)	7.65 (±0.03)	7.37 (±0.13)	7.16 (±0.13)
0.4	57.01(±0.05)	57.88(±0.05)	58.95(±0.06)	59.76(±0.07)	8.24 (±0.15)	8.31 (±0.17)	7.47 (±0.18)	7.39 (±0.22)
0.7	57.98(±0.05)	58.78(±0.05)	59.86(±0.04)	60.65(±0.04)	8.24 (±0.17)	8.45 (±0.16)	7.64 (±0.11)	7.66 (±0.13)
				Lactobionic Acid				
0.0	219.24 (±0.06)	223.11(±0.04)	226.31 (±0.09)	228.25 (±0.07)	17.36(±0.20)	17.23(±0.15)	14.76(±0.27)	14.40 (±0.22)
0.1	221.01 (±0.06)	224.53(±0.10)	227.91(±0.09)	229.74 (±0.07)	20.84 (±0.19)	19.73(±0.32)	18.65(±0.28)	19.82(±0.22)
0.4	223.43(±0.04)	225.60 (±0.08)	228.53 (±0.13)	230.72 (±0.08)	20.85 (±0.15)	20.60 (±0.26)	19.49(±0.41)	19.49 (±0.25)
0.7	223.40 (±0.11)	226.37 (±0.07)	229.16 (±0.06)	231.15(±0.07)	22.28 (±0.34)	20.62 (±0.22)	20.72 (±0.20)	20.32(±0.22)

m_B states the molality of water-soluble sodium benzoate: standard uncertainties are $u_r(m) = 0.01$; $u(V_{\phi}^{0}) = 0.38 \times 10^{6}$/(m^3·mol^{-1}); $u(S_V^*) = 1.07 \times 10^{6}$/(m^3·kg·mol^{-2}); $u(T)$=0.001 K.

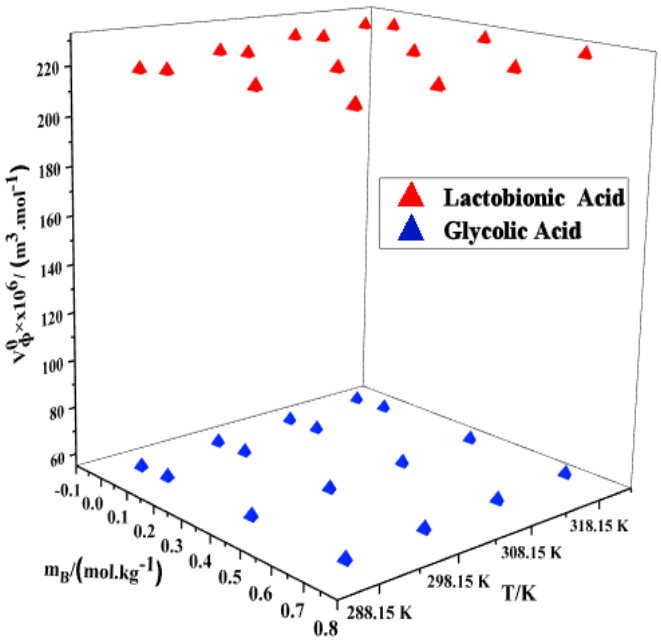

Figure 4.4 The plot illustrates the changes in ($V_\emptyset^0$) for glycolic acid [Blue] and lactobionic acid [Red] in aqueous sodium benzoate solution.

4.1.4 Transfer of partial molar volume

This parameter is used to evaluate the interactions within the solutes and the components of the mixed solvent. The number of solutes that are carried from water to aqueous sodium benzoate (SB) may be acquired by employing the equation as follows:

$$\Delta_{tr}V_{\emptyset}^{0} = V_{\phi}^{0}{}_{(in\ aqueous\ SB)} - V_{\phi}^{0}{}_{(in\ water)} \quad (4.3)$$

The obtained data of $\Delta_{tr}V_{\emptyset}^{0}$ are indicated in **Table 4.3**, which are all positive. The transferability of this property is a fundamental factor in analyzing the characteristics of mixtures as it infers insight into the solute as well as solvent associations. The positive $\Delta_{tr}V_{\emptyset}^{0}$ values may be explained by the occurrence of a solute's capacity to construct or sustain organized compositions due to its solvophobic nature and structural interactions between the two cospheres. A hydrophobic ion is a charged ion with poor water solubility due to its large nonpolar surface or long hydrocarbon chains, making it behave similarly to nonpolar molecules. Unlike typical ions, which are generally hydrophilic and soluble in aqueous solutions due to their charge, hydrophobic ions have a considerable portion of their structure that resists interaction with water molecules [11,12]. On the basis of the co-sphere overlap concept, $\Delta_{tr}V_{\emptyset}^{0}$ are adversely affected by ion-hydrophobic as well as hydrophobic and hydrophobic bonds, while positive values have been attributed to hydrophilic-hydrophilic and ion-hydrophilic groups [13].

Table 4.3 Transfer parameter $\Delta_{tr}V_{\emptyset}^{0}$ of Sodium Benzoate in aqueous glycolic and lactobionic acids solution at several temperatures.

Molality m_B/ (mol·kg^{-1})	**$\Delta_{tr}V_{\emptyset}^{0} \times 10^{6}$/(m^3·mol^{-1})**			
	288.15K	**298.15K**	**308.15K**	**318.15K**
		Glycolic Acid		
0.1	1.02	1.01	1.02	1.04
0.4	1.86	1.69	1.88	1.91
0.7	2.83	2.59	2.80	2.80
		Lactobionic Acid		
0.1	1.77	1.43	1.60	1.48
0.4	3.19	2.50	2.22	2.47
0.7	4.16	3.27	2.85	2.89

m_B states the molality of water-soluble sodium benzoate: standard uncertainties are $u_r(m)$ = 0.01; $u(\Delta_{tr}V_{\emptyset}^{0})$= 0.05×10^6/(m^3·mol^{-1}); $u(T)$=0.001 K.

.

4.1.5 Temperature dependent partial molar volume

Temperature variations are found to have a significant effect on the V_ϕ^0 as illustrated by this method.

$$V_\phi^0 = a^* + b^*\left(T - T_{ref}\right) + c^*\left(T - T_{ref}\right)^2 \tag{4.4}$$

where a^*, b^*, c^* are empirical coefficients for glycolic and lactobionic acids in an aqueous medium of sodium benzoate as recorded in **Table 4.4**. V_ϕ^0 is being investigated with the primary objective of determining the limiting apparent molar expansibility [14,15].

The subsequent equation is applied to acquire the ARD (Average Relative Deviation) values:

$$\sigma = \left(\frac{1}{n}\right)\sum\left[abs\left(\left(Y_{Exptl.} - Y_{calc.}\right)/Y_{Exptl.}\right)\right] \tag{4.5}$$

The computed deviation (σ) is quite tiny and they align precisely with the polynomial's equation. The expression for the $E_\emptyset^0$ (limiting apparent molar expansion), is given by the $\partial V_\emptyset^0/\partial T$ (partial derivatives of the volume in relation to the temperature), evaluated at constant pressure p is considered as the most crucial method for analyzing the interactions between solute along with solvent in a mixture [16]:

$$E_\phi^0 = b^* + 2c^*(T - T_{ref}) \tag{4.6}$$

The findings of limiting apparent molar expansion with $\left(\frac{\partial E_\Phi^0}{\partial T}\right)_P$ for the liquid combination are stated in **Table 4.5**. The positive E_ϕ^0 data support the existence of solute and solvent associations in the examined mixture. The occurrence of the packaging/caging effect may lead to higher $E_\emptyset^0$ data, which further highlights the existence of the interactions [17]. Hepler [18,19] proposed the following thermodynamic model to evaluate whether the solute tends to enhance structure formation or disrupt the structure within the liquid combination:

$$\left(\frac{\partial E_\Phi^0}{\partial T}\right)_P = \left(\frac{\partial^2 V_\phi^0}{\partial T}\right)_P = 2c^* \tag{4.7}$$

The sign of $\left(\frac{\partial E_\Phi^0}{\partial T}\right)_P$ offers an understanding of the solution's potential to either form or disrupt structures [20]. In the present study, Hepler's constant for glycolic and lactobionic acids in water is found to be negative, listed in **Table 4.5,** indicating a structure-breaking behavior in the liquid combination.

Table 4.4 Empirical constants, a^*, b^*, c^* of sodium benzoate solutions with glycolic and lactobionic acids were calculated using equation (4.4) to describe their relationship with molality.

Molality m_B/ (mol·kg^{-1})	**$a^* \times 10^6$/ (m^3·mol^{-1})**	**$b^* \times 10^6$/ (m^3·mol^{-1}·K^{-1})**	**$c^* \times 10^6$/ (m^3·mol^{-1}·K^{-2})**	**R^2**	**ARD**
			Glycolic Acid		
0.1	57.19	0.0963	-0.00058	0.9999	0.0000
0.4	57.95	0.0947	-0.00016	0.9999	0.0000
0.7	58.87	0.0916	-0.00004	0.9999	0.0007
			Lactobionic Acid		
0.1	224.74	0.3376	-0.00423	0.9999	0.0000
0.4	225.68	0.3025	-0.00245	0.9999	0.0000
0.7	226.46	0.2847	-0.00245	0.9999	0.0000

m_B is the molality of water-soluble sodium benzoate solution: standard uncertainties are $u_r(m)$ = 0.01; $u(p)$ =0.01 MPa; $u(T)$=0.001 K.

Table 4.5 Expansibility coefficient '$E^0_{\phi,p}$' and its derivative values were obtained of sodium benzoate in glycolic and lactobionic acids mixtures.

Molality m_B/ (mol·kg^{-1})	**$E^0_{\phi,p} \times 10^6$/(m^3·mol^{-1}·K^{-1})**				**$\left(\frac{\partial E^0_\phi}{\partial T}\right)_p \times 10^6$/ (m^3·mol^{-1}·K^{-2})**
	288.15K	**298.15K**	**308.15K**	**318.15K**	
			Glycolic Acid		
0.1	0.108	0.096	0.085	0.073	-0.0012
0.4	0.098	0.095	0.091	0.088	-0.0003
0.7	0.092	0.092	0.091	0.090	-0.0001
			Lactobionic Acid		
0.1	0.422	0.338	0.253	0.169	-0.0085
0.4	0.352	0.303	0.253	0.204	-0.0049
0.7	0.334	0.285	0.236	0.187	-0.0049

m_B is the molality of water-soluble sodium benzoate solution: standard uncertainties are $u_r(m)$ = 0.01; $u(E^0_{\phi,p})$ = 0.022 /(m^3·mol^{-1}·K^{-1}); $u\left(\frac{\partial E^0_\phi}{\partial T}\right)$ = 0.0014/(m^3·mol^{-1}·K^{-2}); $u(p)$ =0.01 MPa; $u(T)$=0.001 K.

4.1.6 Sound speed

The speed of sound measurements for (Sodium benzoate + water) and (Sodium benzoate +water+ GA/LBA) at a variety of temperatures are included in **Table 4.6** further illustrating that, for a given SB concentration, the sound speed escalates or turn out to be further intense with the molality of (GA/LBA) at 0.1 MPa constant pressure. The existing literature data [2,3] has been used for comparing the experimentally obtained ultrasonic velocity for the mixture of sodium benzoate (SB) and water. It can be scrutinized from **Figure 4.5** that the findings of the experiment are in coherence with the data obtained from the previous studies. The velocity of sound provides significant understanding into the interactions inside solvent-solvent, ion, and solvent as well as between ion-ion in the liquid mixture. The rise in the sound speed in a solution suggests a stronger connection between the solution molecules. The reason behind the significant rise in sound velocity values with increasing molality of lactobionic acid and glycolic acid is the presence of 3-D hydrogen bond networks between the solute and sodium benzoate molecules.

This network is accountable for the reported increase in acoustic speed measurements. In addition, the hydrogen bond that exists between water molecules and sodium benzoate molecules dissociates and becomes resistant as the molar mass of (GA/LBA) rises. Nevertheless, at the same time, new bonds of hydrogen are generated between molecules of the SB and GA/LBA [21-23].

4.1.7 Apparent molar isentropic compressibility

To determine the (K_S) compressibility coefficient of glycolic and lactobionic acid in an aqueous SB solution, a particular approach can be utilized i.e Newton -Laplace equation [24]

$$K_s = 1/c^2\rho \tag{4.8}$$

$K_{\phi,S}$ was acquired by solving the subsequent relation using the above-calculated value of (K_S)-

$$K_{\phi,S} = (MK_s/\rho) - \{(K_{S,0}\rho - K_S\rho_0)/m_A\rho\rho_0\} \tag{4.9}$$

where the symbol 'm_A' indicates the molality of the solutes, 'M' signifies the solute's molecular mass, 'ρ' and 'K_S' represent the density and isentropic compression of the solution, 'ρ_o' and '$K_{S,0}$' implies the density and isentropic compressibilities of the solvent. The data of $K_{\phi,S,}$ and sound speed are stated in **Table 4.6**. The findings are

visually displayed in **Figures 4.6** and **4.7**. The empirical data suggests that the values remain negative, becoming more pronounced with increasing sodium benzoate concentration and rising with higher temperatures. This also enhances the strong connections between the solute and solvent in the existence of GA/LBA and SB fragments [25,26]. The arrangement/pattern of water molecules within the solute is acquired by the potential breaking ability of the water structure due to the hydrophilic group of sodium benzoate (SB) and zwitterions of glycolic and lactobionic acids. This phenomenon demonstrates that the water's compressibility is strongly influenced by the solute which results in stronger solute and solvent interactions [27].

Table 4.6 Sound velocity 'c' and apparent molar isentropic compressibility '$K_{\phi,S}$' values of glycolic and lactobionic acids in sodium benzoate solutions.

m_A/ (mol·kg^{-1})	c/(m·s^{-1})				$K_{\phi,s} \times 10^6$/(m^3·mol^{-1}·GPa^{-1})			
	288.15K	298.15K	308.15K	318.15K	288.15K	298.15K	308.15K	318.15 K
0.0 (mol·kg^{-1}) Sodium Benzoate + Glycolic Acid								
0.00000	1466.59	1495.85	1519.14	1536.02				
0.10004	1468.64	1497.59	1520.42	1536.85	-46.12	-44.33	-42.97	-42.03
0.19904	1470.57	1499.38	1521.55	1537.62	-46.44	-44.63	-43.27	-42.32
0.30994	1472.91	1501.34	1522.99	1538.58	-46.60	-44.79	-43.42	-42.46
0.40849	1474.82	1503.12	1524.27	1539.35	-46.71	-44.89	-43.51	-42.55
0.50487	1476.59	1504.67	1525.61	1540.20	-46.79	-44.96	-43.58	-42.62
0.1 (mol·kg^{-1}) Sodium Benzoate + Glycolic Acid								
0.00000	1477.26	1507.45	1529.52	1546.70				
0.10105	1480.19	1508.26	1530.60	1547.43	-45.46	-43.65	-42.40	-41.45
0.20499	1481.37	1509.32	1531.63	1548.67	-45.77	-43.95	-42.68	-41.73
0.29155	1482.62	1510.31	1532.94	1549.44	-45.90	-44.07	-42.79	-41.84
0.39865	1483.10	1511.24	1533.80	1550.23	-46.00	-44.17	-42.89	-41.93
0.50379	1485.12	1512.35	1534.52	1551.46	-46.08	-44.24	-42.96	-42.00
0.4 (mol·kg^{-1}) Sodium Benzoate + Glycolic Acid								
0.00000	1509.63	1542.98	1559.96	1575.48				
0.10100	1510.65	1543.80	1560.25	1576.63	-43.54	-41.67	-40.76	-39.96
0.20918	1511.20	1544.95	1561.24	1577.22	-43.83	-41.94	-41.03	-40.22
0.29944	1512.77	1545.43	1562.78	1578.14	-43.94	-42.05	-41.13	-40.32
0.40174	1513.44	1546.03	1563.67	1579.48	-44.02	-42.13	-41.21	-40.39
0.49998	1514.17	1547.19	1564.52	1580.36	-44.09	-42.19	-41.26	-40.44
0.7 (mol·kg^{-1}) Sodium Benzoate + Glycolic Acid								
0.00000	1540.95	1571.83	1585.77	1598.87				
0.10835	1541.69	1572.51	1586.07	1600.01	-41.82	-40.19	-39.48	-38.83

0.20196	1542.48	1573.44	1587.29	1601.18	-42.04	-40.40	-39.68	-39.03
0.30857	1544.01	1574.65	1588.13	1602.47	-42.16	-40.51	-39.79	-39.13
0.39608	1545.13	1575.52	1589.44	1604.05	-42.22	-40.56	-39.85	-39.19
0.50753	1546.27	1576.77	1591.02	1605.26	-42.28	-40.62	-39.90	-39.24
0.0 (mol·kg^{-1}) Sodium Benzoate + Lactobionic Acid								
0.00000	1466.59	1495.85	1519.14	1536.02				
0.09680	1476.80	1505.14	1527.15	1543.14	-46.62	-44.80	-43.43	-42.47
0.19782	1486.43	1513.96	1535.73	1551.29	-47.47	-45.60	-44.19	-43.21
0.29589	1496.61	1523.62	1543.46	1558.33	-48.08	-46.17	-44.74	-43.75
0.39959	1507.35	1533.17	1551.95	1567.01	-48.64	-46.70	-45.26	-44.25
0.49383	1516.39	1542.02	1559.19	1573.72	-49.11	-47.14	-45.67	-44.66
0.1 (mol·kg^{-1}) Sodium Benzoate + Lactobionic Acid								
0.00000	1477.26	1507.45	1529.52	1546.70				
0.10419	1485.87	1517.58	1537.74	1552.55	-46.02	-44.16	-42.90	-41.94
0.19155	1494.08	1524.13	1544.23	1558.13	-46.71	-44.82	-43.53	-42.56
0.29453	1503.72	1533.69	1552.16	1564.76	-47.33	-45.40	-44.08	-43.09
0.39723	1512.86	1542.37	1559.05	1572.43	-47.85	-45.90	-44.56	-43.56
0.49377	1522.42	1549.95	1565.68	1578.89	-48.30	-46.32	-44.96	-43.94
0.4 (mol·kg^{-1}) Sodium Benzoate + Lactobionic Acid								
0.00000	1509.63	1542.98	1559.96	1575.48				
0.10162	1517.71	1552.31	1567.2	1581.31	-44.03	-42.14	-41.21	-40.40
0.19582	1525.86	1559.74	1574.72	1587.42	-44.72	-42.78	-41.84	-41.01
0.29255	1534.17	1568.35	1582.25	1593.78	-45.24	-43.28	-42.32	-41.48
0.39458	1543.95	1576.66	1589.96	1602.37	-45.72	-43.73	-42.76	-41.90
0.49139	1553.08	1583.23	1596.72	1609.65	-46.13	-44.11	-43.12	-42.26
0.7 (mol·kg^{-1}) Sodium Benzoate + Lactobionic Acid								
0.00000	1540.95	1571.83	1585.77	1598.87				
0.10275	1548.73	1581.02	1593.24	1605.16	-42.26	-40.61	-39.89	-39.23
0.19691	1556.98	1588.59	1601.33	1611.48	-42.89	-41.20	-40.47	-39.80
0.29223	1565.31	1596.67	1609.18	1619.62	-43.36	-41.66	-40.91	-40.23

0.39881	1574.17	1604.54	1617.91	1628.09	-43.82	-42.09	-41.33	-40.64
0.50361	1584.39	1611.46	1625.14	1636.75	-44.22	-42.47	-41.69	-40.99

m_A is the molality of the glycolic and lactobionic acids in sodium benzoate solution: the standard uncertainty of *u(c)* = 1.0 m·s^{-1}; $u_r(m)$ = 0.01; *u(T)*=0.001 K; $u(K_{\phi,S})$ = 0.18 × 10^6/(m^3·mol^{-1}·GPa^{-1}).

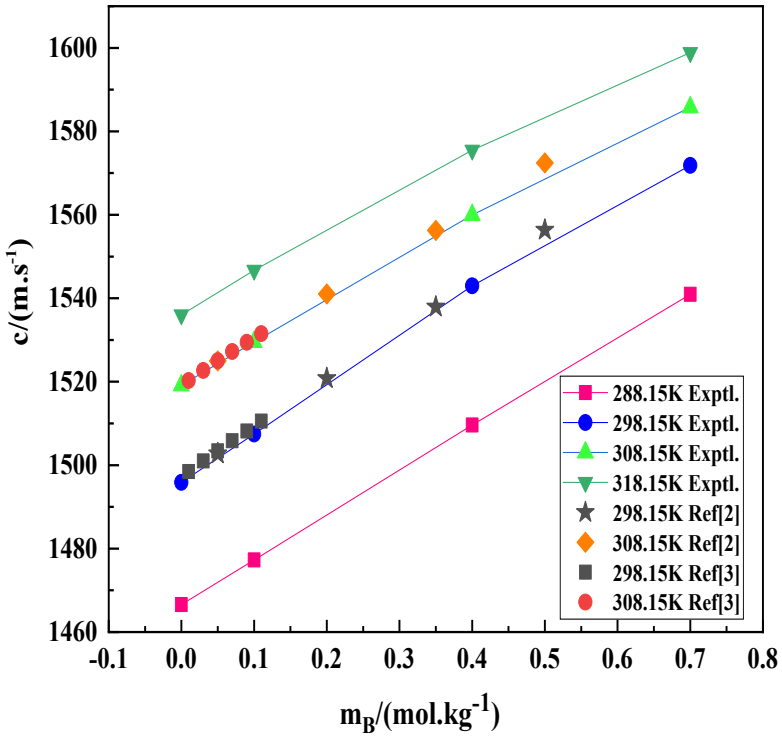

Figure 4.5 The sound velocity of aqueous sodium benzoate was evaluated at several temperatures utilizing experimental and literature data [2,3].

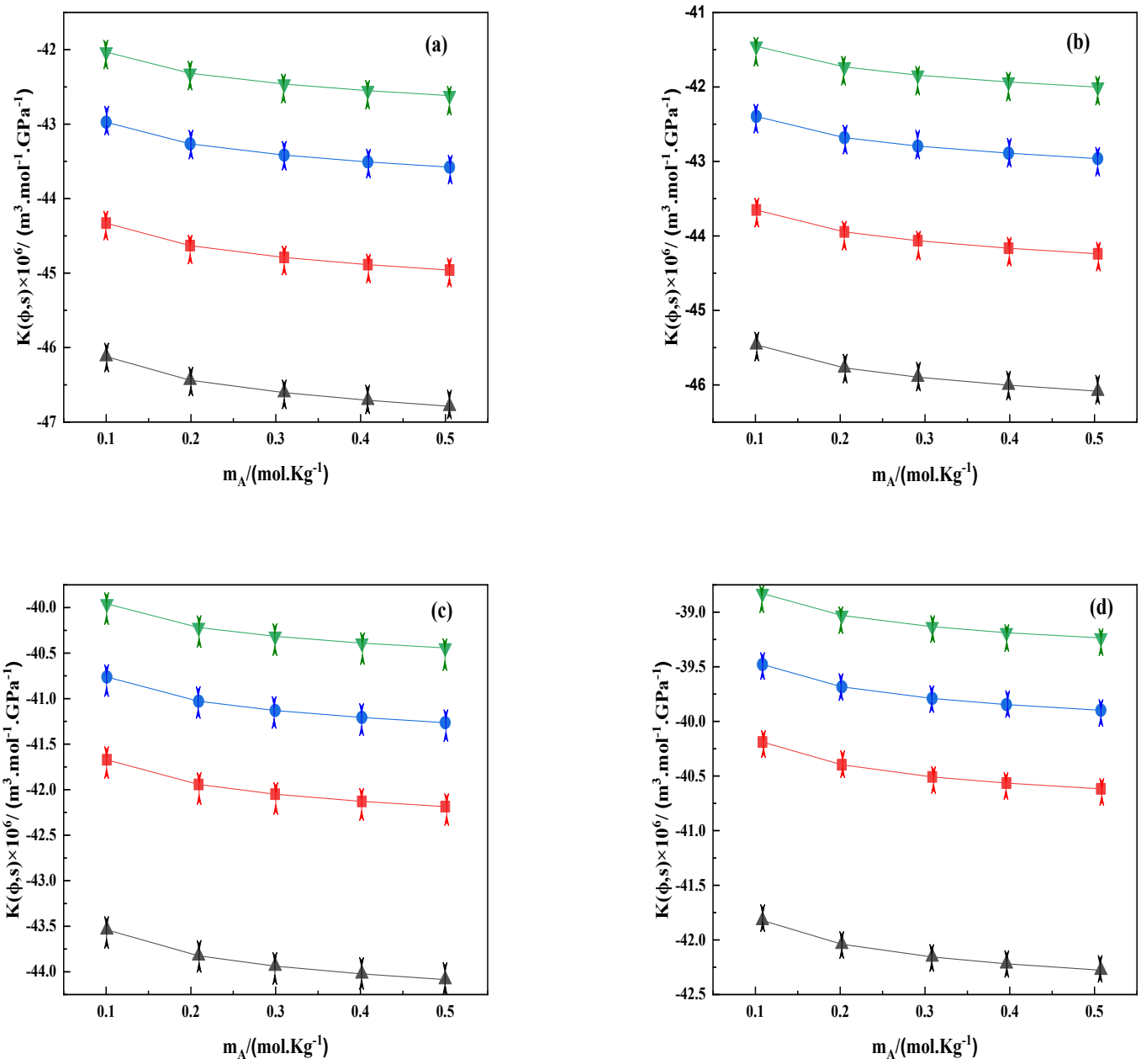

Figure 4.6 Variations in the $K_{\phi,s}$ of glycolic acid in (a) 0.0 sodium benzoate, (b) 0.1 sodium benzoate, (c) 0.4 sodium benzoate and (d) 0.7 sodium benzoate for molality of aqueous glycolic acid solutions.

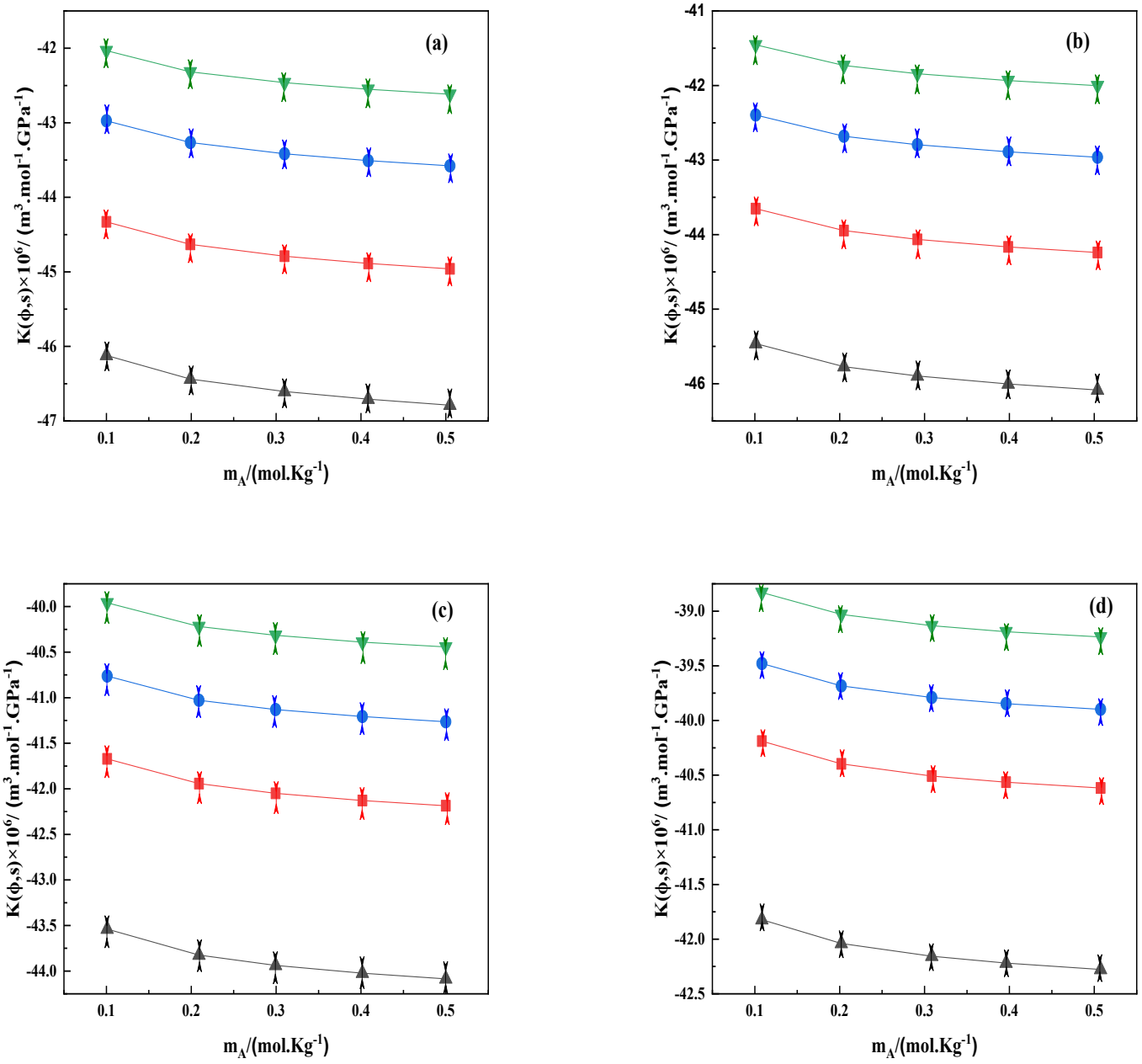

Figure 4.7 Variations in $K_{\phi,s}$ of lactobionic acid in (a) 0.0 sodium benzoate, (b) 0.1 sodium benzoate, (c) 0.4 sodium benzoate and (d) 0.7 sodium benzoate for molality of aqueous lactobionic acid solutions.

4.1.8 Partial molar isentropic compressions

The formula represents the relationship between molality and partial molar isentropic compressibility–

$$K_{\phi,S} = K_{\phi,S}^{0} + S_K^{*} m_A \tag{4.10}$$

The parameter (S_K^{*}) is an acoustic virial coefficient, offering evidence about solute interactions, while ($K_{\phi,S}^{0}$) denotes the limiting partial molar isentropic compressibility.

The computed values along with associated uncertainties are compiled in **Table 4.7.** All the $K_{\phi,S}^{0}$ values are negative (decreases as temperature rises) as represented in **Figure 4.6**. The calculated acoustic virial coefficient demonstrates that the solute-solvent associations become negligible when the solution is infinitely diluted, due to their tiny magnitude [28,29]. It has been noted that when the temperature upsurges, the frequency of negative values of $K_{\phi,S}^{0}$ reduces, resulting in enhanced cohesive forces within solutes and water molecules. This process promotes the movement of H_2O molecules in the bulk solution, a behavior that aligns with the principles outlined in Kirkwood's model [30]. The primary factors contributing to the ($K_{\phi,S}^{0}$) are influenced by two key effects: The positive effect, often linked to the intrinsic compressibility of the solvent, arises from an increase in intermolecular free space, leading to superior compressibility of the solution. Conversely, the negative effect, associated with penetration of solvent, occurs when solvent molecules occupy the free spaces within ions owing to solute as well as solvent interactions [31,32].

At lower concentrations of sodium benzoate, the compressibility of water molecules that are located around carboxylic acids (GA/LBA) diminishes, but increases at greater concentrations of SB due to the predominating combination of sodium benzoate and molecules of water, which begin to dehydrate the solute (GA/LBA) molecules. Since (S_K^{*}) values are much lower than the values of ($K_{\phi,S}^{0}$), it can be inferred that the bonds among the solutes in the liquid system are essentially negligible. This would infer that the interactions inside solute and solvent are more evident in the solution [33,34].

Table 4.7 Obtained values of $K^0_{\phi,S}$ and S^*_K of the combination (sodium benzoate + water + glycolic and lactobionic acids).

m_B/ (mol·kg^{-1})	$K^0_{\phi,S} \times 10^6$/(m^3·mol^{-1}·GPa^{-1})				$S^*_K \times 10^6$/(kg·m^3·kg·mol^{-2}·GPa^{-1})			
	288.15K	**298.15K**	**308.15K**	**318.15K**	**288.15K**	**298.15K**	**308.15K**	**318.15K**
				Glycolic Acid				
0.0	-46.05 (±0.08)	-44.26(±0.08)	-42.91(±0.08)	-41.97(±0.08)	-1.58(±0.26)	-1.49(±0.25)	-1.43(±0.24)	-1.38(±0.23)
0.1	-45.40(±0.08)	-43.60(±0.08)	-42.34(±0.08)	-41.40(±0.08)	-1.47(±0.26)	-1.39(±0.25)	-1.34(±0.24)	-1.29(±0.23)
0.4	-43.49(±0.08)	-41.62(±0.08)	-40.72(±0.07)	-39.92(±0.07)	-1.31(±0.24)	-1.23(±0.24)	-1.20(±0.22)	-1.16(±0.22)
0.7	-41.77(±0.07)	-40.14(±0.07)	-39.43(±0.06)	-38.79(±0.06)	-1.09(±0.20)	-1.03(±0.19)	-1.00(±0.19)	-0.97(±0.19)
				Lactobionic Acid				
0.0	-46.15(±0.13)	-44.36(±0.12)	-43.00(±0.11)	-42.05(±0.11)	-6.18(±0.38)	-5.80(±0.37)	-5.59(±0.35)	-5.44(±0.34)
0.1	-45.53(±0.11)	-43.70(±0.11)	-42.46(±0.10)	-41.52(±0.10)	-5.78(±0.35)	-5.47(±0.33)	-5.23(±0.32)	-5.06(±0.31)
0.4	-43.60±0.11)	-41.73(±0.11)	-40.82(±0.10)	-40.02(±0.10)	-5.31(±0.34)	-5.00(±0.33)	-4.84(±0.32)	-4.71(±0.31)
0.7	-41.87(±0.10)	-40.24(±0.10)	-39.53(±0.10)	-38.88(±0.10)	-4.80(±0.32)	-4.58(±0.30)	-4.44(±0.30)	-4.35(±0.29)

m_B is the molality of water-soluble sodium benzoate: the calculated standard uncertainties u are $u_r(m)$ = 0.01; $u(K^0_{\phi,S})$ = 0.38 × 10^6/(m^3·mol^{-1}·GPa^{-1}); $u(S^*_K)$= 0.39×10^6/(kg·m^3·kg·mol^{-2}·GPa^{-1}); $u(T)$=0.001 K.

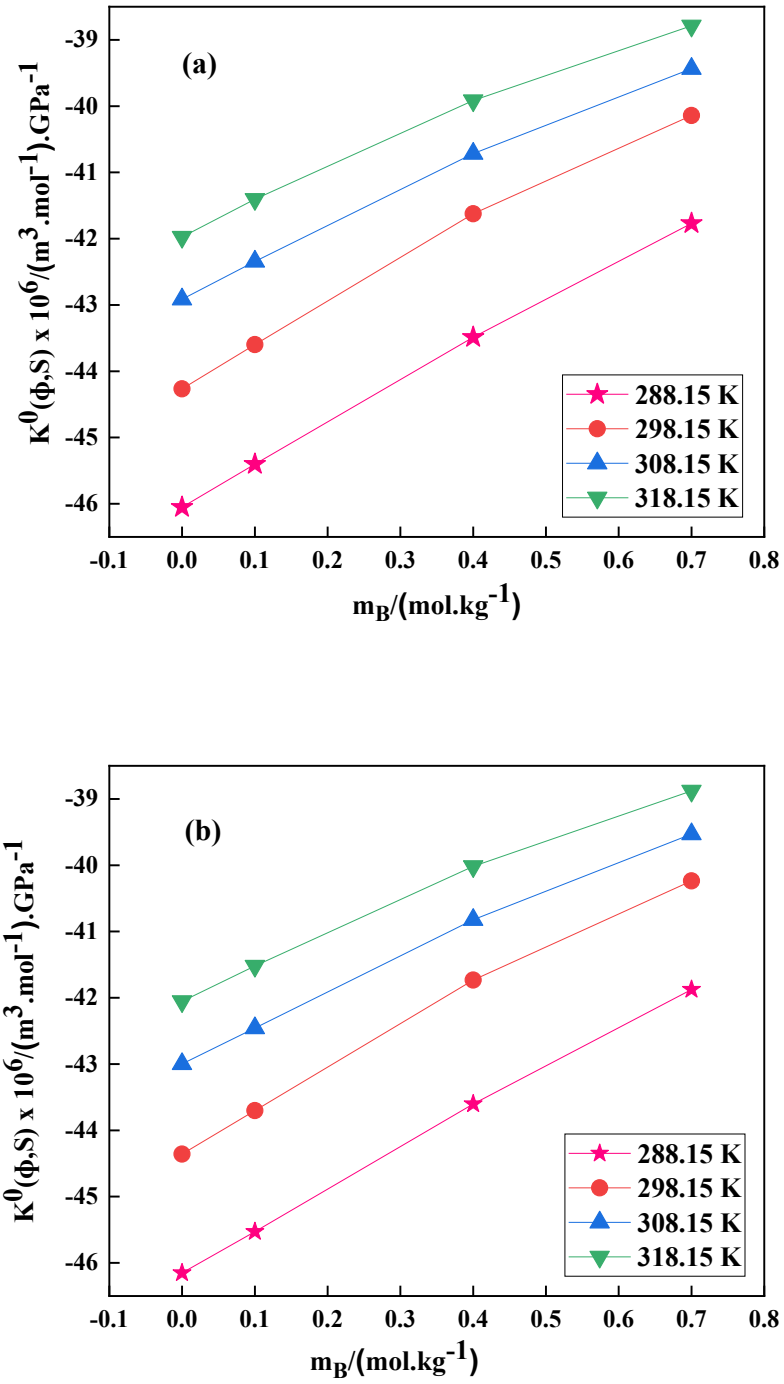

Figure 4.8 Changes in $K^0_{\emptyset,S}$ for (a) glycolic acid and (b) lactobionic acid in aqueous sodium benzoate (SB) at several temperatures.

4.1.9 Transfer parameter of partial molar isentropic compression

The $\Delta_{tr}K^0_{\emptyset,S}$ of glycolic and lactobionic acids produced from water to sodium benzoate mixture is computed by the formula below at the condition of infinite dilution.

$$\Delta K^0_{\emptyset,s} = K^0_{\phi,S_{(in\ aqueous\ SB)}} - K^0_{\phi,S_{(in\ water)}} \quad (4.11)$$

where the determined data of $\Delta_{tr}K^0_{\emptyset,S}$ are positive across different concentrations (0.1,0.4,0.7) mol·Kg^{-1} which has been provided in **Table 4.8**, suggesting the propensity of solutions to form structures. This is caused by the electrostriction decreasing as the concentration of sodium benzoate rises, which enhances the structure-building property [35]. Positive $\Delta_{tr}K^0_{\emptyset,S}$ values cause the molecules of water to interrelate with the glycolic and lactobionic acids, suggesting that the solute's water molecules integrate with the solvent-enhancing intermolecular interactions. The negative $K^0_{\phi,s}$ values observed in solute as well as solvent interaction can be ascribed to the strengthened association of molecules of water with the ion [36,37]. The rise in the molality of GA/LBA is a contributing factor to the rise in the values of $\Delta_{tr}K^0_{\emptyset,S}$ which ultimately in turn enhances the capability of the solute to form structures and intensifies the interactions amid the solute-solvent in the current examination.

Table 4.8 Values of transfer parameter $\Delta_{tr}K^0_{\emptyset,S}$ of sodium benzoate in aqueous glycolic and lactobionic acids at several temperatures.

m_B/ (mol·kg^{-1})	$\Delta_{tr}K^0_{\emptyset,S} \times 10^6$/(m^3·mol^{-1}·GPa^{-1})			
	288.15K	**298.15K**	**308.15K**	**318.15K**
		Glycolic Acid		
0.1	0.65	0.67	0.57	0.57
0.4	2.57	2.64	2.20	2.06
0.7	4.28	4.12	3.48	3.19
		Lactobionic Acid		
0.1	0.62	0.66	0.54	0.54
0.4	2.55	2.63	2.18	2.04
0.7	4.28	4.12	3.47	3.18

m_B states the molality of water-soluble sodium benzoate solution: standard uncertainties are $u_r(m)$ = 0.01; $u(\Delta_{tr}K^0_{\emptyset,S})$ = 0.28×10^6/(m^3·mol^{-1}·GPa^{-1}); $u(T)$=0.001 K.

4.1.10 Interaction Coefficients

The equation yields the interaction coefficients from these transfer parameters i.e. $\Delta_{tr}V_{\emptyset}^{0}$ and $\Delta_{tr}K_{\emptyset,S}^{0}$ which is presented below-

$$\Delta_{tr}V_{\emptyset}^{0} \text{ (from water to sodium benzoate solution)} = 2V_{AB}m_B + 3V_{ABB}m_B^2 \quad (4.12)$$

$$\Delta_{tr}K_{\emptyset,S}^{0}\text{(from water to sodium benzoate solution)} = 2K_{AB}m_B + 3K_{ABB}m_B^2 \quad (4.13)$$

here *A* indicates glycolic and lactobionic acids (solutes), *B* designates sodium benzoate (solvent), m_B specifies the concentration of water-soluble sodium benzoate solution.

The coefficients (K_{AB}, V_{AB}, K_{ABB} and V_{ABB}) have been determined by McMillan and Mayer[58] can be determined from the (eqs. (4.12) and (4.13)) which has been shown in **Table 4.9** that allowed the effects to be separated that might be created to the interactions between the solute fragments or by the interaction between the pairs of fragments. Franks et al. [38,39], Friedman, and Krishnan explored this concept in more detail [40]. The pair interaction coefficients were observed to be positive, while the triplet interaction coefficients were found to be negative at all temperatures. This interaction between the pair interaction results in the electrostriction of water molecules, which eventually leads to a rise in the organization of structure. A positive volume change is the cause of the overlapping of the hydration co-sphere, which is accountable for the phenomenon [41]. To accurately predict and maintain control over the behavior of solute molecules in solution, it is essential to have an inclusive knowledge of the scope of these interactions. According to the findings of the current study, the pair-wise interactions in the liquid combination of (SB+water+GA/LBA) are more effective than the triplet interactions. This is shown with the substantial positive values of V_{AB} and K_{AB}.

Table 4.9 Interaction coefficients for the ternary liquid combination comprising sodium benzoate solutions with glycolic and lactobionic acids.

T/K	$V_{AB} \times 10^6$/(m^3·mol^{-2}· kg)	$V_{ABB} \times 10^6$/(m^3·mol^{-3}·kg^2)	$K_{AB} \times 10^6$(m^3·mol^{-2}· kg·GPa^{-1})	$K_{ABB} \times 10^6$ (m^3·mol^{-3}·kg^2·GPa^{-1})
		Glycolic Acid		
288.15	3.36	-1.31	3.38	-0.30
298.15	3.15	-1.27	3.70	-0.71
308.15	3.42	-1.39	3.05	-0.54
318.15	3.51	-1.47	2.97	-0.66
		Lactobionic Acid		
288.15	6.32	-3.24	3.31	-0.24
298.15	4.98	-2.57	3.65	-0.67
308.15	4.89	-2.79	2.98	-0.47
318.15	5.27	-3.10	2.88	-0.58

T is the temperature in kelvin; where standard uncertainties are $u(T)$=0.001 K, $u(p)$ = 0.01 MPa.

Problem 2

4.2 Title: "Analysis of Molecular Interactions of an Aqueous Benzoates with Glycolic and Lactic Acid: Spectroscopic, Acoustic, and Volumetric Approach"

In this section, the ρ and s of glycolic and lactic acids in aqueous sodium methyl p-hydroxybenzoate solutions of 0.015, 0.025, and 0.035 mol.Kg^{-1} were carried out at temperatures varying from 288.15-318.15 K.

4.2.1 Density and sound velocity

The different volumetric and acoustic characteristics have been investigated using the measured values obtained from experimentation. The densities and sound speeds of AHAs (glycolic acid and lactic acid) in combinations of different concentrations (0.000, 0.015, 0.025, 0.035) mol·Kg^{-1} of SMP were studied at several temperatures and presented the results in **Table 4.10**. Based on the density data, it has been shown that for a specific concentration of SMP, the density of the mixture rises when the concentration of alpha-hydroxy acids (GA and LA) increases, and it slightly decreases with the elevation in temperature. The obtained densities and sound speeds of SMP with water correlate with the published values of the liquid combination [42] as shown in **Figure 4.9.**

It is obvious that the measured densities and sound speeds for the mixture being studied exhibit the similar pattern as recognized in the literature. The primary reason for the rise in density values with concentrations of alpha-hydroxy acids is the expansion of the molar mass of the mixture. An escalation in density also suggests that interactions between solvents and solutes have become more intense [43]. The sound speed data offers significant insights on the interaction of ions with each other, solutes with solvents, and ions with solvents [44]. **Table 4.10** provides additional information that, for a constant SMP concentration, the ultrasonic speed increases or becomes more pronounced when the molality of (GA/LA) rises at a constant pressure of 0.1 MPa. The rise in sound speed data with the increasing molality of solutes can be associated with the existence of three-dimensional H-bond networks inside the solute and solvent molecules [45,46,22]. Furthermore, as the molar mass of alpha hydroxy acids rises from GA to LA, the hydrogen bonding that exists within the molecules of SMP and water decreases and eventually dissolves, whereas new hydrogen bonds are formed within the sodium methyl parahydroxy benzoate molecules and alpha-hydroxy acids [23,47].

Table 4.10 Densities 'ρ', and sound velocity 's' in the liquid mixture of aqueous Sodium Methyl Para-hydroxy Benzoate with Glycolic Acid/Lactic Acid at several temperatures.

m_A/(mol·kg^{-1})	$\rho \times 10^{-3}$/(kg·m^{-3})				s/(m·s^{-1})			
	288.15 (K)	298.15 (K)	308.15 (K)	318.15 (K)	288.15 (K)	298.15 (K)	308.15 (K)	318.15 (K)
0.000 ($mol.kg^{-1}$) SMP + GA								
0.00000	0.99926	0.99705	0.99404	0.99036	1466.59	1495.85	1519.14	1536.02
0.10004	1.00133	0.99904	0.99594	0.99217	1468.59	1497.86	1520.57	1536.89
0.19964	1.00316	1.00078	0.99759	0.99377	1470.67	1499.44	1522.03	1538.84
0.30156	1.00485	1.00239	0.99913	0.99521	1472.53	1501.13	1523.06	1539.72
0.40228	1.00630	1.00375	1.00044	0.99646	1474.46	1502.44	1524.39	1539.66
0.50117	1.00753	1.00491	1.00157	0.99754	1476.37	1504.06	1525.48	1540.33
0.015 ($mol.kg^{-1}$) SMP + GA								
0.00000	1.00007	0.99789	0.99488	0.99114	1468.87	1498.45	1521.84	1537.72
0.10728	1.00220	0.99994	0.99684	0.99303	1470.82	1500.13	1522.47	1538.62
0.20138	1.00388	1.00153	0.99838	0.99450	1472.45	1501.25	1523.35	1539.19
0.29914	1.00543	1.00295	0.99976	0.99580	1474.04	1502.43	1524.22	1539.83
0.39983	1.00680	1.00424	1.00101	0.99698	1475.79	1503.74	1525.03	1540.57
0.50045	1.00791	1.00532	1.00203	0.99797	1477.84	1504.96	1526.06	1541.04
0.025 ($mol.kg^{-1}$) SMP + GA								
0.00000	1.00054	0.99841	0.99537	0.99155	1469.84	1499.31	1521.56	1538.27
0.10093	1.00250	1.00030	0.99718	0.99330	1472.76	1501.04	1523.13	1539.19

0.20152	1.00423	1.00195	0.99877	0.99482	1473.68	1502.35	1524.07	1539.97
0.30264	1.00573	1.00342	1.00017	0.99617	1475.33	1503.68	1525.12	1540.61
0.39951	1.00700	1.00461	1.00133	0.99728	1477.05	1505.03	1526.28	1541.48
0.50479	1.00818	1.00577	1.00241	0.99836	1478.95	1506.23	1527.14	1542.15
0.035 ($mol.kg^{-1}$) SMP + GA								
0.00000	1.00098	0.99879	0.99570	0.99196	1471.24	1500.56	1524.42	1539.23
0.09554	1.00278	1.00051	0.99735	0.99355	1473.11	1501.85	1525.02	1540.26
0.19783	1.00452	1.00219	0.99897	0.99510	1474.77	1503.23	1526.13	1541.37
0.30141	1.00604	1.00366	1.00040	0.99649	1476.53	1505.09	1527.29	1542.21
0.40117	1.00732	1.00480	1.00157	0.99763	1478.34	1506.47	1528.49	1543.35
0.49611	1.00840	1.00590	1.00252	0.99851	1480.27	1507.74	1529.36	1544.05
0.000 ($mol.kg^{-1}$) SMP + LA								
0.00000	0.99926	0.99705	0.99404	0.99036	1466.59	1495.85	1519.14	1536.02
0.08468	1.00081	0.99858	0.99556	0.99186	1469.51	1497.66	1520.75	1537.27
0.19654	1.00279	1.00054	0.99749	0.99379	1472.84	1500.43	1522.87	1538.79
0.30226	1.00459	1.00231	0.99925	0.99553	1476.07	1503.23	1524.50	1540.36
0.38747	1.00598	1.00368	1.00060	0.99688	1478.65	1505.47	1526.21	1541.81
0.49639	1.00771	1.00537	1.00227	0.99853	1481.37	1508.44	1528.05	1543.28
0.015 ($mol.kg^{-1}$) SMP + LA								
0.00000	1.00007	0.99789	0.99488	0.99114	1468.87	1498.45	1521.84	1537.72
0.10228	1.00184	0.99963	0.99661	0.99285	1471.68	1500.60	1523.18	1538.77

0.19533	1.00336	1.00114	0.99809	0.99432	1474.23	1502.73	1524.71	1540.09
0.30046	1.00500	1.00275	0.99968	0.99589	1477.44	1505.14	1526.56	1541.41
0.39841	1.00643	1.00416	1.00108	0.99728	1480.05	1508.02	1528.17	1542.88
0.50262	1.00787	1.00558	1.00249	0.99868	1482.62	1510.44	1530.29	1544.23
0.025 ($mol.kg^{-1}$) SMP + LA								
0.00000	1.00054	0.99841	0.99537	0.99155	1469.84	1499.31	1521.96	1538.27
0.09862	1.00219	1.00004	0.99699	0.99316	1473.28	1501.39	1524.23	1539.82
0.20130	1.00383	1.00165	0.99858	0.99473	1476.25	1503.95	1525.90	1541.24
0.29579	1.00524	1.00305	0.99996	0.99610	1478.65	1506.11	1527.75	1542.64
0.40646	1.00681	1.00459	1.00147	0.99760	1481.38	1509.22	1529.79	1544.12
0.50484	1.00812	1.00587	1.00275	0.99886	1484.04	1511.57	1531.90	1545.48
0.035 ($mol.kg^{-1}$) SMP + LA								
0.00000	1.00098	0.99879	0.99570	0.99196	1471.24	1500.56	1524.42	1539.23
0.10176	1.00263	1.00042	0.99731	0.99356	1475.03	1502.69	1525.68	1540.72
0.19773	1.00411	1.00188	0.99876	0.99498	1478.09	1505.05	1527.29	1542.25
0.30564	1.00568	1.00342	1.00029	0.99650	1480.74	1507.83	1529.38	1543.99
0.39479	1.00691	1.00464	1.00150	0.99771	1483.31	1510.46	1531.14	1545.37
0.49148	1.00820	1.00591	1.00277	0.99895	1486.04	1512.73	1533.04	1546.67

m_A implies the molality of the solutes (GA/LA) in an aqueous Sodium methyl p-hydroxy benzoate solution: standard errors are u(m) = 0.02 (mol·kg^{-1}); u(ρ)= 0.31 (kg·m^{-3}); u(T)=0.001 K; u(s)= 1.80 m·s^{-1}.

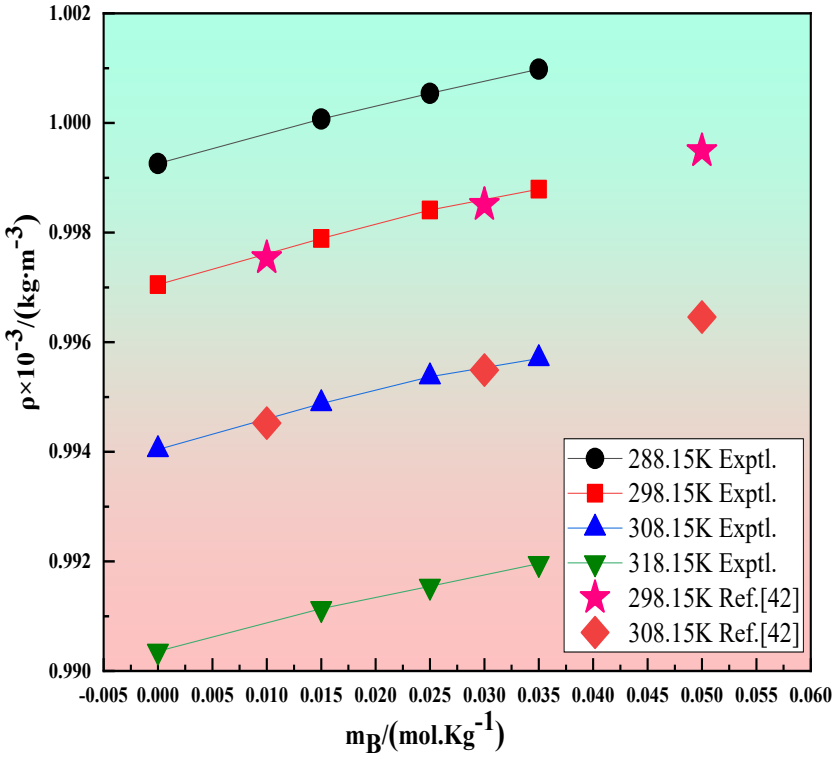

Figure 4.9 The density of a binary combination of an aqueous SMP was shown at different temperatures utilizing literature as well as experimental data [42].

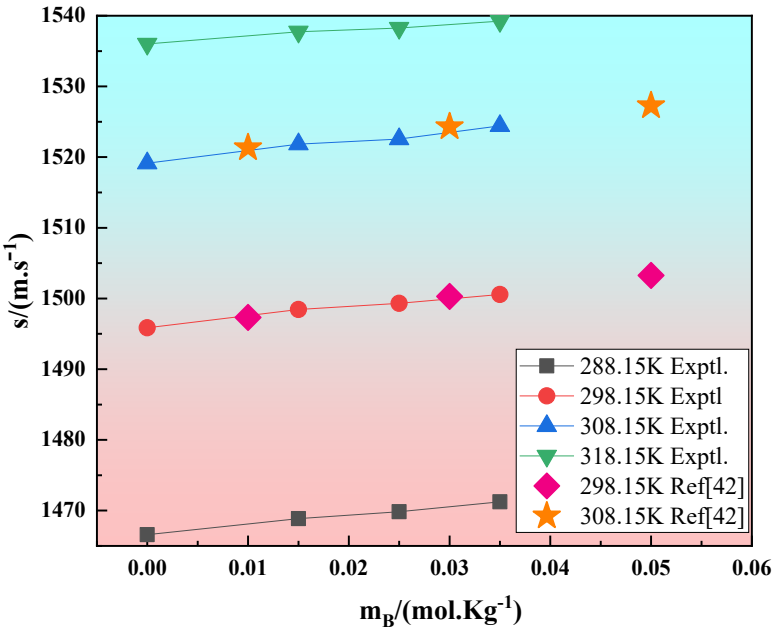

Figure 4.10 Ultrasonic speed of a binary liquid combination (SMP + Water) was shown at different temperatures utilizing literature as well as experimental data [42].

4.2.2 Apparent molar volumes

Using the density measurements, the **equation (4.1)** can be utilized for the computation of the ($V_{\emptyset}$) [48]. **Table 4.11** lists the values obtained for apparent molar volumes from experimental density data. **Figure 4.11** highlights the increasing molecular interaction from GA to LA in SMP aqueous solution. The data obtained through the calculations indicate that the V_{ϕ} in the GA/LA system increases in accordance with both the temperature and SMP concentration. The 3D graphical representation of the liquid system is vividly illustrated in **Figure 4.12.** The substantial inherent volume of the solute indicates significant solute-solvent bonds in the present liquid combinations which may account for the positive values of all computed $V_{\emptyset}$. It is possible to get a substantial amount of knowledge regarding the interactions that occur inside the solutes and the solvent within a solution [15]. The electrostriction of water molecules decreases with the elevation in the concentration mainly due to the interactions inside the solvent and the solute, which leads to a rise in the V_{ϕ}. The rise in the data of V_{ϕ} may be ascribed to a variety of physical factors, such as interactions between dipoles, the hydrophilic effect along with dipole-induced-dipole connections in the region that is abundant in water [49].

Table 4.11 Computed data of $V_{\emptyset}$ for glycolic and lactic acids in aqueous sodium methyl para-hydroxybenzoate at several temperatures and concentrations.

m_A/ (mol·kg^{-1})	$V_\phi \times 10^6$/(m^3·mol^{-1})				$^a m_A$/(mol · kg^{-1})	$V_\phi \times 10^6$/(m^3·mol^{-1})			
	288.15(K)	298.15(K)	308.15(K)	318.15(K)		288.15(K)	298.15(K)	308.15(K)	318.15(K)
	GA + 0.000 $mol \cdot kg^{-1}$ SMP					**LA + 0.000 $mol \cdot kg^{-1}$ SMP**			
0.10004	55.29	56.19	57.22	58.21	0.08468	71.72	72.03	72.38	72.76
0.19964	56.31	57.28	58.28	59.19	0.19654	71.92	72.25	72.59	72.93
0.30156	57.23	58.15	59.13	60.11	0.30226	72.11	72.46	72.81	73.14
0.40228	58.17	59.12	60.01	60.95	0.38747	72.28	72.66	73.01	73.33
0.50117	59.09	60.02	60.84	61.74	0.49639	72.49	72.87	73.23	73.57
	GA + 0.015 $mol \cdot kg^{-1}$ SMP					**LA + 0.015 $mol \cdot kg^{-1}$ SMP**			
0.10728	56.11	56.93	57.86	58.73	0.10228	72.65	73.02	73.35	73.75
0.20138	56.89	57.84	58.69	59.55	0.19533	72.98	73.33	73.69	74.07
0.29914	57.82	58.92	59.67	60.58	0.30046	73.31	73.67	74.06	74.42
0.39983	58.81	59.88	60.58	61.49	0.39841	73.65	74.01	74.36	74.73
0.50045	59.91	60.85	61.57	62.41	0.50262	73.97	74.34	74.68	75.05

GA+ 0.025 $mol \cdot kg^{-1}$ SMP					LA + 0.025 $mol \cdot kg^{-1}$ SMP				
0.10093	56.47	57.27	58.17	58.97	0.09862	73.15	73.51	73.84	74.17
0.20152	57.53	58.34	59.18	60.02	0.20130	73.48	73.82	74.16	74.53
0.30264	58.56	59.25	60.12	60.88	0.29579	73.81	74.13	74.49	74.85
0.39951	59.48	60.23	60.97	61.76	0.40646	74.15	74.52	74.85	75.24
0.50479	60.42	61.09	61.89	62.55	0.50484	74.47	74.85	75.18	75.56
GA + 0.035 $mol \cdot kg^{-1}$ SMP					**LA + 0.035 $mol \cdot kg^{-1}$ SMP**				
0.09554	57.05	57.97	58.81	59.63	0.10176	73.66	73.99	74.35	74.71
0.19783	57.93	58.73	59.49	60.32	0.19773	73.95	74.31	74.64	75.05
0.30141	58.91	59.66	60.38	61.12	0.30564	74.29	74.65	74.97	75.37
0.40117	59.82	60.58	61.27	61.95	0.39479	74.56	74.89	75.21	75.58
0.49611	60.59	61.34	62.09	62.83	0.49148	74.79	75.13	75.42	75.82

m_A implies the molality of the solutes (GA/LA) in Sodium methyl p-hydroxy benzoate (SMP) solution: standard uncertainties are $u(V_\phi)$ = ± (0.05 − 0.07) × 10^6/ (m^3. mol^{-1}).

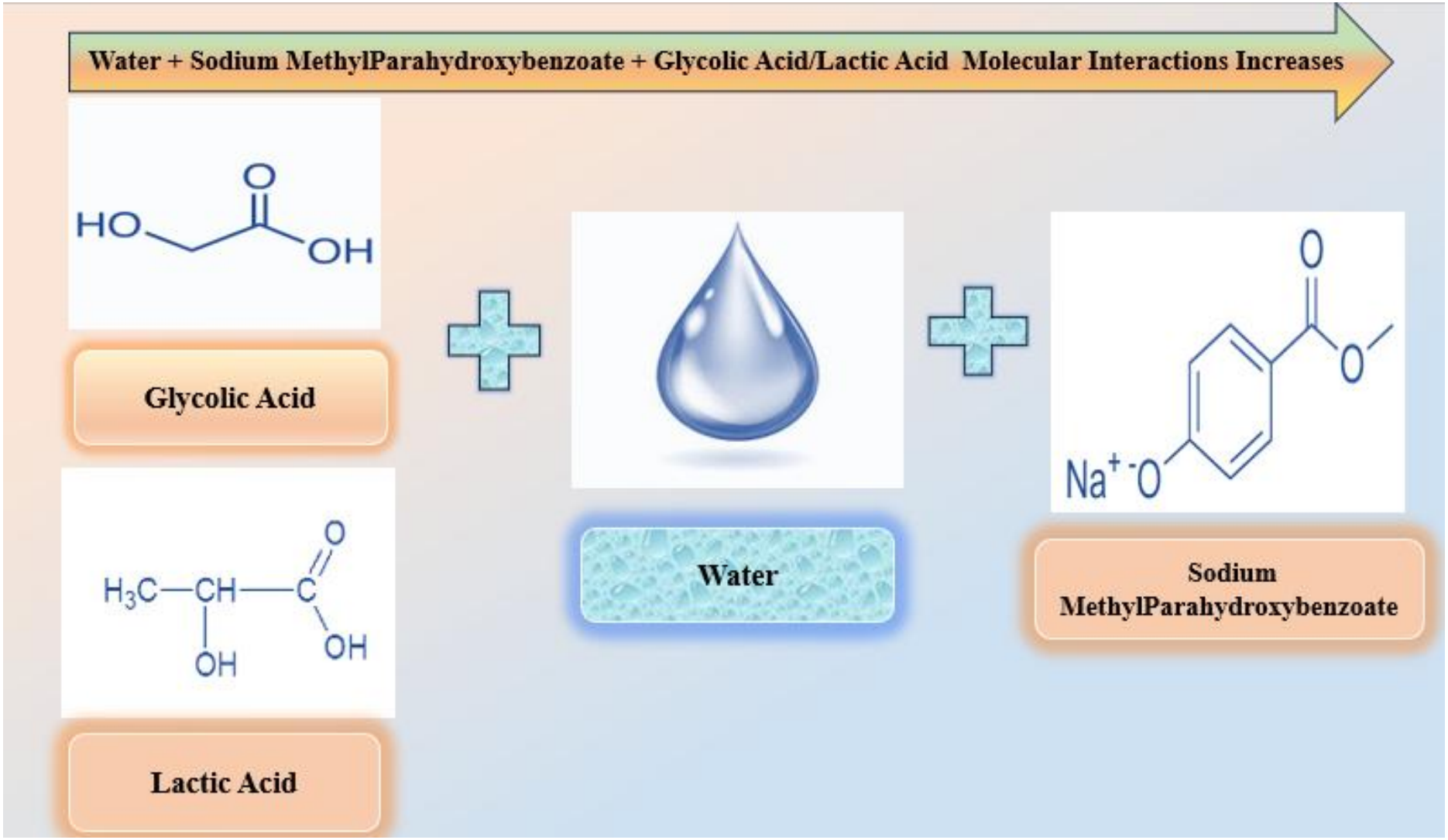

Figure 4.11 GA/LA and Sodium methyl para-hydroxy benzoate molecular interactions.

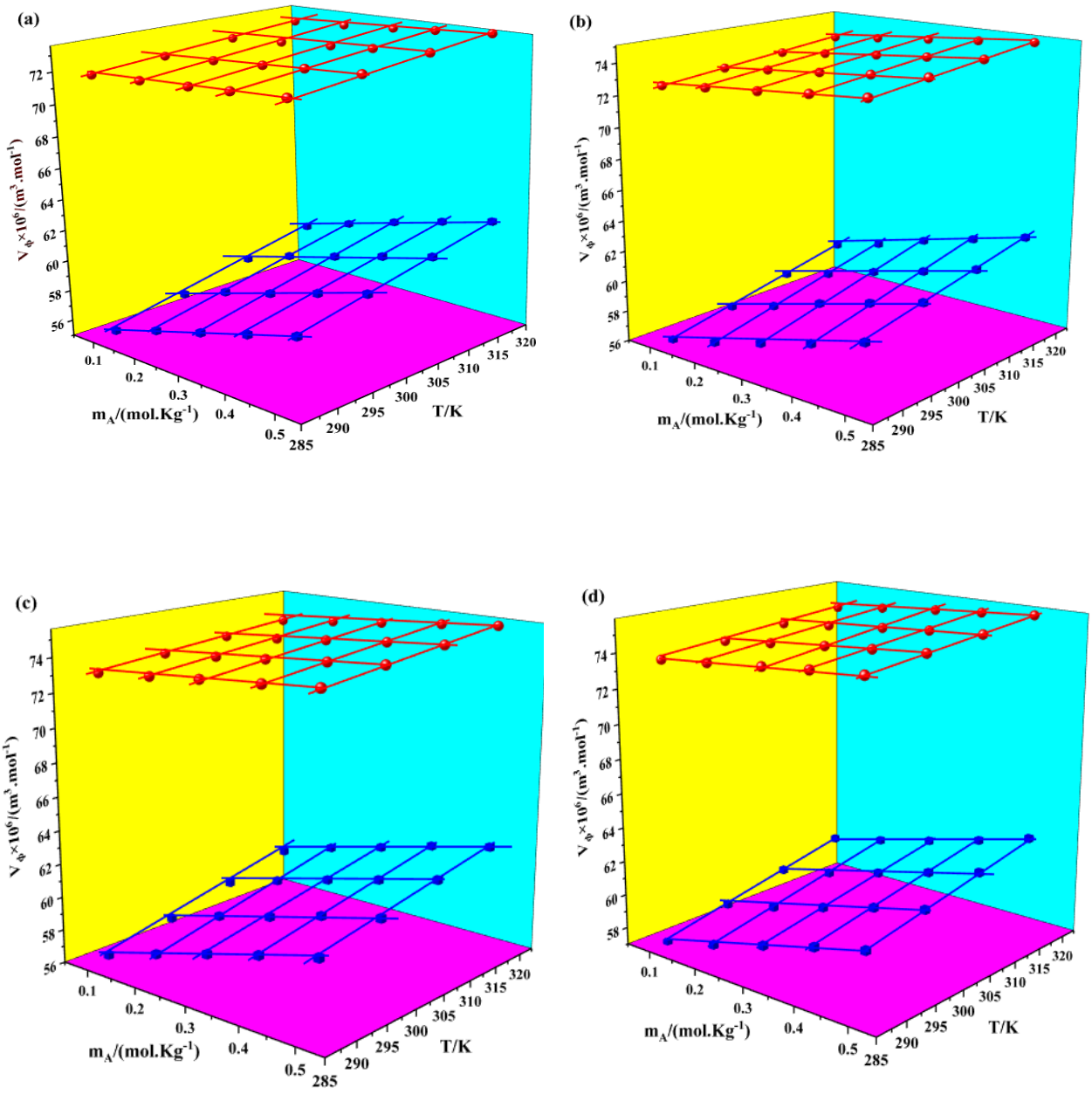

Figure 4.12 Three-dimensional Plots illustrate the variations in ($V_\emptyset$) of (a) 0.000 SMP; (b) 0.015 SMP; (c) 0.025 SMP;(d) 0.035 SMP for molality of glycolic acid (blue; cube) and lactic acid (red; sphere) at varying temperatures.

4.2.3 Apparent molar isentropic compression

The Newton-Laplace equation [50] explains the isentropic compressibility of a liquid system, where isentropic compressibility 'K_S' is calculated using **equation 4.8**. For the purpose of determining the $K_{\phi,s}$ of GA and LA in aqueous SMP mixtures, the **equation 4.9** is utilized [51]. **Table 4.12** confirms that the obtained ($K_{\phi,s}$) data are consistently negative and decrease with the rise in the temperature, there is a corresponding rise in the concentration of SMP inferred that the water molecules around the solute have lesser ability to be compressed relative to those in a bulk solution [25,52]. The findings are visually shown in **Figures 4.13** and **4.14.** These negative values can be explained by the solute molecules being removed from the solvent as a consequence of thermal motion, which raises the solvent volume and also increases its compressibility. Furthermore, the observed behavior of $K_{\phi,s}$ values is influenced by the disruption of the solvent (SMP) molecules along with the hydration shells of the solutes (glycolic and lactic acids). In addition, the negative values demonstrate that the reduction is due to the water's structural compressibility and the aligning impact on the solvent is carried out by the solute that is present in the solvent [53,54]. Through the formation of intermolecular hydrogen bonding, alpha-hydroxy acids and SMP solutions have the ability to generate more compact structures, which leads to reduces their compressibility.

Table 4.12 Values of $K_{\phi,s}$ were calculated for glycolic and lactic acids in aqueous Sodium methyl parahydroxybenzoate solutions at several temperatures and concentrations.

m_A/ (mol·kg^{-1})	$K_{\phi,s} \times 10^6$/(m^3·mol^{-1}·GPa^{-1})				m_A/ (mol·kg^{-1})	$K_{\phi,s} \times 10^6$/(m^3·mol^{-1}·GPa^{-1})			
	288.15(K)	298.15(K)	308.15(K)	318.15(K)		288.15(K)	298.15(K)	308.15(K)	318.15(K)
	GA + 0.000 $mol \cdot kg^{-1}$ SMP					**LA + 0.000 $mol \cdot kg^{-1}$ SMP**			
0.10004	-46.13	-44.33	-42.98	-42.03	0.08468	-46.02	-44.23	-42.88	-41.94
0.19964	-46.45	-44.64	-43.27	-42.32	0.19654	-46.42	-44.62	-43.26	-42.31
0.30156	-46.59	-44.77	-43.40	-42.44	0.30226	-46.59	-44.78	-43.42	-42.46
0.40228	-46.70	-44.88	-43.50	-42.54	0.38747	-46.69	-44.87	-43.51	-42.55
0.50117	-46.79	-44.96	-43.57	-42.61	0.49639	-46.79	-44.98	-43.60	-42.65
	GA + 0.015 $mol \cdot kg^{-1}$ SMP					**LA + 0.015 $mol \cdot kg^{-1}$ SMP**			
0.10728	-46.02	-44.21	-42.86	-41.97	0.10228	-45.98	-44.18	-42.83	-41.94
0.20138	-46.30	-44.48	-43.11	-42.22	0.19533	-46.27	-44.45	-43.10	-42.21
0.29914	-46.44	-44.62	-43.25	-42.35	0.30046	-46.42	-44.61	-43.24	-42.35
0.39983	-46.55	-44.71	-43.34	-42.43	0.39841	-46.53	-44.71	-43.34	-42.45
0.50045	-46.62	-44.78	-43.40	-42.50	0.50262	-46.62	-44.79	-43.42	-42.53
	GA+ 0.025 $mol \cdot kg^{-1}$ SMP					**LA + 0.025 $mol \cdot kg^{-1}$ SMP**			

0.10093	-45.92	-44.13	-42.79	-41.91	0.09862	-45.90	-44.11	-42.77	-41.89
0.20152	-46.23	-44.42	-43.07	-42.19	0.20130	-46.21	-44.41	-43.06	-42.18
0.30264	-46.38	-44.56	-43.20	-42.32	0.29579	-46.35	-44.54	-43.19	-42.31
0.39951	-46.47	-44.65	-43.29	-42.40	0.40646	-46.47	-44.65	-43.30	-42.41
0.50479	-46.55	-44.73	-43.36	-42.47	0.50484	-46.55	-44.73	-43.37	-42.49
	GA + 0.035 $mol \cdot kg^{-1}$ SMP					**LA + 0.035 $mol \cdot kg^{-1}$ SMP**			
0.09554	-45.80	-44.02	-42.65	-41.83	0.10176	-45.82	-44.05	-42.68	-41.86
0.19783	-46.13	-44.34	-42.96	-42.13	0.19773	-46.11	-44.33	-42.95	-42.12
0.30141	-46.28	-44.48	-43.09	-42.26	0.30564	-46.27	-44.47	-43.09	-42.26
0.40117	-46.38	-44.57	-43.18	-42.34	0.39479	-46.36	-44.56	-43.17	-42.35
0.49611	-46.45	-44.64	-43.24	-42.40	0.49148	-46.44	-44.64	-43.25	-42.42

m_A implies the molality of the solutes (GA/LA) in an aqueous Sodium methyl p-hydroxy benzoate (SMP) solution: standard uncertainties u is u(m) = 0.02 (mol·kg^{-1}); $u(K_{\phi,s})$ = ±0.25 × 10^6/(m^3. mol^{-1}.GPa^{-1}); u(p)=0.01MPa.

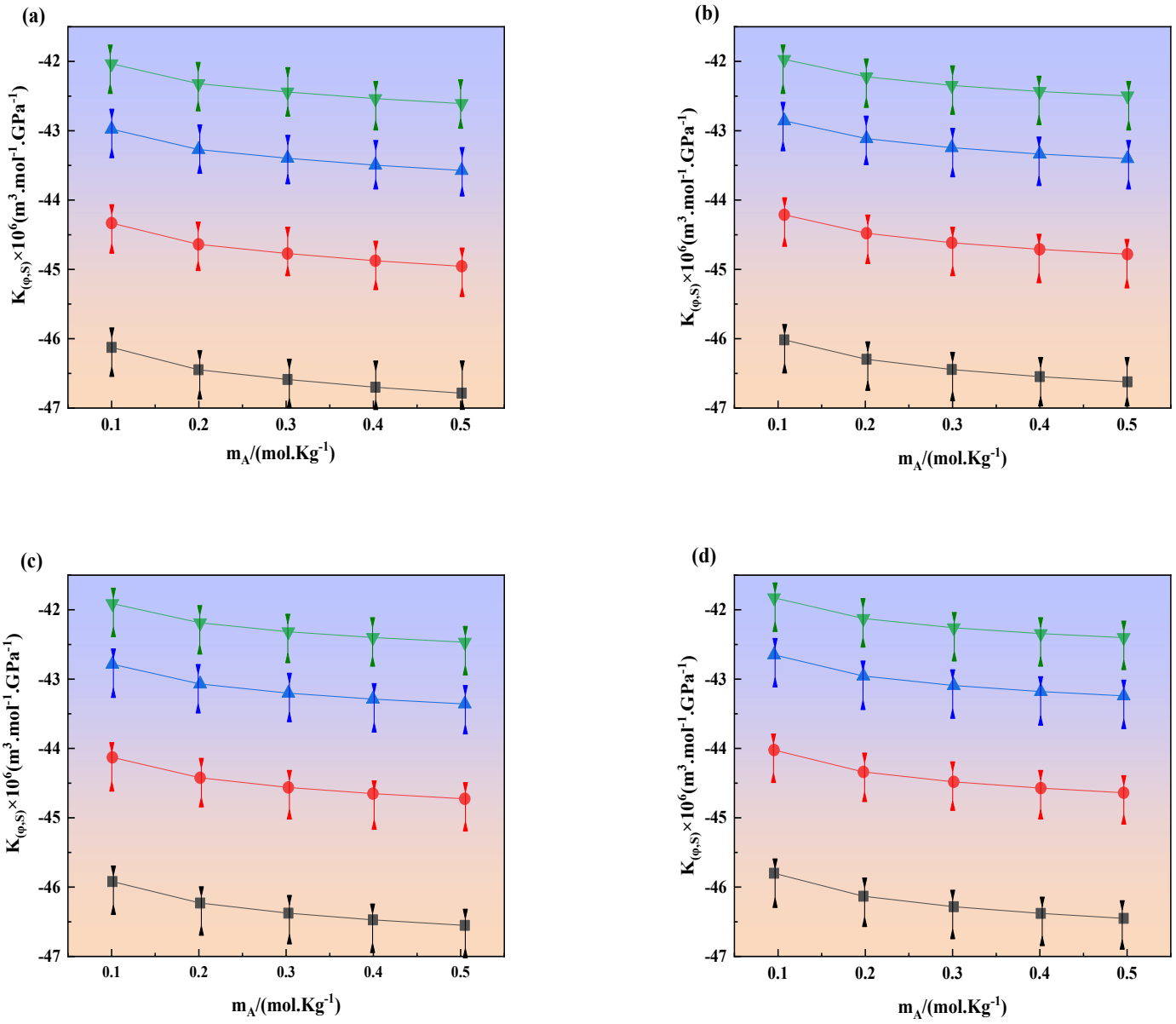

Figure 4.13 Changes of $K_{\phi,s}$ of Glycolic acid (GA) in (a) 0.000 SMP, (b) 0.015 SMP, (c) 0.025 SMP and (d) 0.035 SMP for molality of glycolic acid aqueous solutions.

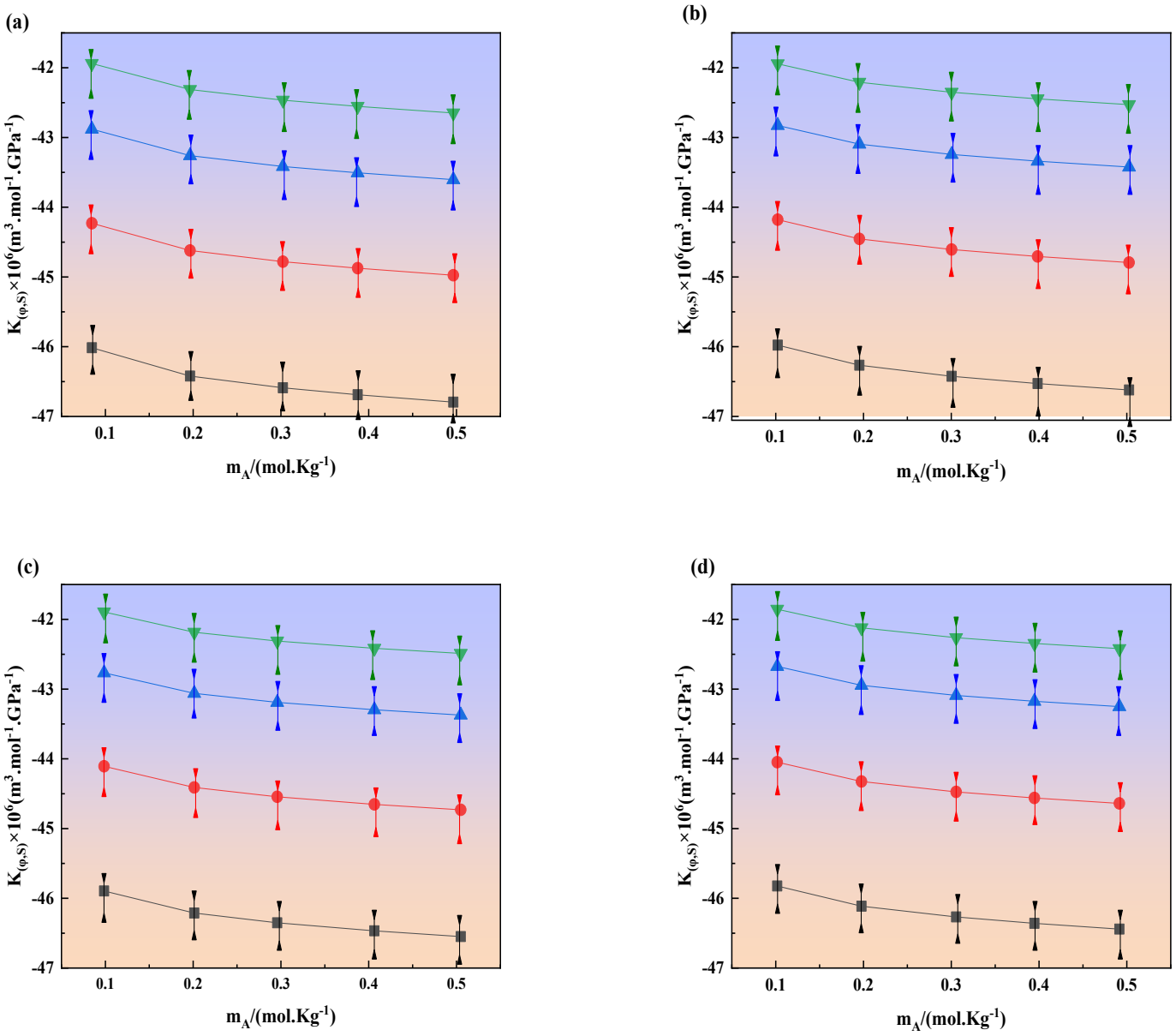

Figure 4.14 Changes of $K_{\phi,s}$ of Lactic Acid (LA) in (a) 0.000 SMP, (b) 0.015 SMP, (c) 0.025 SMP and (d) 0.035 SMP for molality of lactic acid aqueous solutions.

4.2.4 Partial molar volumes

The **equation 4.2** is utilized for the determination of $V_{\emptyset}^{0}$, of ternary combinations that contain SMP and alpha-hydroxy acids (GA/LA) at infinite dilution [55]. The slope of the data that was acquired via experimentation is indicated by S_V^* and the molality of GA/LA is given by m_A. The findings that were obtained for $V_{\emptyset}^{0}$ are provided in **Table 4.13** along with the deviations. It has been noted that the magnitude of S_V^* has consistently demonstrated a positive value throughout all operating temperatures for SMP molecules. The absence of regular patterns in S_V^* values suggest that there are more factors that impact the interactions of solutes [21,7,56]. For all temperatures, the $V_{\emptyset}^{0}$ is always positive and escalates as the concentration of SMP rises. This might be contributed to the enhanced interactions within the solute-solvent as depicted in **Figure 4.15**. In the theory of cosphere overlap, two groups of ions overlap with hydrating cospheres to create bulk reduction, pair overlap between hydrophobic and hydrophobic, and volume expansion. The reason for the positive value of $V_{\emptyset}^{0}$ is that it is derived from the presence of ion hydrophilic bonds, which are more prevalent than interactions between hydrophobic and hydrophobic ions or between ions and hydrophobic bonds [57,8,10]. It may be inferred from the detail that the values of $V_{\emptyset}^{0}$ are higher than the S_V^* values suggests that the interactions inside the solutes and solvents are more prominent than the interactions within the solute molecules.

Table 4.13 Values of $'V_{\phi}^{0}'$, and , $'S_V^*'$ values of SMP in an aqueous Glycolic Acid and Lactic Acid solutions with their standard errors.

m_B/ (mol. Kg^{-1})	$V_{\phi}^{0} \times 10^{6}/\ (m^3.mol^{-1})$				$S_V^* \times 10^6\ /(m^3.kg.mol^{-2})$			
	288.15(K)	**298.15(K)**	**308.15(K)**	**318.15(K)**	**288.15(K)**	**298.15(K)**	**308.15(K)**	**318.15(K)**
				Glycolic Acid				
0.000	54.39(±0.07)	55.31(±0.07)	56.41(±0.08)	57.40(±0.07)	9.41(±0.20)	9.45(±0.20)	8.93(±0.24)	8.78(±0.21)
0.015	54.99(±0.09)	55.86(±0.05)	56.82(±0.03)	57.70(±0.05)	9.67 (±0.27)	10.03(±0.15)	9.46(±0.10)	9.44(±0.15)
0.025	55.54(±0.06)	56.38(±0.06)	57.30(±0.05)	58.17(±0.09)	9.80(±0.17)	9.48(±0.19)	9.18(±0.16)	8.86(±0.26)
0.035	56.19(±0.04)	57.10(±0.06)	57.93(±0.08)	58.79(±0.09)	8.93(±0.12)	8.55(±0.18)	8.30(±0.25)	7.99(±0.27)
				Lactic Acid				
0.000	71.55 (±0.01)	71.85(±0.01)	72.19(±0.01)	72.56 (±0.03)	1.87(±0.03)	2.06(±0.03)	2.09(±0.04)	1.99 (±0.09)
0.015	72.32 (±0.01)	72.68(±0.01)	73.03(±0.03)	73.43 (±0.01)	3.30 (±0.04)	3.31(±0.02)	3.32(±0.08)	3.25(±0.04)
0.025	72.83(±0.01)	73.16 (±0.02)	73.50(±0.02)	73.84 (±0.01)	3.25 (±0.03)	3.32 (±0.05)	3.34(±0.05)	3.43(±0.02)
0.035	73.37 (±0.03)	73.72 (±0.03)	74.09 (±0.04)	74.46(±0.04)	2.94(±0.08)	2.93(±0.11)	2.78 (±0.11)	2.82(±0.14)

m_B states the concentration of aqueous SMP solution: calculated standard uncertainties *u* are *u(m)* = 0.02, *u(T)*=0.001 K, *u* (V_{ϕ}^{0})= (0.14-0.23) × 10^{-6}/(m^3·mol^{-1}) and *u* (S_V^*)=±0.37 × 10^{-6}/(m^3·kg·mol^{-2}).

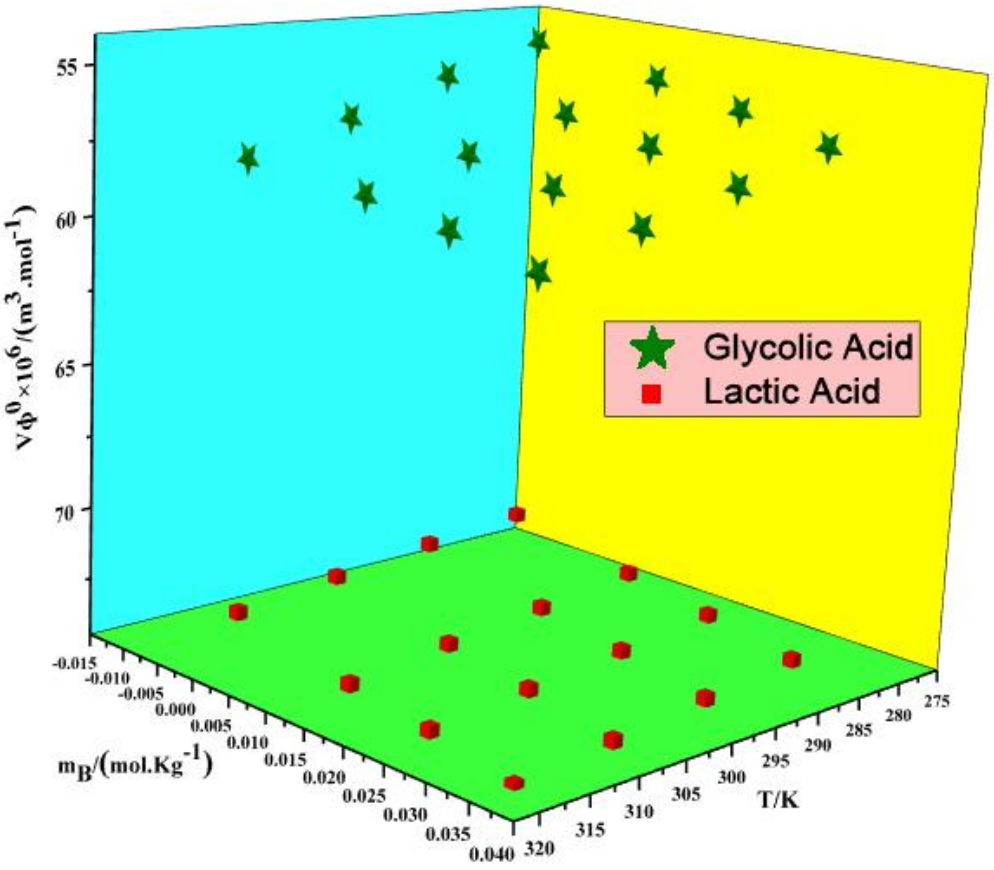

Figure 4.15 The scatter plot represents the variations in V_{ϕ}^{0} for Glycolic Acid (Red) and Lactic Acid (Green) within a SMP aqueous solution at several temperatures.

4.2.5 Partial molar isentropic compressibility

The **equation 4.10** illustrates the variations within molality (m_A) and partial molar isentropic compressibility, which is symbolized by ($K^0_{\emptyset,s}$) [58]. The term (S^*_K) is acoustic virial coefficient, which provides insights among the solutes interaction, ($K^0_{\phi,s}$) implies the limiting partial molar isentropic compressibility and their determined data are indexed in **Table 4.14**, included with their respective errors. All the $K^0_{\phi,s}$ values are negative as shown in **Figure 4.16**. The interaction between solute molecules becomes negligible due to the comparatively small (tiny) size of S^*_K, indicating that solute-solvent interactions dominate within the liquid combination [28,29,31]. It has been noticed that rise in temperature outcomes in a reduction in the occurrence of negative values of $K^0_{\phi,s}$, which strengthens the strong interactions within solutes and molecules of water. This causes the molecules of water to be released into the bulk solution. Kirkwood's model offers a valuable explanation for this phenomenon [30,59,33]. The primary aspects that contribute to the $K^0_{\phi,s}$ are mostly attributable to these effects: The positive impact, known as the inherent compressibility of the solvent, occurs as the amount of free space inside solution molecules rises, leading to greater compression of the solution [60]. The negative impact, referred to as solvent penetration, arises when solvent molecules penetrate the vacant spaces between ions due to interactions inside the solute and solvent [32].

Table 4.14 Obtained data of $K^0_{\phi,S}$ and S^*_K of the liquid system (SMP +water+GA/LA).

m_B/	$K^0_{\phi,S} \times 10^6/(m^3.mol^{-1}.GPa^{-1})$				$S^*_K \times 10^6/(kg.m^3.mol^{-2}.GPa^{-1})$			
(mol. Kg^{-1})	288.15(K)	298.15(K)	308.15(K)	318.15(K)	288.15(K)	298.15(K)	308.15(K)	318.15(K)
				Glycolic Acid				
0.000	-46.06 (±0.09)	-44.27(±0.09)	-42.92(±0.08)	-41.98(±0.08)	-1.58(±0.27)	-1.49(±0.26)	-1.42(±0.25)	-1.37(±0.25)
0.015	-45.94(±0.08)	-44.14(±0.08)	-42.79(±0.08)	-41.91(±0.07)	-1.48(±0.25)	-1.38(±0.24)	-1.33(±0.23)	-1.28(±0.22)
0.025	-45.86(±0.09)	-44.07(±0.08)	-42.73(±0.08)	-41.86(±0.08)	-1.49(±0.26)	-1.42(±0.25)	-1.35(±0.25)	-1.32(±0.24)
0.035	-45.75(±0.09)	-43.97(±0.09)	-42.60(±0.09)	-41.78(±0.09)	-1.55(±0.28)	-1.47(±0.27)	-1.40(±0.26)	-1.37(±0.26)
				Lactic Acid				
0.000	-45.97(±0.10)	-44.19(±0.10)	-42.84(±0.10)	-41.90(±0.10)	-1.81(±0.32)	-1.74(±0.31)	-1.68(±0.30)	-1.65(±0.30)
0.015	-45.90(±0.08)	-44.11(±0.08)	-42.76(±0.07)	-41.88(±0.07)	-1.54(±0.24)	-1.47(±0.23)	-1.42(±0.23)	-1.40(±0.22)
0.025	-45.83±0.09)	-44.05(±0.08)	-42.71(±0.08)	-41.84(±0.08)	-1.53(±0.26)	-1.47(±0.25)	-1.42(±0.24)	-1.39(±0.24)
0.035	-45.75(±0.08)	-43.97(±0.08)	-42.61(±0.07)	-41.79(±0.07)	-1.52(±0.24)	-1.46(±0.23)	-1.42(±0.22)	-1.39(±0.22)

m_B is the molality of water-soluble sodium methyl-hydroxybenzoate: the calculated standard uncertainties u are $u(m)$ = 0.02, $u(T)$ = 0.001 K, $u(K^0_{\phi,S})$ = 0.27 × 10^{-6}/(m^3·mol^{-1}·GPa^{-1}), $u(S^*_K)$ = ±0.23 × 10^{-6}/(kg·m^3·kg·mol^{-2}·GPa^{-1}).

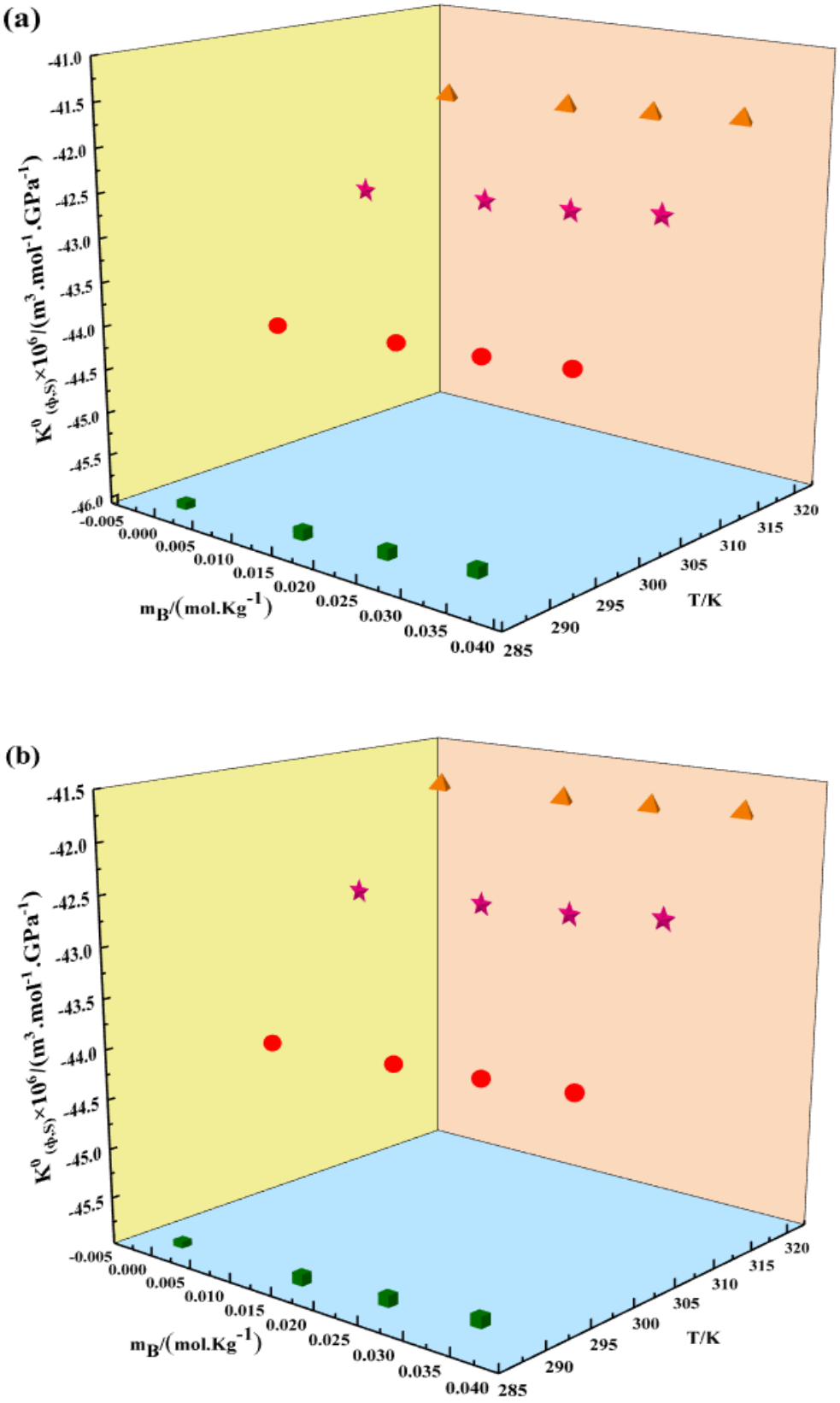

Figure 4.16 Plots of variations of $K^0_{\emptyset,S}$ for (a) glycolic acid and (b) lactic acid in aqueous SMP solution at varying temperatures.

4.2.6 Transfer of partial molar volume

This transfer property is essential to the understanding of solutions as it offers insights on the solutes and solvents interactions. The data that was attained for $\Delta V_{\emptyset}^{0}$ is tabulated in **Table 4.15.** The **equation 4.3** is utilized to evaluate the amount of alpha-hydroxy acids that were transferred from water to SMP solutions [61]. In the context of the current research, which involves the combination of SMP, water, with glycolic acid (GA)/lactic acid (LA), it is essential to account for the fact that both the solute and the solvent are electrolytes. Hence, it is noticed that the $\Delta V_{\emptyset}^{0}$ values indicate the existence of ion-ion interaction within aqueous SMP and AHAs (GA/LA). The positive values of $\Delta V_{\emptyset}^{0}$ may be ascribed to the ability of the solutes to construct or break structured compositions as a result of the solvophobic characteristics of a solute and the structural interactions that occur between the two cospheres [62,9]. The $\Delta V_{\emptyset}^{0}$ values indicate that the interaction between the solute-solute is extremely less and nearly insufficient based on the principle of co-sphere overlap. Furthermore, valuable insights on the solute-solvent interaction may be acquired from the aforementioned information. The current research demonstrates the occurrence of hydrophilic-hydrophilic along with ion-hydrophilic interactions, which is evidenced by the positive values documented for $\Delta V_{\emptyset}^{0}$ in the (SMP + water + GA/LA) system [13,63,34].

4.2.7 Transfer of partial molar isentropic compression

In order to examine the $\Delta K_{\emptyset,s}^{0}$ that were shifted from water to SMP solutions, the **equation 4.11** utilized [64]. The values of $\Delta K_{\emptyset,s}^{0}$ are determined to be positive at varied concentrations (0.015, 0.025, 0.035) mol. Kg^{-1} are tabulated in **Table 4.15.** It demonstrates the solution's tendency to form structures, although they also emphasize the preponderance of zwitterionic interactions between alpha-hydroxy acids and SMP molecules. The electrostriction declines as the concentration of SMP surges, facilitating the ability to build structures [35]. Increasing the concentration of the SMP results in the less compression of the solution mixture in comparison to the pure solvent, which in turn causes the structure building propensity of solutes. On account of this, there is a significant decrease in compressibility in relation to an increase in the concentration of SMP [37,65]. The water molecules interact with the glycolic and lactic acids (solutes) when the $\Delta K_{\emptyset,s}^{0}$ values are positive. This implies that the water molecules of solutes combine with the solvent that rises as a result of the molecular interactions [66]. The reason for the negative $K_{\phi,s}^{0}$ values observed between the solute and solvent interaction may be contributed to the increased attachment of water molecules to the ion [6,36]. In the current

investigation, the increase in the values of $\Delta K^{0}_{\emptyset,s}$ is a contributing factor to the enhancement of their capability to construct structures and the intensity of interactions within solute-solvent.

Table 4.15 Transfer parameters ΔV_{ϕ}^{0} and $\Delta K_{\phi,S}^{0}$ of SMP in Glycolic Acid/Lactic Acid aqueous solution.

m_B/ (mol.Kg^{-1})	$\Delta V_{\phi}^{0} \times 10^{6}/(m^{3}.mol^{-1})$				$\Delta K_{\phi,S}^{0} \times 10^{6}/(m^{3}.mol^{-1}.GPa^{-1})$			
	288.15(K)	298.15(K)	308.15(K)	318.15(K)	288.15(K)	298.15(K)	308.15(K)	318.15(K)
Glycolic Acid								
0.015	0.61	0.55	0.41	0.31	0.12	0.13	0.13	0.07
0.025	1.16	1.07	0.89	0.77	0.20	0.20	0.19	0.12
0.035	1.81	1.79	1.52	1.39	0.31	0.30	0.32	0.20
Lactic Acid								
0.015	0.77	0.83	0.84	0.87	0.07	0.08	0.08	0.02
0.025	1.28	1.31	1.31	1.27	0.14	0.14	0.13	0.06
0.035	1.82	1.87	1.90	1.90	0.22	0.21	0.23	0.11

m_B is the molality of water-soluble sodium methyl p-hydroxybenzoate: the calculated standard uncertainties u are $u(m)$ = 0.02, $u(T)$ = 0.001 K, $u(\Delta V_{\phi}^{0}) = \pm 0.13\times10^{-6}$/(m^{3}·mol^{-1}), $u(\Delta K_{\phi,S}^{0}) = 0.02\times10^{-6}$/(m^{3}·mol^{-1}·GPa^{-1}).

4.2.8 Temperature dependent partial molar volume

The relationship between the V_ϕ^0 and temperature may be stated using the **equation 4.4** [67]. Here a^*, b^*, c^* are empirical parameters for GA/LA in an aqueous SMP solutions which are presented in **Table 4.16** and reference temperature (T_{ref}=298.15K). The **equation 4.5** is used to obtain the ARD (Average Relative Deviation) values [68]. The deviations between the measured ($Y_{exptl.}$) and determined ($Y_{calc.}$) values are derived using these empirical constants. The investigation of V_ϕ^0 aims to examine the limiting apparent molar expansibilities and its determination is crucial for comprehending the interactions within solute-solvent in a solution [14,69,17]. The **equation 4.6** can be acquired through differentiating the **equation 4.4** with respect to the temperature in order to determine the E_ϕ^0. The apparent molar expansibility values along with $(\partial E_\phi^0/\partial T)_P$ for the liquid system is enumerated in **Table 4.17**. The validation of the information acquired on the apparent molar property of volumes is provided by the positive E_ϕ^0 values, which indicate the survival of solute and solvent associations in the liquid combination that is being investigated. The E_ϕ^0 values are more prevalent, which additionally emphasizes the extent of the solute-solvent interactions due to the packaging/caging effect [70,18]. The **equation 4.7** is used by Hepler [19] as a thermodynamic representation to verify the propensity of the solute to structure-building or breaking properties in the liquid mixture. The sign of $(\partial E_\phi^0/\partial T)_P$ provides understanding into the solution's ability to form or disrupt structures. The positive value for $(\partial E_\phi^0/\partial T)_P$ indicates that the solute has the tendency to build structures, although the negative value shows that the solute has an ability to break structures [71,72]. The Hepler's constant for glycolic acid and lactic acid in an aqueous medium was shown to be positive, excluding for glycolic acid at 0.035 mol. Kg^{-1} in the present investigation, as indexed in **Table 4.17** which infers the overall structure-building tendency in the mixture.

Table 4.16 Calculation of empirical coefficients, a^*, b^*, c^* of SMP solutions with GA and LA along with ARD (Average relative deviations).

$a_{m_B/(mol \cdot kg^{-1})}$	$a^* \times 10^6 (m^3 . mol^{-1})$	$b^* \times 10^6 (m^3 . mol^{-1} . K^{-1})$	$c^* \times 10^6 (m^3 . mol^{-1} . K^{-2})$	R^2	*ARD*
Glycolic Acid					
0.015	55.8851	0.0907	0.0000	0.9999	0.0000
0.025	56.4017	0.0873	0.0001	0.9999	0.0000
0.035	57.0854	0.0873	-0.0001	0.9999	0.0000
Lactic Acid					
0.015	72.6745	0.0358	0.0001	0.9999	0.0000
0.025	73.1661	0.0335	0.0000	0.9999	0.0000
0.035	73.7220	0.0357	0.0001	0.9999	0.0000

m_B is the molality of water-soluble sodium methyl p-hydroxybenzoate: calculated standard uncertainties are $u(m)$ = 0.02, $u(T)$ = 0.001 K, $u(p)$ = 0.01 MPa.

Table 4.17 Partial molar expansibilities 'E_ϕ^0' values of Sodium methyl p-hydroxybenzoate in aqueous solutions with GA and LA.

m_B/ (mol.Kg^{-1})	$E_\phi^0 \times 10^6/(m^3.mol^{-1}.K^{-1})$				$\left(\frac{\partial E_\phi^0}{\partial T}\right)_P$ $/(m^3.mol^{-1}.K^{-2})$
	288.15(K)	298.15(K)	308.15(K)	318.15(K)	
			Glycolic Acid		
0.015	0.0900	0.0907	0.0914	0.0920	0.00007
0.025	0.0859	0.0873	0.0888	0.0902	0.00014
0.035	0.0899	0.0873	0.0848	0.0823	-0.00025
			Lactic Acid		
0.015	0.03387	0.03577	0.03767	0.03957	0.00019
0.025	0.03345	0.03349	0.03353	0.03357	0.00000
0.035	0.03429	0.03574	0.03719	0.03863	0.00014

m_B is the molality of water-soluble sodium methyl p-hydroxybenzoate: calculated standard uncertainties are $u(m)$ = 0.02, $u(T)$ = 0.001 K, $u(E_\phi^0)$ = 0.0024 ×10^{-6}/(m^3·mol^{-1}·K^{-1}), $u(\frac{\partial E_\phi^0}{\partial T})$ = 0.00012/(m^3·mol^{-1}·K^{-2}), $u(p)$ = 0.01 MPa.

4.2.9 Interaction Coefficients

The transfer parameters (ΔV_{ϕ}^{0}) and ($\Delta K_{\phi,S}^{0}$) are calculated by the stated **equation 4.12** and **4.13** [38]. The interaction coefficients values are indicated in **Table 4.18**. It is significant to consider that these interaction coefficients give an indication of the intensity of the associations and can change based on the particular chemical properties of the molecules of the solute that are being studied. Solute molecule behavior in solution can only be predicted and controlled by having an extensive understanding of the type and extent of these interactions. Interaction coefficients are positive for glycolic and lactic acid over all temperatures except for the triplet coefficient of isentropic compression, where the values for lactic acid are negative at four temperatures varying from 298.15 to 318.15 K. McMillan and Mayer determined the coefficients for isentropic compression and volumetric pair (K_{AB} and V_{AB}) and (K_{ABB} and V_{ABB}) triplet interactions. This concept emphases exclusively on the phenomena of effect separations in a liquid combination, which occurs due to pairs and triplets interactions. Friedman and Krishnan [40] and Franks et al. explored this concept in more detail [39].

Table 4.18 Interaction Coefficients (V_{AB}, K_{AB} ;V_{ABB} and K_{ABB}) for SMP solutions with Glycolic Acid and Lactic Acid.

T/K	$V_{AB} \times 10^6 (m^3.mol^{-2}.kg)$	$V_{ABB} \times 10^6 (m^3.mol^{-3}.kg^2)$	$K_{AB} \times 10^6$ ($m^3 \cdot mol^{-2} \cdot kg \cdot GPa^{-1}$)	$K_{ABB} \times 10^6$ ($m^3 \cdot mol^{-3} \cdot kg^2 \cdot GPa^{-1}$)
		Glycolic Acid		
288.15	16.07	186.37	3.33	20.70
298.15	12.33	251.50	4.05	3.46
308.15	7.87	264.37	3.35	20.19
318.15	3.47	312.68	1.91	16.65
		Lactic Acid		
288.15	25.06	16.62	1.52	31.68
298.15	27.37	-15.29	2.28	13.97
308.15	27.11	-3.78	1.68	30.48
318.15	27.06	-4.79	0.13	28.27

Standard uncertainties are u(T)=0.001 K.

References

1. A. Haghani, H. Iloukhani and M. M. Hoffmann, J. Chem. Eng. Data 61, 2960 (2016).
2. I. A. Mou, Kuet.ac.bd (2018).
3. H. Singh, Q. Majid, Richu, M. Singh, T. S. Kang and A. Kumar, J. Chem. Eng. Data 68, 2563 (2023).
4. M. A. Jamal, M. Rashad, M. K. Khosa, I. A. Bhatti and K. M. Zia, Food Chem. 153, 140 (2014).
5. H. Kumar, I. Behal and M. Singla, J. Chem. Thermodyn. 95, 1 (2016).
6. H. Kaur, N. Chakraborty, K. C. Juglan and A. Upmanyu, J. Mol. Liq. 392, 123403 (2023).
7. R. C. Thakur, R. Sharma, A. Kumar, S. Kumar and M. L. Parmar, Orient. J. Chem. 30, 2037 (2014).
8. M. T. Zafarani-Moattar and H. Shekaari, J. Chem. Thermodyn. 37, 1029 (2005).
9. A. K. Mishra and J. C. Ahluwalia, J. Phys. Chem. 88, 86 (1984).
10. H. Kumar and I. Behal, J. Chem. Thermodyn. 102, 48 (2016).
11. W. Blokzijl and J. B. F. N. Engberts, Angew. Chem. Int. Ed. Engl. 32, 1545 (1993).
12. L. R. Pratt and A. Pohorille, Chem. Rev. 102, 2671 (2002).
13. R. Rani, A. Kumar, T. Sharma, B. Saini and R. K. Bamezai, Acta Chim. Slov. 63, 589 (2016).
14. S. Devi, M. Kumar, N. Sawhney, U. Syal, A. K. Sharma and M. Sharma, J. Chem. Thermodyn. 154, 106321 (2021).
15. T. Sharma, R. Rani, A. Kumar and R. K. Bamezai, J. Mol. Liq. 300, 111985 (2020).
16. B. A. Ali, Z. Phys. Chem. 222, 1519 (2008).
17. B. Sinha, A. Sarkar, P. K. Roy and D. Brahman, Int. J. Thermophys. 32, 2062 (2011).
18. X. Chen, Z. Huang, W. Hua, H. Castada and H. C. Allen, Langmuir 26, 18902 (2010).
19. L. G. Hepler, Can. J. Chem. 47, 4613 (1969).
20. K. Kaur, K. C. Juglan and H. Kumar, J. Chem. Thermodyn. 127, 8 (2018).
21. A. Thakur, K. C. Juglan and H. Kumar, Results Chem. 2, 100049 (2020).
22. M. Sethu Raman, M. Kesavan, K. Senthilkumar and V. Ponnuswamy, J. Mol. Liq. 202, 115 (2015).
23. K. Kaur, I. Behal, K. C. Juglan and H. Kumar, J. Chem. Thermodyn. 125, 93 (2018).
24. N. Muñoz-Rujas, J. P. Bazile, F. Aguilar, G. Galliero, E. Montero and J. L. Daridon, Fluid Ph. Equilib. 449, 148 (2017).
25. R. Sadeghi and A. Gholamireza, J. Chem. Thermodyn. 43, 200 (2011).

26. I. Bahadur and N. Deenadayalu, Thermochim. Acta 566, 77 (2013).
27. S. S. Dhondge, R. L. Paliwal and N. S. Bhave, J. Chem. Thermodyn. 59, 158 (2013).
28. S. K. Lomesh, M. Bala and V. Nathan, J. Mol. Liq. 283, 133 (2019).
29. A. K. Nain, J. Mol. Liq. 298, 112006 (2020).
30. J. G. Kirkwood, Chem. Rev. 24, 233 (1939).
31. C. M. Romero and F. Negrete, Phys. Chem. Liq. 42, 261 (2004).
32. S. Panda, V. Singh, N. Islam and R. L. Gardas, Fluid Ph. Equilib. 445, 35 (2017).
33. S. Baluja and S. Oza, Fluid Ph. Equilib. 178, 233 (2001).
34. H. Kumar and I. Behal, J. Mol. Liq. 219, 756 (2016).
35. N. Chakraborty, K. C. Juglan and H. Kumar, Braz. J. Chem. Eng. 39, 869 (2022).
36. S. K. Sharma and A. Thakur, J. Mol. Liq. 322, 114527 (2021).
37. A. Salabat, L. Shamshiri and F. Sahrakar, J. Mol. Liq. 118, 67 (2005).
38. W. G. McMillan and J. E. Mayer, J. Chem. Phys. 13, 276 (1945).
39. F. Franks, M. Pedley and D. S. Reid, J. Chem. Soc. Faraday Trans. 72, 359 (1976).
40. C. V Krishnan and H. L. Friedman, J. Solution Chem. 2, 37 (1973).
41. H. Kumar, M. Singla and H. Mittal, J. Chem. Thermodyn. 94, 204 (2016).
42. A. Thakur, K.C. Juglan and H. Kumar, J. Chem. Thermodyn. 140, 105916 (2020).
43. A. Thakur, K.C. Juglan, H. Kumar and K. Kaur, J. Mol Liq. 288, 111014 (2019).
44. I. Bahadur and N. Deenadayalu, J. Solution Chem. 40,1528–1543 (2011).
45. S. Parveen, S. Singh, D. Shukla, M. Yasmin, M. Gupta and J.P. Shukla, J. Solution Chem. 41, 156–172 (2012).
46. F.M. Sannaningannavar, B.S. Navati and N.H. Ayachit, J. Therm. Anal. Calorim. 112, 1573–1578 (2013).
47. N. Chakraborty, K.C. Juglan and H. Kumar, J. Mol Liq. 332, 115869 (2021).
48. H.S. Harned, B.B. Owen and C.V. King, J. Electrochem. Soc. 106, 15C (1959).
49. K. Kaur, K.C. Juglan and H. Kumar, J. Mol Liq. 268, 700–706 (2018).
50. P.S. Laplace, Ann. Chim. Phys. 3, 238 (1816).
51. F.J. Millero, Chem. Rev. 71, 147-176 (1971).
52. T.S. Banipal, D. Kaur, P.K. Banipal and G. Singh, J. Chem. Thermodyn. 39, 371–384 (2007).
53. H.S. Franks and M.W. Evans, J. Chem. Phys. 1945 13, 507–532 (1945).
54. H. Kumar, K. Kaur, S. Arti and M. Singla, J. Mol Liq. 221, 526–534 (2016).
55. D.O. Masson, London Edinburgh Philos. Mag. & J. Sci.8, 218-235 (1929).
56. Z. Yan, J. Wang, H. Zheng and D. Liu, J. Solution Chem. 27, 473–483 (1998).

57. E. Ayranci E and M.J. Sahin, Chem. Thermodyn. 40, 1200–1207 (2008).
58. B.E. Conway, J. Solution Chem. 7, 721-770 (1978).
59. N. Chakraborty, K.C. Juglan and H. Kumar, J. Chem. Thermodyn. 154, 106326 (2021).
60. J. Wang, D. Zhang, Q. Chu and J. Ye, Chin. J. Chem. 28, 313–319 (2010).
61. F.J. Millero, J. Phys. Chem. 76, 3795-3799 (1972).
62. M.J. Iqbal and M.A. Chaudhry, J. Chem. Thermodyn. 42, 951–956 (2010).
63. N. Chakraborty, K.C. Juglan and H. Kumar, J. Mol Liq. 337, 116605 (2021).
64. R.H. Stokes and R.A. Robinson, J. Am. Chem. Soc. 71, 8-12 (1949).
65. R. Sadeghi and F.J. Ziamajidi, Chem. Eng. Data. 52, 1037–1044 (2007).
66. H. Kumar, M. Singla and R. Jindal, Monatsh Chem. 145, 1063–1082 (2014).
67. F.J. Millero, J. Phys. Chem. 75, 3107-3112 (1971).
68. K.R. Brower, J. Chem. Phys. 47, 4526-4530 (1967).
69. I. Gheorghe, C. Stoicescu and F. Sirbu, J. Mol Liq. 218, 515–524 (2016).
70. T. Sharma, H. Singh, R.K. Bamezai and A. Kumar, J. Mol Liq. 349, 118412 (2022).
71. A. Beri, P.K. Banipal and T.S. Banipal, Food Chem. 266, 110–118 (2018).
72. B. Ghosh, A. Sinha, N. Roy, B. Rajbanshi, M. Mondal, D. Roy, A. Das, N. Ghosh, V. Dakua and M. Roy, Fluid Ph. Equilib. 557, 113415 (2022).

Section III

Problem 3

4.3 Title: "Volumetric and ultrasonic investigation of glycolic and malic acids with water-soluble potassium benzoate solutions at different temperatures"

In this section, the ρ and c of glycolic and malic acids in aqueous potassium benzoate solutions with 0.04, 0.05, and 0.06 mol·kg^{-1} were reported at various temperatures using the Anton Paar DSA 5000M.

4.3.1 Density measurements

The density measurements for alpha-hydroxy acids (GA/MA) in aqueous potassium benzoate solutions are recorded in **Table 4.19.** The density of the mixture increases for a given concentration of potassium benzoate as the molality of glycolic and malic acids rises, and it slightly reduces when the temperature rises, according to the density data. The measured densities of glycolic and malic acids with water are correlated with the reported data of the liquid system as represented in **Figure 4.17** [1-3]. For the combination that is being investigated, it is clear that the experimental densities reflect the same pattern that has been stated in previous studies. An upsurge in the molecular mass of the mixture is the primary contributor to the rise in density values that occurs as the concentration of glycolic and malic acids rises. The intensification of interactions within solvents and solutes is also indicated by an increase in density [4,5].

Table 4.19 Densities 'ρ' were investigated in the ternary combination of potassium benzoate in water-soluble glycolic and malic acids at four varying temperatures.

Molality m_A/ (mol·kg^{-1})	$\rho \times 10^{-3}$/(kg·m^{-3})				Molality m_A/ (mol·kg^{-1})	$\rho \times 10^{-3}$/(kg·m^{-3})			
	T=288.15K	T=298.15K	T=308.15K	T=318.15K		T=288.15K	T=298.15K	T=308.15K	T=318.15K
	0.00 (mol·kg^{-1}) PB + Glycolic Acid					**0.00 (mol·kg^{-1}) PB + Malic Acid**			
0.10319	1.00138	0.99909	0.99598	0.99223	0.10506	1.00445	1.00212	0.99899	0.99521
0.20403	1.00324	1.00085	0.99767	0.99383	0.20070	1.00900	1.00654	1.00331	0.99943
0.30101	1.00483	1.00235	0.99909	0.99517	0.30051	1.01354	1.01095	1.00763	1.00364
0.40254	1.00627	1.00374	1.00043	0.99644	0.39822	1.01780	1.01510	1.01167	1.00761
0.50847	1.00759	1.00504	1.00166	0.99757	0.49038	1.02166	1.01881	1.01530	1.01115
	0.04 (mol·kg^{-1}) PB + Glycolic Acid					**0.04 (mol·kg^{-1}) PB + Malic Acid**			
0.00000	1.00175	0.99951	0.99628	0.99241	0.00000	1.00175	0.99951	0.99628	0.99241
0.10018	1.00315	1.00086	0.99758	0.99368	0.10650	1.00678	1.00443	1.00110	0.99714
0.19938	1.00442	1.00207	0.99875	0.99481	0.19723	1.01090	1.00846	1.00504	1.00100
0.30121	1.00560	1.00320	0.99984	0.99586	0.30402	1.01556	1.01300	1.00947	1.00535
0.40118	1.00663	1.00420	1.00078	0.99678	0.40170	1.01963	1.01698	1.01337	1.00914
0.50251	1.00761	1.00513	1.00170	0.99766	0.49141	1.02323	1.02050	1.01682	1.01253
	0.05 (mol·kg^{-1}) PB + Glycolic Acid					**0.05 (mol·kg^{-1}) PB + Malic Acid**			
0.00000	1.00236	1.00015	0.99682	0.99296	0.00000	1.00236	1.00015	0.99682	0.99296
0.10390	1.00374	1.00146	0.99808	0.99416	0.09504	1.00684	1.00454	1.00113	0.99718
0.19919	1.00489	1.00255	0.99912	0.99516	0.19764	1.01149	1.00908	1.00557	1.00154
0.30132	1.00599	1.00359	1.00010	0.99610	0.30178	1.01600	1.01350	1.00989	1.00579

0.40084	1.00695	1.00448	1.00096	0.99692	0.40447	1.02027	1.01765	1.01396	1.00976
0.50425	1.00784	1.00531	1.00173	0.99770	0.49797	1.02400	1.02127	1.01749	1.01323
	0.06 (mol·kg^{-1}) PB + Glycolic Acid					**0.06 (mol·kg^{-1}) PB + Malic Acid**			
0.00000	1.00301	1.00094	0.99765	0.99374	0.00000	1.00301	1.00094	0.99765	0.99374
0.10901	1.00438	1.00223	0.99887	0.99491	0.10315	1.00786	1.00568	1.00230	0.99829
0.20228	1.00542	1.00321	0.99979	0.99579	0.20569	1.01247	1.01019	1.00671	1.00264
0.30387	1.00643	1.00413	1.00067	0.99663	0.30582	1.01677	1.01442	1.01083	1.00670
0.40155	1.00729	1.00491	1.00141	0.99732	0.39428	1.02042	1.01796	1.01432	1.01012
0.50191	1.00804	1.00558	1.00204	0.99792	0.50092	1.02465	1.02209	1.01837	1.01408

m_A specifies the molality of both the acids in the water-soluble potassium benzoate solution: standard uncertainties u are $u_r(m)$ = 0.02, $u(\rho)$=0.55(kg·m^{-3}), $u(T)$=0.001 K, $u(p)$ =0.01 MPa.

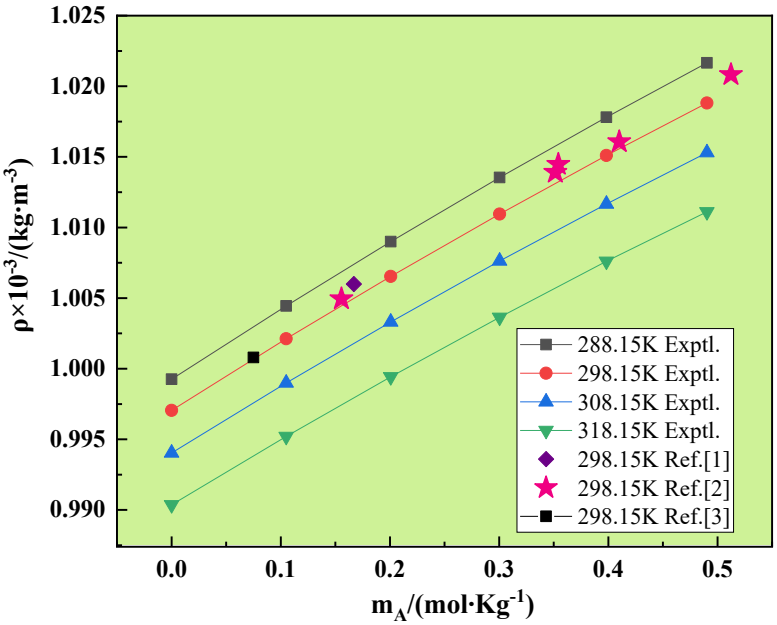

Figure 4.17 The density of malic acid with water was presented at several temperatures applying measured and literature results [1-3].

4.3.2 Apparent molar volume

It is possible to compute the apparent molar volumes by employing the **equation 4.1**, which was derived from the density measurements. M, m_A, ρ_0 and ρ signify the molecular mass of the glycolic and malic acids, molality of the solutes (GA/MA) per kg of the potassium benzoate, and density of the solvent and solution. The rising molecular interactions from glycolic to malic acids in water-soluble potassium benzoate solution are highlighted in **Figure 4.18**. It can be deduced that as the concentration of potassium benzoate (PB) rises, V_ϕ also rises in accordance with temperature and molalities of glycolic and malic acids, indicating stronger bonds within solute and solvent bonds from the values provided in **Table 4.20**. This pattern can be obtained in **Figures 4.19** and **4.20**, which demonstrate favorable solute and solvent groups due to the denser packing of molecules of solute in the solution compared to their pure state. Glycolic acid with its hydroxyl (-OH) and carboxyl (-COOH) groups, engages in hydrogen bonding with benzoate ions and water molecules. Malic acid, containing two carboxyl (-COOH) groups and one hydroxyl (-OH), exhibits stronger molecular interactions due to enhanced hydrogen bonding. The greater than (>) symbol emphasizes the increasing strength of interactions from glycolic acid to malic acid, attributed to the additional carboxyl group.

The interactions occur amid the solute and solvent within a solution can be comprehensively analyzed, providing valuable insights into their dynamic behavior [6]. This is due to the fact that the present liquid mixtures exhibit robust solute and solvent interactions, which is shown by the significant intrinsic volume of the solute. The upsurge in concentration leads to a drop in the electrostriction of molecules of water. This drop is mostly attributed to the interactions that occur within the solvent and the solute, which ultimately upsurge in the V_ϕ values [7–9]. There are a number of different physical processes that might be ascribed to the rise in the values of V_ϕ. These interactions comprise various phenomena, including the influence of the hydrophilic effect, dipoles, and dipole-induced dipole interactions, all occurring in regions with high water content. Such interactions show a vigorous role in defining the solubility and stability of solutes in aqueous solutions, significantly impacting their chemical behavior and interactions [10-12].

Table 4.20 Apparent molar volumes 'V_ϕ' investigated in the liquid system of soluble glycolic and malic acids in potassium benzoate at varying temperatures.

Molality m_A/ (mol·kg^{-1})	$V_\phi \times 10^6$/(m^3·mol^{-1})				Molality m_A/ (mol·kg^{-1})	$V_\phi \times 10^6$/(m^3·mol^{-1})			
	T=288.15K	T=298.15K	T=308.15K	T=318.15K		T=288.15K	T=298.15K	T=308.15K	T=318.15K
	0.00 (mol·kg^{-1}) PB + Glycolic Acid					**0.00 (mol·kg^{-1}) PB + Malic Acid**			
0.10319	55.39	56.32	57.33	58.18	0.10506	84.27	85.52	86.77	87.93
0.20403	56.37	57.31	58.29	59.25	0.20070	84.76	86.11	87.34	88.52
0.30101	57.26	58.26	59.23	60.21	0.30051	85.37	86.75	87.92	89.15
0.40254	58.25	59.17	60.05	61.02	0.39822	85.96	87.32	88.53	89.68
0.50847	59.21	59.98	60.88	61.89	0.49038	86.51	87.93	89.11	90.35
	0.04 (mol·kg^{-1}) PB + Glycolic Acid					**0.04 (mol·kg^{-1}) PB + Malic Acid**			
0.10018	61.90	62.51	63.14	63.71	0.10650	86.35	87.44	88.52	89.57
0.19938	62.43	63.06	63.67	64.27	0.19723	86.83	87.95	89.07	90.11
0.30121	62.95	63.58	64.21	64.76	0.30402	87.38	88.53	89.68	90.72
0.40118	63.49	64.09	64.73	65.29	0.40170	87.92	89.06	90.19	91.28
0.50251	63.92	64.52	65.12	65.68	0.49141	88.41	89.52	90.62	91.69
	0.05 (mol·kg^{-1}) PB + Glycolic Acid					**0.05 (mol·kg^{-1}) PB + Malic Acid**			
0.10390	62.55	63.36	64.02	64.75	0.09504	86.43	87.51	88.54	89.63
0.19919	63.08	63.85	64.53	65.23	0.19764	86.98	88.09	89.16	90.24
0.30132	63.64	64.42	65.11	65.80	0.30178	87.58	88.67	89.74	90.76

0.40084	64.17	64.97	65.62	66.31	0.40447	88.12	89.25	90.32	91.37
0.50425	64.71	65.48	66.17	66.74	0.49797	88.60	89.78	90.87	91.89
	0.06 (mol·kg^{-1}) PB + Glycolic Acid					**0.06 (mol·kg^{-1}) PB + Malic Acid**			
0.10901	63.26	64.12	64.91	65.60	0.10315	86.51	87.68	88.73	89.81
0.20228	63.81	64.65	65.48	66.13	0.20569	87.13	88.26	89.34	90.29
0.30387	64.42	65.29	66.03	66.71	0.30582	87.75	88.79	89.91	90.84
0.40155	64.96	65.84	66.57	67.26	0.39428	88.27	89.35	90.42	91.35
0.50191	65.53	66.45	67.14	67.82	0.50092	88.83	89.92	90.95	91.93

m_A denotes the molality of both the acids in the potassium benzoate solution: the calculated standard uncertainties u are $u_r(m)$ = 0.02, $u(V_\phi)$ = ± 1.03 × 10^6/(m^3·mol^{-1}), $u(T)$=0.001 K, $u(p)$ =0.01 MPa.

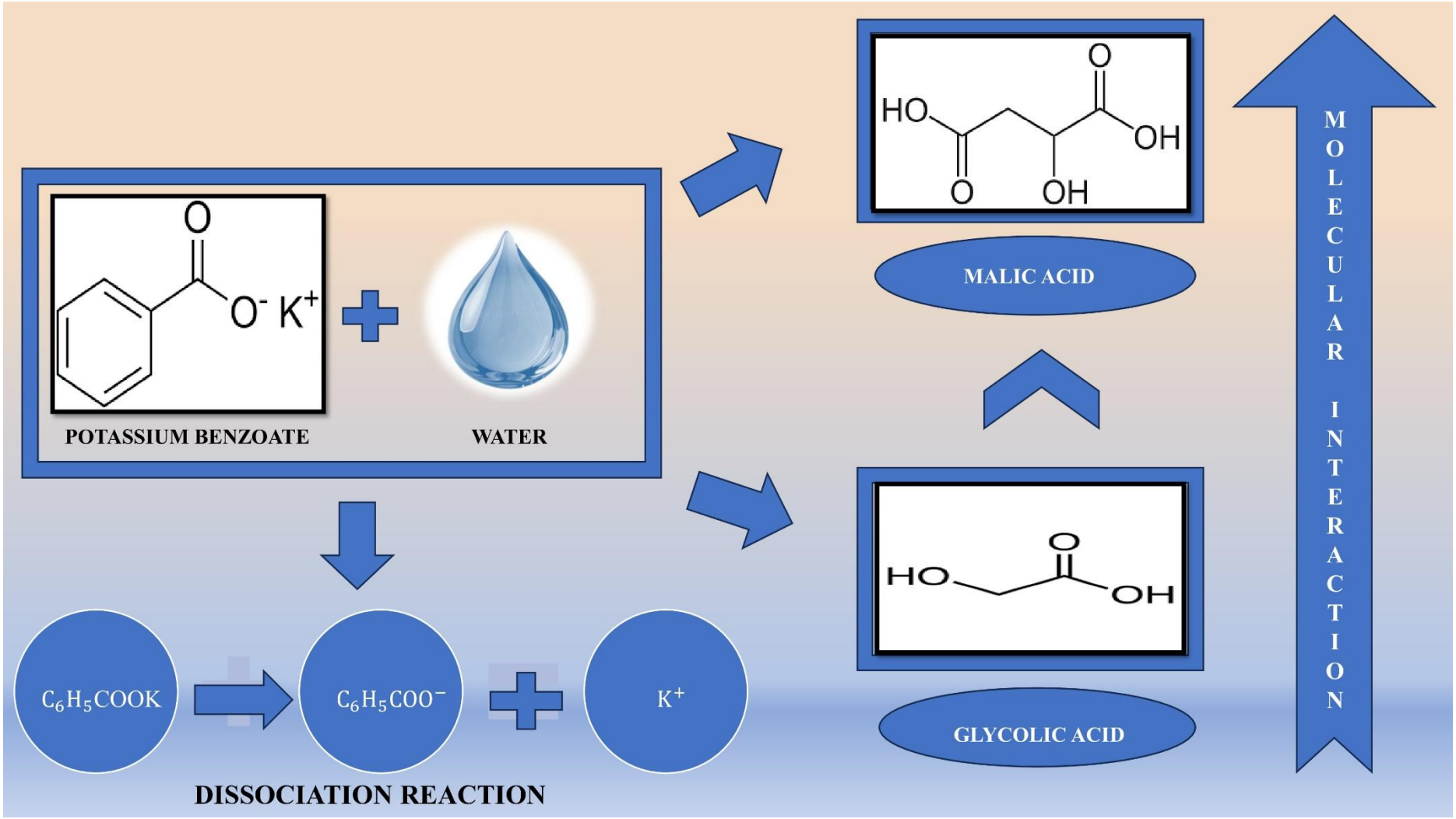

Figure 4.18 Glycolic and Malic Acids with Potassium Benzoate interactions.

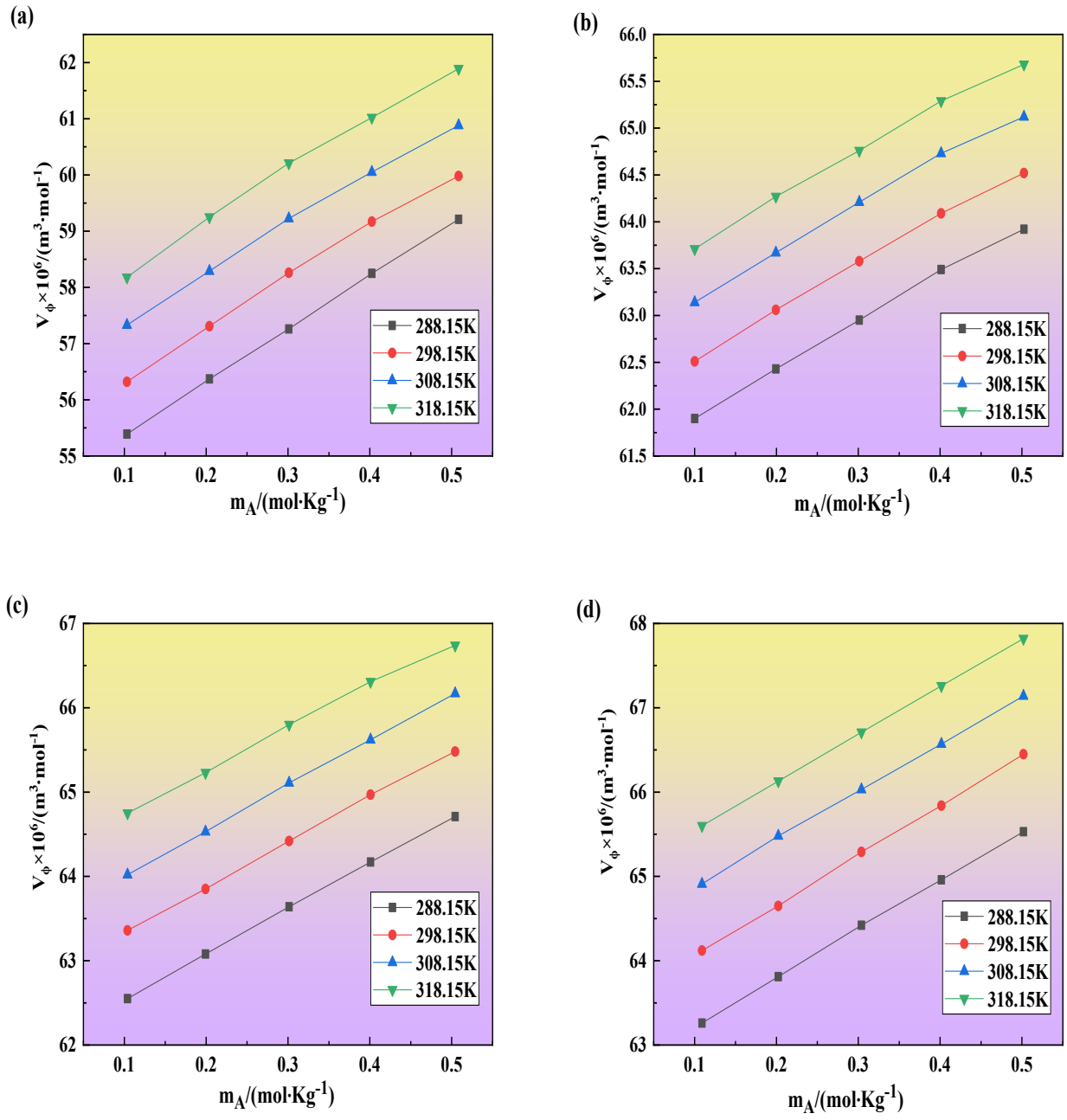

Figure 4.19 Plots demonstrate the changes in $(V_\emptyset)$ of (a) 0.00 PB; (b) 0.04 PB; (c) 0.05 PB; (d) 0.06 PB with the molality of glycolic acid at varying temperatures.

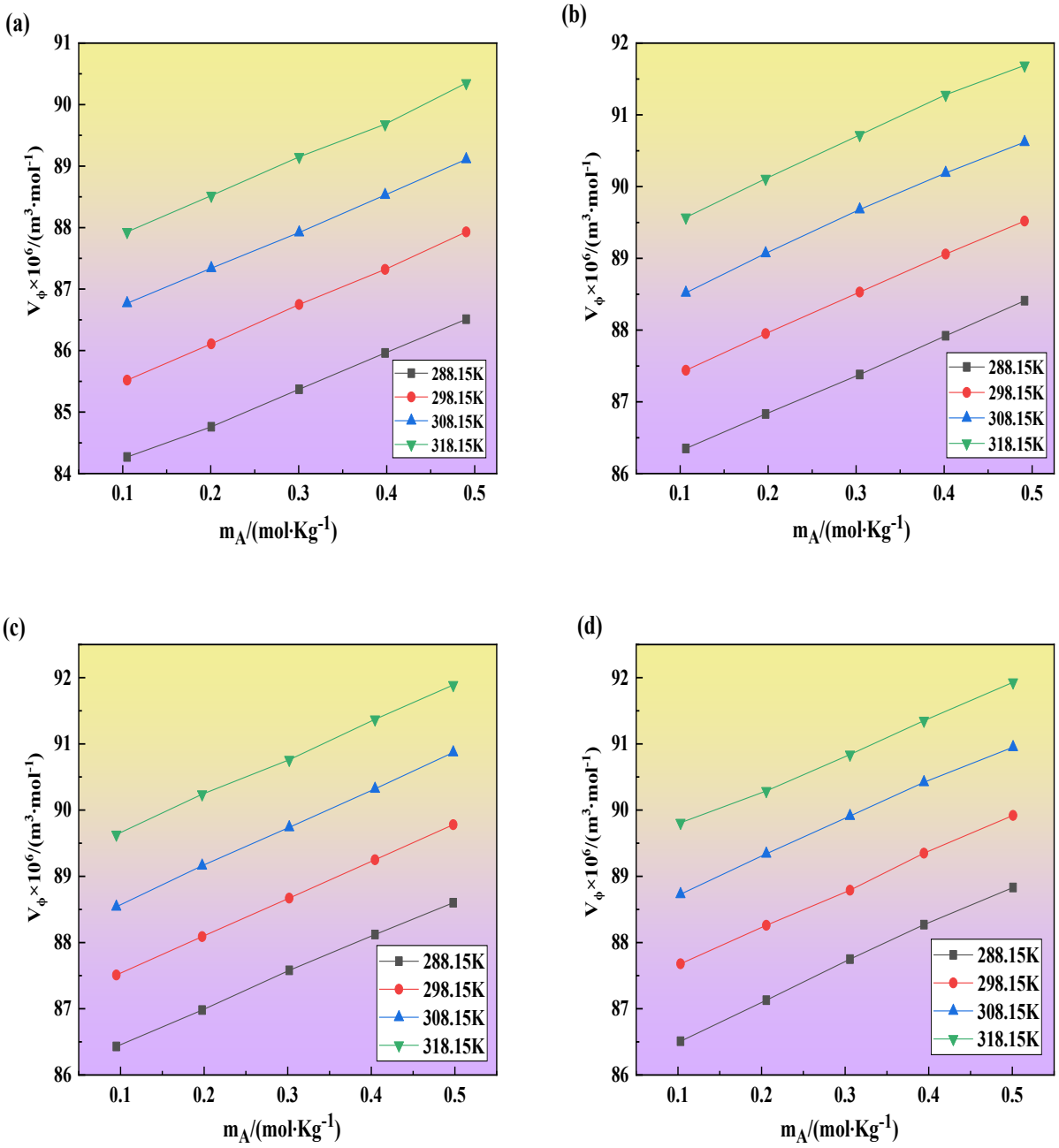

Figure 4.20 Plots demonstrate the changes in ($V_\emptyset$) of (a) 0.00 PB; (b) 0.04 PB; (c) 0.05 PB; (d) 0.06 PB with the molality of malic acid at varying temperatures.

4.3.3 Partial molar volume

The **equation 4.2** has been applied to acquire the partial molar volumes based on the ($V_{\emptyset}$). The partial molar volumes at infinitely dilutions (V_{ϕ}^{0}) and the experimental slopes (S_{V}^{*}) are evaluated with the standard uncertainties and documented in **Table 4.21**. The V_{ϕ}^{0} continues to be positive and rises as the concentration of potassium benzoate also increases at all varying temperatures. The interactions observed within the solute and solvent system, as shown in **Figure 4.21**, may be a contributing factor to this phenomenon. These interactions include interactions between solutes and solvents, interactions within ions and ions, and interactions between ions and solvents. The cosphere overlap model states that the volume rises when the hydration co-spheres of two separate ionized species overlaps with one another which contributes to the hydrophilic-hydrophilic and ion-hydrophilic bonds [13-15].

The S_{V}^{*} value consistently remains positive at all examined temperatures for potassium benzoate molecules. There are no consistent patterns in the S_{V}^{*} values; it is reasonable to assume that there are more variables that influence the interactions between solutes. However, the S_{V}^{*} values are much lesser than the V_{ϕ}^{0} data, representing that the solute along with solvent groups in the liquid combinations prevail over the solute-solute interactions [16,17].

Table 4.21 Values of $'V_{\phi}^{0}'$, and $'S_V^*'$ for potassium benzoate in water-soluble glycolic and malic acids at numerous temperatures.

m_B/ (mol·kg^{-1})	$V_{\phi}^{0} \times 10^6$/(m^3·mol^{-1})				$S_V^* \times 10^6$ /(m^3·kg·mol^{-2})			
	T=288.15K	T=298.15K	T=308.15K	T=318.15K	T=288.15K	T=298.15K	T=308.15K	T=318.15 K
Glycolic Acid								
0.00	54.43(±0.02)	55.45(±0.09)	56.49(±0.08)	57.34(±0.12)	9.43(±0.07)	9.09(±0.27)	8.77(±0.25)	9.10(±0.34)
0.04	61.41(±0.04)	62.04(±0.04)	62.67(±0.06)	63.26(±0.06)	5.07 (±0.12)	5.02(±0.13)	4.99 (±0.17)	4.93 (±0.17)
0.05	62.00(±0.01)	62.80(±0.02)	63.47(±0.02)	64.24(±0.05)	5.40 (±0.04)	5.35 (±0.02)	5.38 (±0.02)	5.05 (±0.05)
0.06	62.64(±0.02)	63.47(±0.02)	64.32(±0.02)	64.99(±0.01)	5.78(±0.05)	5.94(±0.05)	5.63 (±0.06)	5.65(±0.02)
Malic Acid								
0.00	83.62 (±0.03)	84.86(±0.02)	86.12 (±0.02)	87.27 (±0.05)	5.87(±0.10)	6.23(±0.06)	6.06(±0.06)	6.19(±0.14)
0.04	85.77 (±0.01)	86.88(±0.02)	87.98(±0.05)	89.01 (±0.05)	5.35(±0.04)	5.41(±0.05)	5.46(±0.14)	5.56(±0.14)
0.05	85.92(±0.02)	86.98(±0.01)	88.01(±0.04)	89.11 (±0.08)	5.41 (±0.06)	5.63 (±0.01)	5.75(±0.04)	5.58(±0.08)
0.06	86.02 (±0.04)	87.09 (±0.03)	88.18 (±0.04)	89.22(±0.04)	5.87 (±0.11)	5.06 (±0.08)	5.61 (±0.11)	5.38(±0.11)

m_B is the concentration of potassium benzoate solution: standard uncertainties *u* is $u_r(m)$ = 0.01; $u(V_{\phi}^{0})$ = ±(0.31-0.36) × 10^6/(m^3·mol^{-1}) and $u\ (S_V^*)$ = ±0.03 × 10^6/(m^3·kg·mol^{-2}), $u(p)$ =0.01 MPa.

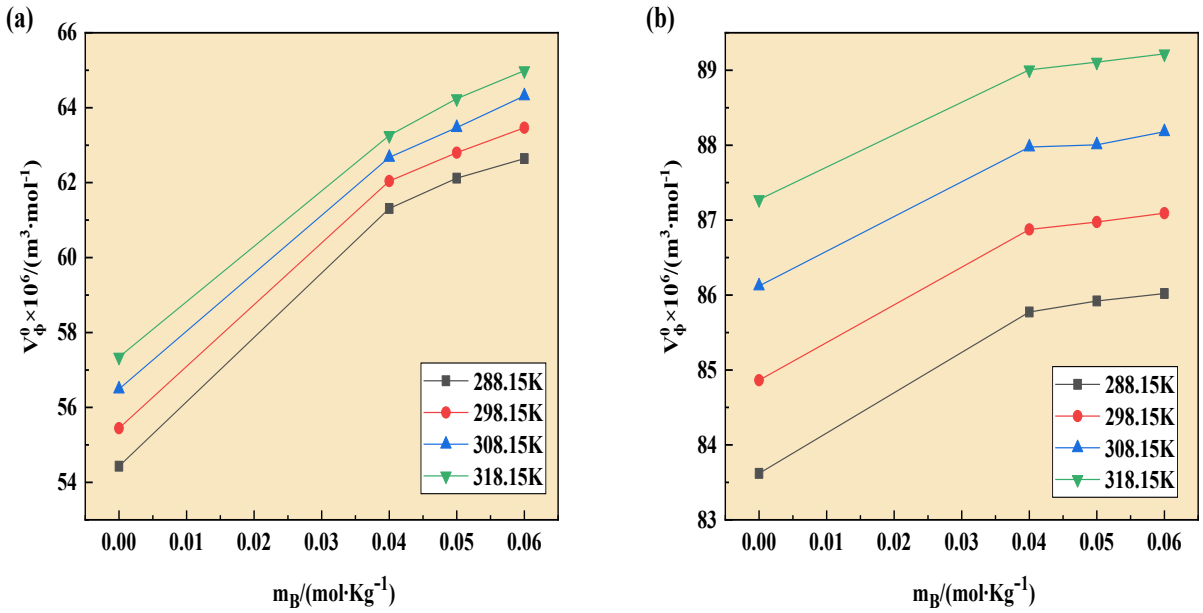

Figure 4.21 Plots representing the variations in $V_{\emptyset}^{0}$, for (a) glycolic acid, (b) malic acid inside a PB water-soluble solution at numerous temperatures.

4.3.4 Tranfer property of partial molar volumes

The transfer of alpha-hydroxy acids from water to PB solution was calculated at infinite dilutions using **equation 4.3**. This transfer characteristic is vital to an extensive knowledge of solutions because it infers evidence on the bonds within the solute and the solvent. It can be detected from the **Table 4.22** that the data of $\Delta_{tr}V_{\emptyset}^{0}$ continues to be positive and rises as the concentration of potassium benzoate rises at all varying temperatures.

The tendency of a solute to build or disrupt structured compositions due to its solvophobic nature and the structural interactions within the two cospheres can be an explanation for the positive values of $\Delta_{tr}V_{\emptyset}^{0}$ as per the hypothesis of co-sphere overlap [18,19]. It is crucial to take into consideration the evidence that solute as well as the solvent are electrolytes in the studies that are currently being conducted, which involve the combination of potassium benzoate (PB), H_2O, glycolic acid (GA) and malic acid (MA). Consequently, it is seen that the values of $\Delta_{tr}V_{\emptyset}^{0}$ imply the occurrence of ion-ion interactions within the aqueous PB and alpha-hydroxy acids (GA/MA). As per the cosphere overlap theory, the data of $\Delta_{tr}V_{\emptyset}^{0}$ show that the solute-solute interaction is extremely low and approximately inadequate. Due to the positive values that have been reported for $\Delta_{tr}V_{\emptyset}^{0}$ in the (PB + water + GA/MA) system, the current research provides evidence that hydrophilic and hydrophilic as well as with ion and hydrophilic interactions are present [20,21].

Table 4.22 Transfer property $\Delta_{tr}V_{\phi}^{0}$, of PB in water-soluble with glycolic and malic acids were determined at several temperatures.

m_B/ (mol·kg^{-1})	$\Delta_{tr}V_{\phi}^{0} \times 10^{6}$/(m^3·mol^{-1})			
	T=288.15K	T=298.15K	T=308.15K	T=318.15K
		Glycolic Acid		
0.04	6.98	6.60	6.18	5.91
0.05	7.57	7.36	6.98	6.90
0.06	8.21	8.02	7.83	7.64
		Malic Acid		
0.04	2.15	2.01	1.85	1.73
0.05	2.30	2.11	1.88	1.83
0.06	2.40	2.23	2.06	1.94

m_B signifies the concentration of potassium benzoate solution: the standard uncertainties *u* are $u_r(m)$= 0.01 (mol·kg^{-1}), $u(\Delta_{tr}V_{\phi}^{0})$= ±(0.05-0.20)×10^6/(m^3·mol^{-1}), *u(T)*=0.001 K, *u(p)* =0.01 MPa.

4.3.5 Effect of temperature on partial molar volume

It is possible to derive the (V_ϕ^0) as a function of temperature at infinite dilution. The variables a^*, b^*, and c^* are empirical parameters for glycolic and malic acid in water-soluble potassium benzoate solution were acquired from **equation 4.4,** which are represented in **Table 4.23.** This table also includes the deviations in the theoretical and measured V_ϕ^0 results, which are assessed using **equation 4.5**. Empirical constants are used to derive the differences between the measured ($Y_{Exptl.}$) and determined ($Y_{calc.}$) values. The calculated deviation, shown by the symbol σ and the polynomial equation that is shown from the R^2 results in this investigation may be explained by the extremely small deviation values. The purpose of studying V_ϕ^0 is to acquire the expansibilities, and its observation is essential for gaining an understanding of the associations that arise amongst the solute along with the solvent in a solution [22,23]. In order to calculate the E_ϕ^0, it is possible to obtain **equation 4.6** by differentiating **equation 4.4** to the temperature (T).

Table 4.24 lists the apparent molar expansion values and $\left(\frac{\partial E_\Phi^0}{\partial T}\right)_P$ for the liquid systems. The positive E_ϕ^0 results highlight the continued existence of solute and solvent associations in the studied combinations and confirm the suggestion attained on the property of apparent molar volume. Due to the caging or packaging effect, the expansibility values are predominant, which supplementary highlights the scope of interactions [24,25]. The **equation 4.7** [26] act as a theory of thermodynamics to confirm the solute's tendency to construct or break structures in the liquid combination. The capability of the solution to construct or disrupt structures may be concluded from the sign of $\left(\frac{\partial E_\Phi^0}{\partial T}\right)_P$. The solute has been demonstrated to have a tendency to create structures by the positive value for $\left(\frac{\partial E_\Phi^0}{\partial T}\right)_P$, whereas its capability to break structures is specified by the negative value [27,28]. Hepler's constant was determined to be negative for both glycolic and malic acids in an aqueous medium, with the exception of malic acid, which was found to be positive at 0.05 mol·Kg^{-1} aqueous PB solutions in this current investigation. This information is indexed in **Table 4.24**, which provides an indication of the inclusive structure-breaking propensity in the liquid combination.

Table 4.23 Computed data of constants, a^*, b^*, c^* of potassium benzoate in water-soluble glycolic and malic acids.

m_B/ (mol·kg^{-1})	$a^* \times 10^6$/(m^3·mol^{-1})	$b^* \times 10^6$/(m^3·mol^{-1}·K^{-1})	$c^* \times 10^6$/ (m^3·mol^{-1}·K^{-2})	R^2	ARD
			Glycolic Acid		
0.04	62.05	0.0628	-0.0001	0.9999	0.0000
0.05	62.76	0.0745	-0.0001	0.9999	0.0000
0.06	63.50	0.0827	-0.0004	0.9999	0.0000
			Malic Acid		
0.04	86.89	0.1098	-0.0002	0.9999	0.0000
0.05	86.96	0.1047	0.0001	0.9999	0.0000
0.06	87.10	0.1077	-0.0001	0.9999	0.0000

m_B implies the concentration of potassium benzoate solution: standard uncertainties are $u_r(m)$ = 0.01, $u(T)$ = 0.001 K, $u(p)$ =0.01 MPa.

Table 4.24 Data of expansibilities 'E_{Φ}^{0}' for PB in water-soluble glycolic and malic acids at several temperatures.

m_B/ (mol·kg^{-1})	$E_{\Phi}^{0} \times 10^{6}$/(m^{3}·mol^{-1}·K^{-1})				$\left(\frac{\partial E_{\Phi}^{0}}{\partial T}\right)_P$ /(m^{3}·mol^{-1}·K^{-2})
	T=288.15K	T=298.15K	T=308.15K	T=318.15K	
			Glycolic Acid		
0.04	0.0649	0.0628	0.0606	0.0585	-0.00021
0.05	0.0758	0.0745	0.0733	0.0720	-0.00013
0.06	0.0903	0.0827	0.0750	0.0674	-0.00076
			Malic Acid		
0.04	0.1135	0.1098	0.1062	0.1025	-0.00036
0.05	0.1022	0.1047	0.1071	0.1096	0.00024
0.06	0.1093	0.1077	0.1060	0.1043	-0.00017

m_B implies the concentration of potassium benzoate solution: standard uncertainties are $u_r(m)$ = 0.01, $u(E_{\phi}^{0})$ = 0.0083 ×10^{6}/(m^{3}·mol^{-1}·K^{-1}), $u(\frac{\partial E_{\phi}^{0}}{\partial T})$ = 0.00024/(m^{3}·mol^{-1}·K^{-2}), $u(p)$ =0.01 MPa.

4.3.6 Ultrasonic speed

Several measures were carried out to attain the objective of determining the sound speed (*c*) in solutions of glycolic acid (GA) and malic acid (MA) with potassium benzoate. While the pressure was continued at 0.1 MPa during the experiment, these measurements were carried out at a variety of temperatures. The values that were obtained are listed in **Table 4.25**. A substantial amount of information regarding the ions interactions with each other, ions with solvents, and solutes with solvents may be obtained from the sound speed data [29]. The presence of hydrogen bond structures within the molecules of the alpha-hydroxy acids and potassium benzoate is the cause for the substantial escalation in sound velocity values that occurs when the molality of glycolic and malic acid increases. The expansion in the values of the sound speed is recognized as the creation of intermolecular and intramolecular H-bonds in the solute and solvent system [30,31]. The H_2 bonds that are present inside the molecules of potassium benzoate and water decline and finally dissolve as the molecular weight grows from GA to MA. However, new H- bonds are formed inside the molecules of potassium benzoate and alpha-hydroxy acids [32].

Table 4.25 Sound velocity 'c' of alpha-hydroxy acids (glycolic and malic acids) were determined in water-soluble potassium benzoate solution at several temperatures.

Molality m_A/ (mol·kg^{-1})	c/(m·s^{-1})				Molality m_A/ (mol·kg^{-1})	c/(m·s^{-1})			
	T=288.15K	T=298.15K	T=308.15K	T=318.15K		T=288.15K	T=298.15K	T=308.15K	T=318.15K
	0.00 (mol·kg^{-1}) PB + Glycolic Acid					**0.00 (mol·kg^{-1}) PB + Malic Acid**			
0.10319	1468.76	1497.91	1520.53	1536.82	0.10506	1471.29	1499.51	1521.85	1538.19
0.20403	1470.58	1499.58	1522.06	1537.88	0.20070	1475.15	1502.82	1524.18	1540.03
0.30101	1472.54	1501.19	1523.12	1538.69	0.30051	1478.43	1505.75	1526.51	1541.69
0.40254	1474.44	1502.93	1524.65	1539.76	0.39822	1482.26	1508.85	1528.87	1543.26
0.50847	1476.31	1504.47	1525.78	1540.95	0.49038	1485.77	1511.21	1530.94	1544.70
	0.04 (mol·kg^{-1}) PB + Glycolic Acid					**0.04 (mol·kg^{-1}) PB + Malic Acid**			
0.00000	1471.38	1501.25	1523.36	1540.28	0.00000	1471.38	1501.25	1523.36	1540.28
0.10018	1472.84	1503.08	1524.89	1541.63	0.10650	1474.01	1502.99	1524.93	1541.32
0.19938	1474.19	1504.55	1526.04	1542.69	0.19723	1476.89	1504.58	1526.59	1542.27
0.30121	1475.81	1506.07	1527.42	1543.75	0.30402	1480.03	1507.07	1528.57	1543.54
0.40118	1477.05	1507.45	1528.49	1544.62	0.40170	1483.74	1509.64	1530.27	1544.48
0.50251	1478.47	1508.73	1529.78	1545.77	0.49141	1486.92	1511.77	1531.91	1545.65
	0.05 (mol·kg^{-1}) PB + Glycolic Acid					**0.05 (mol·kg^{-1}) PB + Malic Acid**			
0.00000	1472.53	1502.67	1524.75	1541.82	0.00000	1472.53	1502.67	1524.75	1541.82
0.10390	1473.78	1504.17	1526.12	1543.16	0.09504	1475.11	1504.05	1526.15	1542.78
0.19919	1475.06	1505.49	1527.33	1544.25	0.19764	1478.33	1505.72	1527.86	1543.91
0.30132	1476.53	1507.12	1528.34	1545.34	0.30178	1481.52	1508.14	1529.49	1545.11

0.40084	1478.11	1508.38	1529.58	1546.29	0.40447	1485.05	1510.86	1531.17	1546.12
0.50425	1479.69	1509.56	1530.84	1547.47	0.49797	1488.49	1513.03	1532.96	1547.19
	0.06 (mol·kg^{-1}) PB + Glycolic Acid					**0.06 (mol·kg^{-1}) PB + Malic Acid**			
0.00000	1473.54	1503.44	1525.49	1542.95	0.00000	1473.54	1503.44	1525.49	1542.95
0.10901	1474.85	1505.28	1527.13	1544.47	0.10315	1476.73	1505.29	1527.34	1543.97
0.20228	1476.13	1506.59	1528.26	1545.55	0.20569	1479.94	1507.31	1528.95	1545.17
0.30387	1477.59	1508.12	1529.57	1546.71	0.30582	1483.48	1509.58	1530.62	1546.23
0.40155	1479.05	1509.64	1530.83	1547.82	0.39428	1486.15	1511.67	1532.08	1547.18
0.50191	1480.36	1510.87	1531.98	1548.89	0.50092	1490.07	1514.49	1534.05	1548.36

m_A is the molality of both the acids in potassium benzoate solution: the standard uncertainties u are $u_r(m)$ = 0.02, $u(c)$ = 1.82 m·s^{-1}, $u(T)$ = 0.001 K, $u(p)$ =0.01 MPa.

4.3.7 Apparent molar isentropic compressibility

This apparent molar property ($K_{\phi,S}$) has been investigated for glycolic and malic acids in water-soluble PB solution. The evaluation was carried out as shown in **equation 4.9**. The Newton-Laplace law describes the isentropic compression of the liquid combination with the help of **equation 4.8**. Based on the values documented in **Table 4.26**, it is obvious that the acquired ($K_{\phi,S}$) information is continuously negative and drops as the temperature rises. **Figures 4.22** and **4.23** provide a graphical illustration of the findings for glycolic and malic acids in water-soluble potassium benzoate solutions. A corresponding increase in the PB concentration indicates that the surrounding water molecules exhibit reduced compressive strength compared to those in the bulk solution. Thermal agitation, which expands the solvent volume and also enhances its compressibility, might be a possible explanation for these negative values [33,34].

The behavior of the $K_{\phi,S}$ values observed can also be affected by the interruption of the potassium benzoate molecules and the alteration of hydration shells surrounding the solutes (glycolic and malic acids) are also factors that affect the behavior of the values of $K_{\phi,S}$ that have been reported. Due to the fact that greater temperatures have the potential to alter the water's structure surrounding the hydrophilic group of potassium benzoate and zwitter ions of alpha-hydroxy acids, a particular rearrangement of molecules of water can be observed around the solute. Additionally, the negative values suggest that the decrease results from the compressibilities of the H_2O structure, with the solute that exists in the solvent contributing to the aligning effect within the solvent [35]. Alpha-hydroxy acids (GA/MA) and PB solutions can build more compact structures through the establishment of intermolecular hydrogen bonds. This eventually leads these compounds to become less compressible. Strong interactions between solutes and solvents are facilitated by the interactions (dipole-dipole) that take place between water molecules that are in close proximity to one another, as well as by the OH groups of alpha-hydroxy acids [36,37].

Table 4.26 Data of '$K_{\phi,S}$' were obtained in the water-soluble mixtures of PB with glycolic and malic acids at numerous temperatures.

Molality m_A/ (mol·kg^{-1})	$K_{\phi,s} \times 10^6$/(m^3·mol^{-1}·GPa^{-1})				Molality m_A/ (mol·kg^{-1})	$K_{\phi,s} \times 10^6$/(m^3·mol^{-1}·GPa^{-1})			
	288.15K	298.15K	308.15 K	318.15 K		288.15K	298.15K	308.15 K	318.15 K
	0.00 (mol·kg^{-1}) PB + Glycolic Acid					**0.00 (mol·kg^{-1}) PB + Malic Acid**			
0.10319	-46.14	-44.35	-42.99	-42.05	0.10506	-46.27	-44.47	-43.14	-42.38
0.20403	-46.45	-44.64	-43.28	-42.33	0.20070	-46.69	-44.87	-43.53	-42.76
0.30101	-46.60	-44.78	-43.41	-42.45	0.30051	-46.98	-45.15	-43.79	-43.02
0.40254	-46.71	-44.88	-43.50	-42.54	0.39822	-47.22	-45.37	-44.00	-43.22
0.50847	-46.79	-44.96	-43.58	-42.61	0.49038	-47.42	-45.56	-44.18	-43.40
	0.04 (mol·kg^{-1}) PB + Glycolic Acid					**0.04 (mol·kg^{-1}) PB + Malic Acid**			
0.10018	-45.79	-44.00	-42.76	-41.80	0.10650	-45.98	-44.18	-42.94	-41.98
0.19938	-46.07	-44.27	-43.03	-42.07	0.19723	-46.37	-44.55	-43.30	-42.33
0.30121	-46.21	-44.40	-43.15	-42.18	0.30402	-46.67	-44.84	-43.57	-42.59
0.40118	-46.29	-44.48	-43.23	-42.26	0.40170	-46.90	-45.05	-43.77	-42.79
0.50251	-46.36	-44.54	-43.29	-42.32	0.49141	-47.08	-45.22	-43.94	-42.95
	0.05 (mol·kg^{-1}) PB + Glycolic Acid					**0.05 (mol·kg^{-1}) PB + Malic Acid**			
0.10390	-45.73	-43.94	-42.70	-41.74	0.09504	-45.83	-44.04	-42.80	-41.83
0.19919	-46.00	-44.19	-42.95	-41.98	0.19764	-46.30	-44.48	-43.23	-42.25
0.30132	-46.12	-44.31	-43.06	-42.09	0.30178	-46.59	-44.76	-43.49	-42.51
0.40084	-46.21	-44.39	-43.13	-42.16	0.40447	-46.82	-44.98	-43.70	-42.71
0.50425	-46.27	-44.45	-43.19	-42.22	0.49797	-47.02	-45.16	-43.87	-42.88
	0.06 (mol·kg^{-1}) PB + Glycolic Acid					**0.06 (mol·kg^{-1}) PB + Malic Acid**			

0.10901	-45.68	-43.89	-42.66	-41.69	0.10315	-45.82	-44.02	-42.78	-41.82
0.20228	-45.92	-44.12	-42.88	-41.91	0.20569	-46.25	-44.44	-43.18	-42.21
0.30387	-46.05	-44.24	-42.99	-42.02	0.30582	-46.52	-44.70	-43.43	-42.45
0.40155	-46.12	-44.31	-43.05	-42.08	0.39428	-46.73	-44.89	-43.61	-42.62
0.50191	-46.18	-44.36	-43.10	-42.13	0.50092	-46.94	-45.09	-43.81	-42.81

m_A specifies the molality of both the acids in water-soluble potassium benzoate solutions: the standard uncertainties u are $u_r(m) = 0.02$, $u\ (K_{\phi,S}) = 0.13 \times 10^6/(m^3 \cdot mol^{-1} \cdot GPa^{-1})$, $u(T)$=0.001 K, $u(p)$ =0.01 MPa.

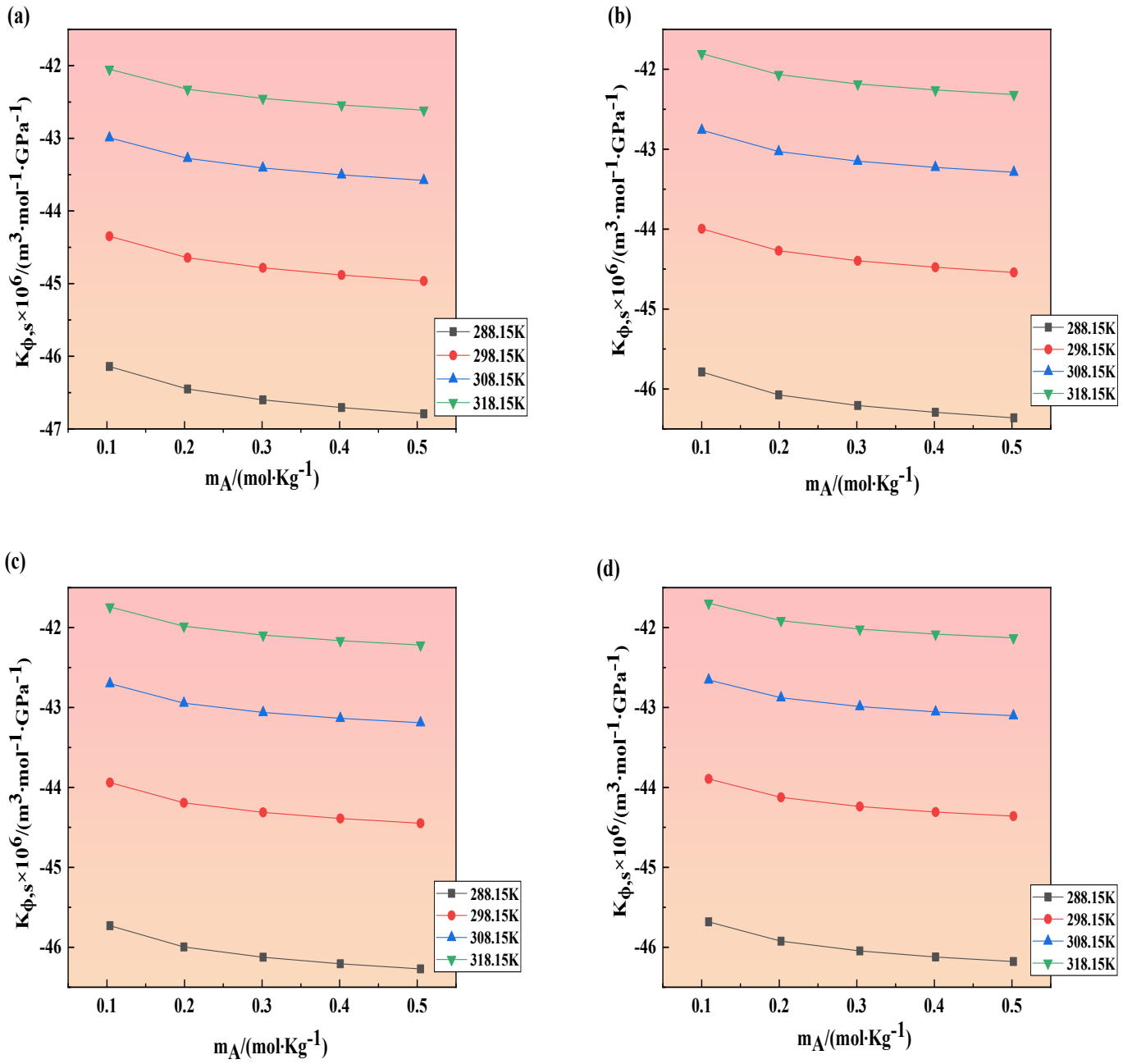

Figure 4.22 Variations in $K_{\phi,s}$, of glycolic acid in (a) 0.00 PB, (b) 0.04 PB, (c) 0.05 PB and (d) 0.06 PB at several temperatures.

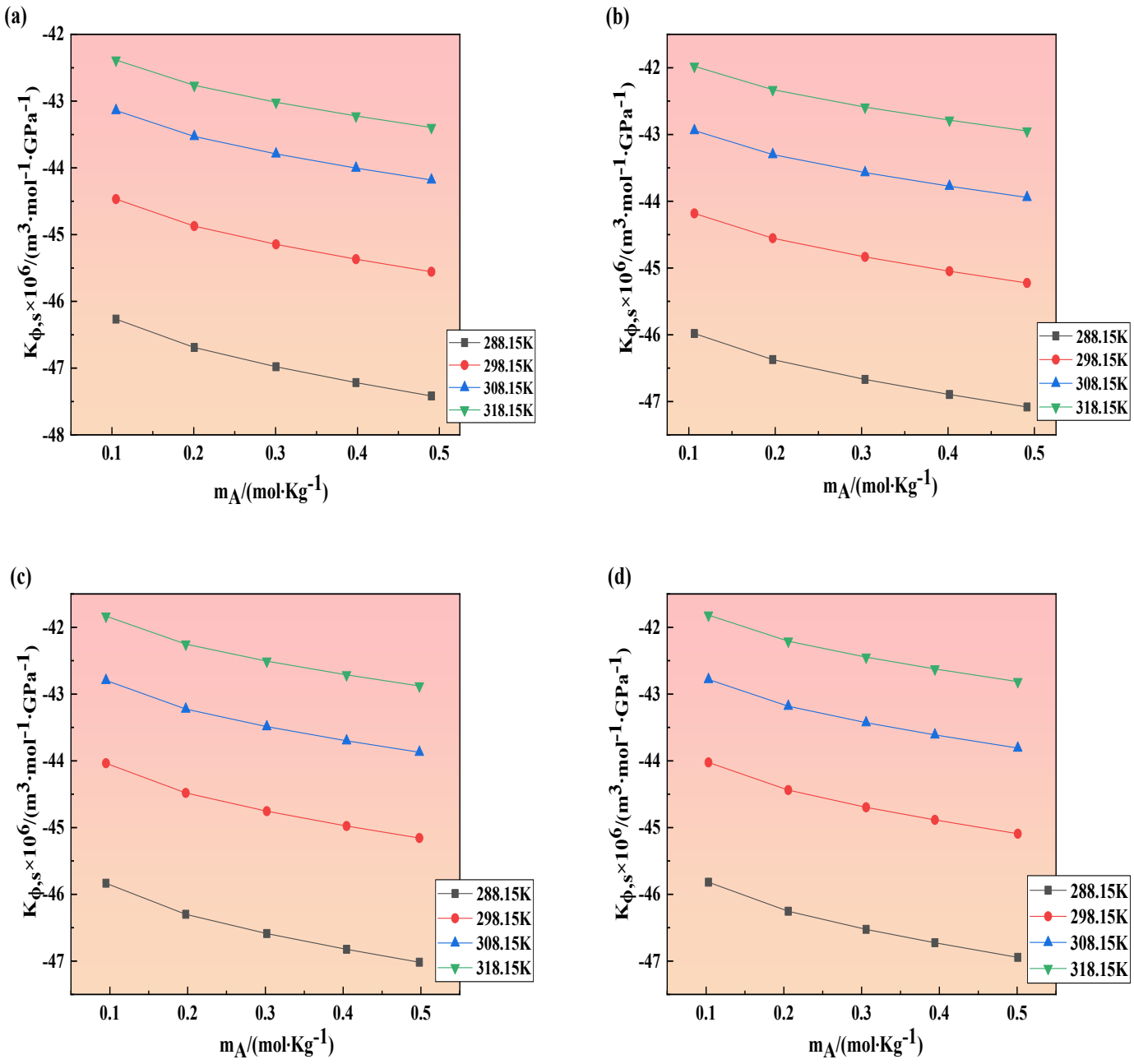

Figure 4.23 Variations in $K_{\phi,s}$, of malic acid in (a) 0.00 PB, (b) 0.04 PB, (c) 0.05 PB and (d) 0.06 PB at several temperatures.

4.3.8 Partial molar isentropic compressions

This property can be obtained by monitoring the change of apparent molar isentropic compressibility against molalities. This variation can be obtained by **equation 4.10.** The acoustic virial coefficient, denoted by S_K^*, offers an understanding into the interactions amongst the solutes. The obtained values of these variables, together with their corresponding uncertainties, are recorded in **Table 4.27**. **Figure 4.24** demonstrates that all of the $K_{\phi,s}^0$ values are negative. The following effects are primarily responsible for the $K_{\phi,s}^0$: The positive effect, referred to as the solvent's inherent compression, ascends when the volume of available space amid solution molecules rises and the solution is compressed further. The negative impact, which is recognized as solvent penetration, takes place when solvent molecules enter the vacant spaces amid ions as a result of interactions that take place among the solvent and solute [38,39].

When the temperature increases, it has been shown that there is a drop in the rate of negative values of $K_{\phi,s}^0$. The strong interactions that occur inside solutes and water molecules are further strengthened by this decrease in the occurrence of negative values. This results in the water molecules being released into the bulk solution when they are released. An insightful explanation for this occurrence may be found in the model that Kirkwood presented [40]. Due to the relatively insignificant size of S_K^*, the interaction amid molecules of solute becomes insignificant, which signifies that interactions of solute as well as solvent are the most prevalent inside the liquid combinations [41].

Table 4.27 Data of $K^0_{\phi,S}$, and S^*_K, of the ternary system of potassium benzoate in glycolic and malic acids at several temperatures.

m_B/ (mol·kg^{-1})	$K^0_{\phi,S} \times 10^6$/(m^3·mol^{-1}·GPa^{-1})				$S^*_K \times 10^6$ /(m^3·kg·mol^{-2})			
	T=288.15K	T=298.15K	T=308.15K	T=318.15K	T=288.15K	T=298.15K	T=308.15K	T=318.15 K
				Glycolic Acid				
0.00	-46.07 (±0.09)	-44.28(±0.08)	-42.93(±0.08)	-41.99(±0.08)	-1.54(±0.26)	-1.45(±0.25)	-1.38(±0.24)	-1.33(±0.23)
0.04	-45.74(±0.08)	-43.95(±0.08)	-42.72(±0.08)	-41.76(±0.08)	-1.36(±0.25)	-1.29(±0.24)	-1.24(±0.24)	-1.21(±0.23)
0.05	-45.68(±0.08)	-43.89(±0.08)	-42.66(±0.07)	-41.70(±0.07)	-1.28(±0.24)	-1.21(±0.23)	-1.16(±0.22)	-1.13(±0.22)
0.06	-45.62(±0.07)	-43.84(±0.07)	-42.61(±0.07)	-41.65(±0.07)	-1.21(±0.22)	-1.13(±0.21)	-1.08(±0.21)	-1.05(±0.21)
				Malic Acid				
0.00	-46.04(±0.08)	-44.26(±0.08)	-42.94(±0.08)	-42.19(±0.08)	-2.92(±0.25)	-2.76(±0.24)	-2.64(±0.24)	-2.56(±0.23)
0.04	-45.76(±0.08)	-43.97(±0.07)	-42.74(±0.07)	-41.79(±0.07)	-2.79(±0.24)	-2.65(±0.23)	-2.54(±0.22)	-2.46(±0.22)
0.05	-45.66±0.09)	-43.87(±0.09)	-42.64(±0.09)	-41.68(±0.09)	-2.86(±0.28)	-2.71(±0.27)	-2.60(±0.26)	-2.52(±0.26)
0.06	-45.62(±0.09)	-43.83(±0.08)	-42.60(±0.08)	-41.64(±0.08)	-2.77(±0.26)	-2.63(±0.25)	-2.53(±0.24)	-2.45(±0.24)

m_B implies the concentration of potassium benzoate solution: the calculated standard uncertainties *u* are $u_r(m) = 0.01$, $u(K^0_{\phi,S}) = 0.32 \times 10^6$/(m^3·mol^{-1}·GPa^{-1}), $u(S^*_K)$= ±0.13×10^6/(kg·m^3·kg·mol^{-2}·GPa^{-1}), $u(p)$ =0.01 MPa.

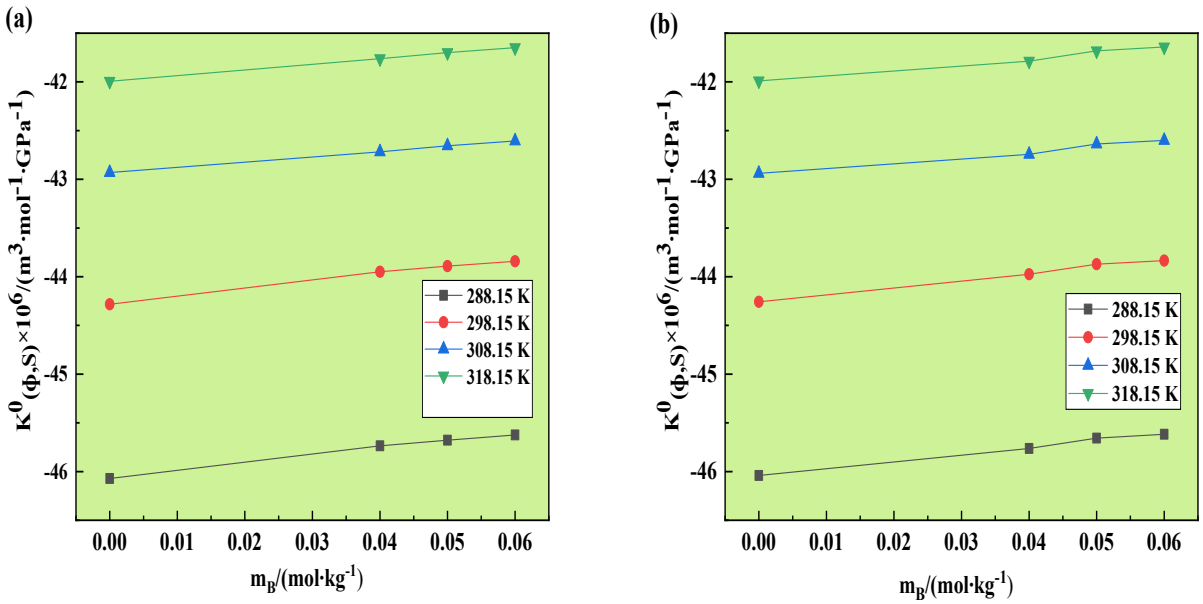

Figure 4.24 Changes of $K^0_{\emptyset,S}$ for (a) glycolic acid (b) malic acid in PB solutions at numerous temperatures.

4.3.9 Transfer of partial molar isentropic compressions

The $\Delta_{tr}K^{0}_{\emptyset,S}$ of alpha-hydroxy acids produced from water to PB aqueous solution is calculated using **equation 4.11** at the condition of infinite dilution. The determined data of $\Delta_{tr}K^{0}_{\emptyset,S}$ are positive at different concentrations (0.04,0.05,0.06) mol·Kg^{-1}. These computed values are reported in **Table 4.28**.

The strength of the interactions inside the molecules of alpha-hydroxy acids and potassium benzoate leads to an increased ability for the formation of structures. Due to this, the compressibility of potassium benzoate reduces as the concentration of the compound rises, which results in the mixture being more compressible than the pure solvent. Due to the reduction in electrostriction, the structure of the solute undergoes a change when the concentration of potassium benzoate increases. This is because the zwitterionic-center of glycolic and malic acids interacts with aqueous PB more effectively [42,43]. The solutes (glycolic and malic acids) interact with the water molecules when the $\Delta_{tr}K^{0}_{\emptyset,S}$ values are positive. This suggests that the solvent, which upsurges as a significance of intermolecular interactions combines with the water molecules of solutes. The enhanced ion-to-water molecule attachment is the cause for the negative $\Delta_{tr}K^{0}_{\emptyset,S}$ data within the solute and solvent bonds [44,45].

Table 4.28 Data of transfer parameter $\Delta_{tr}K^0_{\emptyset,S}$, of water-soluble solutions of PB with glycolic and malic acids at several temperatures.

m_B/ (mol·kg^{-1})	$\Delta_{tr}K^0_{\emptyset,S} \times 10^6$/(m^3·mol^{-1}·GPa^{-1})			
	288.15K	298.15K	308.15K	318.15K
		Glycolic Acid		
0.04	0.34	0.33	0.21	0.23
0.05	0.39	0.39	0.27	0.29
0.06	0.45	0.44	0.32	0.34
		Malic Acid		
0.04	0.28	0.28	0.20	0.40
0.05	0.38	0.39	0.30	0.51
0.06	0.42	0.42	0.34	0.55

m_B infers the concentration of potassium benzoate solution: the calculated standard uncertainties u are $u_r(m)$ = 0.01 (mol·kg^{-1}), $\Delta_{tr}K^0_{\emptyset,S}$= 0.01×10^6/(m^3·mol^{-1}·GPa^{-1}), $u(p)$ =0.01 MPa.

4.3.10 Interaction coefficients

The coefficients for isentropic compression and volumetric pair (K_{AB} and V_{AB}) and triplet (K_{ABB} and V_{ABB}) interactions can be determined from the **equations 4.12** and **4.13**. The values of these variables are listed in **Table 4.29**. McMillan and Mayer [46] concept investigates the possibility of independent effects in a liquid combination resulting from interactions within the molecules in pairs and triplets. Franks et al. [47] and Friedman and Krishnan [48] had both contributed to the discussion of the similar theory in more detail. In order to accurately predict and exert control over the behavior of solute molecules in solution, it is necessary to have a comprehensive understanding of both the scope and nature of the interactions that occur [49]. Across all temperatures, the pair coefficients are positive for both the glycolic and malic acids. The only exception to this is the triplet coefficient for isentropic compression, where the values for glycolic and malic acids are positive at 308.15 K suggests a temperature-induced shift which increases molecular volume and compressibility. Based on the overall positive data of V_{AB} and K_{AB}, it is anticipated that pairwise interactions will be the most prevalent in combinations of glycolic or malic acids, potassium benzoate, and water.

Table 4.29 Calculated pair and triplet parameters of glycolic and malic acids in water-soluble PB solutions at numerous temperatures.

T/K	$V_{AB} \times 10^6$/(m^3·mol^{-2}· kg)	$V_{ABB} \times 10^6$/(m^3·mol^{-3}·kg^2)	$K_{AB}\times10^6$/(m^3·mol^{-2}· kg·GPa^{-1})	$K_{ABB}\times10^6$/(m^3·mol^{-3}·kg^2·GPa^{-1})
		Glycolic Acid		
288.15	122.75	-608.86	5.09	-15.18
298.15	112.66	-511.91	5.18	-16.81
308.15	99.78	-387.64	2.64	0.86
318.15	94.47	-341.61	2.98	-1.07
		Malic Acid		
288.15	40.28	-226.40	3.73	-1.42
298.15	37.53	-212.59	3.93	-3.70
308.15	33.84	-188.66	2.10	9.05
318.15	31.93	-176.11	6.26	-18.11

Standard uncertainties are $u(T)$=0.001 K, $u(p)$ =0.01 MPa.

Problem 4

4.4 Title: "Investigating Interactions of Alpha-Hydroxy Acids with Sodium Benzoate for Advanced Formulation and Translational Applications: An Ultrasonic Approach"

In this investigation, lactic acid and malic acid were studied in combination with aqueous sodium benzoate to assess variations in density and sound speed across different concentrations and temperatures.

4.4.1 Density measurements

The densities for lactic and malic acids in aqueous (0.00 to 0.03) mol·kg^{-1} were attained at various temperatures, as shown in **Table 4.30**. The experimentally obtained densities of aqueous malic acid are shown to be consistent with the reported data of the liquid system [1-3] as shown in **Figure 4.17**. Through the analysis of figures, it has been noted that the experimental densities for the investigated combination demonstrate similar trends as the densities shown in previous studies. The increase in density data with higher concentrations of lactic and malic acids is primarily attributed to the expansion in the molecular mass of the system. It is also evident from **Table 4.30** that for a given sodium benzoate concentration, the density of the ternary system increases with rising molality of lactic and malic acids but decreases with rising temperatures. It is also possible that the interactions within solvents and solutes have grown stronger, as shown by the increase in density [5].

Table 4.30 Values of densities 'ρ' were determined in the combination of sodium benzoate solutions with lactic and malic acids at four different temperatures.

m_A/ (mol·kg^{-1})	$\rho \times 10^{-3}$/(kg·m^{-3})				m_A/ (mol·kg^{-1})	$\rho \times 10^{-3}$/(kg·m^{-3})			
	288.15K	298.15K	308.15K	318.15K		288.15K	298.15K	308.15K	318.15K
0.00 (mol·kg^{-1}) Sodium Benzoate + Lactic Acid					**0.00 (mol·kg^{-1}) Sodium Benzoate + Malic Acid**				
0.00000	0.99926	0.99705	0.99404	0.99036	0.00000	0.99926	0.99705	0.99404	0.99036
0.09931	1.00107	0.99884	0.99581	0.99212	0.09930	1.00417	1.00184	0.99872	0.99494
0.19903	1.00283	1.00058	0.99754	0.99383	0.20136	1.00904	1.00656	1.00334	0.99946
0.30437	1.00462	1.00234	0.99929	0.99558	0.29949	1.01350	1.01091	1.00758	1.00360
0.39491	1.00610	1.00380	1.00073	0.99701	0.40764	1.01823	1.01550	1.01208	1.00800
0.49638	1.00769	1.00538	1.00229	0.99855	0.49042	1.02163	1.01882	1.01530	1.01113
0.01 (mol·kg^{-1}) Sodium Benzoate + Lactic Acid					**0.01 (mol·kg^{-1}) Sodium Benzoate + Malic Acid**				
0.00000	0.99976	0.99764	0.99461	0.99084	0.00000	0.99976	0.99764	0.99461	0.99084
0.09292	1.00144	0.99931	0.99626	0.99248	0.09918	1.00464	1.00240	0.99925	0.99538
0.19681	1.00325	1.00109	0.99803	0.99423	0.20125	1.00946	1.00709	1.00383	0.99987
0.30545	1.00504	1.00286	0.99979	0.99597	0.29686	1.01381	1.01130	1.00794	1.00388
0.39357	1.00642	1.00422	1.00115	0.99732	0.40372	1.01848	1.01583	1.01234	1.00817
0.51301	1.00817	1.00597	1.00291	0.99907	0.49841	1.02242	1.01967	1.01604	1.01177
0.02 (mol·kg^{-1}) Sodium Benzoate + Lactic Acid					**0.02 (mol·kg^{-1}) Sodium Benzoate + Malic Acid**				
0.00000	1.00023	0.99823	0.99516	0.99125	0.00000	1.00023	0.99823	0.99516	0.99125
0.09514	1.00211	1.00010	0.99702	0.99309	0.10647	1.00544	1.00332	1.00012	0.99611

0.19723	1.00368	1.00165	0.99856	0.99463	0.20876	1.01027	1.00800	1.00469	1.00058
0.30553	1.00544	1.00339	1.00029	0.99636	0.30821	1.01476	1.01235	1.00894	1.00472
0.40625	1.00699	1.00491	1.00181	0.99787	0.40950	1.01916	1.01661	1.01306	1.00875
0.51246	1.00852	1.00642	1.00331	0.99938	0.50775	1.02322	1.02055	1.01692	1.01245
0.03 (mol·kg^{-1}) Sodium Benzoate + Lactic Acid					**0.03 (mol·kg^{-1}) Sodium Benzoate + Malic Acid**				
0.00000	1.00086	0.99882	0.99572	0.99173	0.00000	1.00086	0.99882	0.99572	0.99173
0.10639	1.00275	1.00070	0.99759	0.99359	0.09874	1.00568	1.00352	1.00030	0.99621
0.19865	1.00430	1.00224	0.99912	0.99511	0.21348	1.01108	1.00876	1.00539	1.00121
0.30468	1.00598	1.00391	1.00077	0.99676	0.30371	1.01513	1.01267	1.00922	1.00494
0.39963	1.00741	1.00531	1.00217	0.99815	0.41664	1.02002	1.01743	1.01385	1.00947
0.50672	1.00890	1.00680	1.00367	0.99961	0.51397	1.02402	1.02131	1.01764	1.01311

m_A denotes the molality of alpha-hydroxy acids in sodium benzoate solution: the calculated standard uncertainties u are u(m) = 0.03 (mol·kg^{-1}), u(T)=0.001 K, u(ρ)=0.55(kg·m^{-3}).

4.4.2 Apparent molar volumes

This parameter is essential in formulating beverages, pharmaceuticals, and cosmetics, where solvation and volume effects influence product stability and efficacy [50,51] . The density data obtained from experiments are utilized to compute the V_ϕ using the **equation 4.1** [52]. Understanding the interactions between solutes and solvents in a mixture can be achieved by analyzing the variations in apparent molar volume [53]. Based on the experimental density data, the values that were obtained for V_ϕ are presented in **Table 4.31**. A clear and concise illustration of the three-dimensional graphical depiction of the liquid systems may be shown in **Figure 4.25**. The present ternary system of lactic and malic acids in sodium benzoate solutions suggests significant solute-solvent associations, as seen by the positive V_ϕ results that upsurge with increasing sodium benzoate concentration and molality of solutes (LA/MA). If the concentration is increased, there will be a lessening in the electrostriction of the molecules of water. The intensification in V_ϕ values is mainly accredited to the interactions taking place inside the molecules of solutes and solvents [54,55].

Table 4.31 Values of 'V_ϕ' were determined in the combination of sodium benzoate solutions with lactic and malic acids at four different temperatures.

m_A/ (mol·kg^{-1})	$V_\phi \times 10^6$/(m^3·mol^{-1})				m_A/ (mol·kg^{-1})	$V_\phi \times 10^6$/(m^3·mol^{-1})			
	288.15K	298.15K	308.15K	318.15K		288.15K	298.15K	308.15K	318.15K
0.00 (mol·kg^{-1}) Sodium Benzoate + Lactic Acid					**0.00 (mol·kg^{-1}) Sodium Benzoate + Malic Acid**				
0.09931	71.73	72.07	72.41	72.74	0.09930	84.22	85.53	86.75	87.91
0.19903	71.92	72.26	72.58	72.91	0.20136	84.73	86.14	87.32	88.50
0.30437	72.14	72.47	72.79	73.10	0.29949	85.34	86.72	87.94	89.13
0.39491	72.31	72.65	72.98	73.29	0.40764	85.95	87.34	88.51	89.69
0.49638	72.53	72.85	73.20	73.53	0.49042	86.57	87.91	89.12	90.32
0.01 (mol·kg^{-1}) Sodium Benzoate + Lactic Acid					**0.01 (mol·kg^{-1}) Sodium Benzoate + Malic Acid**				
0.09292	71.89	72.15	72.48	72.79	0.09918	84.53	85.81	87.07	88.25
0.19681	72.17	72.43	72.75	73.11	0.20125	85.06	86.42	87.69	88.82
0.30545	72.49	72.75	73.06	73.42	0.29686	85.56	86.97	88.23	89.41
0.39357	72.74	73.01	73.28	73.66	0.40372	86.13	87.54	88.85	90.02
0.51301	73.09	73.36	73.59	73.96	0.49841	86.67	88.06	89.42	90.65
0.02 (mol·kg^{-1}) Sodium Benzoate + Lactic Acid					**0.02 (mol·kg^{-1}) Sodium Benzoate + Malic Acid**				
0.09514	72.01	72.26	72.56	72.89	0.10647	84.67	85.94	87.22	88.41
0.19723	72.32	72.58	72.84	73.17	0.20876	85.15	86.53	87.83	88.96
0.30553	72.65	72.92	73.19	73.48	0.30821	85.69	87.11	88.37	89.57
0.40625	72.94	73.24	73.49	73.81	0.40950	86.22	87.68	89.01	90.19

0.51246	73.29	73.59	73.85	74.13	0.50775	86.81	88.23	89.51	90.84
0.03 (mol·kg^{-1}) Sodium Benzoate + Lactic Acid					**0.03 (mol·kg^{-1}) Sodium Benzoate + Malic Acid**				
0.10639	72.15	72.35	72.61	72.92	0.09874	84.85	86.09	87.49	88.65
0.19865	72.49	72.69	72.97	73.28	0.21348	85.32	86.71	88.11	89.19
0.30468	72.84	73.08	73.38	73.66	0.30371	85.84	87.34	88.62	89.78
0.39963	73.17	73.44	73.72	74.03	0.41664	86.41	87.83	89.15	90.31
0.50672	73.58	73.82	74.06	74.42	0.51397	86.97	88.39	89.67	90.95

m_A is the molality of alpha-hydroxy acids in sodium benzoate solution: the calculated standard uncertainties u are u(m) = 0.02520 (mol·kg^{-1}), u(T)=0.001 K, u (V_ϕ) = (0.07-0.19) × 10^6/(m^3·mol^{-1}).

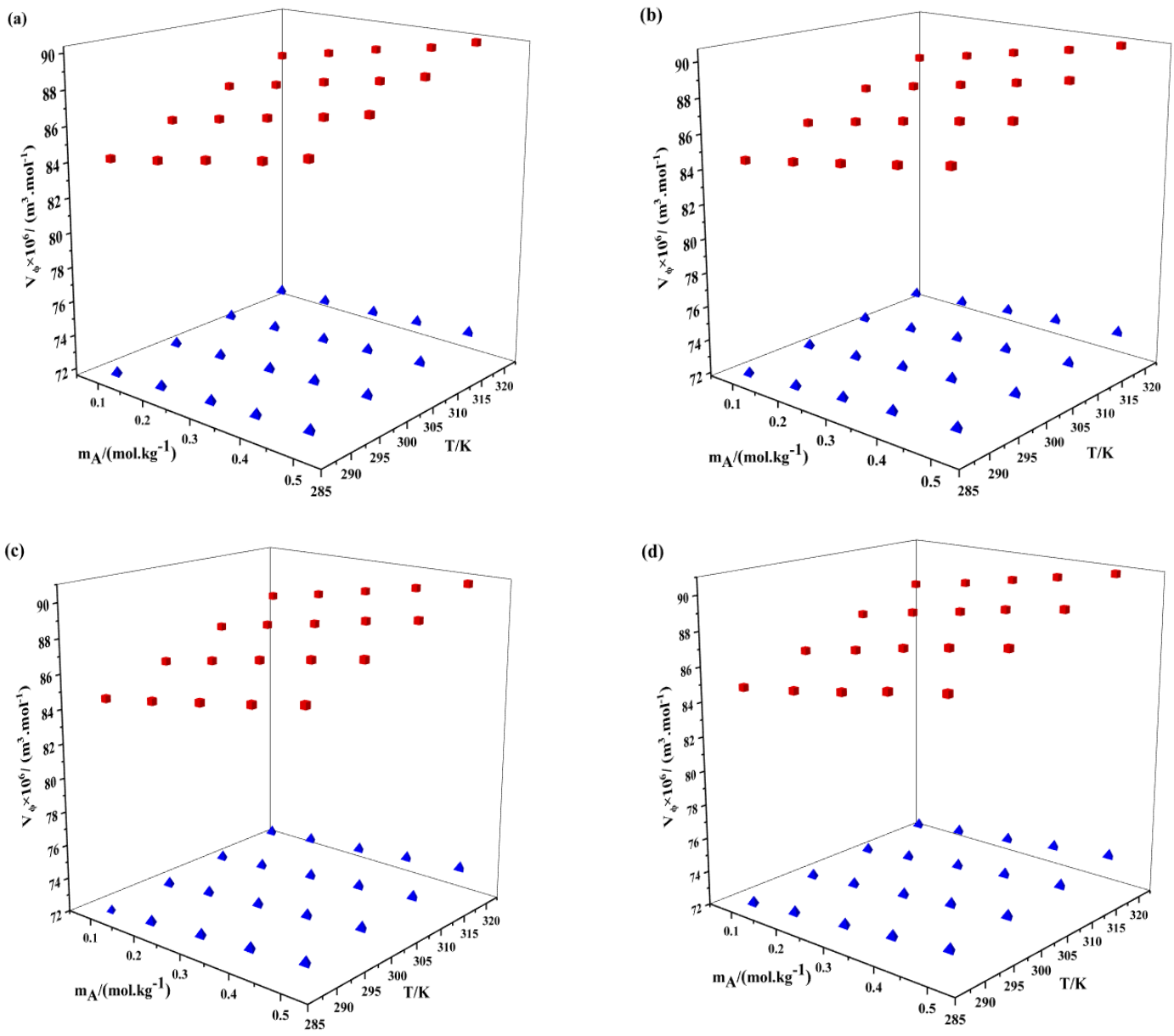

Figure 4.25 Three-dimensional plots illustrate the variations in ($V_\emptyset$) of (a) 0.00 SB; (b) 0.01 SB; (c) 0.02 SB;(d) 0.03 SB for molality of lactic acid (blue; tetrahedron) and malic acid (red; cube) at varying temperatures.

4.4.3 Partial molar volumes

This is a key property that represents the change in the total volume of a solution when one mole of solute is added. It provides an understanding of the associations and the structural arrangement of molecules in the solution [20]. The **equation 4.2** can be employed to govern the V_ϕ^0 of ternary liquid systems that consist of lactic and malic acids mixed with sodium benzoate in aqueous solutions [56]. **Table 4.32** presents the results of evaluating the (V_ϕ^0) and (S_V^*) through the use of the least square fitting technique. At all different temperatures, the V_ϕ^0 remains positive and rises following the sodium benzoate concentration. Enhanced interactions within the solute-solvent system could have a significant role in this phenomenon as observed in **Figure 4.26.** The variation of V_ϕ^0 with temperature reveals the nature of these interactions- whether they are strengthening or weakening with increasing thermal energy [57].

It has been observed that for SB molecules, the magnitude of S_V^* has continuously remained positive across all operating temperatures. The lack of consistent trends in S_V^* values indicate that additional variables influence solute interactions [58]. The cosphere overlaps hypothesis states that when two groups of ions interact, their hydration spheres merge, resulting in a decrease in bulk properties, overlap between hydrophobic ions, and an increase in volume. The positive value of V_ϕ^0 is due to the existence of ion and hydrophilic bonds, which are generally more predominant than interactions inside ions and hydrophobic bonds or within hydrophobic and hydrophobic ions. The interactions that take place between solutes and solvents have a more substantial impact on the interactions that take place inside solute molecules in a solution than the interactions that take place between solutes interacting with one another [59,16,60]. Solute-solvent bonds dominate in the current study due to the very small S_V^* values relative to the V_ϕ^0 values. In practical applications, V_ϕ^0 helps predict solubility, stability, and interaction mechanisms in systems like food preservatives, pharmaceuticals, and chemical solutions, making it essential for understanding and optimizing solution behavior.

Table 4.32 Values of 'V_ϕ^0' and 'S_V^*' of sodium benzoate with lactic and malic acids solutions along with their standard errors.

m_B/ (mol·kg^{-1})	$V_\phi^0 \times 10^6$/(m^3·mol^{-1})				$S_V^* \times 10^6$ /(m^3·kg·mol^{-2})			
	288.15K	298.15K	308.15K	318.15K	288.15K	298.15K	308.15K	318.15K
				Lactic Acid				
0.00	71.53(±0.01)	71.87(±0.00)	72.19(±0.02)	72.52(±0.03)	2.01(±0.03)	1.97(±0.01)	2.00(±0.05)	1.98(±0.08)
0.01	71.57(±0.05)	71.89(±0.01)	72.21(±0.01)	72.55(±0.02)	2.87(±0.14)	2.89(±0.03)	2.65(±0.03)	2.79(±0.07)
0.02	71.61(±0.01)	71.93(±0.01)	72.22(±0.01)	72.57(±0.01)	3.11(±0.04)	3.24(±0.03)	3.16(±0.03)	3.05(±0.03)
0.03	71.65(±0.02)	71.96(±0.01)	72.24(±0.03)	72.61(±0.01)	3.53(±0.05)	3.68(±0.02)	3.64(±0.09)	3.74(±0.03)
				Malic Acid				
0.00	83.57(±0.07)	84.92(±0.03)	86.13(±0.05)	87.29(±0.06)	5.98(±0.21)	6.02(±0.10)	5.99(±0.16)	6.07(±0.18)
0.01	83.99(±0.02)	85.28(±0.02)	86.50(±0.01)	87.63(±0.03)	5.34(±0.06)	5.61(±0.07)	5.85(±0.04)	5.99(±0.10)
0.02	84.07(±0.04)	85.34(±0.01)	86.62(±0.03)	87.72(±0.04)	5.33(±0.13)	5.71(±0.03)	5.74(±0.10)	6.07(±0.12)
0.03	84.29(±0.06)	85.56(±0.07)	86.84(±0.03)	87.96(±0.06)	5.15(±0.17)	5.53(±0.20)	5.22(±0.09)	5.52(±0.19)

m_B implies the concentration of the sodium benzoate solution: standard uncertainties u are u(m) = 0.01 (mol·kg^{-1}), u(T)=0.001 K, u (V_ϕ^0)= ±1.46 × 10^6/(m^3·mol^{-1}) and u (S_V^*)=±0.27 × 10^6/(m^3·kg·mol^{-2}).

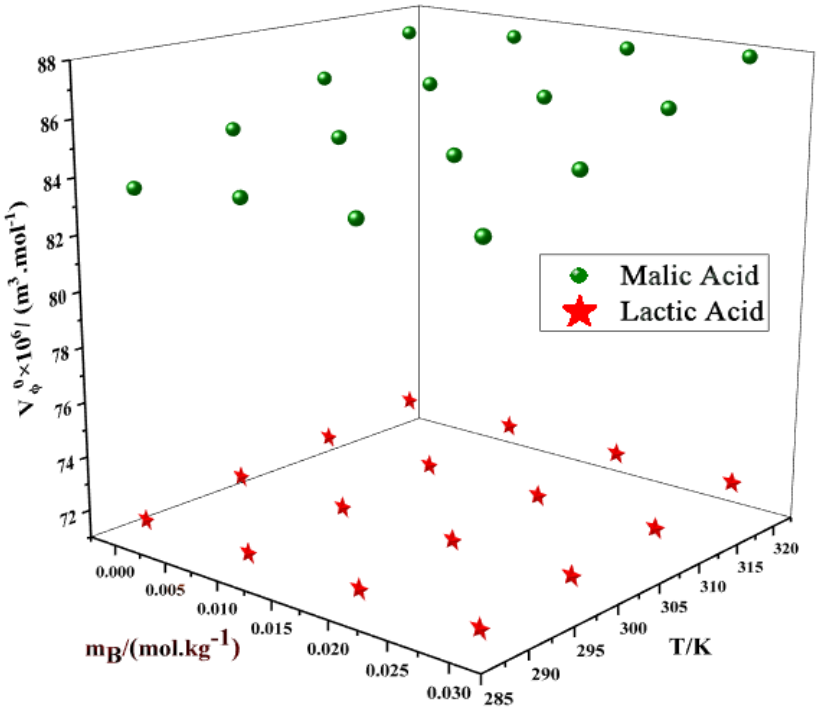

Figure 4.26 The plots represent the variations in $V_{\emptyset}^{0}$, for lactic and malic acid within a sodium benzoate aqueous solution at several temperatures.

4.4.4 Partial molar volume of transfer

This parameter reflects the interaction of the solutes with the pure solvent and provides insights into how the solute behaves in different environments [61]. **Equation 4.3** was applied to evaluate the transfer volumes of lactic and malic acids from aqueous medium into sodium benzoate solutions at infinite dilution. It is significant to recognize that both the solute and the solvent are electrolytes in this study, which focuses on the combination of sodium benzoate (SB), water, and lactic acid (LA)/malic acid (MA). All of these compounds are electrolytes. Due to this, it has been shown that the values of ΔV_{ϕ}^{0} reflect the presence of ionic interaction inside aqueous SB, LA, and MA. When considering the concept of co-sphere overlap, it is evident from the findings of ΔV_{ϕ}^{0} that the interaction within the solute and the solute is minimal [62]. The values of this transfer parameter for lactic and malic acids in sodium benzoate are positive and indexed in **Table 4.33**. In the present ternary systems, the solute possesses the capability to create structures, and the solute and solvent interactions have been identified which has been shown by the positive values of ΔV_{ϕ}^{0} [63–65]. The positive trend highlights the strengthening of solute-solvent interaction, indicating that the solute molecules are effectively integrated into the solution, potentially influencing the overall properties such as solubility, stability, and biological activity in various applications like food and pharmaceutical formulations.

Table 4.33 Values of transfer, ΔV_{ϕ}^{0}, of the combination of Sodium Benzoate in water-based lactic and malic acids solutions at several temperatures.

m_B/ (mol·kg^{-1})	$\Delta V_{\phi}^{0} \times 10^{6}$/(m^3·mol^{-1})			
	288.15K	298.15K	308.15K	318.15K
		Lactic Acid		
0.01	0.04	0.02	0.02	0.03
0.02	0.09	0.06	0.03	0.04
0.03	0.12	0.09	0.05	0.09
		Malic Acid		
0.01	0.42	0.35	0.36	0.34
0.02	0.49	0.41	0.49	0.43
0.03	0.71	0.64	0.71	0.67

m_B denotes the molality of sodium benzoate solution: the calculated standard uncertainties u are u(m) = 0.01 (mol·kg^{-1}), u(T)=0.001 K, u(ΔV_{ϕ}^{0})= ±0.05×10^6/(m^3·mol^{-1}).

4.4.5 Temperature-dependent partial molar volume

Variations in this parameter reveal the nature of molecular interactions, such as whether they strengthen or weaken with temperature, which is crucial for understanding solubility, stability, and the overall behavior of solutions in different temperature conditions [66,67]. **Equation 4.4** may be utilized to determine the distinction of V_ϕ^0 associated with the temperature at infinite dilutions. **Table 4.34** presents the empirical constants for lactic and malic acids in sodium benzoate solutions, denoted by the variables a, b, c . In this particular investigation, the R^2 values demonstrate that variations in values are exceedingly small, hence completely satisfying the polynomial equation. In order to acquire a comprehensive knowledge of the interactions inside the solute-solvent in a mixture, it is crucial to identify the limiting apparent molar expansibilities, as shown by **equation 4.6** [36,33].

The **equation 4.7** was used to estimate the structure constructing and disrupting capabilities of the solute in solvent by means of the general thermodynamic expression, which was derived by Hepler [26]. Since the E_ϕ^0 values, which are provided in **Table 4.35,** are positive for all of the analyzed solutions over the entire range of operating temperatures, it is possible to conclude that there are significant ion-hydrophilic interactions within molecules of solute and solvent. The packaging/caging effect is responsible for the increased prevalence of the E_ϕ^0 values, which further emphasize the importance of the solute as well as solvent interactions [68].

The sign of the Hepler's constant provides useful insights into the ability of the solution to create or break structure, as tabulated in **Table 4.35**. A significant positive value for the $\left(\frac{\partial E_\Phi^0}{\partial T}\right)_P$ specifies that the solute possesses the inclination to construct structures, whereas a negative value suggests that the solute possesses the capability to break structures [69,70]. This constant was determined to be positive for lactic acid in an aqueous solution of SB which suggests the structure-making behavior of the liquid systems whereas $\left(\frac{\partial E_\Phi^0}{\partial T}\right)_P$ was found to be negative for malic acid in an aqueous solution of SB which gives evidence of the structure-breaking properties of the combinations in the current study.

Table 4.34 Calculation of empirical constants of sodium benzoate in aqueous lactic and malic acids solutions.

m_B/ (mol·kg^{-1})	$a \times 10^6$/ (m^3·mol^{-1})	$b \times 10^6$/ (m^3·mol^{-1}·K^{-1})	$c \times 10^6$/ (m^3·mol^{-1}·K^{-2})	R^2	ARD
		Lactic Acid			
0.01	71.89	0.0323	0.00004	0.9999	0.0000
0.02	71.92	0.0308	0.00007	0.9999	0.0000
0.03	71.94	0.0302	0.00014	0.9999	0.0000
		Malic Acid			
0.01	85.28	0.1254	-0.00038	0.9999	0.0000
0.02	85.37	0.1268	-0.00042	0.9999	0.0000
0.03	85.59	0.1269	-0.00039	0.9999	0.0000

m_B specifies the concentration of sodium benzoate solution: standard uncertainties are u(m) = 0.01 (mol·kg^{-1}), u(T)=0.001 K, u(p) =0.01 MPa.

Table 4.35 Coefficient of expansibilities 'E_ϕ^0' for sodium benzoate in aqueous solutions with lactic and malic acids.

m_B/ (mol·kg^{-1})	$E_\phi^0 \times 10^6$/(m^3·mol^{-1}·K^{-1})				$\left(\frac{\partial E_\phi^0}{\partial T}\right)_P$ /(m^3·mol^{-1}·K^{-2})
	288.15K	298.15K	308.15K	318.15K	
			Lactic Acid		
0.01	0.0314	0.0323	0.0332	0.0340	0.00009
0.02	0.0293	0.0308	0.0322	0.0337	0.00014
0.03	0.0274	0.0302	0.0331	0.0359	0.00029
			Malic Acid		
0.01	0.1330	0.1254	0.1178	0.1101	-0.00076
0.02	0.1351	0.1268	0.1184	0.1100	-0.00084
0.03	0.1348	0.1269	0.1191	0.1112	-0.00079

m_B specifies the concentration of sodium benzoate solution: standard uncertainties are u(m) = 0.01 (mol·kg^{-1}), u(T)=0.001 K, u(E_ϕ^0) = 0.0095 ×10^6/(m^3·mol^{-1}·K^{-1}), u$\left(\frac{\partial E_\phi^0}{\partial T}\right)$= 0.00022/(m^3·mol^{-1}·K^{-2}), u(p) =0.01 MPa.

4.4.6 Speed of sound

The ultrasonic speed in a mixture including water, sodium benzoate, and lactic acid/malic acid has been measured at varied temperatures and the investigated data is recorded in **Table 4.36.** The significant increase in sound speed data observed with increasing molality of lactic and malic acids can be ascribed to the occurrence of 3-D hydrogen bond networks between the molecules of the LA/MA and an increase in the concentration of sodium benzoate. The mechanism behind the rise in the ultrasonic speed values when LA/MA and sodium benzoate are combined is the creation of H_2 bonds among the solute and solvent associations. Additionally, as the molecular mass of the solutes rises from lactic acid (LA) to malic acid (MA), the H-bonding within the sodium benzoate (SB) and H_2O molecules diminishes and eventually dissolves. Concurrently, new hydrogen bonds form within the molecules of the resulting liquid systems [31,71,72].

Table 4.36 Values of sound velocity 's' were determined in the combination of sodium benzoate with lactic and malic acids mixtures at several temperatures.

m_A/	s/(m·s^{-1})				m_A/	s/(m·s^{-1})			
(mol·kg^{-1})	288.15K	298.15K	308.15K	318.15K	(mol·kg^{-1})	288.15K	298.15K	308.15K	318.15K
0.00 (mol·kg^{-1}) Sodium Benzoate + Lactic Acid					**0.00 (mol·kg^{-1}) Sodium Benzoate + Malic Acid**				
0.00000	1466.59	1495.85	1519.14	1536.02	0.00000	1466.59	1495.85	1519.14	1536.02
0.09931	1470.18	1498.79	1521.32	1537.51	0.09930	1470.76	1499.04	1521.54	1537.83
0.19903	1473.29	1501.64	1523.38	1538.94	0.20136	1474.85	1502.13	1524.02	1539.51
0.30437	1476.74	1504.38	1525.52	1540.61	0.29949	1478.44	1505.30	1526.28	1541.16
0.39491	1479.45	1507.03	1527.47	1541.97	0.40764	1482.46	1508.75	1528.87	1543.06
0.49638	1482.51	1509.56	1529.42	1543.44	0.49042	1485.56	1511.27	1530.69	1544.39
0.01 (mol·kg^{-1}) Sodium Benzoate + Lactic Acid					**0.01 (mol·kg^{-1}) Sodium Benzoate + Malic Acid**				
0.00000	1468.32	1498.32	1520.45	1537.12	0.00000	1468.32	1498.32	1520.45	1537.12
0.09292	1471.07	1500.89	1522.34	1538.44	0.09918	1472.52	1501.04	1523.01	1538.87
0.19681	1474.18	1503.55	1524.58	1539.99	0.20125	1476.54	1503.86	1525.24	1540.75
0.29545	1477.15	1505.98	1526.77	1541.51	0.29686	1480.27	1506.65	1527.36	1542.46
0.39362	1480.36	1508.46	1528.64	1542.92	0.40372	1483.83	1509.98	1529.78	1544.14
0.51301	1484.27	1511.35	1530.92	1544.67	0.49841	1486.96	1512.94	1531.81	1545.51
0.02 (mol·kg^{-1}) Sodium Benzoate + Lactic Acid					**0.02 (mol·kg^{-1}) Sodium Benzoate + Malic Acid**				
0.00000	1470.12	1500.26	1521.28	1538.06	0.00000	1470.12	1500.26	1521.28	1538.06
0.10514	1472.77	1502.53	1523.45	1539.37	0.10647	1473.88	1502.3	1524.17	1539.95

0.19723	1475.65	1504.86	1525.73	1541.03	0.20876	1477.54	1504.69	1526.38	1541.66
0.30553	1479.10	1507.68	1527.94	1542.75	0.30821	1481.83	1507.94	1528.86	1543.78
0.40625	1482.26	1510.07	1529.72	1544.28	0.40950	1484.99	1510.62	1530.67	1545.21
0.51246	1485.58	1512.75	1531.81	1545.92	0.50775	1488.61	1513.78	1532.91	1546.76
0.03 (mol·kg^{-1}) Sodium Benzoate + Lactic Acid					**0.03 (mol·kg^{-1}) Sodium Benzoate + Malic Acid**				
0.00000	1471.29	1501.32	1522.67	1539.28	0.00000	1471.29	1501.32	1522.67	1539.28
0.10639	1474.41	1504.11	1524.92	1540.73	0.09874	1475.04	1503.57	1525.28	1540.92
0.19865	1477.15	1506.46	1526.98	1542.25	0.21348	1479.14	1506.56	1527.64	1543.03
0.30468	1480.53	1508.83	1529.02	1543.79	0.30371	1482.87	1508.97	1529.72	1544.68
0.39963	1483.38	1511.15	1530.79	1545.33	0.41664	1485.95	1511.88	1531.71	1546.25
0.50672	1487.09	1513.66	1532.83	1546.84	0.51397	1489.75	1514.89	1533.84	1547.86

m_A denotes the molality of alpha-hydroxy acids in sodium benzoate aqueous solution: the calculated standard uncertainties u are u(m) = 0.02520 (mol·kg^{-1}), u(T)=0.001 K, u(s)=1.77 (m·s^{-1}).

4.4.7 Apparent molar isentropic compression

This parameter provides information about how the compression of a solution changes upon the addition of one mole of solute. It reflects the solute-solvent interactions, where a lower compressibility value indicates strong bonds amid the solute and solvent molecules, leading to a denser and stable mixture. However, a higher value suggests weaker interactions, where the molecules are loosely associated, and the solution is more easily compressed [73,74] . This is important in understanding the structural and thermodynamic behavior of solutions, especially in applications like food preservation, pharmaceuticals, and chemical engineering. The Laplace **equation 4.8** is used to calculate isentropic compressibility [75].

In an aqueous sodium benzoate solution, the **equation 4.9** that has been provided is associated with the estimation of the $K_{\phi,S}$ of alpha-hydroxy acids (LA/MA). The findings of $K_{\phi,S}$ that were estimated at a variety of temperatures and concentrations of sodium benzoate are recorded in **Table 4.37** and visually presented in **Figures 4.27** and **4.28**. Water molecules are particularly attracted to sodium benzoate ions due to their strong electrolytic properties. It is possible to observe from **Table 4.36** that the values of $K_{\phi,S}$ are negative, and although the negative trend drops with higher temperatures and sodium benzoate concentrations, it becomes more pronounced with the enhancement of the molality of lactic and malic acids. This occurs as a result of the solute bonds being released from the solvent, which is due to thermal agitation, leading to a rise in volume and a larger degree of compressibility [76,45]. Due to this, the volume of the solution significantly increases. This demonstrates that there is a certain rearrangement of water molecules nearby the solute, as indicated by the negative $K_{\phi,S}$, which implies that the H_2O molecules that surround the charged ionic clusters of the solute are lesser compressed than those that are present in the bulk solution [77,78].

Table 4.37 Data of '$K_{\phi,s}$' of alpha-hydroxy acids (lactic and malic acids) in sodium benzoate aqueous solution.

m_A/ (mol·kg^{-1})	$K_{\phi,s} \times 10^6$/(m^3·mol^{-1}·GPa^{-1})				m_A/ (mol·kg^{-1})	$K_{\phi,s} \times 10^6$/(m^3·mol^{-1}·GPa^{-1})			
	288.15K	298.15K	308.15K	318.15K		288.15K	298.15K	308.15K	318.15K
0.00 (mol·kg^{-1}) Sodium Benzoate + Lactic Acid					**0.00 (mol·kg^{-1}) Sodium Benzoate + Malic Acid**				
0.09931	-46.08	-44.30	-42.98	-42.03	0.09930	-46.62	-44.80	-43.43	-42.47
0.19903	-46.40	-44.60	-43.27	-42.32	0.20136	-47.47	-45.60	-44.19	-43.21
0.30437	-46.56	-44.76	-43.42	-42.47	0.29949	-48.08	-46.17	-44.74	-43.75
0.39491	-46.67	-44.86	-43.51	-42.56	0.40764	-48.64	-46.70	-45.26	-44.25
0.49638	-46.77	-44.95	-43.60	-42.65	0.49042	-49.11	-47.14	-45.67	-44.66
0.01 (mol·kg^{-1}) Sodium Benzoate + Lactic Acid					**0.01 (mol·kg^{-1}) Sodium Benzoate + Malic Acid**				
0.09292	-45.97	-44.09	-42.87	-41.92	0.09918	-46.02	-44.16	-42.90	-41.94
0.19681	-46.32	-44.42	-43.19	-42.24	0.20125	-46.71	-44.82	-43.53	-42.56
0.29545	-46.48	-44.58	-43.35	-42.39	0.29686	-47.33	-45.40	-44.08	-43.09
0.39362	-46.58	-44.68	-43.44	-42.48	0.40372	-47.85	-45.90	-44.56	-43.56
0.51301	-46.69	-44.78	-43.54	-42.58	0.49841	-48.30	-46.32	-44.96	-43.94
0.02 (mol·kg^{-1}) Sodium Benzoate + Lactic Acid					**0.02 (mol·kg^{-1}) Sodium Benzoate + Malic Acid**				
0.10514	-45.91	-44.04	-42.81	-41.85	0.10647	-44.03	-42.14	-41.21	-40.40
0.19723	-46.24	-44.35	-43.12	-42.15	0.20876	-44.72	-42.78	-41.84	-41.01
0.30553	-46.40	-44.51	-43.27	-42.31	0.30821	-45.24	-43.28	-42.32	-41.48
0.40625	-46.51	-44.61	-43.37	-42.41	0.40950	-45.72	-43.73	-42.76	-41.90
0.51246	-46.61	-44.70	-43.46	-42.49	0.50775	-46.13	-44.11	-43.12	-42.26

0.03 (mol·kg^{-1}) Sodium Benzoate + Lactic Acid					**0.03 (mol·kg^{-1}) Sodium Benzoate + Malic Acid**				
0.10639	-45.89	-44.01	-42.79	-41.82	0.09874	-42.26	-40.61	-39.89	-39.23
0.19865	-46.17	-44.28	-43.04	-42.08	0.21348	-42.89	-41.20	-40.47	-39.80
0.30468	-46.33	-44.43	-43.19	-42.22	0.30371	-43.36	-41.66	-40.91	-40.23
0.39963	-46.43	-44.53	-43.29	-42.32	0.41664	-43.82	-42.09	-41.33	-40.64
0.50672	-46.52	-44.62	-43.38	-42.40	0.51397	-44.22	-42.47	-41.69	-40.99

m_A denotes the molality of alpha-hydroxy acids in solution of sodium benzoate: the calculated standard uncertainties u are u(m) = 0.02520 (mol·kg^{-1}), u(T)=0.001 K, u ($K_{\phi,S}$) = (0.17 - 0.18) × 10^6/(m^3·mol^{-1}·GPa^{-1}).

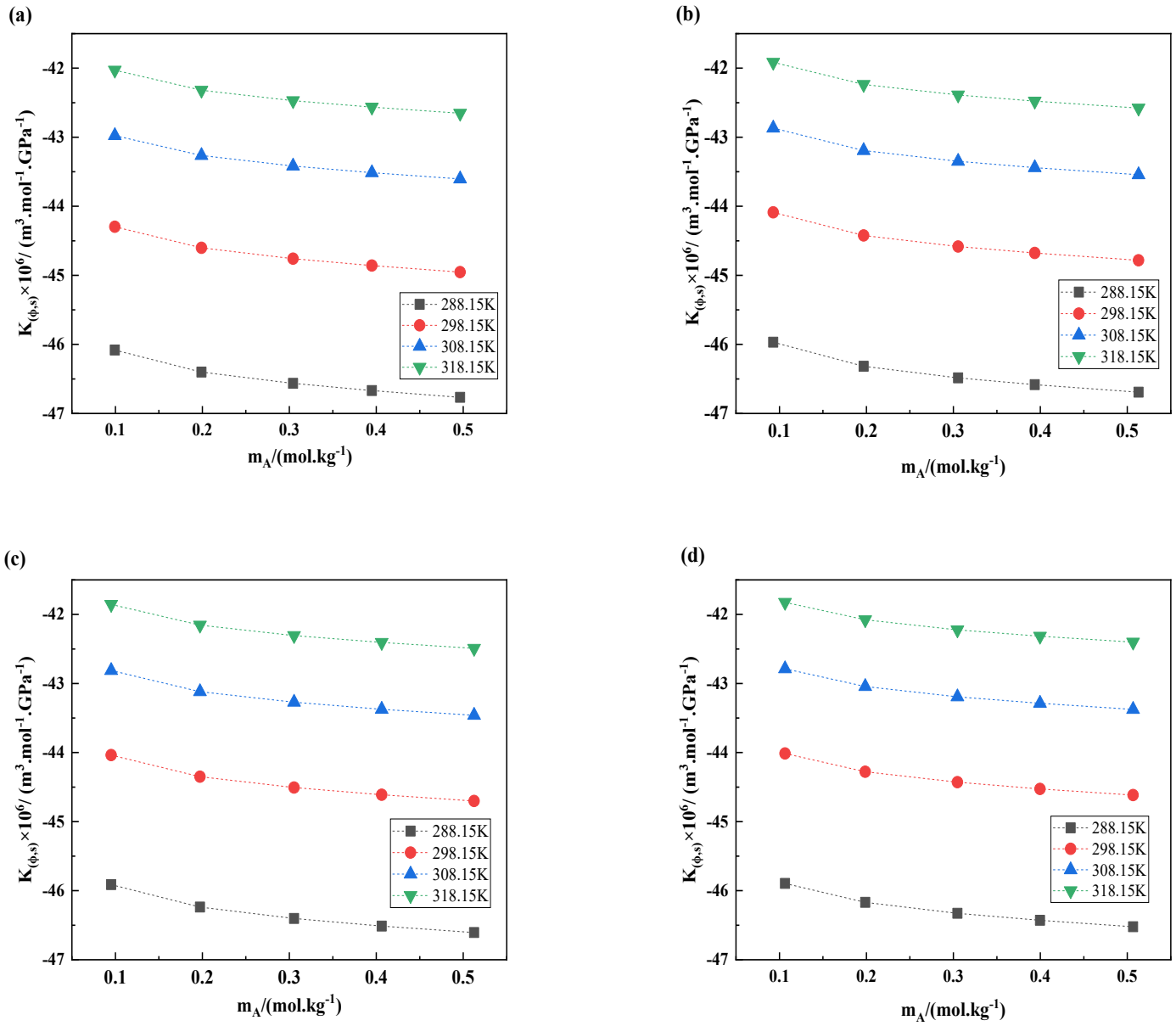

Figure 4.27 Changes of $K_{\phi,S}$, of Lactic Acid (LA) in (a) 0.00 SB; (b) 0.01 SB; (c) 0.02 SB; (d) 0.03 SB for molality of lactic acid aqueous solutions at several temperatures.

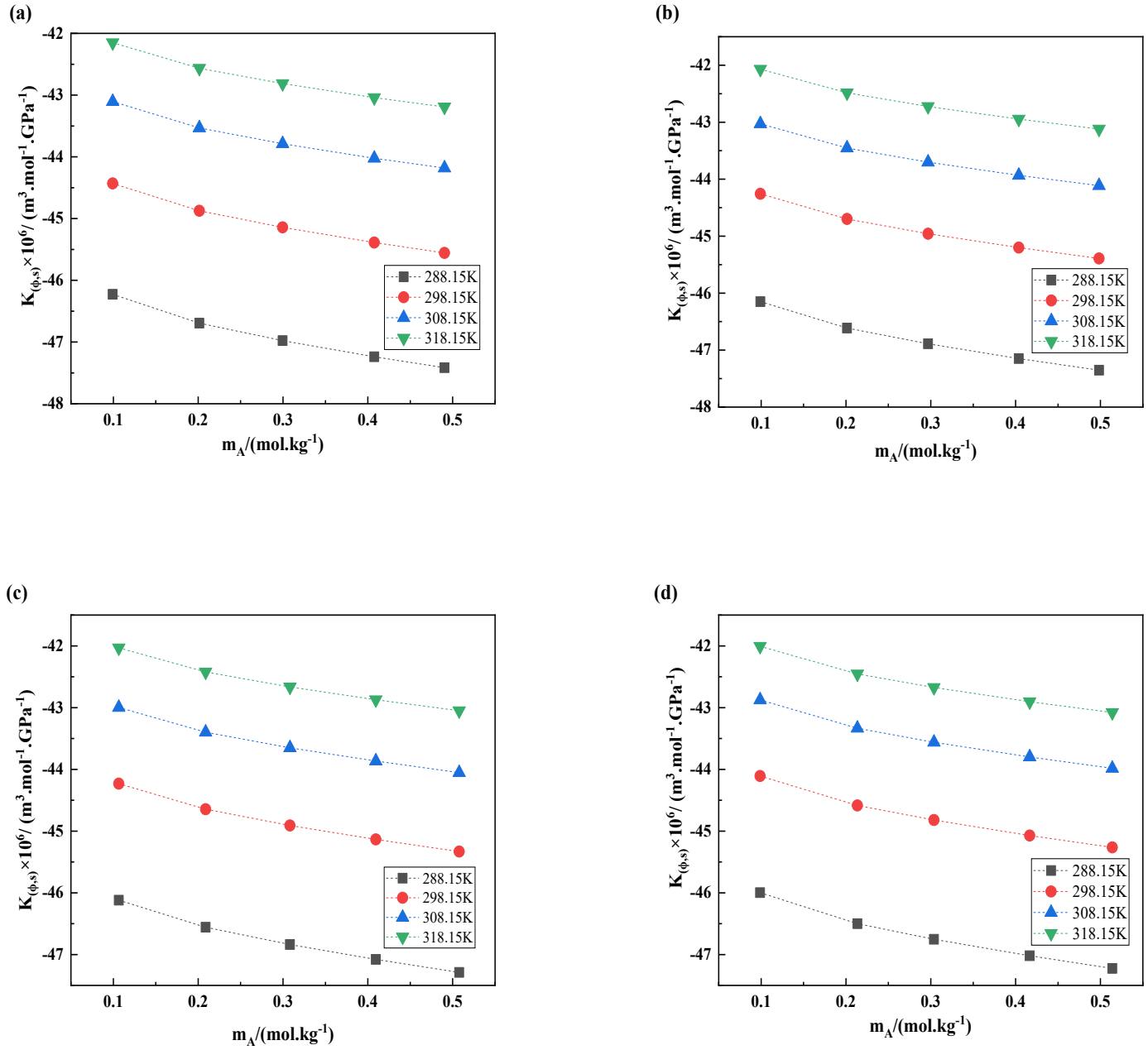

Figure 4.28 Changes of $K_{\phi,S}$, of Malic Acid (MA) in (a) 0.00 SB; (b) 0.01 SB; (c) 0.02 SB; (d) 0.03 SB for molality of malic acid aqueous solutions at several temperatures.

4.4.8 Partial molar isentropic compression

It refers to the variation in the compressibility of a solution when one mole of solute is added under 0.1 MPa pressure, considering the contributions of each component in the mixture. It provides insights into how the solute affects the overall solution's compressibility, reflecting the strength of solute-solvent interactions and the structures induced by adding the solute [79]. The **equation 4.10** illustrates the changes that occur within the concept of molality (m_A) and $K_{\phi,S}^{0}$. **Table 4.38** includes the computed values of the acoustic virial coefficient (S_K^*), along with their corresponding errors. This coefficient offers insights into the interaction between the solutes. Consequently, the presence of alpha-hydroxy acids (LA/MA) and water diminishes the electrostriction contact within the mixtures, thereby enhancing the interaction between sodium benzoate and molality of lactic and malic acids which is described by the Kirkwood model [40]. The results of $K_{\phi,S}^{0}$ tend to become more negative at low temperatures, which shows that there are extremely favorable interactions within lactic/malic acids and water molecules as depicted in **Figure 4.29**. The key factors that ascribe to the \ $K_{\phi,S}^{0}$ are the impacts that are listed below: - The positive impact, commonly known as the intrinsic compressibility of the solvent, arises when the amount of free space within the molecules of the solution increases, leading to further compression of the solution. The negative effect, known as solvent penetration, occurs when solvent molecules occupy the vacant spaces between ions. The contacts between molecules of solute in the system are negligible, as the values of S_K^* are slight as compared to the $K_{\phi,S}^{0}$, highlighting the prevalence of associations of solute-solvent in the investigated liquid combination[41,80].

Table 4.38 Calculated $K^0_{\phi,s}$ and S^*_K, of alpha-hydroxy acids (lactic and malic acids) in sodium benzoate aqueous solution.

m_B/ (mol·kg^{-1})	$K^0_{\phi,s} \times 10^6$/(m^3·mol^{-1})				$S^*_K \times 10^6$ /(m^3·kg·mol^{-2})			
	288.15K	298.15K	308.15K	318.15K	288.15K	298.15K	308.15K	318.15K
				Lactic Acid				
0.00	-46.00(±0.08)	-44.22(±0.08)	-42.90(±0.07)	-41.96(±0.08)	-1.66(±0.25)	-1.59(±0.24)	-1.52(±0.23)	-1.51(±0.23)
0.01	-45.91(±0.09)	-44.04(±0.09)	-42.82(±0.09)	-41.87(±0.09)	-1.65(±0.28)	-1.58(±0.27)	-1.54(±0.26)	-1.51(±0.26)
0.02	-45.85(±0.09)	-43.98(±0.08)	-42.76(±0.08)	-41.80(±0.08)	-1.59(±0.26)	-1.52(±0.25)	-1.49(±0.24)	-1.46(±0.24)
0.03	-45.81(±0.08)	-43.93(±0.07)	-42.71(±0.07)	-41.75(±0.07)	-1.51(±0.23)	-1.45(±0.22)	-1.41(±0.21)	-1.38(±0.21)
				Malic Acid				
0.00	-46.02(±0.09)	-44.24(±0.09)	-42.92(±0.08)	-41.97(±0.08)	-2.97(±0.27)	-2.80(±0.26)	-2.68(±0.25)	-2.59(±0.25)
0.01	-45.95(±0.09)	-44.07(±0.09)	-42.85(±0.08)	-41.90(±0.08)	-2.94(±0.27)	-2.77(±0.26)	-2.65(±0.26)	-2.56(±0.25)
0.02	-45.90(±0.08)	-44.02(±0.08)	-40.80(±0.08)	-41.84(±0.08)	-2.85(±0.24)	-2.68(±0.23)	-2.57(±0.23)	-2.48(±0.23)
0.03	-45.81(±0.09)	-43.93(±0.09)	-42.70(±0.09)	-41.80(±0.09)	-2.89(±0.27)	-2.72(±0.26)	-2.60(±0.25)	-2.52(±0.25)

m_B implies the concentration of sodium benzoate solution: the calculated standard uncertainties u are u(m) = 0.01 (mol·kg^{-1}), u(T)=0.001 K, u($K^0_{\phi,S}$) = 0.32 × 10^6/(m^3·mol^{-1}·GPa^{-1}), u(S^*_K)= ±0.13×10^6/(kg·m^3·kg·mol^{-2}·GPa^{-1}).

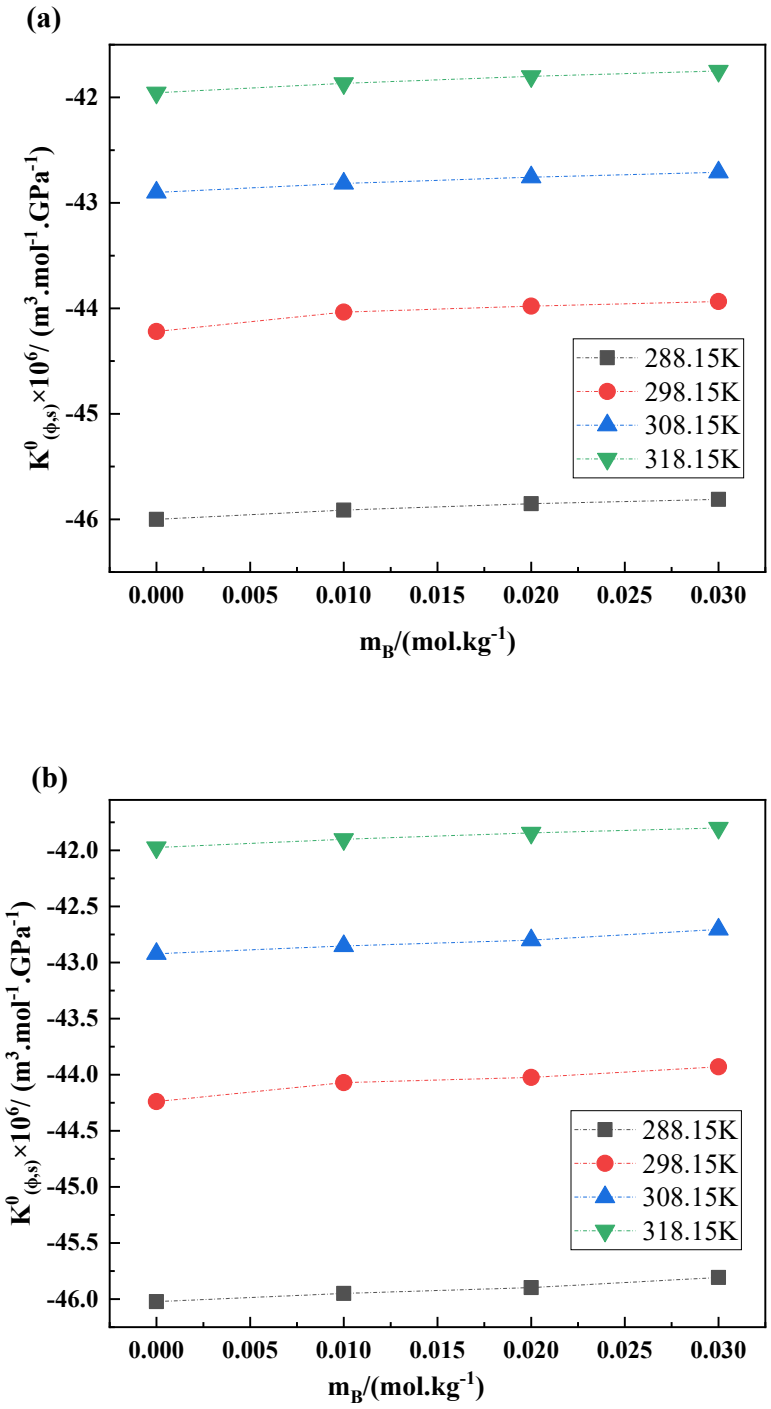

Figure 4.29 Plots of variations of $K^0_{\emptyset,S}$ for (a) lactic acid and (b) malic acid in aqueous sodium benzoate solution at varying temperatures.

4.4.9 Transfer characteristics of partial molar isentropic compression

It reflects the variation in solution compressibility when a solute is shifted from one solvent to another, i.e. from water to sodium benzoate solution. It indicates how the solute affects the compressibility in the sodium benzoate solution, reflecting the strength of associations within the solute and the solvent. If the value is positive, it means the solute makes the solution less compressible, suggesting stronger interactions within the solvent. If the value is negative, the solute makes the solution more compressible, indicating weaker interactions [81]. The **equation 4.11** has been applied to determine the amount of lactic and malic acids shifted from water to sodium benzoate solutions at infinite dilutions.

Values of $\Delta K_{\phi,s}^{0}$ are positive which are presented in **Table 4.39.** The zwitterionic center of lactic and malic acids interacts with sodium benzoate more strongly as its concentration rises, changing the structure of the liquid systems with a lessening in the electrostriction. The ability to construct structures is facilitated by the reduction in electrostriction that occurs when the concentration of SB rises [44]. The observed $K_{\phi,S}^{0}$ values might be ascribed to the enhanced binding of molecules of water to the ions. In this study, the rise in the $\Delta K_{\phi,s}^{0}$ values contribute to the improved ability of solute-solvent bonds to form structures and the strength of these interactions [82].

Table 4.39 Values of transfer $\Delta K^0_{\phi,S}$, of alpha-hydroxy acids (lactic and malic acids) in aqueous sodium benzoate solution at several temperatures.

m_B/ (mol·kg^{-1})	$\Delta K^0_{\phi,S} \times 10^6$/(m^3·mol^{-1}·GPa^{-1})			
	288.15K	298.15K	308.15K	318.15K
		Lactic Acid		
0.01	0.09	0.18	0.08	0.09
0.02	0.15	0.24	0.14	0.16
0.03	0.19	0.28	0.19	0.21
		Malic Acid		
0.01	0.07	0.17	0.07	0.07
0.02	0.12	0.22	0.12	0.13
0.03	0.22	0.31	0.22	0.17

m_B implies the concentration of the sodium benzoate solution: the calculated standard uncertainties u are u(m) = 0.01 (mol·kg^{-1}), u(T)=0.001 K, u($\Delta K^0_{\phi,S}$) = 0.01×10^6/(m^3·mol^{-1}·GPa^{-1}).

4.4.10 Interaction coefficients

The pair coefficient refers to the interaction between two molecules, such as solute-solvent or solute-solute pairs, whereas the triplet coefficient considers the interaction between three molecules or ions simultaneously [43]. McMillian and Mayer derived the coefficients for isentropic compression and volumetric interactions. This theory specifically examines the separation effects in a liquid system, resulting from interactions between pairs and triplets [46]. The **equations 4.12** and **4.13** illustrate the transfer parameters for these interaction coefficients (V_{AB}, V_{ABB}; K_{AB}, K_{ABB}).

Values for interaction coefficients are recorded in **Table 4.40**. Franks et al. conducted an in-depth investigation into the McMillian theory, examining the underlying principles and implications of the interactions involved [47]. Pair-wise coefficients are found to be positive for lactic and malic acids, while triplet constants are negative for both acids across the studied temperature range, with the exception of the triplet coefficient for volume in lactic acid, which is positive between 298.15 K and 318.15 K, and the triplet coefficient for isentropic compression in malic acid, which is positive at 288.15 K and 308.15 K, respectively. It has been noticed that the pair-wise interactions remain constantly positive across all tested temperatures for both acids, specifically lactic and malic acids. This finding suggests stable and favorable interactions, between these components, highlighting the significance of their molecular interactions in the current investigation. The positive data highlight that the presence of the lactic and malic acids contributes to enhanced structural stability and cohesion within the liquid combinations at varying temperatures.

Table 4.40 Interaction coefficients for the ternary liquid combination of aqueous sodium benzoate solutions with lactic and malic acids.

T/K	$V_{AB} \times 10^6/(m^3 \cdot mol^{-2} \cdot kg)$	$V_{ABB} \times 10^6/(m^3 \cdot mol^{-3} \cdot kg^2)$	$K_{AB} \times 10^6/(m^3 \cdot mol^{-2} \cdot kg \cdot GPa^{-1})$	$K_{ABB} \times 10^6/(m^3 \cdot mol^{-3} \cdot kg^2 \cdot GPa^{-1})$
		Lactic Acid		
288.15	2.26	-3.76	4.92	-39.09
298.15	1.00	10.63	10.05	-120.30
308.15	0.60	4.55	4.59	-31.73
318.15	0.90	11.47	4.93	-33.43
		Malic Acid		
288.15	19.79	-184.49	2.98	12.41
298.15	15.97	-126.98	8.15	-69.77
308.15	17.45	-132.76	2.71	18.76
318.15	15.52	-105.13	4.03	-24.79

T/K is the temperatures in kelvin.

References

1. A.-P. Hyvärinen, H. Lihavainen, A. Gaman, L. Vairila, H. Ojala, M. Kulmala and Y. Viisanen, J. Chem. Eng. Data 51, 255–260 (2006).
2. E. Manzurola and A. Apelblat, J. Chem. Thermodyn. 17, 579–584 (1985).
3. M. A. Raza, P. D. Hallett, X. Liu, M. He and W. Afzal, J. Chem. Eng. Data 64, 5049–5056 (2019).
4. T. S. Banipal, H. Singh, P. K. Banipal and V. Singh, Thermochim. Acta 553, 31–39 (2013).
5. A. Thakur, K. C. Juglan, H. Kumar and K. Kaur, J. Mol. Liq. 288, 111014 (2019).
6. R. Rani, A. Kumar, T. Sharma and R. K. Bamezai, J. Chem. Thermodyn. 135, 260–277 (2019).
7. H. Kaur, R. C. Thakur, H. Kumar and A. Katal, J. Chem. Thermodyn. 158, 106433 (2021).
8. V. Pathania, S. Sharma, B. K. Vermani, H. Kaur and R. C. Thakur, J. Mol. Liq. 371, 121067 (2023).
9. H. Kaur, R. C. Thakur, V. S. Pathania and S. Sharma, J. Mol. Liq. 346, 118247 (2022).
10. H. Kumar, I. Behal and M. Singla, J. Chem. Thermodyn. 95, 1–14 (2016).
11. X. Ren, C. Zhu and Y. Ma, J. Chem. Thermodyn. 93, 179–192 (2016).
12. A. Ali, S. Hyder and A. K. Nain, J. Mol. Liq. 79, 89–99 (1999).
13. N. Chakraborty, H. Kumar, K. Kaur and K. C. Juglan, J. Chem. Thermodyn. 126, 137–146 (2018).
14. R. C. Thakur, R. Sharma, A. Kumar, S. Kumar and M. L. Parmar, Orient. J. Chem. 30, 2037–2041 (2014).
15. M. T. Zafarani-Moattar and H. Shekaari, J. Chem. Thermodyn. 37, 1029–1035 (2005).
16. Z. Yan, J. Wang, H. Zheng and D. Liu, J. Solution Chem. 27, 473–483 (1998).
17. K. Kaur, K. C. Juglan and H. Kumar, J. Mol. Liq. 268, 700–706 (2018).
18. M. Lamba, N. Chakraborty, K. C. Juglan, R. Sharma and M. Singla, J. Chem. Eng. Data 69, 171–184 (2024).
19. F. Shahidi, P. G. Farrel and J. T. Edward, J. Solution Chem. 5, 807–816 (1976).
20. M. J. Iqbal and M. A. Chaudhry, J. Chem. Thermodyn. 42, 951–956 (2010).
21. R. Rani, A. Kumar, T. Sharma, B. Saini and R. K. Bamezai, Acta Chim. Slov. 63, 589-601 (2016).
22. N. Chakraborty, K. C. Juglan and H. Kumar, Braz. J. Chem. Eng. 39, 864-884 (2021).

23. S. Devi, M. Kumar, N. Sawhney, U. Syal, A. K. Sharma and M. Sharma, J. Chem. Thermodyn. 154, 106321 (2021).
24. N. G. Tsierkezos and I. E. Molinou, J. Chem. Eng. Data 43, 989–993 (1998).
25. A. Apelblat and E. Manzurola, J. Chem. Thermodyn. 33, 581–595 (2001).
26. L. G. Hepler, Can. J. Chem. 47, 4613–4617 (1969).
27. K. C. Juglan and H. Kumar, Results Chem. 2, 100049 (2020).
28. B. Ghosh, A. Sinha, N. Roy, B. Rajbanshi, M. Mondal, D. Roy, A. Das, N. N. Ghosh, V. K. Dakua and M. N. Roy, Fluid Ph. Equilib. 557, 113415 (2022).
29. I. Bahadur and N. Deenadayalu, J. Solution Chem. 40, 1528–1543 (2011).
30. N. Chakraborty, K. C. Juglan and H. Kumar, J. Chem. Eng. Data 66, 2391–240 (2021).
31. M. S. Raman, M. Kesavan, K. Senthilkumar and V. Ponnuswamy, J. Mol. Liq. 202, 115–124 (2015).
32. K. Kaur, I. Behal, K. C. Juglan and H. Kumar, J. Chem. Thermodyn. 125, 93–106 (2018).
33. H. Kumar and I. Behal, J. Chem. Thermodyn. 99, 16–29 (2016).
34. H. S. Frank, M. W. Evans, J. Chem. Phys. 13, 507–532 (1945).
35. N. Chakraborty, K. Kaur, K. C. Juglan and H. Kumar, J. Chem. Eng. Data 65, 1435–1446 (2020).
36. N. Chakraborty, K. C. Juglan and H. Kumar, J. Chem. Thermodyn. 163, 106584 (2021).
37. M. S. Raman, V. Ponnuswamy, P. Kolandaivel and K. Perumal, J. Mol. Liq. 142, 10–16 (2008).
38. J. Wang, D. Zhang, Q. Chu and J. Ye, Chin. J. Chem. 28, 313–319 (2010).
39. S. Panda, V. Singh, N. Islam and R. L. Gardas, Fluid Ph. Equilib. 445, 35–44 (2017).
40. J. G. Kirkwood, Chem. Rev. 24, 233–251 (1939).
41. H. Kumar and I. Behal, J. Mol. Liq. 219, 756–764 (2016).
42. K. Kaur, K. C. Juglan and H. Kumar, J. Chem. Thermodyn. 127, 8–16 (2018).
43. R. Sadeghi and F. Ziamajidi, J. Chem. Eng. Data 52, 1037–1044 (2007).
44. A. Salabat, L. Shamshiri and F. Sahrakar, J. Mol. Liq. 118, 67–70 (2005).
45. S. K. Sharma and A. Thakur, J. Mol. Liq. 322, 114527 (2021).
46. W. G. McMillan Jr and J. E. Mayer, J. Chem. Phys. 13, 276–305 (1945).
47. F. Franks, M. Pedley and D. S. Reid, J. Chem. Soc., Faraday Trans. 72, 359–367 (1976).
48. C. V Krishnan and H. L. Friedman, J. Solution Chem. 2, 37–51 (1973).
49. K. S. Pitzer, C.R.C. Press. 2, (1991).
50. K.D. Amirchand, S. Kaur, T.S. Banipal and V. Singh, J. Mol. Liq. 334, 116077 (2021).

51. R. Sharma, N.R. Kar, M. Ahmad, P. Gadipelli, S. Misra, R. Karodi, V.K. Pathak, S. Sarkar, B. Das and S. Mandal, Community Pract. 21, 1812–1826 (2024).
52. H.S. Harned, B.B. Owen and C. V King, J Electrochem. Soc. 106, 15C (1959).
53. P. Kaur, K.C. Juglan, H. Kumar and M. Singla, Braz. J. Chem. Eng. 40, 1213–1226 (2023).
54. Y. Marcus, Chem. Rev. 111, 2761–2783 (2011).
55. H. Kaur, N. Chakraborty, K.C. Juglan, A. Upmanyu, J. Mol. Liq. 392, 123403 (2023).
56. D.O. Masson, XXVIII. Lond. Edinb. Dubl. Phil. Mag. 8, 218–235 (1929).
57. M. Talukdar, S. Dey, A. Panda, S. Pan and S. Singh, J. Solution Chem. 53, 387–415 (2024).
58. A. Thakur, K.C. Juglan, H. Kumar and K. Kaur, Phys. Chem. Liq. 58, 803–819 (2020).
59. V. Dhir and R.P.S. Grewal, J. Adv. Res. Appl. Sci. 2, 37–42 (2015).
60. H. Kumar and I. Behal, J. Chem. Eng. Data. 61, 3740–3751 (2016).
61. A.K. Mishra and J.C. Ahluwalia, J. Phys. Chem. 88, 86–92 (1984).
62. H.L. Friedman and C. V Krishnan, J. Sol. Chem. 2, 119–140 (1973).
63. A.K. Nain, J. Mol. Liq. 318, 114190 (2020).
64. T. Sharma, S.S. Shah and R.K. Bamezai, J. Sol. Chem. 50, 1363–1390 (2021).
65. S. Li, W. Sang and R. Lin, J. Chem. Thermodyn. 34, 1761–1768 (2002).
66. R. Xu, G. Tang, X.-L. Fu and Q.-L. Yan, Cryst. Growth. Des. 22, 909–936 (2021).
67. E.L. Smith, A.P. Abbott and K.S. Ryder, Chem. Rev. 114, 11060–11082 (2014).
68. A. Ghosh and K.S. Schweizer, Macromol. 53, 4366–4380 (2020).
69. K. Dhal, S. Singh and M. Talukdar, J. Mol. Liq. 361, 119578 (2022).
70. P. Kaur, N. Chakraborty, H. Kumar, M. Singla and K.C. Juglan, J. Sol. Chem. 51, 1268–1291 (2022).
71. N. Chakraborty, K.C. Juglan and H. Kumar, J. Mol. Liq. 332, 115869 (2021).
72. V. Pathania and A. Garg, J. Mol. Liq. 404, 124886 (2024).
73. K. Singh and S. Chauhan, J. Chem. Eng. Data 65, 4536–4546 (2020).
74. K. Klimaszewski, E. Stronka-Lewkowska, K. Abramczyk, A. Bald, J. Chem. Thermodyn. 89, (2015) 212–222.
75. N. Chakraborty, K.C. Juglan, H. Kumar and M. Singla, J. Chem. Thermodyn. 174, 106876 (2022).
76. R. Sadeghi and A. Gholamireza, J. Chem. Thermodyn. 43, 200–215 (2011).
77. M.T. Zafarani-Moattar and S. Sarmad, J. Chem. Thermodyn. 42, 1213–1221 (2010).
78. A. Purchala and I. Cibulka, J. Chem. Eng. Data 59, 4205–4216 (2014).

79. N. Chakraborty, K.C. Juglan and H. Kumar, J. Mol. Liq. 337, 116605 (2021).
80. A. Thakur, S.K. Sharma and M. Kumar, J. Mol. Liq. 351, 118653 (2022).
81. H. Kaur, N. Chakraborty and K.C. Juglan, J. Chem. Eng. Data. 69, 2461–2474 (2024).
82. D. Chawla, N. Chakraborty, K.C. Juglan and H. Kumar, Chem. Pap. 75, 1497–1506 (2021).

Section III

Problem 5

4.5 Title: "Molecular Interactions of Butyric and L(+)-lactic Acids in Water-Soluble Potassium Benzoate Solutions: An Acoustic and Thermodynamic Study"

In this section, the volumetric behavior of water + potassium benzoate + lactic acid and butyric acid mixtures was evaluated through "density" and "sound speed" measurements at distinct temperatures and at three potassium benzoate concentrations.

4.5.1 Density

The density measurements for L(+)-lactic and butyric acids in potassium benzoate solutions at concentrations of 0.00, 0.01, 0.02, 0.03 $\mathrm{mol \cdot kg^{-1}}$ across varying temperatures are summarized in **Table 4.41**. **Figures 4.30** and **4.31** compare the experimental density data with previously reported data for butyric acid and L(+)-lactic acid with water. The experimental findings for the density align well with the documented data in the literature [1-6,7,8] under the studied temperatures. The values in **Table 4.41** indicate that for a constant potassium benzoate concentration, an increase in the molality of L(+)-lactic and butyric acids leads to a rise in density, whereas an intensification in temperature leads to a reduction in density. The rise in molality of solute enhances molecular interactions within the solution, promoting tighter packing of molecules and an increase in density. On the other hand, at a particular PB concentration, an increase in temperature declines density due to elevated molecular kinetic energy, which weakens the intermolecular cohesion and increases the separation between molecules. As the temperature rises, the solution undergoes expansion, leading to a decrease in densities. This phenomenon corresponds to the general principle of thermal expansion in liquids, where an increase in temperature causes a reduction in density [9,10].

4.5.2 Apparent molar volume

The stability and functionality of beverages, cosmetics, and pharmaceuticals are strongly influenced by apparent molar volume, which reflects solvation effects and volumetric properties. This parameter is calculated from experimentally obtained density data through **equation 4.1**. **Table 4.41** shows the positive apparent molar volume values for L(+)-lactic and butyric acids derived from experimental density measurements. The molecular interactions within LA and BA in potassium benzoate water-soluble solution are highlighted in **Figure 4.32**. Comparative three-dimensional plots in **Figure 4.33** illustrate the variations in apparent molar volume of L(+)-lactic acid (represented by blue spheres) and butyric acid (represented by red cubes). In the absence of potassium benzoate as depicted in **Figure 4.33(a)**, butyric acid consistently exhibits higher V_ϕ values compared to L(+)-lactic acid, reflecting differences in molecular size and solute-solvent interactions. As the PB concentration escalates , a progressive increase in V_ϕ is observed for L(+)-lactic acid as shown in **Figure 4.33(b-d)**, the detected positive V_ϕ values with rising potassium benzoate concentration suggest enhanced solute-solvent interactions showing a more pronounced sensitivity to PB concentration and temperature, primarily owing to the strong hydrogen bonding and dipole-dipole associations within the hydroxyl and carboxyl group of L(+)-lactic acid and benzoate anion[11–13]. This suggests that L(+)-lactic acid engages more strongly in specific interactions with PB which influence the solvation and volumetric behavior. The examined ternary systems exhibit a consistent elevation in V_ϕ with increasing temperatures for both acids. The detected positive values suggest the occurrence of stronger interactions amongst solute and solvent bonds. The hydrophilic nature of L(+)-lactic acid allows it to form stable H_2 bonds with water and PB molecules which leads to greater structural organization and a net volumetric expansion. The determined data of the apparent molar volume of L(+)-lactic acid in the present study align closely with the reported literature value demonstrating the accuracy of the obtained data[14]. Conversely, butyric acid exhibits a falling trend in V_ϕ with growing PB concentration as represented in **Fig. 4.33(b-d)** which can be ascribed to its relatively weaker hydrogen-bonding ability and the dominance of hydrophobic interactions from its longer alkyl chain. This decreasing trend suggests comparatively weaker solute-solvent interactions due to the predominance of hydrophobic effects. As PB concentration rises, the solvation shell around butyric acid molecules weakens due to competitive hydrogen

bonding between PB and water, reducing the effective hydration of butyric acid and leading to a contraction in volume[15,16].

Table 4.41 Densities 'ρ' and apparent molar volumes 'V_ϕ' were determined in the combination of potassium benzoate in L(+)-lactic and butyric acids at four different temperatures.

m_A	ρ(g·cm^{-3})				$V_\phi \times 10^6$(m^3·mol^{-1})			
(mol·kg^{-1})	288.15K	298.15K	308.15K	318.15K	288.15K	298.15K	308.15K	318.15K
0.00 mol·kg^{-1} Potassium Benzoate + L(+)-lactic Acid								
0.00000	0.99926	0.99705	0.99404	0.99036				
0.10457	1.00116	0.99893	0.99591	0.99221	71.78	72.09	72.41	72.79
0.19782	1.00280	1.00056	0.99751	0.99381	71.95	72.26	72.60	72.94
0.30149	1.00457	1.00229	0.99923	0.99552	72.13	72.47	72.81	73.13
0.40528	1.00626	1.00396	1.00088	0.99715	72.34	72.69	73.05	73.37
0.50361	1.00781	1.00547	1.00238	0.99863	72.53	72.91	73.25	73.59
0.01 mol·kg^{-1} Potassium Benzoate + L(+)-lactic Acid								
0.00000	0.99986	0.99776	0.99466	0.99081				
0.10026	1.00160	0.99948	0.99636	0.99250	72.56	72.91	73.25	73.58
0.20527	1.00337	1.00122	0.99809	0.99421	72.75	73.11	73.42	73.77
0.31457	1.00513	1.00295	0.99982	0.99593	72.95	73.32	73.59	73.97
0.40530	1.00654	1.00435	1.00121	0.99730	73.11	73.47	73.74	74.13
0.50392	1.00803	1.00582	1.00267	0.99875	73.27	73.62	73.91	74.28
0.02 mol·kg^{-1} Potassium Benzoate + L(+)-lactic Acid								
0.00000	1.00039	0.99848	0.99532	0.99134				
0.10953	1.00226	1.00032	0.99714	0.99316	72.86	73.22	73.57	73.81

0.20277	1.00379	1.00183	0.99864	0.99465	73.02	73.41	73.72	74.02
0.30191	1.00538	1.00338	1.00018	0.99617	73.18	73.56	73.88	74.21
0.40631	1.00698	1.00496	1.00175	0.99773	73.35	73.75	74.05	74.38
0.50265	1.00841	1.00636	1.00315	0.99912	73.51	73.91	74.20	74.53
0.03 mol·kg^{-1} Potassium Benzoate + L(+)-lactic Acid								
0.00000	1.00109	0.99909	0.99577	0.99186				
0.10554	1.00285	1.00082	0.99749	0.99358	73.19	73.58	73.87	74.13
0.19767	1.00434	1.00229	0.99894	0.99503	73.36	73.72	74.03	74.28
0.30422	1.00600	1.00392	1.00057	0.99666	73.51	73.89	74.18	74.43
0.40821	1.00757	1.00546	1.00210	0.99818	73.67	74.06	74.35	74.61
0.50845	1.00903	1.00689	1.00353	0.99960	73.82	74.21	74.49	74.77
0.00 mol·kg^{-1} Potassium Benzoate +Butyric Acid								
0.00000	0.99926	0.99705	0.99404	0.99036				
0.09887	0.99950	0.99729	0.99429	0.99062	85.72	85.89	86.06	86.22
0.20651	0.99977	0.99757	0.99457	0.99092	85.66	85.81	85.98	86.13
0.29671	1.00000	0.99780	0.99482	0.99118	85.61	85.75	85.92	86.07
0.40733	1.00030	0.99810	0.99513	0.99151	85.54	85.68	85.83	85.99
0.49683	1.00055	0.99836	0.99539	0.99178	85.47	85.61	85.77	85.93
0.01 mol·kg^{-1} Potassium Benzoate +Butyric Acid								
0.00000	0.99986	0.99776	0.99466	0.99081				
0.09974	1.00008	0.99798	0.99489	0.99106	85.91	86.08	86.22	86.37

0.19896	1.00032	0.99822	0.99514	0.99132	85.78	85.95	86.10	86.25
0.29999	1.00058	0.99848	0.99541	0.99161	85.66	85.83	85.99	86.14
0.39998	1.00087	0.99877	0.99569	0.99191	85.51	85.69	85.88	86.03
0.49996	1.00117	0.99907	0.99599	0.99222	85.39	85.57	85.78	85.94
0.02 mol·kg^{-1} Potassium Benzoate +Butyric Acid								
0.00000	1.00039	0.99848	0.99532	0.99134				
0.09873	1.00059	0.99868	0.99553	0.99157	86.05	86.23	86.38	86.52
0.19785	1.00081	0.99890	0.99576	0.99182	85.93	86.09	86.24	86.39
0.29957	1.00106	0.99915	0.99602	0.99209	85.80	85.96	86.10	86.26
0.39923	1.00132	0.99941	0.99630	0.99238	85.67	85.82	85.96	86.13
0.49780	1.00160	0.99970	0.99659	0.99269	85.54	85.69	85.84	86.01
0.03 mol·kg^{-1} Potassium Benzoate +Butyric Acid								
0.00000	1.00109	0.99909	0.99577	0.99186				
0.09955	1.00127	0.99927	0.99596	0.99207	86.21	86.37	86.53	86.67
0.19843	1.00147	0.99947	0.99618	0.99230	86.09	86.24	86.39	86.54
0.29785	1.00169	0.99969	0.99641	0.99255	85.95	86.11	86.26	86.41
0.39856	1.00194	0.99994	0.99667	0.99283	85.81	85.98	86.12	86.27
0.49941	1.00221	1.00021	0.99696	0.99313	85.68	85.84	85.97	86.14

m_A signifies the molality of the solutes (L(+)-lactic and butyric acids) per kg of the potassium benzoate: the calculated standard uncertainties u are $u_r(m_{PB})$ =0.01, $u_r(m_{LA})$ = 0.03 and, $u_r(m_{BA})$ = 0.03, $u(T)$=0.01 K, $u(\rho)$= (0.00032) g·cm^{-3}, $u(V_\phi)$ = (0.50 × 10^{-6})m^3·mol^{-1}, $u(p)$ = 0.01 MPa.

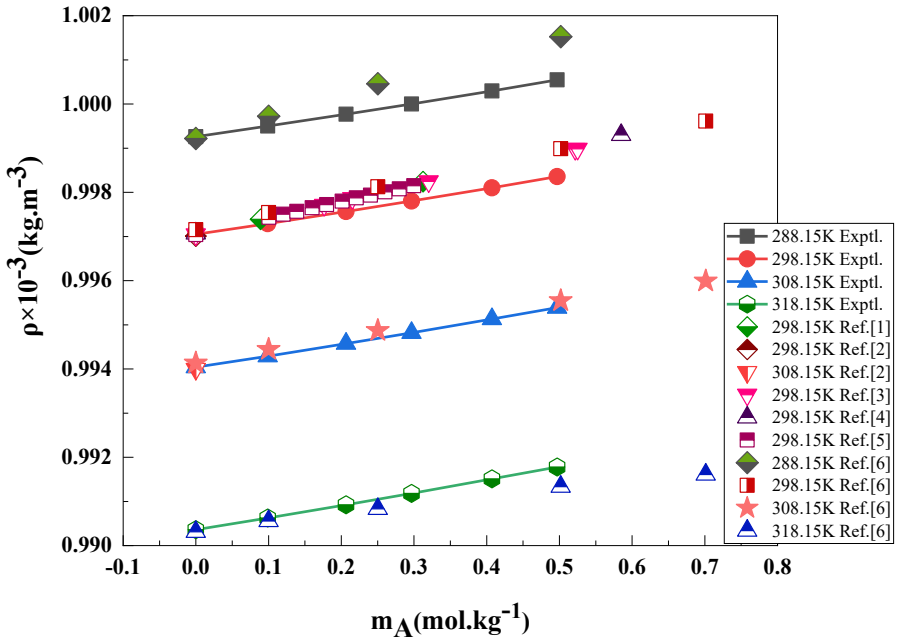

Figure 4.30 The density of a binary combination of aqueous butyric acid was shown at different temperatures utilizing experimental as well as literature data [1-6]**.**

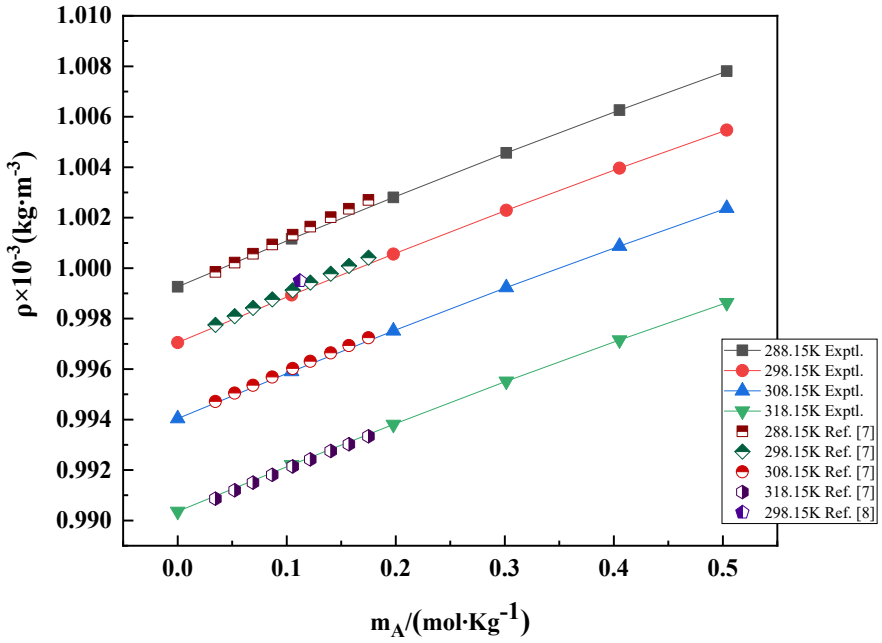

Figure 4.31 The density of a binary combination of an aqueous L(+)-lactic acid was shown at different temperatures utilizing experimental as well as literature data [7,8].

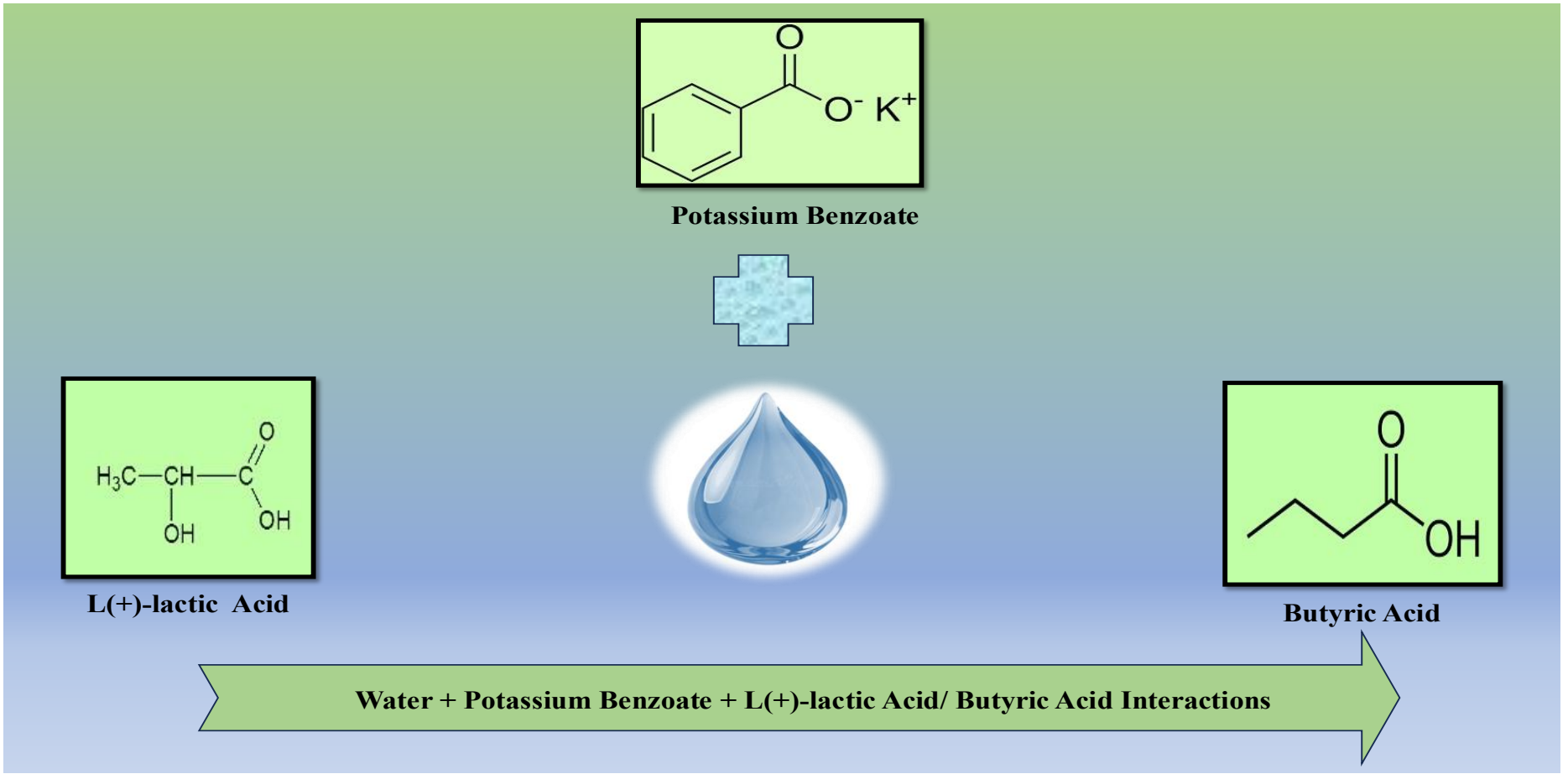

Figure 4.32 L(+)-lactic Acid/ Butyric Acid and Potassium Benzoate interactions.

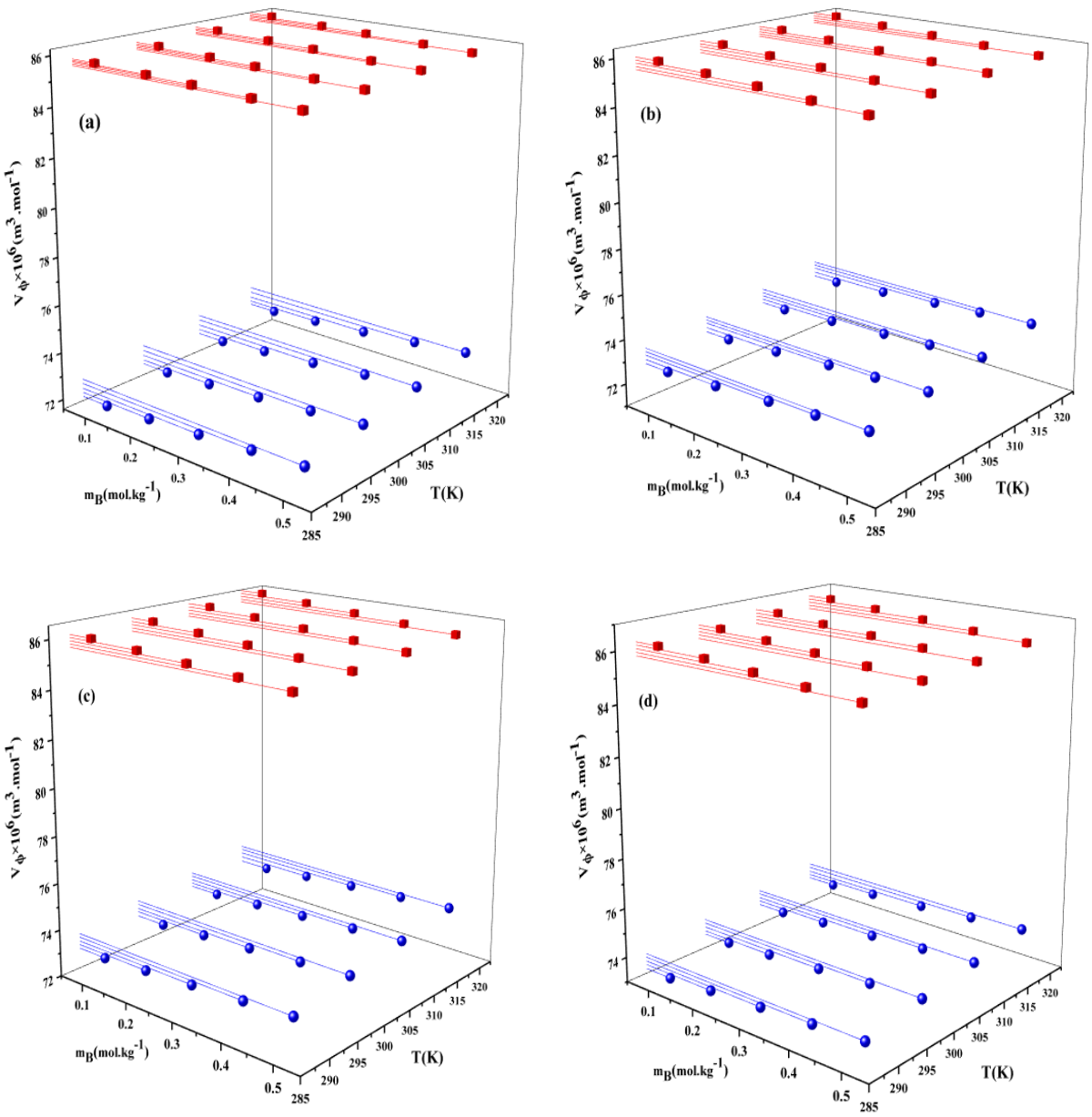

Figure 4.33 Comparative three-dimensional plots illustrate the variations in $(V_\emptyset)$ of (a) 0.00 PB; (b) 0.01 PB; (c) 0.02 PB;(d) 0.03 PB for molality of L(+)-lactic acid (blue; sphere) and butyric acid (red; cube) at varying temperatures.

4.5.3 Partial molar volume

The **equation 4.2** can be utilized to calculate the V_ϕ^0 for ternary liquid mixtures containing L(+)-lactic acid, butyric acid, and potassium benzoate in water ($V_\emptyset$). The application of the least squares fitting technique provided the data of (V_ϕ^0) and the (S_V^*) as presented in **Table 4.42**. The V_ϕ^0 values for L(+)-lactic and butyric acids remain positive and display an increasing pattern with the escalation in potassium benzoate concentration as observed in comparative plot of **Figure 4.34.**

Partial molar volume values for L(+)-lactic acid increase gradually with both temperature and potassium benzoate concentration, ranging from (71.58 to 73.96) × 10^6 $m^3 \cdot mol^{-1}$, accompanied by positive S_V^* values. In contrast, butyric acid exhibits higher V_ϕ^0 values (85.79 to 86.80) × 10^6 $m^3 \cdot mol^{-1}$ with negative S_V^* values. As the molality of L(+)-lactic and butyric acids rises, the V_ϕ^0 of PB also rises, indicating that bonds between ions and hydrophilic groups are more significant than those involving hydrophobic groups [17–19].

Variations in S_V^* values suggest that factors beyond the apparent solute-solute interactions might influence the behavior of PB and LA/BA. Furthermore, the observed positive results do not follow a uniform trend for the solvent composition or temperature changes. This observation proposes that solute as well as solvent interactions show a substantial role in defining the behavior of solute molecules within the solution compared to solute-solute interactions. This study highlights the prevalence of solute and solvent molecules as shown by the relatively low S_V^* values as compared to V_ϕ^0 [20,21].

Table 4.42 Data of $'V_{\phi}^{0}'$, and $'S_V^*'$ values of Potassium Benzoate in L(+)-lactic and butyric acids solutions with their standard errors.

m_B	$V_{\phi}^{0} \times 10^{6}$(m^3·mol^{-1})				$S_V^* \times 10^6$ (m^3·kg·mol^{-2})			
(mol·kg^{-1})	288.15K	298.15K	308.15K	318.15K	288.15K	298.15K	308.15K	318.15 K
				L(+)-lactic Acid				
0.00	71.58(±0.01)	71.86(±0.01)	72.18(±0.01)	72.55(±0.03)	1.88(±0.03)	2.06(±0.04)	2.12(±0.03)	2.02(±0.09)
0.01	72.39(±0.01)	72.74(±0.02)	73.08(±0.01)	73.41(±0.01)	1.77(±0.02)	1.77(±0.05)	1.63(±0.02)	1.75(±0.03)
0.02	72.68(±0.00)	73.04(±0.01)	73.39(±0.00)	73.64(±0.03)	1.65(±0.01)	1.74(±0.04)	1.61(±0.01)	1.82(±0.08)
0.03	73.04(±0.01)	73.41(±0.00)	73.72(±0.01)	73.96(±0.01)	3.53(±0.04)	1.57(±0.01)	1.53(±0.03)	1.58(±0.03)
				Butyric Acid				
0.00	85.79(±0.01)	85.96(±0.00)	86.13(±0.00)	86.29(±0.01)	-0.63(±0.02)	-0.69(±0.01)	-0.72(±0.01)	-0.72(±0.02)
0.01	86.04(±0.01)	86.21(±0.01)	86.32(±0.01)	86.47(±0.01)	-1.31(±0.03)	-1.28(±0.02)	-1.10(±0.02)	-1.08(±0.03)
0.02	86.18(±0.00)	86.36(±0.00)	86.51(±0.01)	86.64(±0.00)	-1.28(±0.01)	-1.35(±0.01)	-1.36(±0.02)	-1.28(±0.01)
0.03	86.35(±0.01)	86.50(±0.00)	86.67(±0.01)	86.80(±0.00)	-1.34(±0.02)	-1.32(±0.01)	-1.39(±0.02)	-1.33(±0.01)

m_B specifies the molality of potassium benzoate per kg of the pure water: standard uncertainties *u* are $u_r(m_{PB})$ = 0.01, $u(T)$=0.01 K, $u(V_{\phi}^{0})$ = (±1.38 × 10^{-6})m^3·mol^{-1} and $u(S_V^*)$=±(0.26 × 10^{-6})m^3·kg·mol^{-2}, $u(p)$ = 0.01 MPa.

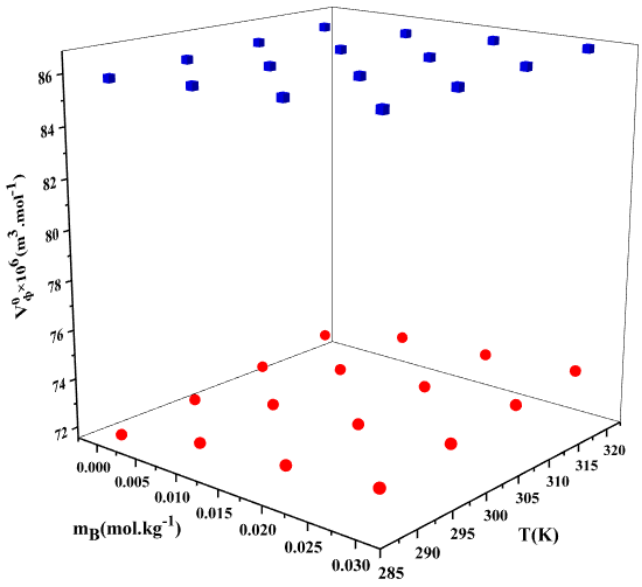

Figure 4.34 The comparative plot represents the variations in V_ϕ^0, for L(+)-lactic acid (red; dot) and butyric acid (blue; cube) within a potassium benzoate aqueous solution at several temperatures.

4.5.4 Transfer of partial molar volumes

In the context of thermodynamics, $\Delta_{tr}V_{\emptyset}^{0}$ signifies the change in volume accompanying the phase transition of a solute molecule. The **equation 4.3** is used to compute the amount of solutes transferred from water to the potassium benzoate solution.

The $\Delta_{tr}V_{\emptyset}^{0}$ values for L(+)-lactic and butyric acids in water-soluble potassium benzoate solutions are tabulated in **Table 4.43,** are positive, and show an upward trend with increasing solvent concentrations, the data show a non-uniform pattern with varying temperatures.

This transfer property is crucial for understanding solution behavior as it infers evidence on the associations within the solute and the solvent. The positive $\Delta_{tr}V_{\emptyset}^{0}$ values may be ascribed to the solute's propensity to either promote or weaken structured arrangements due to its solvophobic approach and the interactions within overlapping cospheres [22,23]. According to the cosphere overlap theory, these values indicate minimal solute-solute interactions, suggesting that such interactions are weak or nearly negligible. It is essential to recognize that the solvent (PB) and solutes (LA/BA) act as electrolytes, dissociating into ions when dissolved. The determined positive values emphasize stronger ion-ion interactions between potassium benzoate and L(+)-lactic /butyric acids [24]. Pauling introduced the concept of clathrates, which describes void spaces in the water structure that can be penetrated by other molecules. L(+)-lactic and butyric acids rather than filling these spaces, disrupt the water network and potentially form new structural arrangements by bonding with water molecules. Due to the positive values that have been reported for $\Delta_{tr}V_{\emptyset}^{0}$ in the (PB + water + LA/BA) system, the present research specifies the existence of both hydrophilic and ion-hydrophilic associations through hydrogen bonding in L(+)-lactic and butyric acids [25,26].

Table 4.43 Transfer, ΔV_{ϕ}^{0} values of the combination of potassium benzoate in L(+)-lactic and butyric acids solutions at various temperatures.

m_B ($\mathrm{mol \cdot kg^{-1}}$)	$\Delta V_{\phi}^{0} \times 10^{6}$($\mathrm{m^3 \cdot mol^{-1}}$)			
	288.15K	298.15K	308.15K	318.15K
		L(+)-lactic Acid		
0.01	0.81	0.88	0.90	0.86
0.02	1.11	1.18	1.21	1.08
0.03	1.46	1.55	1.53	1.41
		Butyric Acid		
0.01	0.25	0.25	0.19	0.18
0.02	0.39	0.40	0.38	0.35
0.03	0.56	0.54	0.54	0.51

m_B specifies the molality of potassium benzoate per kg of the pure water: the calculated standard uncertainties *u* are $u_r(m_{PB})$ = 0.01, $u(T)$=0.01 K, $u(\Delta V_{\phi}^{0})$= (±0.09×10^{-6})$\mathrm{m^3 \cdot mol^{-1}}$, $u(p)$ = 0.01 MPa.

4.5.5 Temperature-dependent partial molar volume

To evaluate the impact of temperature on V_ϕ^0 at infinite dilution, the **equation 4.4** can be utilized. The data exhibit the constants for L(+)-lactic and butyric acids with potassium benzoate in **Table 4.44.** The table also comprises the differences within the obtained and the measured V_ϕ^0 results which are evaluated using the **equation 4.5**.

here, $Y = V_\phi^0$. In this study, the polynomial equation, as reflected by the values, exhibits very slight deviations, demonstrating a good fit [27,28]. The observed scatter in the V_ϕ^0 values are specified by the negative c values in the table. The investigation of these values primarily focused on obtaining partial molar expansibilities through the **equation 4.6**. The validation of the apparent molar parameter of volume is reflected in the positive E_ϕ^0 data, suggesting the perseverance of solute and solvent bonds in the combination as indicated in **Table 4.45**.

The increased prevalence of E_ϕ^0 data further highlight the occurrence of solute and solvent interactions caused by the packing or caging effect[29,30]. The Hepler's thermodynamic **equation 4.7** [31] helps determine the solute's capability to promote and disrupt structures within the solution. The formation of structures by the solute is reflected in the positive sign of $\left(\frac{\partial E_\Phi^0}{\partial T}\right)_P$ whereas a negative sign demonstrates the solute's tendency to make or disrupt structures [32,33]. The data of $\left(\frac{\partial E_\Phi^0}{\partial T}\right)_P$ is provided in **Table 4.45**, which is negative for both the L(+)-lactic and butyric acids in aqueous media with potassium benzoate, suggests structure breaking tendency, implying disruption of structures in the current investigation.

Table 4.44 Calculation of empirical constants of potassium benzoate in aqueous solutions with L(+)-lactic and butyric acids.

$m_B(\mathrm{mol\cdot kg^{-1}})$	$a \times 10^6$ ($m^3 \cdot mol^{-1}$)	$b \times 10^6$ ($m^3 \cdot mol^{-1} \cdot K^{-1}$)	$c \times 10^6$ ($m^3 \cdot mol^{-1} \cdot K^{-2}$)	R^2	ARD
			L(+)-lactic Acid		
0.01	72.74	0.0349	-0.0001	0.9999	0.0000
0.02	73.06	0.0351	-0.0003	0.9999	0.0000
0.03	73.44	0.0339	-0.0003	0.9999	0.0000
			Butyric Acid		
0.01	86.20	0.0144	0.0000	0.9999	0.0000
0.02	86.36	0.0166	-0.0001	0.9999	0.0000
0.03	86.51	0.0158	0.0000	0.9999	0.0000

m_B specifies the molality of potassium benzoate per kg of the pure water: standard uncertainties are $u_r(m_{PB})$ = 0.01, $u(T)$=0.01 K, $u(p)$ =0.01 MPa.

Table 4.45 Values of expansibilities 'E_{ϕ}^{0}' potassium benzoate in L(+)-lactic and butyric acids at various temperatures.

m_B (mol·kg^{-1})	$E_{\phi}^{0} \times 10^{6}$(m^{3}·mol^{-1}·K^{-1})				$\left(\frac{\partial E_{\phi}^{0}}{\partial T}\right)_P$ (m^{3}·mol^{-1}·K^{-2})
	288.15K	298.15K	308.15K	318.15K	
			L(+)-lactic Acid		
0.01	0.0364	0.0349	0.0333	0.0318	-0.00015
0.02	0.0409	0.0351	0.0293	0.0234	-0.00058
0.03	0.0403	0.0339	0.0275	0.0211	-0.00063
			Butyric Acid		
0.01	0.0154	0.0144	0.0135	0.0125	-0.00010
0.02	0.0189	0.0166	0.0142	0.0119	-0.00023
0.03	0.0168	0.0158	0.0148	0.0138	-0.00010

m_B denotes the molality of potassium benzoate per kg of the pure water: standard uncertainties are $u_r(m_{PB})$ = 0.01, $u(T)$=0.01 K, $u(E_{\phi}^{0})$ = (0.0020 ×10^{-6})m^{3}·mol^{-1}·K^{-1}, $u(\frac{\partial E_{\phi}^{0}}{\partial T})$ = (0.00010)m^{3}·mol^{-1}·K^{-2}, $u(p)$ =0.01 MPa.

4.5.6 Speed of sound

The study focused on the sound velocity of L(+)-lactic and butyric acids in potassium benzoate solutions at numerous concentrations and temperatures with the findings provided in **Table 4.46.** The sound speed measurements for the binary system (LA + Water) align closely with the trends reported in existing literature [7] as displayed in **Figure 4.35.** The investigated data show a consistent upward trend as both temperatures and PB concentrations surge from 0.00 to 0.03 $\mathrm{mol \cdot kg^{-1}}$. The acceleration of sound speed in the (L(+)-lactic acid/butyric acid) is caused by extensive hydrogen bonding in water's three-dimensional structure. This network supports strong molecular associations with hydrogen bonds forming inside solute and solvent molecules and among solute particles, leading to a more compact system. The escalation in molar mass from butyric acid to lactic acid results in weaker water-PB interactions and the formation of new bonds within PB and (LA/BA) [34,35].

4.5.7 Apparent molar isentropic compression

The calculation of k_s values were carried out by applying the Laplace **equation 4.8** to the ultrasonic velocity data collected at varying temperatures. The data of $K_{\phi,S,}$ are specified in **Table 4.46**. The findings are demonstrated in **Figure 4.36 (a)** and **(b).** The **equation 4.9** is utilized to derive the $K_{\phi,S}$ values for L(+)-lactic and butyric acids in a water-containing PB solution. The data show a symmetric trend with a slight decrease in negativity as temperatures escalate. However, as L(+)-lactic and butyric acids molality rise, the negative values become more pronounced. This pattern reveals that H_2O molecules near the ionic-charge groups of both the acids possess lesser compressibility than those in bulk water. Consequently, water experiences a significant reduction in structural compressibility, resulting in an adjustment of the molecules of water surrounding the solute [36,37]. L(+)-lactic and butyric acids exhibit zwitterionic properties having both charges (positive as well as negative) in the same molecule, which is crucial for their interaction with water. This structure enhances the ability of L(+)-lactic and butyric acids to form H_2 bonds with water, which creates hydrophilic clusters around the solute. These properties lead to strong ion-hydrophilic and ion-ion bonds, especially with the polar nature of water [38,39]. Inter-molecular hydrogen bonding in L(+)-lactic/butyric acids and PB solutions leads to the formation of denser structures, which subsequently reduces their compressibility. The hydroxyl groups of

L(+)-lactic and butyric acids form strong solute and solvent bonds with water molecules via dipole-dipole interactions [40].

Table 4.46 Values of 's' and '$K_{\phi,s}$' for L(+)-lactic and butyric acids in aqueous potassium benzoate solution at several temperatures.

m_A ($\mathrm{mol \cdot kg^{-1}}$)	s($\mathrm{m \cdot s^{-1}}$)				$K_{\phi,s} \times 10^6$($\mathrm{m^3 \cdot mol^{-1} \cdot GPa^{-1}}$)			
	288.15K	298.15K	308.15K	318.15K	288.15K	298.15K	308.15K	318.15 K
0.00 mol·kg^{-1} Potassium Benzoate + L(+)-lactic Acid								
0.00000	1466.59	1495.85	1519.14	1536.02				
0.10457	1470.04	1498.36	1521.05	1537.54	-46.11	-44.32	-43.00	-42.25
0.19782	1472.69	1500.73	1522.92	1538.85	-46.40	-44.60	-43.27	-42.52
0.30149	1476.08	1503.35	1524.87	1540.46	-46.56	-44.76	-43.42	-42.67
0.40528	1479.25	1506.07	1526.82	1542.11	-46.68	-44.87	-43.53	-42.77
0.50361	1481.88	1508.56	1528.65	1543.57	-46.77	-44.96	-43.62	-42.86
0.01 mol·kg^{-1} Potassium Benzoate + L(+)-lactic Acid								
0.00000	1468.84	1500.54	1523.15	1540.22				
0.10026	1472.02	1502.32	1525.17	1542.69	-46.01	-44.03	-42.71	-41.75
0.20527	1474.78	1504.65	1527.37	1545.35	-46.33	-44.34	-43.01	-42.05
0.31457	1478.16	1506.79	1529.44	1547.71	-46.49	-44.49	-43.16	-42.19
0.40530	1480.59	1508.68	1531.23	1549.54	-46.59	-44.59	-43.25	-42.28
0.50392	1483.25	1510.94	1533.03	1551.37	-46.68	-44.67	-43.33	-42.36
0.02 mol·kg^{-1} Potassium Benzoate + L(+)-lactic Acid								
0.00000	1472.34	1504.17	1526.56	1541.91				
0.10953	1474.67	1506.24	1528.75	1544.63	-45.78	-43.91	-42.58	-41.72

0.20277	1477.06	1508.12	1530.59	1547.07	-46.05	-44.16	-42.83	-41.96
0.30191	1479.42	1510.41	1532.62	1549.25	-46.20	-44.31	-42.97	-42.10
0.40631	1482.29	1512.48	1534.86	1551.34	-46.31	-44.41	-43.07	-42.20
0.50265	1484.66	1514.84	1536.81	1553.27	-46.40	-44.50	-43.15	-42.28
0.03 mol·kg^{-1} Potassium Benzoate + L(+)-lactic Acid								
0.00000	1474.10	1507.15	1528.82	1543.66				
0.10554	1476.62	1509.12	1531.14	1545.96	-45.70	-43.72	-42.48	-41.62
0.19767	1479.13	1510.53	1533.07	1548.29	-45.97	-43.98	-42.74	-41.88
0.30422	1481.54	1512.76	1535.71	1550.72	-46.13	-44.13	-42.88	-42.02
0.40821	1484.11	1514.68	1538.06	1552.81	-46.24	-44.23	-42.99	-42.12
0.50845	1486.37	1516.91	1540.14	1554.93	-46.33	-44.32	-43.07	-42.20
0.00 mol·kg^{-1} Potassium Benzoate + Butyric Acid								
0.00000	1466.59	1495.85	1519.14	1536.02				
0.09887	1472.07	1501.12	1523.26	1540.22	-46.01	-44.22	-42.91	-41.96
0.20651	1478.23	1506.18	1527.53	1544.88	-46.27	-44.47	-43.15	-42.20
0.29671	1483.32	1510.04	1530.79	1548.51	-46.35	-44.55	-43.23	-42.28
0.40733	1489.16	1514.75	1534.73	1552.76	-46.40	-44.61	-43.28	-42.33
0.49683	1494.11	1518.89	1537.89	1555.61	-46.43	-44.64	-43.31	-42.36
0.01 mol·kg^{-1} Potassium Benzoate + Butyric Acid								
0.00000	1468.84	1500.54	1523.15	1540.22				
0.09974	1475.09	1505.44	1527.27	1544.07	-45.94	-43.96	-42.64	-41.69

0.19896	1480.37	1510.55	1530.75	1547.56	-46.18	-44.20	-42.87	-41.92
0.29999	1485.76	1515.07	1534.63	1550.98	-46.27	-44.29	-42.96	-42.00
0.39998	1490.95	1519.53	1538.08	1554.74	-46.33	-44.34	-43.01	-42.05
0.49996	1495.81	1523.58	1541.17	1557.68	-46.36	-44.37	-43.04	-42.09
0.02 mol·kg^{-1} Potassium Benzoate + Butyric Acid								
0.00000	1472.34	1504.17	1526.56	1541.91				
0.09873	1476.73	1509.44	1529.64	1545.99	-45.66	-43.79	-42.47	-41.61
0.19785	1482.52	1514.39	1532.81	1549.72	-45.91	-44.03	-42.70	-41.84
0.29957	1487.76	1518.85	1536.13	1553.13	-46.00	-44.12	-42.79	-41.92
0.39923	1492.92	1522.83	1539.27	1556.74	-46.05	-44.17	-42.83	-41.97
0.49780	1497.44	1526.66	1542.47	1559.77	-46.08	-44.20	-42.87	-42.01
0.03 mol·kg^{-1} Potassium Benzoate + Butyric Acid								
0.00000	1474.10	1507.15	1528.82	1543.66				
0.09955	1478.46	1512.37	1531.76	1547.57	-45.60	-43.62	-42.39	-41.54
0.19843	1484.11	1517.27	1534.94	1551.63	-45.84	-43.86	-42.62	-41.76
0.29785	1489.47	1521.71	1538.01	1555.48	-45.93	-43.94	-42.70	-41.84
0.39856	1494.59	1525.99	1541.13	1558.72	-45.98	-43.99	-42.75	-41.89
0.49941	1499.19	1529.87	1544.35	1561.81	-46.01	-44.02	-42.78	-41.93

m_A signifies the molalities of the solutes (L(+)-lactic and butyric acids) per kg of the potassium benzoate: the calculated standard uncertainties u are $u_r(m_{PB})$ =0.01, $u_r(m_{LA})$ = 0.03 and, $u_r(m_{BA})$ = 0.03, $u(T)$=0.01 K, $u(s)$=1.89 m·s^{-1}, $u\ (K_{\phi,S})$ = (0.12 × 10^{-6})m^3·mol^{-1}·GPa^{-1}, $u(p)$ = 0.01 MPa.

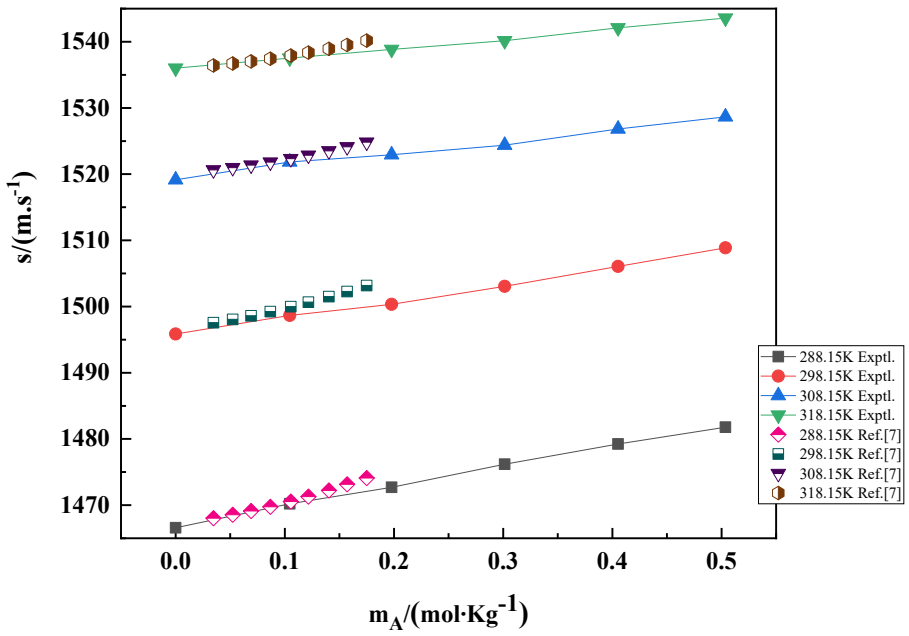

Figure 4.35 Ultrasonic speed of a binary combination of an aqueous L(+)-lactic acid was shown at different temperatures utilizing experimental as well as literature data [7].

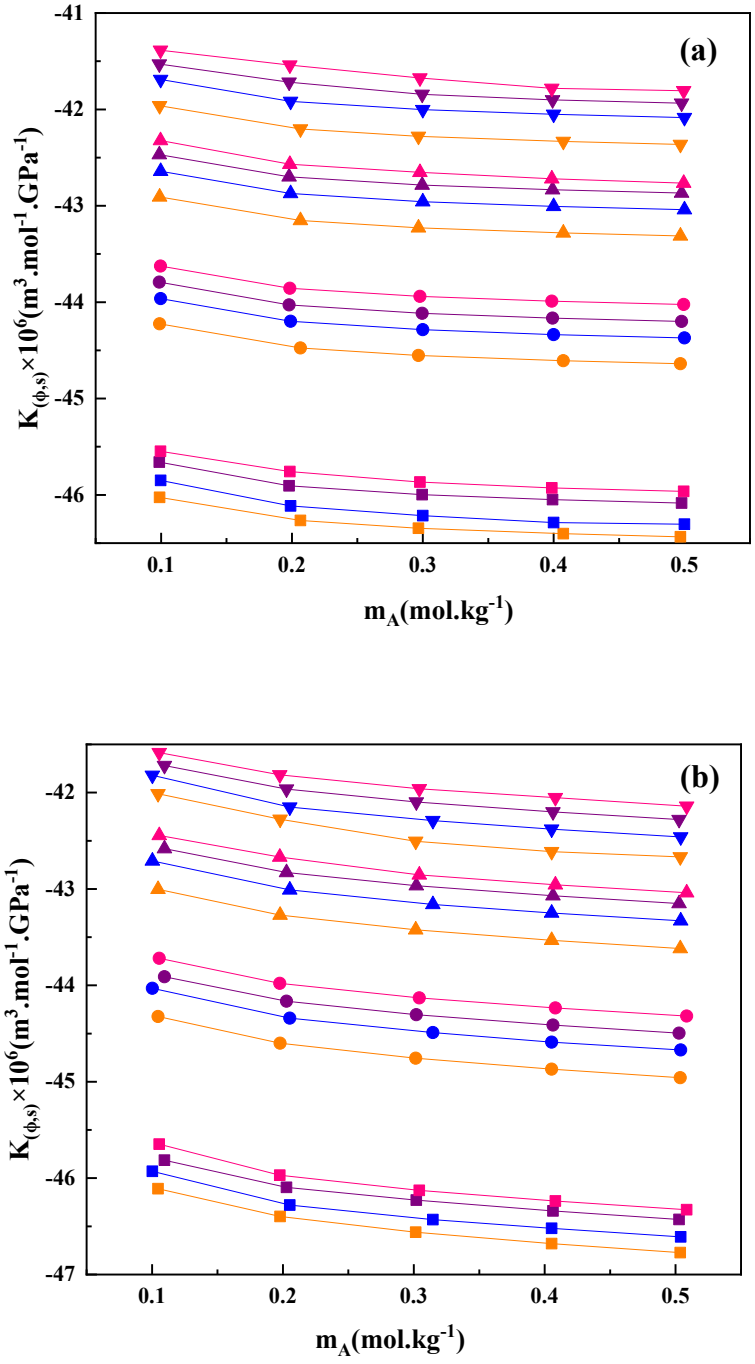

Figure 4.36 Changes of $K_{\phi,s}$, of (a) butyric acid (BA) and (b) L(+)-lactic acid (LA) in potassium benzoate solutions at several concentrations (0.00, orange; 0.01, blue; 0.02, purple; and 0.03, pink) [square: 288.15 K; circle: 298.15 K; upward triangle: 308.15 K; downward triangle: 318.15 K].

4.5.8 Partial molar isentropic compression

The relationship illustrates the dependence of $K_{\phi,S}^{0}$ on molality is expressed by the **equation 4.10.** $K_{\phi,S}^{0}$ and their experimental slope/acoustic virial coefficient (S_k^*) are estimated by the least square regression analysis using the data of $K_{\phi,s}$ and are provided in **Table 4.47.** Negative values were observed with decrease corresponding to elevated temperatures as illustrated in **Figure 4.37.** The temperature and solutes (LA/BA) molality dependence of the negative $K_{\phi,S}^{0}$ values point to an increase in attractive interactions between the PB and (LA/BA) molecules which results in water molecules being less compressible as they are positioned around the L(+)-lactic and butyric acids. The key factors $K_{\phi,s}^{0}$ include a positive effect, recognized as the inherent compression of the solvent, which occurs when molecular spacing in the solution expands, enabling further compression. Conversely, the solvent penetration, a negative effect, arises as solvent molecules occupy voids within ions due to the interactions that take place among the solvent and solutes[41–43].

According to Kirkwood's theory, these interactions lessen electrostriction, releasing H_2O molecules into the bulk phase. Electrostricted water due to its more compact structure has a higher compressibility than bulk water [44]. The weak solute-solute contacts are suggested by the very small S_k^* values when compared to $K_{\phi,s}$, emphasizing that the solute and solvent associations dominate in the examined system [45].

Table 4.47 Calculated $K^0_{\phi,S}$ and S^*_K, of the potassium benzoate in L(+)-lactic and butyric acids solutions at various temperatures.

m_B	$K^0_{\phi,S} \times 10^6$(m^3·mol^{-1})				$S^*_K \times 10^6$ (m^3·kg·mol^{-2})			
(mol·kg^{-1})	288.15K	298.15K	308.15K	318.15K	288.15K	298.15K	308.15K	318.15 K
				L(+)-lactic Acid				
0.00	-46.02 (±0.08)	-44.24(±0.07)	-42.92(±0.07)	-42.17(±0.07)	-1.60(±0.23)	-1.53(±0.22)	-1.48(±0.22)	-1.45(±0.21)
0.01	-45.93(±0.08)	-43.96(±0.08)	-42.64(±0.08)	-41.68(±0.08)	-1.60(±0.24)	-1.53(±0.23)	-1.48(±0.23)	-1.45(±0.22)
0.02	-45.69(±0.07)	-43.82(±0.07)	-42.50(±0.07)	-41.64(±0.07)	-1.50(±0.21)	-1.43(±0.20)	-1.39(±0.20)	-1.37(±0.20)
0.03	-45.61(±0.07)	-43.64(±0.07)	-42.41(±0.07)	-41.55(±0.07)	-1.50(±0.22)	-1.43(±0.21)	-1.39(±0.21)	-1.37(±0.20)
				Butyric Acid				
0.00	-45.99(±0.08)	-44.21(±0.08)	-42.89(±0.08)	-41.95(±0.08)	-1.00(±0.24)	-0.97(±0.24)	-0.95(±0.23)	-0.93(±0.23)
0.01	-45.92(±0.08)	-43.95(±0.08)	-42.62(±0.07)	-41.67(±0.07)	-0.99(±0.24)	-0.95(±0.23)	-0.93(±0.22)	-0.92(±0.22)
0.02	-45.64(±0.08)	-43.78(±0.08)	-42.45(±0.07)	-41.59(±0.07)	-0.99(±0.24)	-0.95(±0.23)	-0.93(±0.22)	-0.93(±0.22)
0.03	-45.58(±0.08)	-43.61(±0.07)	-42.38(±0.07)	-41.52(±0.07)	-0.97(±0.24)	-0.93(±0.23)	-0.91(±0.22)	-0.91(±0.22)

m_B specifies the molality of potassium benzoate per kg of the pure water: the calculated standard uncertainties *u* are $u_r(m_{PB})$ = 0.01, $u(T)$=0.01 K, $u(K^0_{\phi,S})$ = (0.32 × 10^{-6})m^3·mol^{-1}·GPa^{-1}, $u(S^*_K)$ = (±0.05×10^{-6})kg·m^3·kg·mol^{-2}·GPa^{-1}, $u(p)$ = 0.01 MPa.

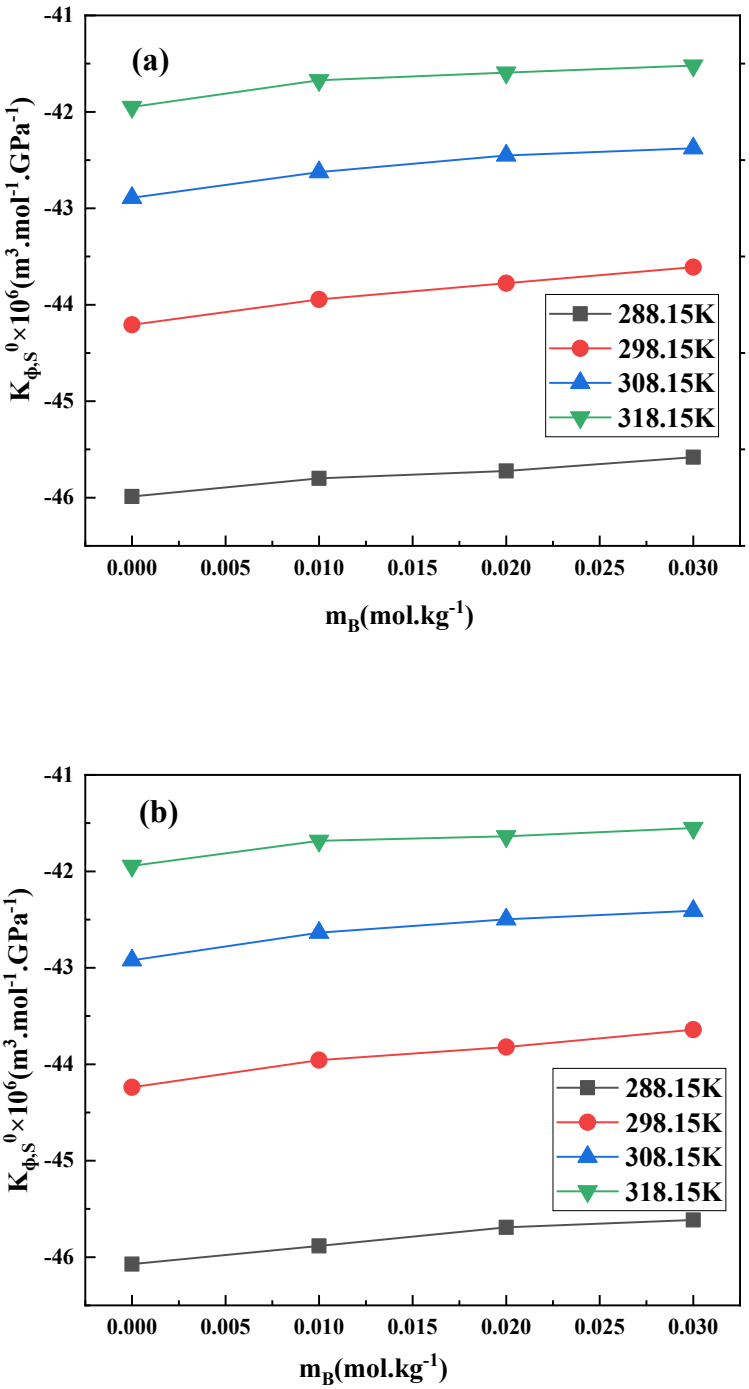

Figure 4.37 Plots of variations of $K_{\emptyset,s}^{0}$ for (a) butyric acid and (b) L(+)-lactic acid in potassium benzoate solution at varying temperatures.

4.5.9 Transfer of Partial molar isentropic compressions

The compression of a solute changes upon transitioning from water to a PB-containing solution, and $\Delta_{tr}K^{0}_{\emptyset,S}$ is determined using the outlined mathematical **equation 4.11**. The computed $\Delta_{tr}K^{0}_{\emptyset,S}$ values illustrating the change from water to infinitely diluted water-PB mixtures for L(+)-lactic and butyric acids are detailed in **Table 4.48.** The data reveals positive values that rise consistently with higher PB concentrations. Krishnan and Friedman [46] advanced the co-sphere overlap concept which explains this behavior by highlighting the part of solute as well as solvent interactions in altering the volume of the solution through expansion or contraction mechanisms. This theory suggests that positive data specify the displacement of H_2O molecules from hydrophilic centres.

With the addition of PB and (LA/BA), the positive $\Delta_{tr}K^{0}_{\emptyset,S}$ values reflect a more structured and less compressible solution. These results highlight the substantial role of the interactions between these components, which play a pivotal part in defining the solution's characteristics. The interactions between LA/BA and potassium benzoate strengthen the structural stability of the system. As a result, higher concentrations of the potassium benzoate lead to reduced compressibility, resulting in a mixture that is more compressible than the pure solvent. The reduction in electrostriction alters the solute's structural arrangement as the concentration of potassium benzoate upsurges. This occurs due to the stronger interactions within the zwitter-ionic centres of L(+)-lactic and butyric acids with water-soluble potassium benzoate [47]. The solutes (L(+)-lactic and butyric acids) interact with the water molecules. When the $\Delta_{tr}K^{0}_{\emptyset,S}$ values are positive, it indicates that L(+)-lactic and butyric acids interact with water molecules, leading to an increase in intermolecular associations. This implies that the solvent molecules integrate with the H_2O molecules surrounding the solutes due to these interactions. Conversely, negative $\Delta_{tr}K^{0}_{\emptyset,S}$ values arise from stronger ion-water interactions, which enhance the binding of solute molecules with the solvent, reducing overall compressibility [48].

Table 4.48 Values of $\Delta K^0_{\phi,S}$, of the ternary system of potassium benzoate in aqueous L(+)-lactic and butyric acids mixtures at various temperatures.

m_B ($\mathrm{mol \cdot kg^{-1}}$)	$\Delta K^0_{\phi,S} \times 10^6$ ($\mathrm{m^3 \cdot mol^{-1} \cdot GPa^{-1}}$)			
	288.15K	298.15K	308.15K	318.15K
		L(+)-lactic Acid		
0.01	0.09	0.28	0.29	0.49
0.02	0.33	0.42	0.43	0.54
0.03	0.41	0.60	0.51	0.62
		Butyric Acid		
0.01	0.07	0.26	0.27	0.28
0.02	0.35	0.43	0.44	0.36
0.03	0.41	0.60	0.51	0.43

m_B specifies the molality of potassium benzoate per kg of the pure water: the calculated standard uncertainties *u* are $u_r(m_{PB})$ = 0.01, $u(T)$=0.01 K, $u(\Delta K^0_{\phi,S})$ = $(0.02\times10^{-6})\mathrm{m^3 \cdot mol^{-1} \cdot GPa^{-1}}$, $u(p)$ = 0.01 MPa.

4.5.10 Interaction coefficients

Substituting the results of ΔV_{ϕ}^{0} and $\Delta K_{\phi,s}^{0}$ into the **equations 4.12** and **4.13** enabled the computation of the interaction coefficients. The parameters $V_{AB,}$ V_{ABB}; $K_{AB,}$ K_{ABB} for volume and isentropic compressibility are stated in **Table 4.49.** The splitting effects observed in solute interactions, as first noted by McMillan and Mayer [49], the concept examines the potential for independent effects in liquid combinations arising from molecular interactions occurring in pairs and triplets. Franks et al. [50] and Friedman and Krishnan [51] have further elaborated on similar theoretical concepts. A thorough understanding of both the extent and nature of these interactions is vital for accurately predicting and governing solute behavior in solutions [52]. At all examined temperatures, the pair coefficients exhibit positive values, although the triplet coefficients remain negative for both L(+)-lactic and butyric acids. The predominance of pair-wise interactions in mixtures of L(+)-lactic and butyric acids with potassium benzoate and water is supported by the consistently positive data of V_{AB} and K_{AB}.

Table 4.49 Interaction coefficients for the liquid system of potassium benzoate solutions with L(+)-lactic and butyric acids at different temperatures.

T/K	$V_{AB} \times 10^6$($m^3 \cdot mol^{-2} \cdot kg$)	$V_{ABB} \times 10^6$($m^3 \cdot mol^{-3} \cdot kg^2$)	$K_{AB} \times 10^6$ ($m^3 \cdot mol^{-2} \cdot kg \cdot GPa^{-1}$)	$K_{ABB} \times 10^6$ ($m^3 \cdot mol^{-3} \cdot kg^2 \cdot GPa^{-1}$)
		L(+)-lactic Acid		
288.15	41.99	-402.70	4.92	-39.09
298.15	45.80	-456.23	10.05	-120.30
308.15	47.95	-509.41	4.59	-31.73
318.15	44.30	-477.00	4.93	-33.43
		Butyric Acid		
288.15	12.61	-76.26	6.55	13.78
298.15	13.10	-91.82	13.65	-83.51
308.15	10.25	-27.55	15.72	-158.85
318.15	9.28	-15.68	15.05	-179.11

T/K is the temperature in kelvin; where standard uncertainties are $u(T)$=0.01 K, $u(p)$ = 0.01 MPa.

Problem 6

4.6 Title: "Acoustic and volumetric analysis of malic and tartaric acids in aqueous medium of sodium methyl p-hydroxybenzoate from 288.15 K to 318.15 K"

The study reports ρ and c data for alpha-hydroxy acids (malic and tartaric acids) in aqueous sodium methyl parahydroxybenzoate solutions at several concentrations of (0.02, 0.04, and 0.06) $mol \cdot kg^{-1}$ using DSA 5000 M.

4.6.1 Densities

In aqueous sodium methyl p-hydroxybenzoate solutions, the density measurements for malic and tartaric acids at several concentrations and a variety of temperatures are compiled in **Table 4.50**. The experimental density information is compared with previously published data for aqueous tartaric acid [53-55] in **Figure 4.38**. Under the investigated temperatures, the investigational results for the density align closely with those reported in previous studies. According to the data in **Table 4.50**, density increases with increasing molality of malic or tartaric acids and decreases with increasing temperatures at a particular concentration of sodium methyl 4-hydroxybenzoate. The molecular interactions inside solute and solvent molecules intensify as the molality of solute particles in a system rises, resulting in tighter molecular packing and an increase in density. However, for a certain SMP concentration, a upsurge in temperature causes a reduction in density because of increased kinetic energy which reduces intermolecular interactions and increases molecular spacing [56,57].

Table 4.50 Densities 'ρ' were determined in the ternary system of sodium methyl 4-hydroxybenzoate (SMP) in water-containing solutions with malic acid (MA) and tartaric acid (TA).

m_A/	$\rho \times 10^{-3}$/(kg·m^{-3})				m_A/	$\rho \times 10^{-3}$/(kg·m^{-3})			
(mol·kg^{-1})	288.15K	298.15K	308.15K	318.15K	(mol·kg^{-1})	288.15K	298.15K	308.15K	318.15K
	0.00 (mol·kg^{-1}) SMP + MA					**0.00 (mol·kg^{-1}) SMP + TA**			
0.00000	0.99926	0.99705	0.99404	0.99036	0.00000	0.99926	0.99705	0.99404	0.99036
0.09930	1.00417	1.00184	0.99872	0.99494	0.10542	1.00630	1.00406	1.00103	0.99734
0.20136	1.00904	1.00656	1.00334	0.99946	0.19266	1.01200	1.00975	1.00671	1.00300
0.29949	1.01350	1.01091	1.00758	1.00360	0.30748	1.01935	1.01708	1.01402	1.01030
0.40764	1.01823	1.01550	1.01208	1.00800	0.39615	1.02491	1.02262	1.01955	1.01581
0.49042	1.02163	1.01882	1.01530	1.01113	0.50027	1.03131	1.02900	1.02590	1.02215
	0.02 (mol·kg^{-1}) SMP + MA					**0.02 (mol·kg^{-1}) SMP + TA**			
0.00000	1.00038	0.99826	0.99525	0.99152	0.00000	1.00038	0.99826	0.99525	0.99152
0.09478	1.00496	1.00275	0.99963	0.99581	0.10157	1.00707	1.00493	1.00189	0.99814
0.19236	1.00950	1.00717	1.00396	1.00004	0.20748	1.01389	1.01171	1.00866	1.00487
0.30185	1.01437	1.01191	1.00859	1.00458	0.30553	1.02006	1.01785	1.01478	1.01098
0.39862	1.01847	1.01593	1.01251	1.00841	0.40342	1.02607	1.02384	1.02074	1.01691
0.49776	1.02248	1.01981	1.01634	1.01216	0.50661	1.03228	1.03002	1.02690	1.02306
	0.04 (mol·kg^{-1}) SMP + MA					**0.04 (mol·kg^{-1}) SMP + TA**			
0.00000	1.00119	0.99931	0.99616	0.99239	0.00000	1.00119	0.99931	0.99616	0.99239
0.10057	1.00602	1.00404	1.00078	0.99691	0.10816	1.00819	1.00628	1.00311	0.99932

0.20382	1.01078	1.00868	1.00532	1.00134	0.20957	1.01458	1.01266	1.00947	1.00567
0.30054	1.01504	1.01281	1.00937	1.00532	0.30996	1.02076	1.01882	1.01561	1.01180
0.39479	1.01902	1.01670	1.01317	1.00902	0.40878	1.02669	1.02474	1.02151	1.01768
0.49544	1.02308	1.02064	1.01703	1.01283	0.50975	1.03261	1.03065	1.02741	1.02356
0.06 (mol·kg^{-1}) SMP + MA					**0.06 (mol·kg^{-1}) SMP + TA**				
0.00000	1.00221	1.00024	0.99712	0.99313	0.00000	1.00221	1.00024	0.99712	0.99313
0.10991	1.00745	1.00537	1.00213	0.99804	0.10241	1.00873	1.00674	1.00360	0.99960
0.19548	1.01136	1.00919	1.00588	1.00166	0.20765	1.01526	1.01325	1.01009	1.00608
0.30981	1.01638	1.01407	1.01062	1.00636	0.30358	1.02106	1.01904	1.01588	1.01186
0.40127	1.02021	1.01781	1.01433	1.00991	0.40476	1.02705	1.02501	1.02184	1.01781
0.50693	1.02445	1.02189	1.01835	1.01387	0.50834	1.03305	1.03099	1.02781	1.02379

m_A is the molality of malic and tartaric acids in sodium methyl p-hydroxy benzoate: the calculated standard uncertainties *u* are u(m) = 0.02, u(T)=0.001 K, u(ρ)=0.59(kg·m^{-3}).

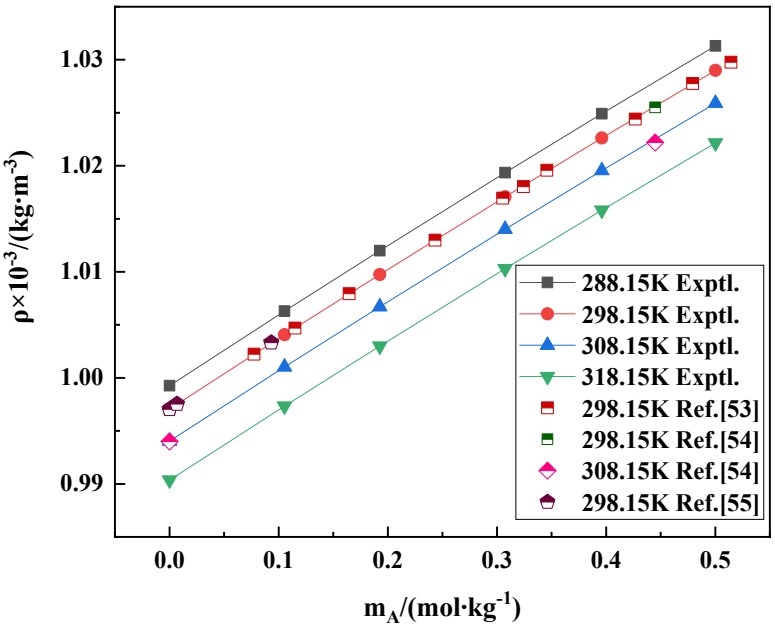

Figure 4.38 Variation of densities for tartaric acid + water between measured and literature values at different concentrations and temperatures [53-55].

4.6.2 Apparent molar volume

The effectiveness and consistency of liquid-based products such as cosmetics and pharmaceuticals depend greatly on their apparent molar volume which are examined from measured density data using **equation 4.1.** At different temperatures, the V_ϕ of malic and tartaric acids in aqueous sodium methyl p-hydroxybenzoate has been calculated as indicated in **Table 4.51.** The results indicate that when the concentration of SMP rises, V_ϕ also rises with a rise in temperature and molalities of alpha-hydroxy acids, which suggests stronger bonds between the solute-solvent molecules. Molecular interactions between these acids and sodium methyl p-hydroxybenzoate are schematically presented in **Figure 4.39.** This effect is primarily due to interactions between malic and tartaric acids with sodium methyl p-hydroxybenzoate, which weaken the electrostriction caused by water molecules, leading to an elevation in apparent molar volume [58]. An upward trend in V_ϕ values is observed with both temperature elevation and rising alpha-hydroxy acids molality at a specific SMP concentration, as depicted in **Figures 4.40** and **4.41**. The interaction pattern among the molecules in the mixture is attributed to the clear linear dependence of V_ϕ on temperature and AHAs molality, driven by effective solvation and solvent affinity. The observed enhancement in apparent molar volume could result from various physical factors, such as dipole and hydrophilic-hydrophilic effects, in the aqueous medium. The outcomes emphasize the role of chemical properties, including polarity and the ability to form hydrogen bonds, in governing solute-solvent associations[59–62].

Table 4.51 Apparent molar volumes 'V_ϕ' were determined in the ternary system of sodium methyl para-hydroxy benzoate in water-based solutions with malic acid (MA) and tartaric acid (TA).

m_A/ (mol·kg^{-1})	$V_\phi \times 10^6$/(m^3·mol^{-1})				m_A/ (mol·kg^{-1})	$V_\phi \times 10^6$/(m^3·mol^{-1})			
	288.15K	298.15K	308.15K	318.15K		288.15K	298.15K	308.15K	318.15K
	0.00 (mol·kg^{-1}) SMP + MA					**0.00 (mol·kg^{-1}) SMP + TA**			
0.09930	84.26	85.55	86.79	87.96	0.10542	82.75	83.01	83.25	83.44
0.20136	84.72	86.16	87.34	88.51	0.19266	82.91	83.16	83.39	83.57
0.29949	85.35	86.73	87.94	89.13	0.30748	83.08	83.34	83.55	83.76
0.40764	85.95	87.34	88.50	89.68	0.39615	83.21	83.47	83.68	83.89
0.49042	86.57	87.91	89.12	90.32	0.50027	83.37	83.61	83.84	84.06
	0.02 (mol·kg^{-1}) SMP + MA					**0.02 (mol·kg^{-1}) SMP + TA**			
0.09478	85.37	86.44	87.65	88.78	0.10157	83.64	83.92	84.21	84.52
0.19236	85.89	87.06	88.24	89.42	0.20748	83.85	84.17	84.43	84.76
0.30185	86.51	87.76	88.91	90.03	0.30553	84.01	84.35	84.62	84.93
0.39862	87.12	88.29	89.47	90.59	0.40342	84.23	84.56	84.83	85.16
0.49776	87.73	88.95	90.05	91.17	0.50661	84.42	84.75	85.03	85.32
	0.04 (mol·kg^{-1}) SMP + MA					**0.04 (mol·kg^{-1}) SMP + TA**			
0.10057	85.57	86.68	87.93	89.05	0.10816	84.75	85.04	85.31	85.59
0.20382	86.19	87.34	88.49	89.71	0.20957	85.02	85.28	85.53	85.75
0.30054	86.74	88.01	89.14	90.27	0.30996	85.25	85.49	85.76	85.96
0.39479	87.31	88.53	89.65	90.82	0.40878	85.51	85.72	85.99	86.21

0.49544	87.92	89.17	90.26	91.35	0.50975	85.73	85.93	86.19	86.43
	0.06 (mol·kg^{-1}) SMP + MA					**0.06 (mol·kg^{-1}) SMP + TA**			
0.10991	85.86	86.94	88.16	89.26	0.10241	85.82	86.07	86.29	86.51
0.19548	86.38	87.53	88.65	89.90	0.20765	86.09	86.31	86.55	86.75
0.30981	87.02	88.21	89.37	90.51	0.30358	86.30	86.52	86.74	86.92
0.40127	87.56	88.74	89.82	91.08	0.40476	86.51	86.73	86.93	87.13
0.50693	88.15	89.43	90.43	91.62	0.50834	86.68	86.91	87.12	87.28

m_A is the molality of malic and tartaric acids in sodium methyl p-hydroxy benzoate: the calculated standard uncertainties *u* are u(m) = 0.02, u(T)=0.001 K, u (V_ϕ) = (0.08-0.19) × 10^6/(m^3·mol^{-1}).

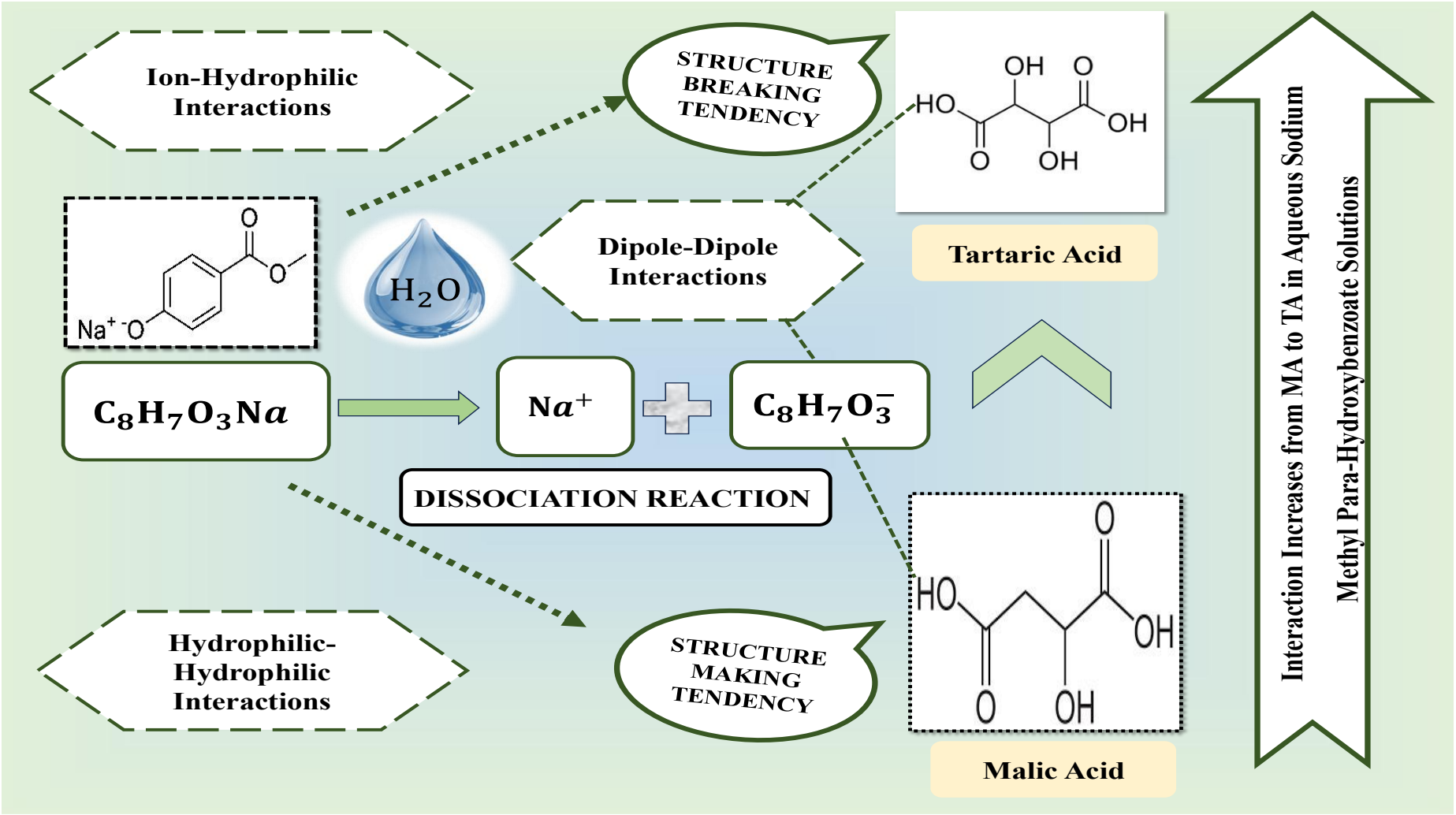

Figure 4.39 Interactions of malic or tartaric acids with sodium methyl p-hydroxybenzoate solutions.

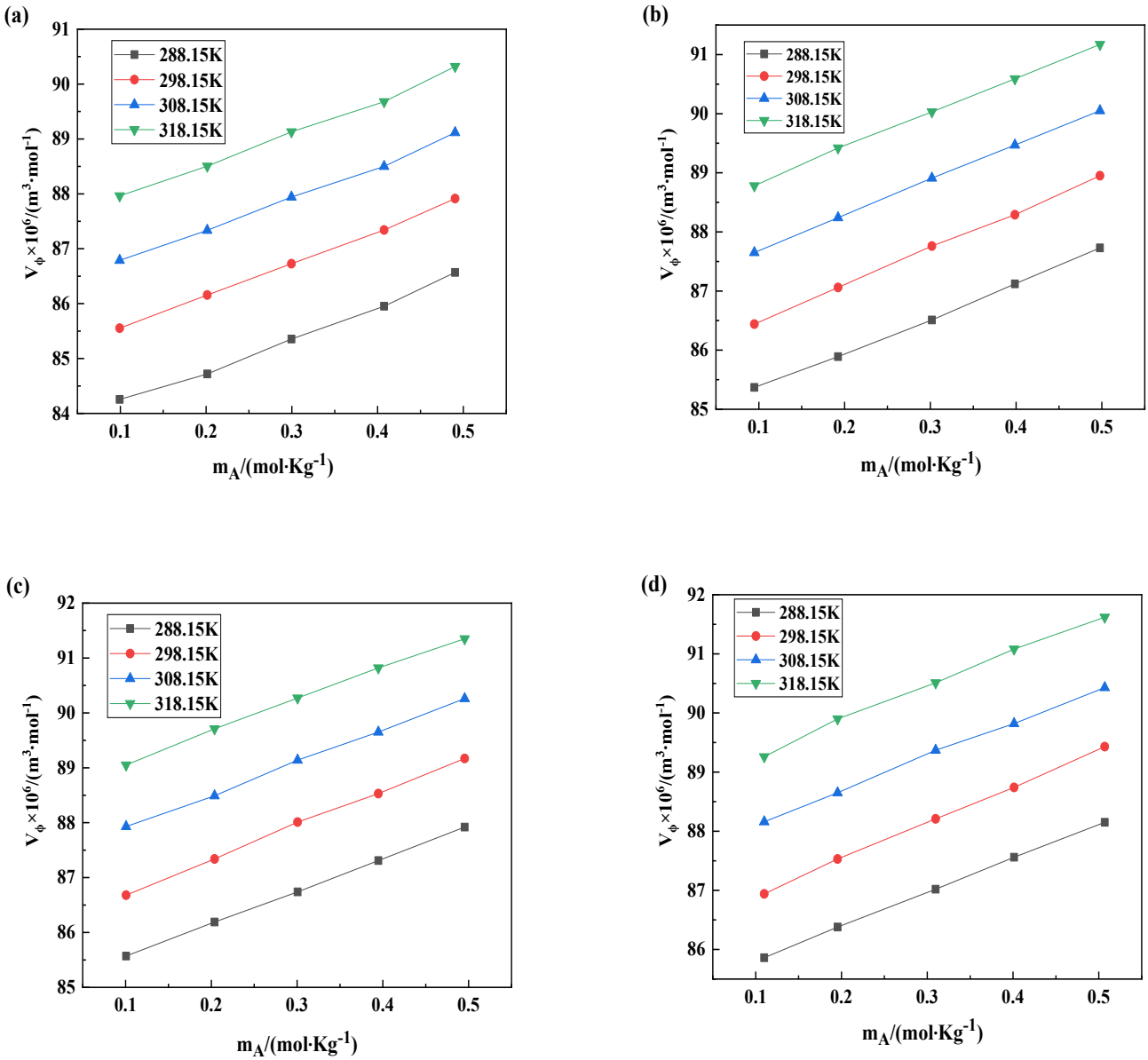

Figure 4.40 Plots demonstrate the changes in ($V_\emptyset$) of (a) 0.00 SMP; (b) 0.02 SMP; (c) 0.04 SMP; (d) 0.06 SMP with the molality of malic acid at varying temperatures.

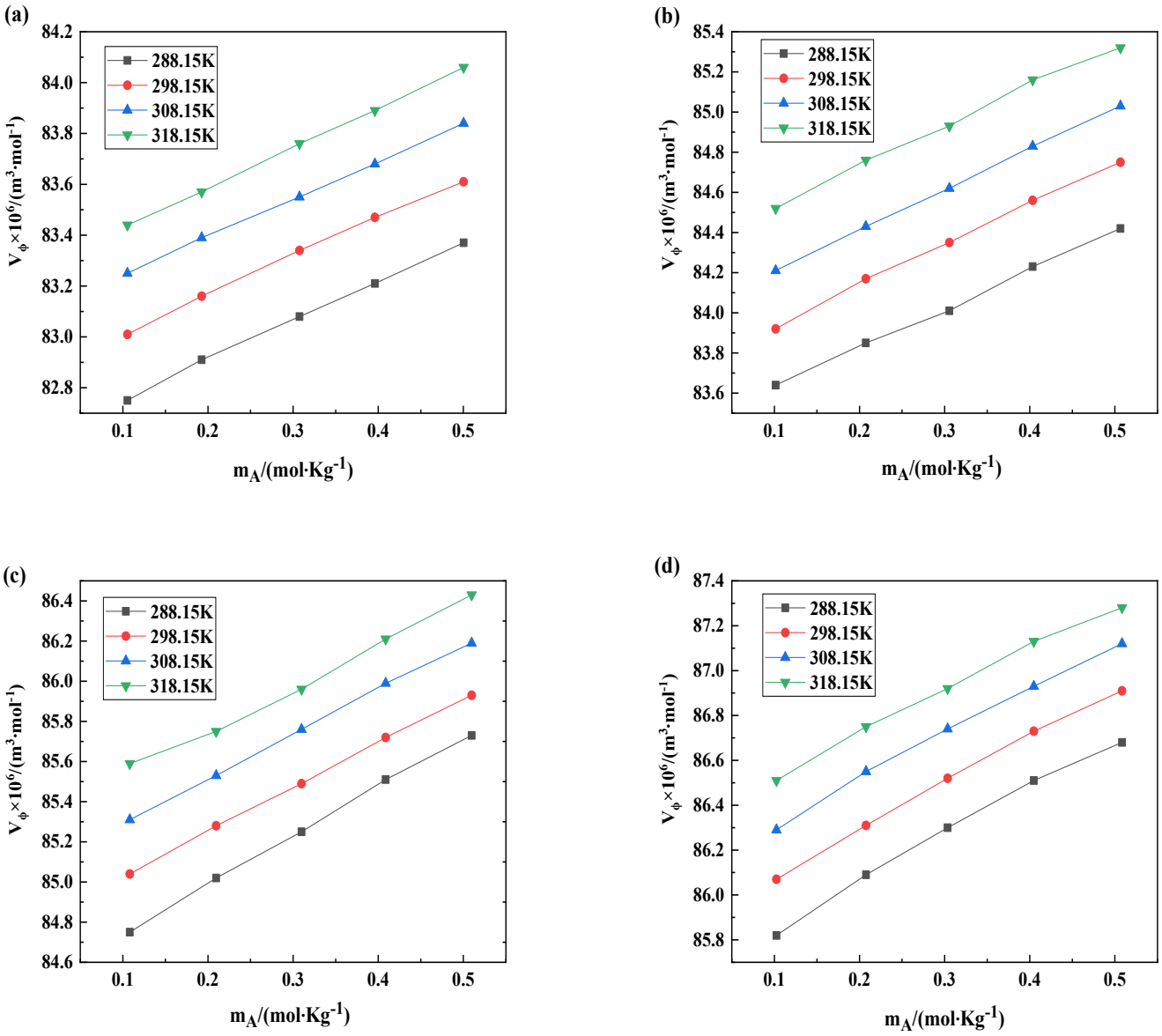

Figure 4.41 Plots demonstrate the changes in ($V_\emptyset$) of (a) 0.00 SMP; (b) 0.02 SMP; (c) 0.04 SMP; (d) 0.06 SMP with the molality of tartaric acid at varying temperatures.

4.6.3 Partial molar volumes

The **equation 4.2** can be applied to evaluate the V_ϕ^0 values for ternary mixtures composed of malic acid, tartaric acid, and sodium methyl 4-hydroxybenzoate in aqueous media. The least squares fitting technique was employed to evaluate the (V_ϕ^0) and the corresponding slopes (S_V^*) as specified in **Table 4.52.** The V_ϕ^0 values for both malic or tartaric acids were found to be positive and exhibited a rising trend with increasing concentrations of SMP as illustrated in **Figure 4.42.**

Throughout the studied temperature range for sodium methyl p-hydroxybenzoate, the S_V^* parameter consistently exhibited positive values reflecting the existence of solute associations. Nonetheless, the inconsistency in S_V^* trends point toward the influence of additional variables affecting solute behavior [63,64]. A predominance of the solute-solvent bond is evident from the lower S_V^* values relative to V_ϕ^0. This can be interpreted using the co-sphere overlap concept, which postulates that overlapping hydration spheres of ions contribute to an overall volumetric expansion in the solution. It can be inferred that solute-solvent interactions predominantly govern the molecular associations in the liquid mixture over solute-solute interactions. The increasing pattern of V_ϕ^0 in SMP with elevated molality of the acids highlights that hydrophilic and ionic bonds show a critical role than the hydrophobic in the current system[65–67].

Table 4.52 $'V_{\Phi}^{0}'$, and $'S_{V}^{*}'$ values of sodium methyl para-hydroxy benzoate (SMP) in water-soluble solutions with malic acid (MA) and tartaric acid (TA) with their standard errors.

m_B/ (mol·kg^{-1})	$V_{\Phi}^{0} \times 10^{6}$/(m^3·mol^{-1})				$S_{V}^{*} \times 10^{6}$ /(m^3·kg·mol^{-2})			
	288.15K	298.15K	308.15K	318.15K	288.15K	298.15K	308.15K	318.15 K
				Malic Acid				
0.00	83.60(±0.08)	84.95(±0.03)	86.18(±0.06)	87.34(±0.07)	5.92(±0.25)	5.97(±0.10)	5.88(±0.18)	5.94(±0.22)
0.02	84.78(±0.04)	85.87(±0.03)	87.09(±0.01)	88.25(±0.03)	5.88(±0.11)	6.18(±0.09)	5.96(±0.04)	5.88(±0.09)
0.04	84.97(±0.01)	86.06(±0.04)	87.32(±0.03)	88.50(±0.04)	5.93(±0.04)	6.29(±0.11)	5.93(±0.11)	5.82(±0.12)
0.06	85.24(±0.01)	86.28(±0.03)	87.56(±0.08)	88.72(±0.10)	5.76(±0.04)	6.19(±0.10)	5.68(±0.25)	5.80(±0.31)
				Tartaric Acid				
0.00	82.60(±0.01)	82.86(±0.01)	83.10(±0.01)	83.27(±0.01)	1.55(±0.03)	1.52(±0.04)	1.48(±0.02)	1.57(±0.02)
0.02	83.44(±0.02)	83.73(±0.02)	84.01(±0.01)	84.33(±0.02)	1.93(±0.05)	2.04(±0.05)	2.03(±0.02)	1.99(±0.07)
0.04	84.50(±0.02)	84.81(±0.01)	85.07(±0.01)	85.33(±0.03)	2.44(±0.05)	2.21(±0.03)	2.21(±0.03)	2.13(±0.10)
0.06	85.63(±0.03)	85.87(±0.02)	86.11(±0.03)	86.34(±0.03)	2.12(±0.10)	2.08(±0.06)	2.02(±0.07)	1.90(±0.08)

m_B is the molality of sodium methyl para-hydroxy benzoate solution: calculated standard uncertainties *u* are u(m) = 0.01, u(T)=0.001 K, u (V_{Φ}^{0})= (0.15-0.40) × 10^6/(m^3·mol^{-1}) and u (S_{V}^{*})=±0.33 × 10^6/(m^3·kg·mol^{-2}).

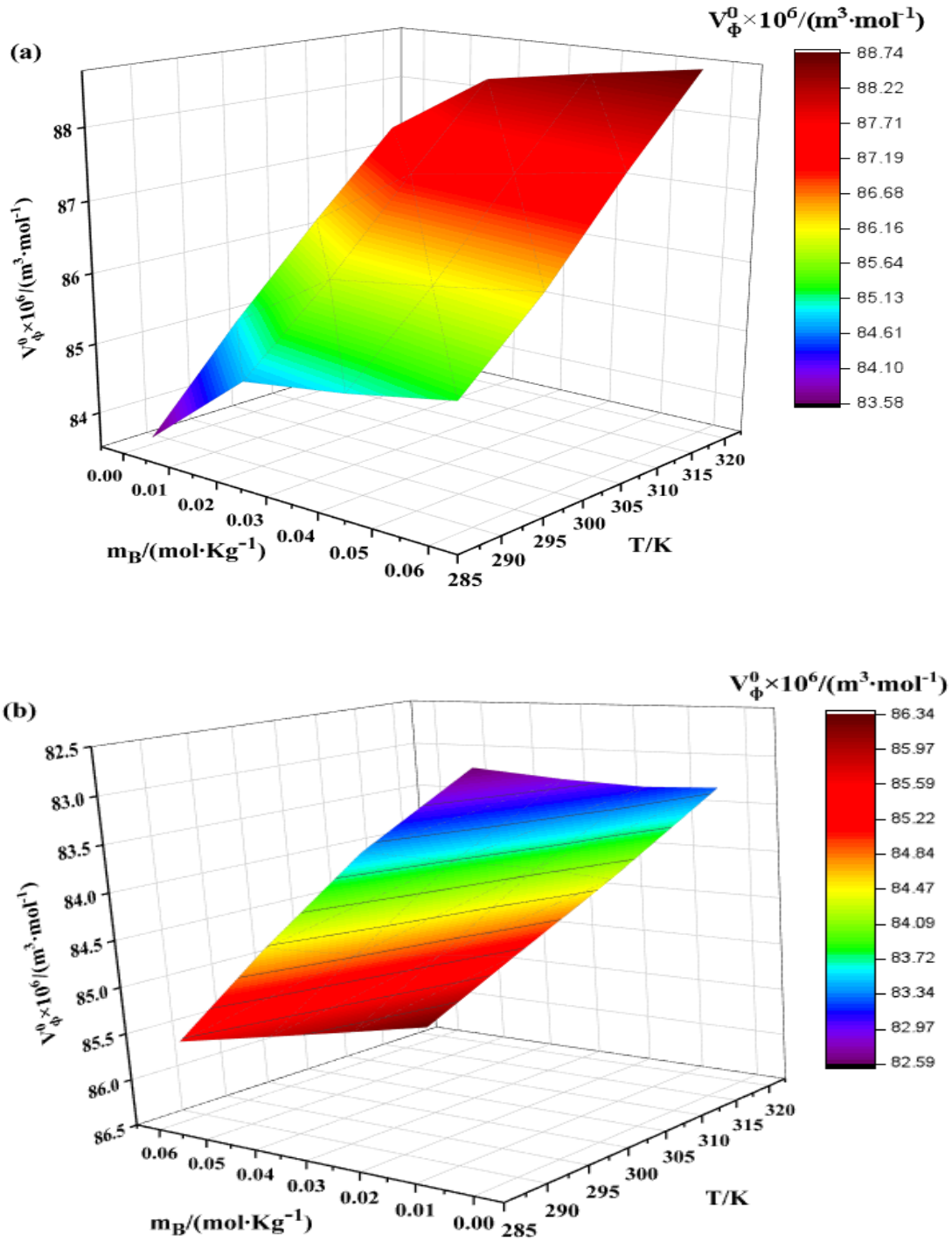

Figure 4.42 Plots representing the variations in $V_\emptyset^0$, for (a) malic acid, (b) tartaric acid inside an SMP water-soluble solution at numerous temperatures.

4.6.4 Transfer of Partial molar volumes

In the realm of thermodynamic interpretation, ΔV_{ϕ}^{0} denotes the volumetric change linked to the solute's phase behavior. The **equation 4.3** is applied to evaluate the extent of solute transfer from water to the SMP-containing solution.

According to **Table 4.53**, the ΔV_{ϕ}^{0} values for malic and tartaric acids in SMP solutions in water are positive and generally rise with increasing solvent concentration, though the trend fluctuates with temperature changes. This transfer parameter is crucial in interpreting the nature of associations in the solution as it reflects the degree of association within solute and solvent. The observed positive ΔV_{ϕ}^{0} data suggest that the solute may disrupt or enhance the organization of the structure through solvophobic effects and overlapping hydration spheres [68]. It is crucial to understand that the sodium methyl Parahydroxybenzoate and malic or tartaric acids function as electrolytes and separate into ions during dissolution. The observed positive values highlight the greater ion-ion interactions within malic/tartaric acids and sodium methyl p-hydroxybenzoate. Pauling's clathrate concept explains the void spaces in water structure that can be filled by other molecules. However, malic and tartaric acids do not fill these spaces but instead disturb the water network, potentially forming new structures by bonding with water molecules [69]. Hydrophilic-hydrophilic, ion-ion, ion-hydrophilic interactions are associated with positive ΔV_{ϕ}^{0} values in the present investigation, as defined by the co-sphere overlap theory [70,71].

Table 4.53 Transfer property 'ΔV_{ϕ}^{0}' of sodium methyl para-hydroxy benzoate (SMP) in water-soluble solutions with malic acid (MA) and tartaric acid (TA) at various temperatures and concentrations.

m_B/ (mol·kg^{-1})	$\Delta V_{\phi}^{0} \times 10^{6}$/(m^3·mol^{-1})			
	288.15K	298.15K	308.15K	318.15K
		Malic Acid		
0.02	1.18	0.92	0.92	0.91
0.04	1.37	1.11	1.14	1.16
0.06	1.64	1.34	1.39	1.38
		Tartaric Acid		
0.02	0.84	0.87	0.91	1.06
0.04	1.90	1.95	1.97	2.06
0.06	3.03	3.01	3.01	3.07

m_B signifies the molality of sodium methyl para-hydroxy benzoate solution: the calculated standard uncertainties *u* are u(m) = 0.01, u(T)=0.001 K, u(ΔV_{ϕ}^{0})= ±0.06×10^6/(m^3·mol^{-1}).

4.6.5 Temperature-dependent partial molar volume

This method illustrates that temperature changes significantly influence the V_ϕ^0 using **equation 4.4**. **Table 4.54** contains the empirical coefficients a, b, and c for malic and tartaric acids in water-soluble sodium methyl 4-hydroxybenzoate solutions. The ARD (σ) deviations, derived from both determined and measured V_ϕ^0 values, are computed using **equation 4.5**. In this study, the polynomial equation, represented by $Y = V_\phi^0$, shows minimal deviations, indicating a strong correlation and a good fit to the data [72].

The main focus of the study was to calculate partial molar expansibilities using **equation 4.6.** The positive E_ϕ^0 data confirm the validity of the apparent molar volume parameter signifies that solute-solvent bonds persist in the system due to caging or packing phenomena [73,30], as shown in **Table 4.55**. The solute's potential to affect the solution structure, either by promoting or disrupting it, can be determined using Hepler's thermodynamic **equation 4.7** [31].

The positive sign of $(\partial E_\phi^0 / \partial T)_P$ exhibits that the solute promotes structure formation, whereas a negative sign indicates that the solute tends to disrupt existing structures [74–76]. In this study, as shown in **Table 4.55**, Hepler's constant for malic acid in water-soluble SMP solution is positive, which suggests a structure-forming behavior, whereas tartaric acid is negative, except at 0.02 mol·kg^{-1}, which points to structure-disrupting properties of the combination in this study.

`

Table 4.54 Calculated empirical parameters of sodium methyl para-hydroxy benzoate (SMP) in water-soluble malic acid (MA) and tartaric acid (TA).

m_B/(mol·kg^{-1})	$a \times 10^6$/ (m^3·mol^{-1})	$b \times 10^6$/ (m^3·mol^{-1}·K^{-1})	$c \times 10^6$/ (m^3·mol^{-1}·K^{-2})	R^2	ARD
			Malic Acid		
0.02	85.90	0.1147	0.0002	0.9999	0.0000
0.04	86.10	0.1162	0.0002	0.9999	0.0000
0.06	86.34	0.1144	0.0003	0.9999	0.0000
			Tartaric Acid		
0.02	83.72	0.0285	0.0001	0.9999	0.0000
0.04	84.80	0.0289	-0.0001	0.9999	0.0000
0.06	85.87	0.0238	0.0000	0.9999	0.0000

m_B signifies the molality of sodium methyl para-hydroxy benzoate solution: calculated standard uncertainties are u(m) = 0.01, u(T)=0.001 K, u(p) =0.01 MPa.

Table 4.55 Data of partial molar expansibilities 'E_{ϕ}^{0}' sodium methyl para-hydroxy benzoate (SMP) in water-soluble solutions with malic acid (MA) and tartaric acid (TA) at various temperatures

m_B/ (mol·kg^{-1})	$E_{\phi}^{0} \times 10^{6}$/(m^3·mol^{-1}·K^{-1})				$\left(\frac{\partial E_{\phi}^{0}}{\partial T}\right)_P$/(m^3·mol^{-1}·K^{-2})
	288.15K	298.15K	308.15K	318.15K	
			Malic Acid		
0.02	0.1112	0.1147	0.1183	0.1218	0.00035
0.04	0.1119	0.1162	0.1205	0.1248	0.00043
0.06	0.1086	0.1144	0.1201	0.1259	0.00058
			Tartaric Acid		
0.02	0.0265	0.0285	0.0305	0.0324	0.00020
0.04	0.0317	0.0289	0.0262	0.0235	-0.00027
0.06	0.0244	0.0238	0.0232	0.0226	-0.00006

m_B signifies the molality of sodium methyl p-hydroxy benzoate solution: calculated standard uncertainties are u(m) = 0.01, u(T)=0.001 K, u(E_{ϕ}^{0}) = 0.0083 ×10^6/(m^3·mol^{-1}·K^{-1}), u($\frac{\partial E_{\phi}^{0}}{\partial T}$) = 0.00022/(m^3·mol^{-1}·K^{-2}), u(p) =0.01 MPa.

4.6.6 Sound speed

The acoustic behavior of malic and tartaric acids was analyzed in sodium methyl p-hydroxybenzoate at selected concentrations under varying temperatures with results compiled in **Table 4.56**. The observed ultrasonic velocities for the binary mixtures of TA + water [53] are consistent with previously reported data, as illustrated in **Figure 4.43.** The propagation sound speed through a solution reflects the strength and type of interactions present between its components. An upward trend in velocity generally implies enhanced intermolecular bonds. The data indicate that as the molality of malic and tartaric acids increases, so does the velocity, which is likely due to the establishment of 3-D hydrogen bond frameworks with sodium methyl parahydroxy benzoate[77].

At higher concentrations, solute molecules occupy the spaces between solvent molecules, reducing the free volume available for molecular movement and enabling sound waves to propagate more efficiently through the denser medium. Additionally, robust solute-solvent interactions become more prominent as the concentration rises. creating a more structured environment that facilitates sound propagation. As temperature rises, thermal agitation enhances molecular interactions by breaking weaker bonds, and strengthening significant ones like hydrogen bonds further supports faster sound wave propagation. This phenomenon is also influenced by a drop in the compressibility of the solution as the structured arrangement of molecules becomes more rigid, allowing sound waves to travel at greater speeds [35,78,79]. With the progression from malic acid to tartaric acid, the rise in solute molar mass disrupts the existing hydrogen bonds between sodium methyl p-hydroxybenzoate and water, leading to their breakdown and the establishment of new hydrogen-bonding interactions among the system components [80-83].

Table 4.56 Sound velocity 's' values of sodium methyl para-hydroxy benzoate (SMP) in water-soluble solutions with malic acid (MA) and tartaric acid (TA) at different temperatures.

m_A/	s/(m·s^{-1})				m_A/	s/(m·s^{-1})			
(mol·kg^{-1})	288.15K	298.15K	308.15K	318.15K	(mol·kg^{-1})	288.15K	298.15K	308.15K	318.15K
	0.00 (mol·kg^{-1}) SMP + MA					**0.00 (mol·kg^{-1}) SMP + TA**			
0.00000	1466.59	1495.85	1519.14	1536.02	0.00000	1466.59	1495.85	1519.14	1536.02
0.09930	1470.76	1499.04	1521.54	1537.83	0.10542	1470.49	1499.64	1522.75	1540.24
0.20136	1474.85	1502.13	1524.02	1539.51	0.19266	1474.07	1502.82	1525.63	1544.08
0.29949	1478.44	1505.30	1526.28	1541.16	0.30748	1478.83	1506.93	1529.85	1547.96
0.40764	1482.46	1508.75	1528.87	1543.06	0.39615	1482.34	1510.28	1532.46	1551.72
0.49042	1485.56	1511.27	1530.69	1544.39	0.50027	1485.92	1514.06	1536.17	1555.27
	0.02 (mol·kg^{-1}) SMP + MA					**0.02 (mol·kg^{-1}) SMP + TA**			
0.00000	1469.69	1499.21	1522.25	1538.68	0.00000	1469.69	1499.21	1522.25	1538.68
0.09478	1473.51	1502.07	1524.14	1539.81	0.10157	1472.75	1501.54	1524.31	1542.37
0.19236	1476.95	1504.78	1525.98	1541.17	0.20748	1476.78	1504.82	1527.67	1546.48
0.30185	1481.11	1507.94	1528.29	1542.97	0.30553	1480.12	1508.01	1531.13	1549.25
0.39862	1484.77	1510.89	1530.56	1544.73	0.40342	1484.03	1512.07	1534.42	1553.47
0.49776	1489.19	1514.61	1533.02	1546.36	0.50661	1487.26	1516.18	1538.59	1557.76
	0.04 (mol·kg^{-1}) SMP + MA					**0.04 (mol·kg^{-1}) SMP + TA**			
0.00000	1472.35	1501.46	1523.82	1539.86	0.00000	1472.35	1501.46	1523.82	1539.86
0.10057	1476.05	1504.37	1526.12	1541.38	0.10816	1474.39	1503.65	1526.71	1544.45

0.20382	1479.88	1507.18	1528.15	1542.89	0.20957	1478.14	1506.82	1529.58	1548.63
0.30054	1483.25	1509.85	1530.24	1544.23	0.30996	1482.75	1510.03	1533.43	1551.19
0.39479	1486.76	1512.91	1532.47	1545.92	0.40878	1486.03	1514.27	1536.39	1555.26
0.49544	1490.81	1516.28	1535.06	1547.64	0.50975	1489.48	1518.61	1540.64	1559.17
0.06 (mol·kg^{-1}) SMP + MA					**0.06 (mol·kg^{-1}) SMP + TA**				
0.00000	1474.8	1503.69	1525.76	1541.63	0.00000	1474.8	1503.69	1525.76	1541.63
0.10991	1478.86	1506.74	1528.19	1542.75	0.10241	1476.54	1505.74	1528.06	1546.36
0.19548	1481.63	1509.13	1529.82	1544.03	0.20765	1480.04	1508.39	1530.62	1550.75
0.30981	1485.72	1511.95	1532.14	1545.84	0.30358	1484.23	1512.45	1534.15	1553.84
0.40127	1489.15	1514.83	1534.05	1547.54	0.40476	1488.02	1516.83	1538.48	1557.41
0.50693	1492.68	1518.04	1536.51	1549.42	0.50834	1491.65	1520.08	1542.24	1561.03

m_A is the molality of malic and tartaric acids in water-soluble sodium methyl p-hydroxy benzoate: the calculated standard uncertainties *u* are u(m) = 0.02, u(T)=0.001 K, u(s)=1.80(m·s^{-1}).

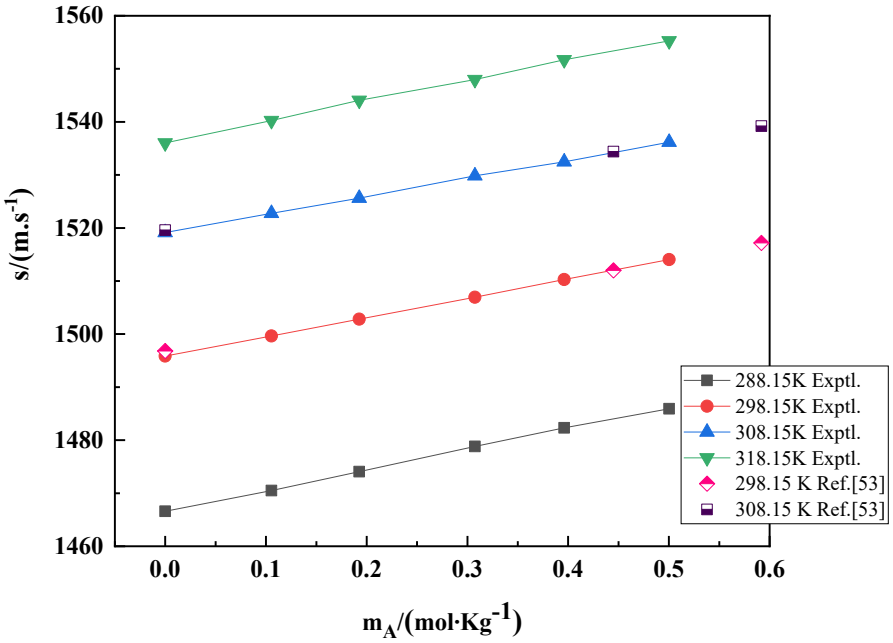

Figure 4.43 Variation of sound speed for tartaric acid + water between measured and literature values at different concentrations and temperatures [53].

4.6.7 Apparent molar isentropic compressibility

The values of k_s were obtained by utilizing the Laplace equation from **equation 4.8** on the ultrasonic velocity measurements obtained at different temperatures. The $K_{\phi,s}$ for malic and tartaric acids in water-soluble SMP mixture is derived using **equation 4.9. Table 4.57** lists the $K_{\phi,s}$ measurements and the results show a symmetric behavior, where the negative magnitude slightly lessens with temperature, but becomes more significant with increasing molality of the alpha-hydroxy acids. All $K_{\phi,s}$ values are found to be negative with the degree of negativity increasing as the molality of malic and tartaric acids rises at a fixed SMP concentration. However, this negativity diminishes with a temperature rise. Furthermore, as the concentration of SMP rises, the $K_{\phi,s}$ values display a trend toward less negative values, as indicated by the linear relationship in **Figures 4.44** and **4.45**.

Due to their zwitterionic nature, malic and tartaric acids carry both positive and negative charges within a single molecule which significantly influences their affinity for water. This dual charge enables these acids to engage in extensive hydrogen bonding with water molecules results to the formation of hydrophilic aggregates around the solutes. These molecular interactions give rise to intense ion-ion and ion-hydrophilic bonding, particularly supported by the polar nature of water molecules [84,85]. The creation of compact structures in malic and tartaric acids in aqueous SMP solutions is attributed to strong inter-molecular hydrogen bonding leads to a decline in compressibility. The hydroxyl groups present in malic and tartaric acids interact intensely with water molecules through dipole-dipole forces, strengthening solute-solvent associations. This tendency specifies that water molecules located adjacent to the ionic groups of malic and tartaric acids exhibit reduced compressibility compared to molecules in the bulk phase. Consequently, the compressibility of the surrounding water structure is lowered which leads to a reorganization of H_2O molecules surrounding the solute [86].

Table 4.57 Values of '$K_{\phi,s}$' for sodium methyl para-hydroxy benzoate in water-soluble solutions with malic acid (MA) and tartaric acid (TA) at different temperatures.

m_A/ (mol·kg^{-1})	$K_{\phi,s} \times 10^6$/(m^3·mol^{-1}·GPa^{-1})				m_A/ (mol·kg^{-1})	$K_{\phi,s} \times 10^6$/(m^3·mol^{-1}·GPa^{-1})			
	288.15K	298.15K	308.15K	318.15K		288.15K	298.15K	308.15K	318.15K
	0.00 (mol·kg^{-1}) SMP + MA					**0.00 (mol·kg^{-1}) SMP + TA**			
0.09930	-46.23	-44.43	-43.10	-42.15	0.10542	-46.35	-44.56	-43.23	-42.28
0.20136	-46.69	-44.87	-43.53	-42.57	0.19266	-46.82	-45.01	-43.67	-42.71
0.29949	-46.98	-45.14	-43.79	-42.81	0.30748	-47.25	-45.42	-44.07	-43.11
0.40764	-47.24	-45.39	-44.02	-43.04	0.39615	-47.55	-45.71	-44.35	-43.37
0.49042	-47.42	-45.56	-44.18	-43.19	0.50027	-47.87	-46.02	-44.65	-43.67
	0.02 (mol·kg^{-1}) SMP + MA					**0.02 (mol·kg^{-1}) SMP + TA**			
0.09478	-46.04	-44.25	-42.93	-41.97	0.10157	-46.17	-44.38	-43.06	-42.10
0.19236	-46.50	-44.69	-43.35	-42.38	0.20748	-46.73	-44.91	-43.57	-42.61
0.30185	-46.82	-44.99	-43.63	-42.66	0.30553	-47.08	-45.26	-43.90	-42.93
0.39862	-47.04	-45.20	-43.84	-42.85	0.40342	-47.40	-45.56	-44.20	-43.22
0.49776	-47.25	-45.40	-44.03	-43.04	0.50661	-47.71	-45.86	-44.49	-43.50
	0.04 (mol·kg^{-1}) SMP + MA					**0.04 (mol·kg^{-1}) SMP + TA**			
0.10057	-45.92	-44.14	-42.80	-41.94	0.10816	-46.06	-44.27	-42.94	-42.08
0.20382	-46.38	-44.57	-43.22	-42.35	0.20957	-46.56	-44.75	-43.41	-42.54
0.30054	-46.65	-44.83	-43.46	-42.59	0.30996	-46.91	-45.10	-43.74	-42.87
0.39479	-46.87	-45.03	-43.66	-42.78	0.40878	-47.22	-45.40	-44.03	-43.15

0.49544	-47.08	-45.23	-43.85	-42.96	0.50975	-47.52	-45.68	-44.30	-43.42
	0.06 (mol·kg^{-1}) SMP + MA					**0.06 (mol·kg^{-1}) SMP + TA**			
0.10991	-45.83	-44.04	-42.80	-41.93	0.10241	-45.86	-44.07	-42.84	-41.97
0.19548	-46.19	-44.38	-43.14	-42.26	0.20765	-46.38	-44.58	-43.33	-42.46
0.30981	-46.51	-44.68	-43.42	-42.54	0.30358	-46.72	-44.90	-43.65	-42.77
0.40127	-46.72	-44.88	-43.61	-42.72	0.40476	-47.03	-45.20	-43.94	-43.06
0.50693	-46.94	-45.08	-43.81	-42.91	0.50834	-47.33	-45.49	-44.22	-43.33

m_A specifies the molality of malic and tartaric acids in water-soluble solutions with sodium methyl p-hydroxy benzoate: the calculated standard uncertainties *u* are u(m) = 0.02, u(T)=0.001 K, u ($K_{\phi,S}$) = 0.12 × 10^6/(m^3·mol^{-1}·GPa^{-1}).

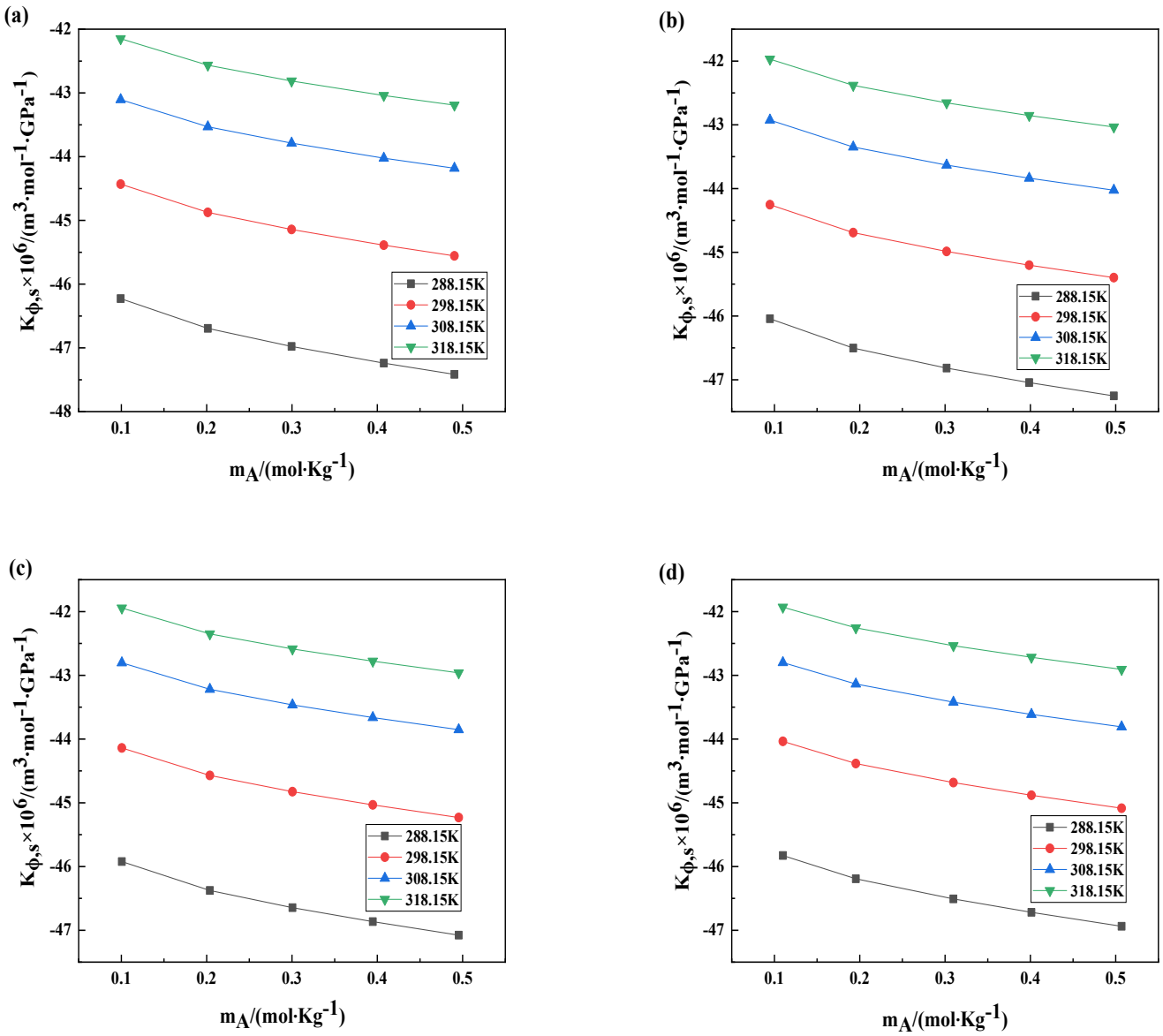

Figure 4.44 Changes of $K_{\phi,s}$, of Malic Acid (MA) in (a) 0.00 SMP; (b) 0.02 SMP; (c) 0.04 SMP; (d) 0.06 SMP for molality of malic acid aqueous solutions.

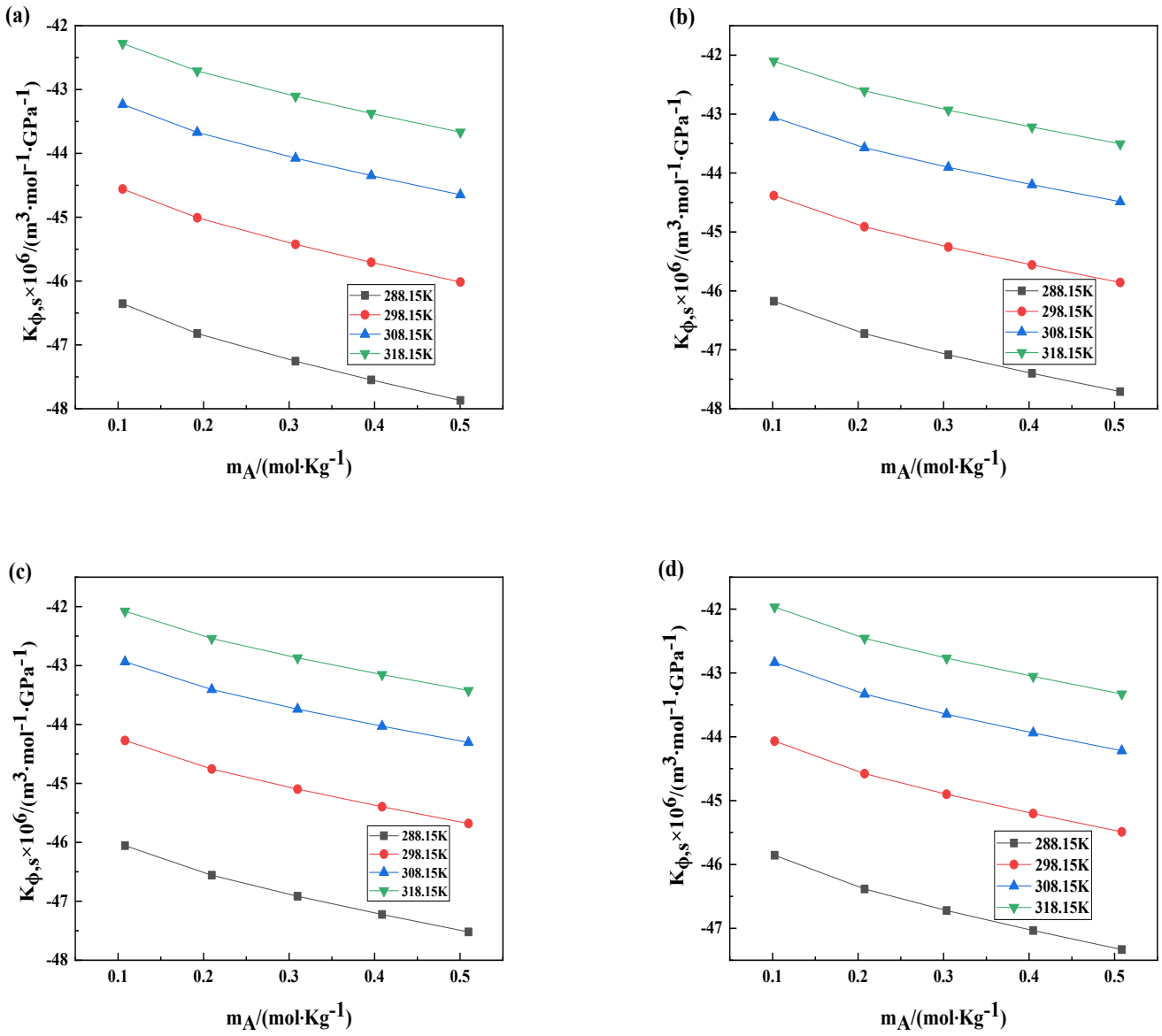

Figure 4.45 Changes of $K_{\phi,s}$, of Tartaric Acid (TA) in (a) 0.00 SMP; (b) 0.02 SMP; (c) 0.04 SMP; (d) 0.06 SMP for molality of tartaric acid aqueous solutions.

4.6.8 Partial molar isentropic compression

The **equation 4.10** given below describes the dependence of partial molar isentropic compressibility on molality. The data of the acoustic virial coefficient (S_K^*) with their associated errors are documented in **Table 4.58**. This coefficient serves as an indicator of the interactions between solutes. As temperatures increased, a corresponding decline into negative values was observed, as illustrated in **Figure 4.46.**

Stronger interactions among water molecules and malic/tartaric acids are observed as the molar mass increases. Based on Kirkwood's theory [44], this intensified interactions with water diminishes electrostriction and liberates H_2O molecules into the bulk solution. The compact nature of electrostricted water results in a higher compressibility than that observed in bulk water. The comparatively low values of S_K^* relative to $K_{\phi,s}$ indicate that interactions among solutes are minimal, and solute-solvent bonds are the primary contributors to the observed behavior of the investigated system. The dependence of negative $K_{\phi,s}^0$ values on temperature and malic or tartaric acids molality reflects stronger attractive forces between SMP and (MA/TA) molecules, causing the surrounding water molecules to become lesser compressible [36,39].

Table 4.58 Evaluated $K^0_{\phi,S}$ and S^*_K, for sodium methyl para-hydroxybenzoate (SMP) in water-soluble solutions with malic acid (MA) and tartaric acid (TA) at various temperatures.

m_B/ (mol·kg^{-1})	$K^0_{\phi,s} \times 10^6$/(m^3·mol^{-1})				$S^*_K \times 10^6$ /(m^3·kg·mol^{-2})			
	288.15K	298.15K	308.15K	318.15K	288.15K	298.15K	308.15K	318.15 K
				Malic Acid				
0.00	-46.02 (±0.09)	-44.24(±0.09)	-42.92(±0.08)	-41.97(±0.08)	-2.97(±0.27)	-2.80(±0.26)	-2.68(±0.25)	-2.60(±0.25)
0.02	-45.86(±0.09)	-44.08(±0.09)	-42.77(±0.09)	-41.82(±0.09)	-2.93(±0.29)	-2.77(±0.27)	-2.66(±0.27)	-2.57(±0.26)
0.04	-45.72(±0.09)	-43.95(±0.09)	-42.63(±0.08)	-41.77(±0.08)	-2.86(±0.27)	-2.70(±0.26)	-2.59(±0.25)	-2.52(±0.25)
0.06	-45.60(±0.08)	-43.83(±0.07)	-42.60(±0.07)	-41.74(±0.07)	-2.74(±0.22)	-2.59(±0.22)	-2.49(±0.21)	-2.41(±0.21)
				Tartaric Acid				
0.00	-46.04(±0.08)	-44.25(±0.08)	-42.93(±0.07)	-41.99(±0.07)	-3.78(±0.24)	-3.63(±0.24)	-3.53(±0.22)	-3.46(±0.22)
0.02	-45.88(±0.09)	-44.10(±0.08)	-42.78(±0.08)	-41.83(±0.08)	-3.72(±0.26)	-3.58(±0.25)	-3.47(±0.24)	-3.40(±0.24)
0.04	-45.74(±0.08)	-43.97(±0.08)	-42.65(±0.07)	-41.79(±0.07)	-3.59(±0.23)	-3.45(±0.22)	-3.35(±0.22)	-3.30(±0.22)
0.06	-45.58(±0.08)	-43.80(±0.08)	-42.57(±0.08)	-41.71(±0.08)	-3.57(±0.25)	-3.44(±0.24)	-3.35(±0.24)	-3.29(±0.23)

m_B signifies the molality of sodium methyl p-hydroxy benzoate solution: the calculated standard uncertainties *u* are u(m) = 0.01, u(T)=0.001 K, u($K^0_{\phi,S}$) = 0.31 × 10^6/(m^3·mol^{-1}·GPa^{-1}), u(S^*_K)= ±0.17×10^6/(kg·m^3·kg·mol^{-2}·GPa^{-1}).

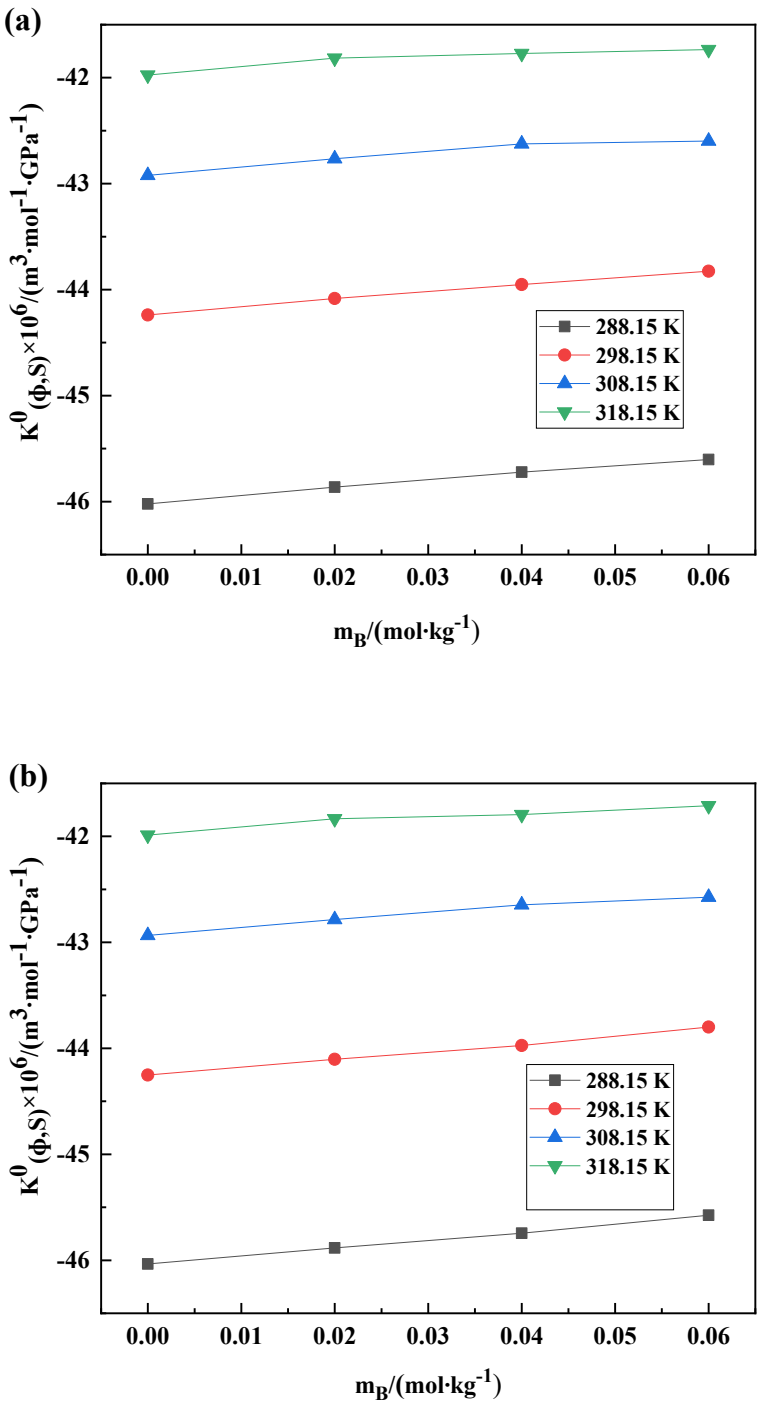

Figure 4.46 Plots representing $K^0_{\emptyset,S}$ for (a) malic acid and (b) tartaric acid in water-soluble sodium methyl p-hydroxybenzoate solution at varying temperatures.

4.6.9 Transfer of Partial molar isentropic compressions

The **equation 4.11** was utilized to examine the transfer of malic and tartaric acids from water to sodium methyl p-hydroxybenzoate solutions. **Table 4.59** details the computed $\Delta K_{\phi,S}^{0}$ parameter, highlighting the transition behavior of malic and tartaric acids from water-soluble solutions to infinitely diluted SMP mixtures. The positive values recorded with the incorporation of SMP and (MA/TA) imply that the solution becomes increasingly structured and less prone to compression. This emphasizes the significant contribution of interactions to the system's overall behavior.

The co-sphere overlap hypothesis clarifies this behavior by emphasizing that interaction within solutes and solvents can modify the solution's volume [51]. This theory explains that positive data reflect the relocation of water molecules from hydrophilic groups. An upward trend in positive values of $\Delta K_{\phi,S}^{0}$ is evident with the progressive enhancement of SMP concentration levels exhibits a stronger solute structure formation and more pronounced solute-solvent interactions in this investigation [46,48].

Table 4.59 Values of transfer parameter, $\Delta K^{0}_{\phi,S}$, of sodium methyl para-hydroxy benzoate (SMP) in water-soluble solutions with malic acid (MA) and tartaric acid (TA).

m_B/ (mol·kg^{-1})	$\Delta K^{0}_{\phi,S} \times 10^{6}$/(m^{3}·mol^{-1}·GPa^{-1})			
	288.15K	298.15K	308.15K	318.15K
		Malic Acid		
0.02	0.16	0.16	0.16	0.16
0.04	0.30	0.29	0.30	0.20
0.06	0.42	0.41	0.32	0.24
		Tartaric Acid		
0.02	0.15	0.15	0.15	0.15
0.04	0.29	0.28	0.29	0.19
0.06	0.46	0.45	0.36	0.28

m_B implies the molality of sodium methyl p-hydroxy benzoate solution: the calculated standard uncertainties *u* are u(m) = 0.01, u(T)=0.001 K, u($\Delta K^{0}_{\phi,S}$) = 0.02×10^{6}/(m^{3}·mol^{-1}·GPa^{-1}).

4.6.10 Interaction coefficients

These coefficients of interaction were obtained by substituting the derived values into **equations 4.12** and **4.13**. Values for the volume ($V_{AB,}$ V_{ABB}) and isentropic compressibility ($K_{AB,}$ K_{ABB}) are provided in **Table 4.60**. The splitting phenomena observed during solute interactions, originally reported by McMillian-Mayer [49] and later validated by Friedman and Krishnan [51], arise from non-covalent interactions. This phenomenon occurs when hydration co-spheres overlap, leading to the expulsion of water molecules into the surrounding solution [26,37]. The pairwise interactions for V_{AB} and K_{AB} have consistently shown positive values at all examined temperatures for malic and tartaric acids. This observation indicates sustainable and advantageous interactions inside the components, emphasizing the importance of their molecular behavior in this study. The results of this study indicate that pair-wise interactions within the liquid system (SMP + Water + MA/TA) are more influential than the triplet interactions.

Table 4.60 Calculated coefficients of interaction for (MA/TA) in water-soluble SMP solutions at numerous temperatures.

T/K	V_{AB} × 10^6/(m^3·mol^{-2}· kg)	V_{ABB} × 10^6/(m^3·mol^{-3}·kg^2)	K_{AB}×10^6 /(m^3·mol^{-2}· kg·GPa^{-1})	K_{ABB}×10^6 /(m^3·mol^{-3}·kg^2·GPa^{-1})
		Malic Acid		
288.15	20.93	-20.41	3.85	-0.99
298.15	16.71	-15.71	3.69	-0.69
308.15	16.98	-15.30	3.93	-3.44
318.15	17.14	-15.77	3.00	-2.82
		Tartaric Acid		
288.15	22.78	7.02	3.64	0.52
298.15	23.51	4.45	3.50	0.75
308.15	24.09	2.81	3.74	-2.04
318.15	25.93	-1.10	2.80	-1.40

Standard uncertainties are u(T)=0.001 K.

References

1. K. Granados and J. Gracia-Fadrique, A. Amigo, R. Bravo, J. Chem. Eng. Data 51, 1356–1360 (2006).
2. F. Suárez and C. M. Romero, J. Chem. Eng. Data 56, 1778-1786 (2011).
3. S.H. Ganatra, V.R. Shaikh, P.A. Tomar and K.J. Patil, J. Mol. Liq. 304, 112658 (2020).
4. J. Grindley, C.R. XCVII Bury, J. Chem. Soc. 679-685 (1929).
5. A. Bald and Z. Kinart, J. Solution Chem. 40, 1-16 (2011).
6. B. R. McRae, B. A. Patterson, M. L. Origlia-Luster, E. C. Sorenson and E. M. Woolley, J. Chem. Thermodyn. 35, 301-329 (2003).
7. A. Mehrdad, H. Shekaari and N. Noorani, Fluid Ph. Equilib. 440, 77-86 (2017).
8. M.A. Raza, P.D. Hallett, X. Liu, M. He and W. Afzal, J. Chem. Eng. Data 64, 5049-5056 (2019).
9. A. Thakur, K.C. Juglan, H. Kumar and K. Kaur, J. Mol. Liq. 288, 111014 (2019).
10. T.S. Banipal, H. Singh, P.K. Banipal and V. Singh, Thermochim. Acta 553, 31–39 (2013).
11. S. Raheem, A. Kumar, G.M. Peerzada and M.A. Rizvi, J. Mol. Liq. 390, 122941 (2023).
12. S.K. Sharma and A. Thakur, J. Mol. Liq. 322, 114527 (2021).
13. N. Chakraborty, K.C. Juglan, H. Kumar and M. Singla, J. Chem. Eng. Data 67, 2292–2306 (2022).
14. S. Shamil, G.G. Birch, M. Mathlouthi and M.N. Clifford, Chem. Senses 12, 397–409 (1987).
15. C. Zhao, G. Liu, Q. Tan, M. Gao, G. Chen, X. Huang, X. Xu, L. Li, J. Wang and Y. Zhang, J. Adv. Res. 44, 53–70 (2023).
16. L.R. Pratt and A. Pohorille, Chem. Rev. 102, 2671–2692 (2002).
17. M.T. Zafarani-Moattar and H. Shekaari, J. Chem. Thermodyn. 37, 1029–1035 (2005).
18. R.C. Thakur, R. Sharma, A. Kumar, S. Kumar and M.L. Parmar, Orient. J. Chem. 30, 2037–2041 (2014).
19. N. Chakraborty, H. Kumar, K. Kaur and K.C. Juglan, J. Chem. Thermodyn. 126, 137–146 (2018).
20. Z. Yan, J. Wang, H. Zheng and D. Liu, J. Solution Chem. 27, 473–483 (1998).
21. K. Kaur, K.C. Juglan and H. Kumar, J. Mol. Liq. 268, 700–706 (2018).
22. M. Lamba, N. Chakraborty, K.C. Juglan, R. Sharma and M. Singla, J. Chem. Eng. Data 69, 171–184 (2024).
23. F. Shahidi, P.G. Farrell and J.T. Edward, J. Solution Chem. 5, 807–816 (1976).

24. A. Zendehbad, M. Bagheri, M. Mokhtarpour, H. Shekaari and M.T. Zafarani-Moattar, J. Chem. Eng. Data 69, 2528–2545 (2024).
25. P. Meena and N. Kishore, J. Mol. Liq. 340, 117166 (2021).
26. R. Rani, A. Kumar, T. Sharma, B. Saini and R.K. Bamezai, Acta Chim. Slov. 63, 589-601 (2016).
27. P. Kaur, K.C. Juglan, H. Kumar and M. Singla, Braz. J. Chem. Eng. 40, 1213–1226 (2023).
28. S. Devi, M. Kumar, N. Sawhney, U. Syal, A.K. Sharma and M. Sharma, J. Chem. Thermodyn. 154, 106321 (2021).
29. N.G. Tsierkezos and I.E. Molinou, J. Chem. Eng. Data 43, 989–993 (1998).
30. A. Apelblat and E. Manzurola, J. Chem. Thermodyn. 33, 581–595 (2001).
31. L.G. Hepler, Can. J. Chem. 47, 4613–4617 (1969).
32. B. Ghosh, A. Sinha, N. Roy, B. Rajbanshi, M. Mondal, D. Roy, A. Das, N.N. Ghosh, V.K. Dakua and M.N. Roy, Fluid Ph. Equilib. 557, 113415 (2022).
33. K.C. Juglan and H. Kumar, Results Chem. 2, 100049 (2020).
34. N. Chakraborty, K.C. Juglan and H. Kumar, J. Chem. Eng. Data 66, 2391–2400 (2021).
35. M.S. Raman, M. Kesavan, K. Senthilkumar and V. Ponnuswamy, J. Mol. Liq. 202, 115–124 (2015).
36. H. Kumar and I. Behal, J. Chem. Thermodyn. 99, 16–29 (2016).
37. H.S. Frank and M.W. Evans, J. Chem. Phys. 13, 507–532 (1945).
38. N. Chakraborty, K.C. Juglan and H. Kumar, J. Chem. Thermodyn. 163, 106584 (2021).
39. N. Chakraborty, K. Kaur, K.C. Juglan and H. Kumar, J. Chem. Eng. Data 65, 1435–1446 (2020).
40. M.S. Raman, V. Ponnuswamy, P. Kolandaivel and K. Perumal, J. Mol. Liq. 142, 10–16 (2008).
41. S. Panda, R.L. Gardas and N. Deenadayalu, J. Mol. Liq. 289, 1110 (2019).
42. V. Ramkumar and R.L. Gardas, J. Chem. Eng. Data 64, 4844–4855 (2019).
43. J. Wang, D. Zhang, Q. Chu and J. Ye, Chin. J. Chem. 28, 313–319 (2010).
44. J.G. Kirkwood, Chem. Rev. 24, 233–251 (1939).
45. H. Kumar and I. Behal, J. Mol. Liq. 219, 756–764 (2016).
46. R. Sadeghi and F. Ziamajidi, J. Chem. Eng. Data 52, 1037–1044 (2007).
47. K. Kaur, K.C. Juglan and H. Kumar, J. Chem. Thermodyn. 127, 8–16 (2018).
48. A. Salabat, L. Shamshiri and F. Sahrakar, J. Mol. Liq. 118, 67–70 (2005).
49. W.G. McMillan Jr and J.E. Mayer, J. Chem. Phys. 13, 276–305 (1945).
50. F. Franks, M. Pedley and D.S. Reid, J. Chem. Soc., Faraday Trans. 72, 359–367 (1976).

51. C. V Krishnan and H.L. Friedman, J. Solution Chem. 2, 37–51 (1973).
52. E.L. Ratkova, D.S. Palmer and M. V Fedorov, Chem. Rev. 115, 6312–6356 (2015).
53. E. Manzurola and A. Apelblat, J. Chem. Thermodyn. 17, 579–584 (1985).
54. S.J. Kharat, Int. J. Thermophys. 31, 585–594 (2010).
55. M. Castaldi, G. D'Errico, L. Paduano and V. Vitagliano, J. Chem. Eng. Data 44, 672–677 (1999).
56. G. Ding, L. Tam and C. Wu, Int. J. Hydrogen Energy 86, 1036–1050 (2024).
57. P.V. Tekade, B.U. Tale, S.D. Bajaj and N. Authankar, Russ. J. Phys. Chem. 92, 2488–2496 (2018).
58. S. Mondal, S.S. Dhondge, L.J. Paliwal, V.M. Tangde and S.P. Jengathe, J. Chem. Thermodyn. 90, 147–157 (2015).
59. Q. Majid, Richu, H. Singh, A. Bandral and A. Kumar, J. Chem. Eng. Data 67, 2974–2985 (2022).
60. R. Li, E. Wang, L. Chai, X. Wang, Y. Wang, K. Ma and J. Zhang, J. Mol. Liq. 408, 125351 (2024).
61. R. Gaba, A. Pal, D. Sharma, H. Kumar and A. Kumar, J. Mol. Liq. 279, 711–718 (2019).
62. A.K. Gill, N. Chakraborty and K.C. Juglan, Chem. Phys. Imp. 10, 100843 (2025).
63. P. Kaur, N. Chakraborty, K.C. Juglan, H. Kumar and M. Singla, J. Mol. Liq. 339, 116810 (2021).
64. K. Bhakri, N. Chakraborty, K.C. Juglan, H. Kumar and R. Sharma, J. Therm. Anal. Calorim. 148, 7185–7205 (2023).
65. M. Lamba, N. Chakraborty and K.C. Juglan, J. Chem. Eng. Data 70, 244–260 (2025).
66. H. Kumar and I. Behal, J. Chem. Eng. Data 61, 3740–3751 (2016).
67. V. Patel, A. Jain and S.P. Zodape, J. Chem. Eng. Data 70, 115–128 (2025).
68. M.J. Iqbal and M.A. Chaudhry, J. Chem. Thermodyn. 42, 951–956 (2010).
69. G.A. Jeffrey, Acc. Chem. Res. 2, 344–352 (1969).
70. P. Kaur, N. Chakraborty, H. Kumar, M. Singla and K.C. Juglan, J. Solution Chem. 51, 1268–1291 (2022).
71. H. Kaur, N. Chakraborty, K.C. Juglan and A. Upmanyu, J. Mol. Liq. 392, 123403 (2023).
72. A.K. Mishra and J.C. Ahluwalia, J. Phys. Chem. 88, 86–92 (1984).
73. A. Ghosh and K.S. Schweizer, 53, 4366–4380 (2020).
74. K. Dhal, S. Singh and M. Talukdar, J. Mol. Liq. 368, 120761 (2022).
75. D. Chawla, N. Chakraborty, K.C. Juglan and H. Kumar, Chem. Pap. 75, 1497–1506 (2021).
76. H. Kaur, N. Chakraborty and K.C. Juglan, J. Chem. Eng. Data 69, 2461–2474 (2024).

77. N. Chakraborty, K.C. Juglan and H. Kumar, Braz. J. Chem. Eng. 39, 869–884 (2022).
78. T.S. Banipal, D. Kaur, P.K. Banipal and G. Singh, J. Chem. Thermodyn. 39, 371–384 (2007).
79. A. Ali, A.K. Nain and M. Kamil, Thermochim. Acta 274, 209–221(1996).
80. M. Dhiman, K. Singh, J. Kaushal and A. Upmanyu, D.P. Singh, Acta Acust. 105, 743–752 (2019).
81. R. Sadeghi and A. Gholamireza, J. Chem. Thermodyn. 43, 200–215 (2011).
82. I. Nadeem, F. Yasmeen, M. Sohail, A. Yaseen Khan and M. Nadeem Asghar, Chem. Phys. 580, 112198 (2024).
83. H. Kitano, M. Imai, K. Sudo and M. Ide, J. Phys. Chem. B 106, 11391–11396 (2002).
84. Ankita and A.K. Nain, J. Mol. Liq. 298, 112006 (2020).
85. N. Chakraborty, K.C. Juglan and H. Kumar, J. Mol. Liq. 332, 115869 (2021).
86. N. Ammari, H. Shekaari, B. Golmohammadi, F. Ghaffari and M.T. Zafarani-Moattar, Sci. Rep. 15, 13867 (2025).

Section IV

Problem 7

4.7 Title: "Thermodynamic Analysis of Tartaric and Lactobionic Acids with Aqueous Potassium Benzoate Mixtures through Volumetric and Acoustic Methods"

In this section, density and sound speed experiments were performed for tartaric and lactobionic acids in potassium benzoate solutions of (0.000-0.035) mol·kg^{-1}.

4.7.1 Density and sound velocity

Volumetrical and acoustical analysis were performed by means of experimentally measured densities and sound velocities for tartaric and lactobionic acids in potassium benzoate at four concentrations (0.000-0.035) mol·kg^{-1} over numerous temperatures. The findings summarized in **Table 4.61** specify that at a constant PB concentration, an increase in organic acids molalities leads to a rise in solution density, whereas a slight decrease in density is observed as the temperature escalates. An increase in potassium benzoate concentration leads to a higher solution density which is primarily due to the elevated molar mass. This trend also reflects intensified interactions amongst solute and solvent molecules.

Sound velocity data serve as valuable indicators of the nature of interactions among ions, solutes and solvents within the system [1,2]. As outlined in **Table 4.61**, at a fixed concentration of PB and a pressure of 0.1 MPa, ultrasonic velocity tends to rise with increasing molality of tartaric or lactobionic acids. The detected enhancement in ultrasonic speed with solute molality is indicative of the development of complex hydrogen-bonded structures involving solute and solvent components. With a shift from TA to LBA, the molar mass rises, leading to the break-down of existing PB-water H_2 bonds and the rise of stronger interactions between PB and the tartaric or lactobionic acids [3-6].

Table 4.61 Measured data of densities 'ρ' and sound velocity 'c' were investigated for potassium benzoate in tartaric and lactobionic acids at several temperatures.

m_A/ (mol·kg^{-1})	$\rho \times 10^{-3}$/(kg·m^{-3})				c/(m·s^{-1})			
	288.15K	298.15K	308.15K	318.15K	288.15K	298.15K	308.15K	318.15K
0.000 (mol·kg^{-1}) Potassium Benzoate + Tartaric Acid								
0.00000	0.99926	0.99705	0.99404	0.99036	1466.59	1495.85	1519.14	1536.02
0.10542	1.00630	1.00406	1.00103	0.99734	1470.49	1499.64	1522.75	1540.24
0.19266	1.01200	1.00975	1.00671	1.00300	1474.07	1502.82	1525.63	1544.08
0.30748	1.01935	1.01708	1.01402	1.01030	1478.83	1506.93	1529.85	1547.96
0.39615	1.02491	1.02262	1.01955	1.01581	1482.34	1510.28	1532.46	1551.72
0.50027	1.03131	1.02900	1.02590	1.02215	1485.92	1514.06	1536.17	1555.27
0.015 (mol·kg^{-1}) Potassium Benzoate + Tartaric Acid								
0.00000	1.00019	0.99810	0.99502	0.99113	1469.07	1498.71	1521.53	1537.98
0.10836	1.00741	1.00529	1.00218	0.99826	1474.42	1503.25	1526.34	1542.65
0.20542	1.01372	1.01158	1.00843	1.00449	1479.73	1508.37	1531.74	1547.36
0.30874	1.02030	1.01812	1.01493	1.01096	1484.54	1514.02	1536.29	1552.09
0.40208	1.02612	1.02389	1.02067	1.01667	1489.11	1519.19	1541.63	1557.38
0.50875	1.03261	1.03033	1.02707	1.02305	1494.61	1524.56	1547.05	1563.11
0.025 (mol·kg^{-1}) Potassium Benzoate + Tartaric Acid								
0.00000	1.00061	0.99851	0.99543	0.99153	1469.80	1499.30	1522.01	1538.39
0.10843	1.00780	1.00566	1.00255	0.99863	1475.82	1504.84	1527.01	1543.64

0.20987	1.01434	1.01217	1.00904	1.00509	1480.62	1509.53	1532.49	1548.78
0.31898	1.02120	1.01899	1.01583	1.01186	1486.04	1515.17	1537.51	1553.24
0.41489	1.02707	1.02482	1.02162	1.01764	1491.36	1521.03	1542.44	1558.61
0.51853	1.03325	1.03097	1.02774	1.02373	1496.28	1526.22	1547.07	1563.39
0.035 (mol·kg^{-1}) Potassium Benzoate + Tartaric Acid								
0.00000	1.00109	0.99909	0.99577	0.99186	1470.79	1500.15	1522.76	1539.06
0.10845	1.00824	1.00563	1.00285	0.99893	1476.06	1505.48	1528.84	1544.65
0.20991	1.01474	1.01210	1.00929	1.00535	1481.33	1510.23	1533.47	1549.85
0.31998	1.02159	1.01893	1.01610	1.01214	1487.42	1516.68	1539.69	1554.19
0.41576	1.02737	1.02469	1.02184	1.01787	1492.54	1522.01	1544.95	1559.72
0.51981	1.03350	1.03078	1.02794	1.02395	1497.67	1527.38	1549.26	1565.07
0.000 (mol·kg^{-1}) Potassium Benzoate +Lactobionic Acid								
0.00000	0.99926	0.99705	0.99404	0.99036	1466.59	1495.85	1519.14	1536.02
0.09680	1.01228	1.00972	1.00646	1.00263	1476.80	1505.14	1527.15	1543.14
0.19782	1.02498	1.02206	1.01857	1.01462	1486.43	1513.96	1535.73	1551.29
0.29589	1.03645	1.03321	1.02958	1.02549	1496.61	1523.62	1543.46	1558.33
0.39959	1.04772	1.04413	1.04043	1.03616	1507.35	1533.17	1551.95	1567.01
0.49383	1.05719	1.05332	1.04953	1.04529	1516.39	1542.02	1559.19	1573.72
0.015 (mol·kg^{-1}) Potassium Benzoate + Lactobionic Acid								
0.00000	1.00019	0.99810	0.99502	0.99113	1469.07	1498.71	1521.53	1537.98
0.10543	1.01433	1.01184	1.00839	1.00423	1479.78	1508.45	1530.30	1545.99

0.20332	1.02653	1.02372	1.02001	1.01558	1488.68	1516.09	1537.28	1552.72
0.29568	1.03723	1.03415	1.03010	1.02547	1497.59	1524.53	1544.90	1559.35
0.40215	1.04887	1.04540	1.04105	1.03615	1507.71	1533.39	1552.83	1566.15
0.50137	1.05876	1.05506	1.05059	1.04544	1517.70	1542.84	1561.59	1574.52
0.025 (mol·kg^{-1}) Potassium Benzoate + Lactobionic Acid								
0.00000	1.00061	0.99851	0.99543	0.99153	1469.80	1499.30	1522.01	1538.39
0.10958	1.01523	1.01272	1.00923	1.00503	1481.71	1509.86	1531.31	1546.66
0.20253	1.02675	1.02394	1.02018	1.01573	1489.50	1517.62	1538.49	1553.81
0.30576	1.03867	1.03553	1.03145	1.02680	1498.40	1525.26	1545.57	1560.94
0.40429	1.04929	1.04588	1.04145	1.03655	1508.35	1534.73	1553.38	1568.41
0.50814	1.05962	1.05593	1.05139	1.04622	1518.23	1543.25	1562.97	1575.89
0.035 (mol·kg^{-1}) Potassium Benzoate + Lactobionic Acid								
0.00000	1.00119	0.99908	0.99599	0.99208	1470.79	1500.15	1522.76	1539.06
0.10989	1.01580	1.01327	1.00977	1.00556	1484.86	1512.18	1532.91	1547.74
0.20115	1.02705	1.02423	1.02045	1.01600	1491.93	1519.25	1539.75	1554.38
0.30554	1.03906	1.03591	1.03182	1.02714	1499.66	1526.29	1546.45	1561.66
0.40882	1.05009	1.04668	1.04223	1.03733	1509.48	1535.61	1554.84	1569.82
0.50961	1.06006	1.05627	1.05182	1.04662	1519.35	1544.85	1563.19	1577.97

m_A denotes the molality of organic (TA/LBA) acids in potassium benzoate solution; the standard uncertainties u are $u(m)$ = 0.02, $u(T)$=0.001 K, $u(\rho)$= 0.83 Kg·m^{-3}, $u(c)$= 1.87 m·s^{-1}.

4.7.2 Apparent molar volume

This is an indispensable parameter for evaluating the nature of interactions within TA/LBA and PB combinations. The data of V_ϕ were computed from investigational density outcomes using the formula stated in **equation 4.1**. The V_ϕ for both the organic acids in potassium benzoate (PB) solutions at numerous temperatures are stated in **Table 4.62**. **Figure 4.47** outlines the molecular interactions of tartaric acid (TA) and lactobionic acid (LBA) in aqueous PB solutions. **Figure 4.48** presents comparative 3D plots illustrating the changes in V_ϕ, where tartaric acid is represented by green spheres and lactobionic acid by pink cubes. The trend of increasing and positive V_ϕ is evident from the calculated values under these variable conditions. Data from **Table 4.62** demonstrate that with rising concentrations of potassium benzoate, the V_ϕ also rises in response to both temperature and organic acid molality. This trend reflects enhanced solute-solvent binding within the TA/LBA system. Positive V_ϕ values suggest effective binding between solute and solvent, which becomes more intense when shifting from TA to LBA at several temperatures. This effect becomes more pronounced because LBA has a larger molecular structure and multiple hydroxyl groups as compared to tartaric acid. As the concentration of PB escalates, it weakens the tight binding of water molecules (electrostriction) [7,8]. The affinity/hydrophilic nature, dipole-dipole interactions of tartaric or lactobionic acids for aqueous solutions facilitate the creation of robust hydrogen bonds with water and potassium benzoate, which promotes the enhanced structural arrangement and results in an overall expansion in volume [9-11].

Table 4.62 Apparent molar volumes 'V_ϕ' were obtained in the liquid system of potassium benzoate in water-based solutions with tartaric acid (TA) and lactobionic acid (LBA).

m_A/ (mol·kg^{-1})	$V_\phi \times 10^6$/(m^3·mol^{-1})				m_A/ (mol·kg^{-1})	$V_\phi \times 10^6$/(m^3·mol^{-1})			
	288.15K	298.15K	308.15K	318.15K		288.15K	298.15K	308.15K	318.15K
0.000 (mol·kg^{-1}) Potassium Benzoate + Tartaric Acid					**0.000 (mol·kg^{-1}) Potassium Benzoate + Lactobionic Acid**				
0.10542	82.75	83.01	83.25	83.44	0.09680	220.98	224.81	227.72	229.66
0.19266	82.91	83.16	83.39	83.57	0.19782	222.62	226.51	229.31	231.09
0.30748	83.08	83.34	83.55	83.76	0.29589	224.35	228.15	230.65	232.47
0.39615	83.21	83.47	83.68	83.89	0.39959	226.13	229.97	232.11	234.11
0.50027	83.37	83.61	83.84	84.06	0.49383	227.87	231.66	233.67	235.32
0.015 (mol·kg^{-1}) Potassium Benzoate + Tartaric Acid					**0.015 (mol·kg^{-1}) Potassium Benzoate + Lactobionic Acid**				
0.10836	82.89	83.18	83.52	83.85	0.10543	221.03	225.05	228.94	231.95
0.20542	83.08	83.39	83.78	84.11	0.19332	222.85	226.69	230.16	233.35
0.30874	83.27	83.61	84.03	84.35	0.29568	224.69	228.36	232.09	235.13
0.40208	83.43	83.82	84.24	84.58	0.39215	226.22	230.01	233.68	236.78
0.50875	83.65	84.06	84.49	84.83	0.49137	228.09	231.72	235.01	238.19
0.025 (mol·kg^{-1}) Potassium Benzoate + Tartaric Acid					**0.025 (mol·kg^{-1}) Potassium Benzoate + Lactobionic Acid**				
0.10843	83.21	83.54	83.91	84.17	0.10958	221.56	225.54	229.62	232.86
0.20987	83.49	83.87	84.18	84.49	0.20253	223.34	227.11	230.87	234.11
0.31898	83.79	84.19	84.51	84.81	0.30576	225.18	228.89	232.63	235.63
0.41489	84.08	84.48	84.83	85.12	0.40429	226.79	230.38	234.24	237.32

0.51853	84.38	84.77	85.13	85.44	0.50814	228.61	232.15	235.56	238.72
0.035 (mol·kg^{-1}) Potassium Benzoate + Tartaric Acid					**0.035 (mol·kg^{-1}) Potassium Benzoate + Lactobionic Acid**				
0.10845	83.56	83.87	84.25	84.49	0.10989	222.04	226.09	230.17	233.39
0.20991	83.91	84.22	84.61	84.82	0.20115	223.85	227.65	231.48	234.65
0.31998	84.28	84.57	84.93	85.17	0.30554	225.69	229.41	233.15	236.23
0.41576	84.62	84.92	85.26	85.49	0.40882	227.44	230.97	234.81	237.84
0.51981	84.95	85.28	85.55	85.79	0.50961	229.15	232.86	236.07	239.27

m_A infers the molality of the organic acids in potassium benzoate: the calculated standard uncertainties u are $u(m)$ = 0.02, $u(T)$=0.001 K, $u\ (V_\phi)$ = (0.08-0.50) × 10^6/(m^3·mol^{-1}).

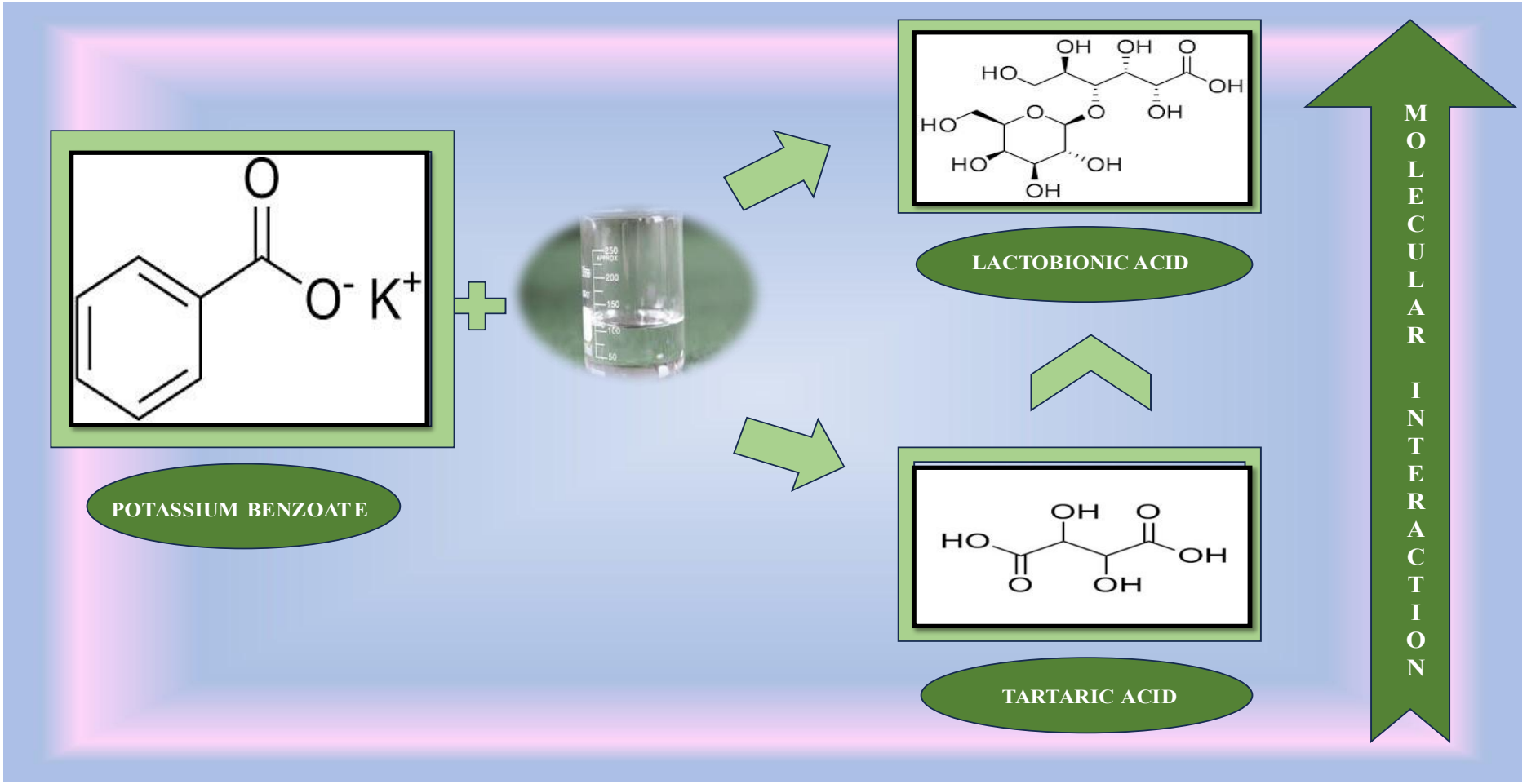

Figure 4.47. Tartaric Acid/ Lactobionic Acid and Potassium Benzoate interactions.

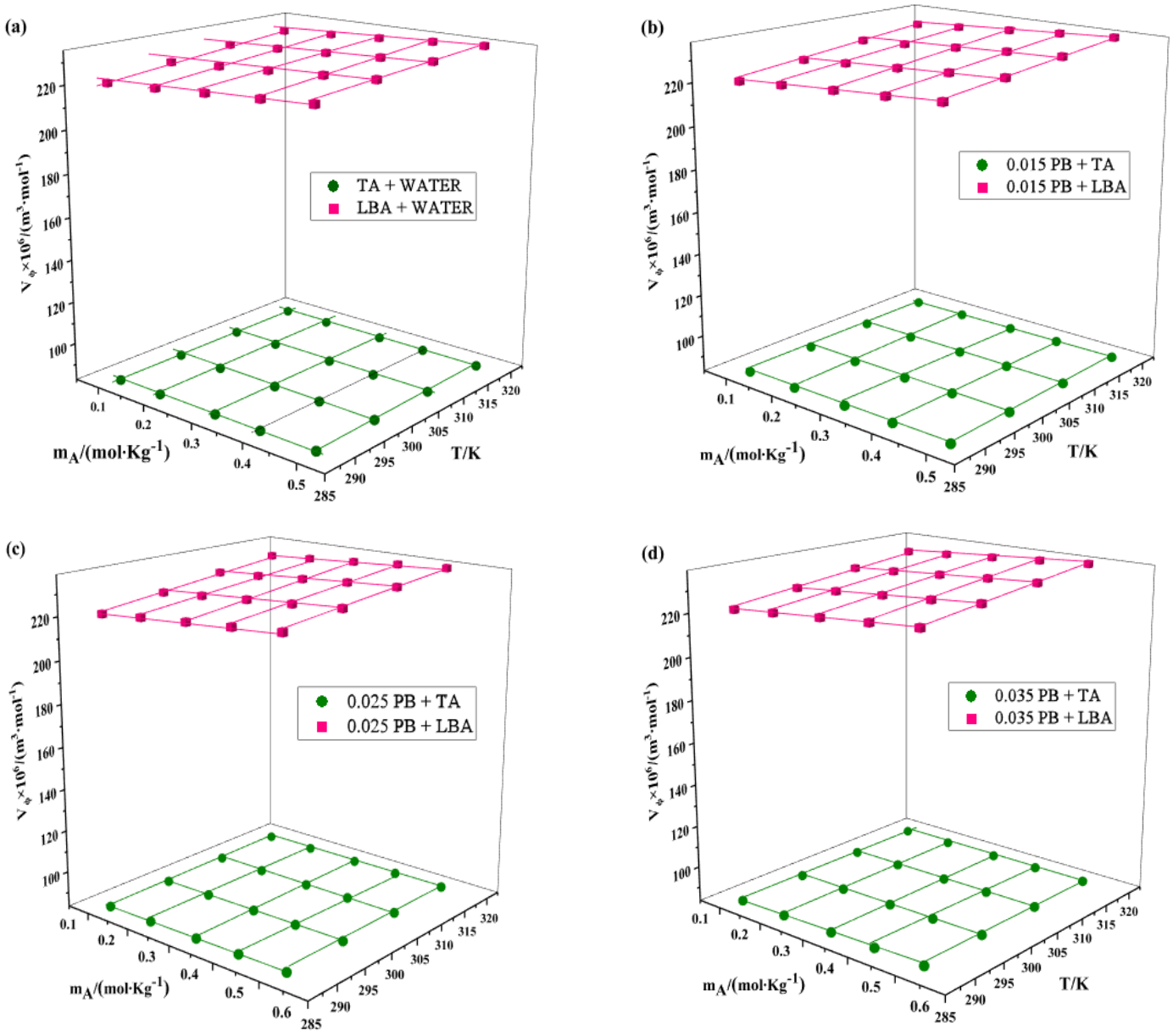

Figure 4.48 Comparative three-dimensional plots demonstrate the variations in $V_\emptyset$ of (a) 0.000 PB; (b) 0.015 PB; (c) 0.025 PB;(d) 0.035 PB for molalities of tartaric acid (green; sphere) and lactobionic acid (pink; cube) at several temperatures.

4.7.3 Apparent molar isentropic compression

The Laplace formula outlined in **equation 4.8** [12] was applied to the ultrasonic velocity data gathered under a range of temperature conditions for the evaluation of compressibility κ_s. The $K_{\phi,S}$ for TA and LBA in potassium benzoate aqueous solutions was determined using **equation 4.9**. **Table 4.63** highlights that the compressibility parameter $K_{\phi,S}$ remains negative under all tested conditions which suggests compressive interaction effects. The magnitude of this negative behavior is enhanced with higher molalities of tartaric or lactobionic acids but shows a slight reduction at elevated temperatures. Moreover, as the PB concentration increases, the values shift toward less negativity, a pattern consistent with the linear trends as illustrated in **Figures 4.49** and **4.50**.

Tartaric and lactobionic acids exhibit zwitterionic character containing both positive and negative functional groups within a single molecule. The observed structural compactness of tartaric and lactobionic acid in PB aqueous media arises from enhanced hydrogen bonding which in turn lowers compressibility [13,14]. Dipole-dipole bonds within the hydroxyl groups of the organic acids and water molecules thereby reinforcing solute-solvent bonds. Water molecules near the ionic sites of the acids demonstrate diminished compressibility which causes a restructuring of the H_2O molecules around the solutes. This structural feature enhances their interaction with water which allows for robust hydrogen bonding [15,16]. As a result, hydrated aggregates form around the solute molecules, promoting stronger interactions which are facilitated by the polar nature of water [17].

Table 4.63 Data of '$K_{\phi,s}$' for potassium benzoate with tartaric acid (TA) and lactobionic acid (LBA) mixtures at different temperatures.

m_A/ (mol·kg^{-1})	$K_{\phi,s} \times 10^6$/(m^3·mol^{-1}·GPa^{-1})				m_A/ (mol·kg^{-1})	$K_{\phi,s} \times 10^6$/(m^3·mol^{-1}·GPa^{-1})			
	288.15K	298.15K	308.15K	318.15K		288.15K	298.15K	308.15K	318.15K
0.000 (mol·kg^{-1}) Potassium Benzoate + Lactobionic Acid					**0.000 (mol·kg^{-1}) Potassium Benzoate + Tartaric Acid**				
0.09680	-46.62	-44.80	-43.43	-42.47	0.10542	-46.35	-44.56	-43.23	-42.28
0.19782	-47.47	-45.60	-44.19	-43.21	0.19266	-46.82	-45.01	-43.67	-42.71
0.29589	-48.08	-46.17	-44.74	-43.75	0.30748	-47.25	-45.42	-44.07	-43.11
0.39959	-48.64	-46.70	-45.26	-44.25	0.39615	-47.55	-45.71	-44.35	-43.37
0.49383	-49.11	-47.14	-45.67	-44.66	0.50027	-47.87	-46.02	-44.65	-43.67
0.015 (mol·kg^{-1}) Potassium Benzoate + Lactobionic Acid					**0.015 (mol·kg^{-1}) Potassium Benzoate + Tartaric Acid**				
0.10543	-46.53	-44.71	-43.36	-42.48	0.10836	-46.22	-44.43	-43.09	-42.23
0.20332	-47.31	-45.45	-44.06	-43.16	0.20542	-46.72	-44.90	-43.56	-42.69
0.29568	-47.88	-45.98	-44.57	-43.65	0.30874	-47.10	-45.27	-43.91	-43.03
0.40215	-48.46	-46.53	-45.08	-44.15	0.40208	-47.40	-45.56	-44.20	-43.31
0.50137	-48.94	-46.98	-45.52	-44.57	0.50875	-47.73	-45.87	-44.50	-43.61
0.025 (mol·kg^{-1}) Potassium Benzoate + Lactobionic Acid					**0.025 (mol·kg^{-1}) Potassium Benzoate + Tartaric Acid**				
0.10958	-46.59	-44.77	-43.41	-42.43	0.10843	-46.24	-44.44	-43.11	-42.15
0.20253	-47.32	-45.46	-44.07	-43.07	0.20987	-46.75	-44.94	-43.59	-42.62
0.30576	-47.95	-46.05	-44.63	-43.61	0.31898	-47.14	-45.31	-43.96	-42.98
0.40429	-48.48	-46.55	-45.10	-44.06	0.41489	-47.45	-45.61	-44.24	-43.25
0.50814	-48.98	-47.02	-45.56	-44.50	0.51853	-47.76	-45.90	-44.53	-43.53

0.035 (mol·kg^{-1}) Potassium Benzoate + Lactobionic Acid					0.035 (mol·kg^{-1}) Potassium Benzoate + Tartaric Acid				
0.10989	-46.52	-44.69	-43.33	-42.45	0.10845	-46.16	-44.34	-43.03	-42.16
0.20115	-47.23	-45.37	-43.98	-43.08	0.20991	-46.67	-44.83	-43.50	-42.63
0.30554	-47.87	-45.96	-44.55	-43.63	0.31998	-47.06	-45.21	-43.87	-42.99
0.40882	-48.41	-46.48	-45.03	-44.10	0.41576	-47.36	-45.50	-44.15	-43.26
0.50961	-48.90	-46.93	-45.47	-44.51	0.51981	-47.67	-45.79	-44.43	-43.54

m_A signifies the molality of the organic acids (TA/LBA) in water-soluble solutions with potassium benzoate: the standard uncertainties u are $u(m)$ = 0.02, $u(T)$=0.001 K, $u\ (K_{\phi,S})$ = 0.14 × 10^6/(m^3·mol^{-1}·GPa^{-1}).

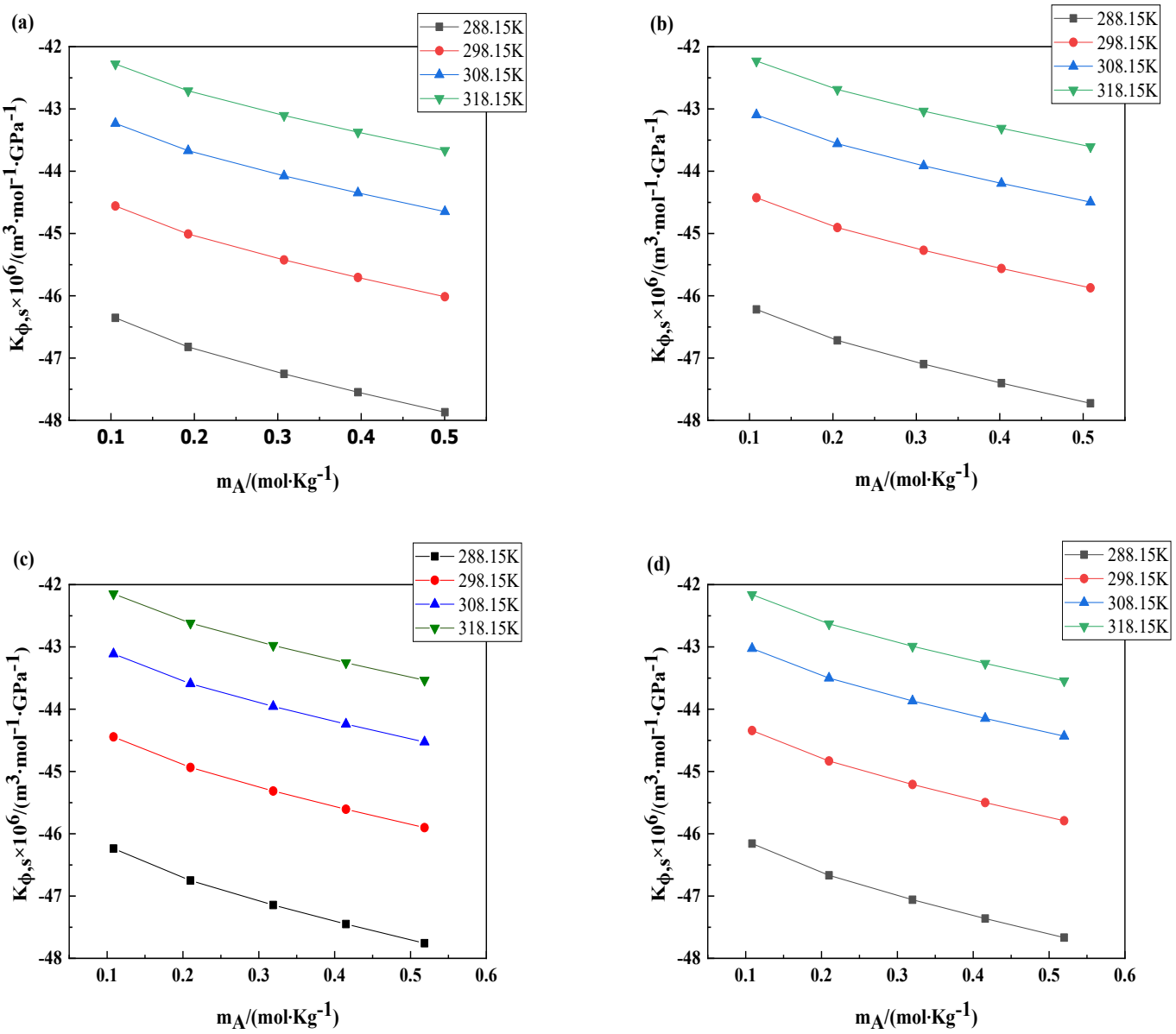

Figure 4.49 Changes of $K_{\phi,s}$, of tartaric acid (TA) in water-soluble potassium benzoate at varying concentrations.

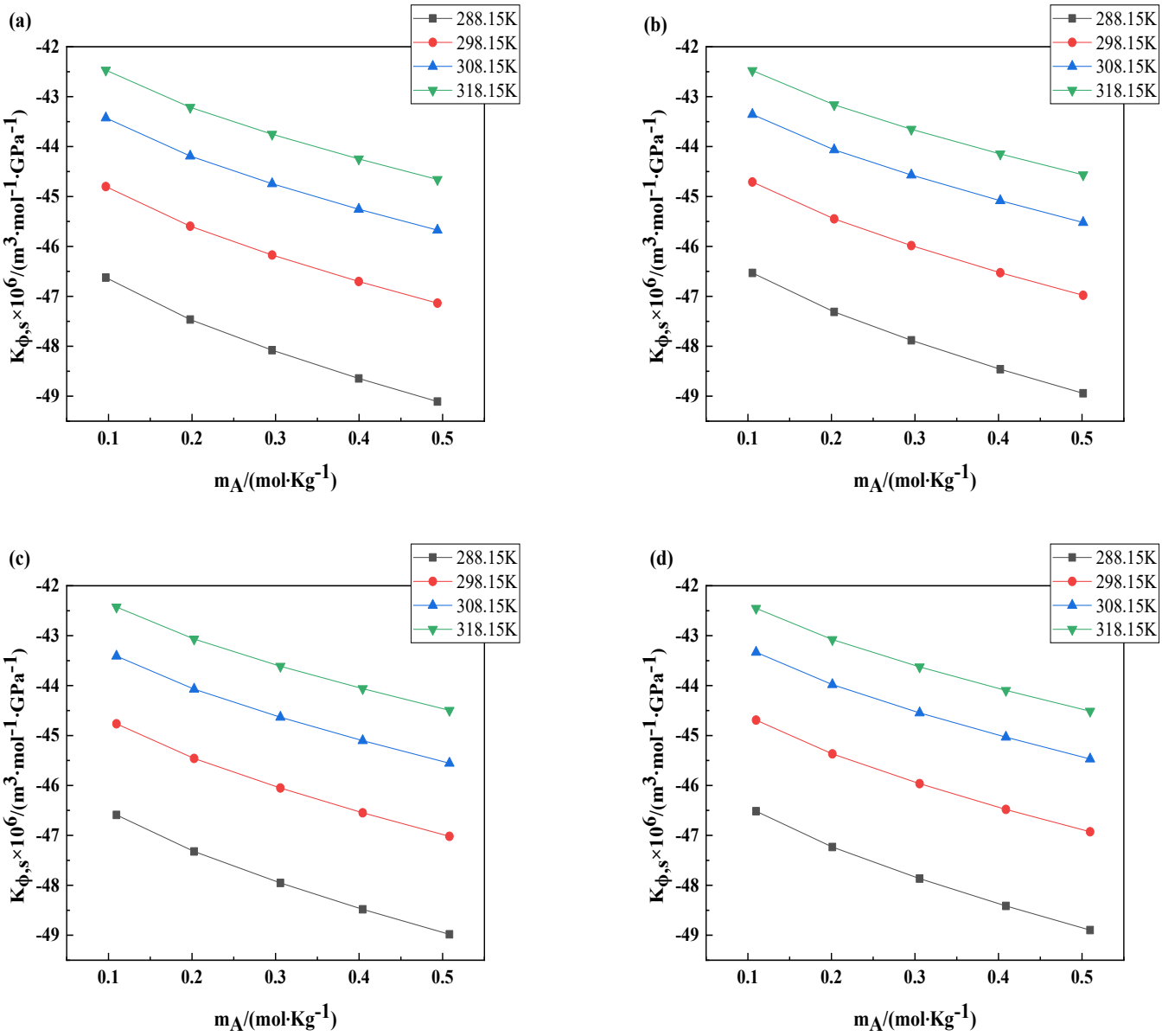

Figure 4.50 Changes of $K_{\phi,s}$, of lactobionic acid (LBA) in water-soluble potassium benzoate at varying concentrations.

4.7.4 Partial molar volumes

The standard mathematical relation stated in **equation 4.2** was employed to evaluate the V_ϕ^0 of the ternary solutions made up of PB and organic acids (tartaric or lactobionic acids). The least squares regression approach was applied to obtain the V_ϕ^0 and S_V^* data which are summarized in **Table 4.64**. At all studied temperatures, V_ϕ^0 values for tartaric or lactobionic acids were positive and showed a consistent increase with rising concentrations of potassium benzoate, all illustrated in the comparative plot (**Figure 4.51**).

When the hydration zones of ions intersect, as outlined in the co-spheres overlap concept, the solution volume increases owing to the additive effect of ion-hydration structures. The increasing V_ϕ^0 values with elevated tartaric or lactobionic acids molalities reveal the predominance of ion-hydrophilic interactions which surpass the effects of hydrophobic effects in these systems [18-20]. The positive and increasing trend in V_ϕ^0 can be attributed to the zwitterionic nature of tartaric and lactobionic acids which enables them to form strong electrostatic and hydrogen-bond interactions with both water and benzoate ions. Throughout the investigated thermal range, potassium benzoate exhibited a consistently positive S_V^* values which point to the occurrence of solute interactions. However, the non-linear or fluctuating pattern in S_V^* suggest that additional molecular interactions or environmental conditions may be influencing the system's behavior.

A clear dominance of solutes and solvent associations is specified by the reduced S_V^* data relative to V_ϕ^0. The co-sphere overlap mechanism suggests that this is due to the expansion effect caused by the intersecting hydration shells which supports the inference that solute-solvent bonds are more influential than solute-solute bonding in the solution [21].

Table 4.64 Values of $'V_{\phi}^{0}'$, and $'S_V^*'$ of potassium benzoate (PB) in water-soluble solutions with tartaric acid (TA) and lactobionic acid (LBA) with their standard errors.

m_B/ (mol·kg^{-1})	$V_{\phi}^{0} \times 10^{6}$/(m^3·mol^{-1})				$S_V^* \times 10^{6}$ /(m^3·kg·mol^{-2})			
	288.15K	298.15K	308.15K	318.15K	288.15K	298.15K	308.15K	318.15 K
Tartaric Acid								
0.000	82.60(±0.01)	82.86(±0.01)	83.10(±0.01)	83.27(±0.01)	1.55(±0.03)	1.52(±0.04)	1.48(±0.02)	1.57(±0.02)
0.015	82.69(±0.01)	82.94(±0.02)	83.27(±0.04)	83.60(±0.03)	1.88(±0.03)	2.20(±0.02)	2.41(±0.04)	2.44(±0.03)
0.025	82.89(±0.01)	83.23(±0.01)	83.57(±0.02)	83.83(±0.01)	2.86(±0.03)	2.99(±0.04)	3.01(±0.06)	3.09(±0.02)
0.035	83.20(±0.01)	83.50(±0.01)	83.93(±0.02)	84.15(±0.01)	3.39(±0.03)	3.42(±0.04)	3.16(±0.07)	3.18(±0.)
Lactobionic Acid								
0.000	219.24(±0.07)	223.11(±0.05)	226.31(±0.09)	228.25(±0.07)	17.36(±0.21)	17.23(±0.15)	14.76(±0.27)	14.40(±0.22)
0.015	219.26(±0.16)	223.30(±0.07)	227.21(±0.23)	230.24(±0.15)	17.64(±0.49)	16.81(±0.20)	15.79(±0.70)	16.05(±0.46)
0.025	219.72(±0.09)	223.76(±0.06)	227.91(±0.15)	231.15(±0.11)	17.56(±0.27)	16.51(±0.19)	15.27(±0.15)	14.95(±0.11)
0.035	220.21(±0.11)	224.26(±0.10)	228.52(±0.12)	231.72(±0.06)	17.67(±0.32)	16.74(±0.28)	15.03(±0.36)	14.85(±0.16)

m_B specifies the molalities of the potassium benzoate solution: calculated standard uncertainties u are $u(m)$ = 0.01, $u(T)$=0.001 K, $u\ (V_{\phi}^{0})$= (0.11-0.45) × 10^6/(m^3·mol^{-1}) and $u\ (S_V^*)$=±1.23 × 10^6/(m^3·kg·mol^{-2}).

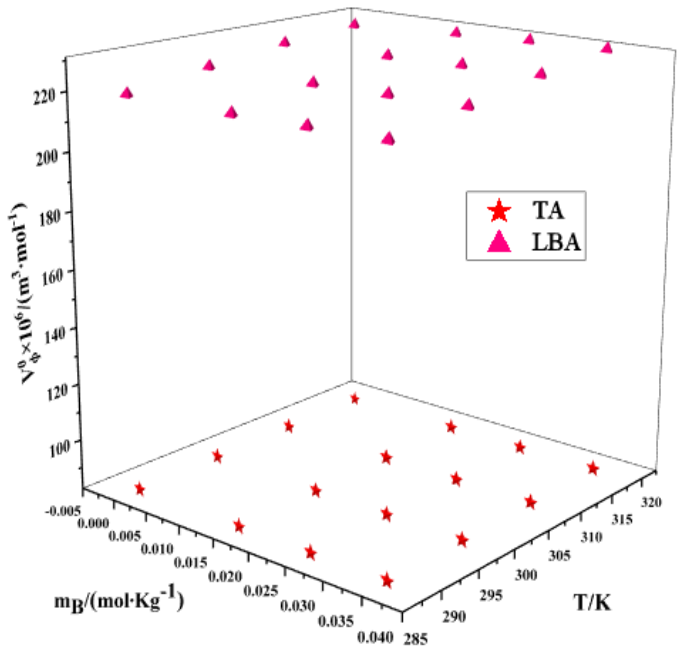

Figure 4.51 The comparative plot presents the changes in $V_{\emptyset}^{0}$, for tartaric acid (red; star) and lactobionic acid (pink; tetrahedron) within a potassium benzoate aqueous solution at several temperatures.

4.7.5 Partial molar isentropic compressions

The dependency of $K_{\phi,S}^{0}$ on solute molality is mathematically illustrated in the **equation 4.10**. The acoustic virial coefficient, which is symbolized by S_K^*, is utilized to assess the nature of interactions among solute particles. Additionally, with a rise in temperature, $K_{\phi,S}^{0}$ values become more negative, indicating stronger interaction effects, which is evident from **Table 4.65** and depicted in **Figure 4.52**.

Stronger hydration and intermolecular forces are observed when tartaric and lactobionic acids with higher molar masses are present in solution. Under Kirkwood's theoretical interpretation, increased interaction with solvent molecules alleviates electrostriction by promoting the displacement of structured water to re-enter the bulk medium. This structured water near solutes exhibits compressibility values higher than those of unbound water [22,23]. The minimal magnitude of S_K^* when compared to $K_{\phi,S}^{0}$ implies weak interactions among the solute species and highlights the dominant influence of solute-solvent associations. This interpretation is consistent with the zwitterionic nature and higher molecular weight of tartaric or lactobionic acids which facilitate structured hydration shells. The trend of more negative $K_{\phi,S}^{0}$ values at higher temperatures and increasing molalities of TA/LBA reflect enhanced molecular attraction, which restricts the mobility and compressibility of adjacent water molecules [14,24,25].

Table 4.65 Evaluated $K^0_{\phi,S}$, and S^*_K, for potassium benzoate (PB) with aqueous tartaric acid (TA) and lactobionic acid (LBA) mixtures at several temperatures.

m_B/ (mol·kg^{-1})	$K^0_{\phi,S} \times 10^6$/(m^3·mol^{-1})				$S^*_K \times 10^6$ /(m^3·kg·mol^{-2})			
	288.15K	298.15K	308.15K	318.15K	288.15K	298.15K	308.15K	318.15 K
				Tartaric Acid				
0.000	-46.04 (±0.08)	-44.25(±0.08)	-42.93(±0.07)	-41.99(±0.07)	-3.78(±0.24)	-3.63(±0.23)	-3.53(±0.22)	-3.46(±0.22)
0.015	-45.89(±0.08)	-44.12(±0.08)	-42.80(±0.07)	-41.94(±0.07)	-3.71(±0.23)	-3.55(±0.23)	-3.44(±0.22)	-3.38(±0.22)
0.025	-45.87(±0.08)	-44.08(±0.08)	-42.75(±0.08)	-41.89(±0.07)	-3.65(±0.23)	-3.50(±0.22)	-3.40(±0.22)	-3.33(±0.22)
0.035	-45.85(±0.08)	-44.04(±0.08)	-42.73(±0.08)	-41.88(±0.07)	-3.61(±0.23)	-3.47(±0.22)	-3.37(±0.22)	-3.31(±0.21)
				Lactobionic Acid				
0.000	-46.15(±0.13)	-44.36(±0.12)	-43.00(±0.11)	-42.05(±0.11)	-6.18(±0.38)	-5.80(±0.37)	-5.59(±0.35)	-5.44(±0.34)
0.015	-46.11(±0.12)	-44.30(±0.11)	-42.98(±0.11)	-42.01(±0.10)	-6.02(±0.35)	-5.66(±0.33)	-5.39(±0.32)	-5.20(±0.31)
0.025	-46.05(±0.11)	-44.26(±0.11)	-42.93(±0.10)	-41.96(±0.10)	-3.59(±0.23)	-3.45(±0.22)	-3.35(±0.22)	-3.30(±0.22)
0.035	-45.98(±0.11)	-44.19(±0.11)	-42.85(±0.10)	-41.91(±0.10)	-5.89(±0.33)	-5.54(±0.31)	-5.28(±0.30)	-5.09(±0.29)

m_B denotes the molalities of potassium benzoate solution: the standard uncertainties u are $u(m)$ = 0.01, $u(T)$=0.001 K, $u(K^0_{\phi,S})$ = 0.27 × 10^6/(m^3·mol^{-1}·GPa^{-1}), $u(S^*_K)$= ±0.19×10^6/(kg·m^3·kg·mol^{-2}·GPa^{-1}).

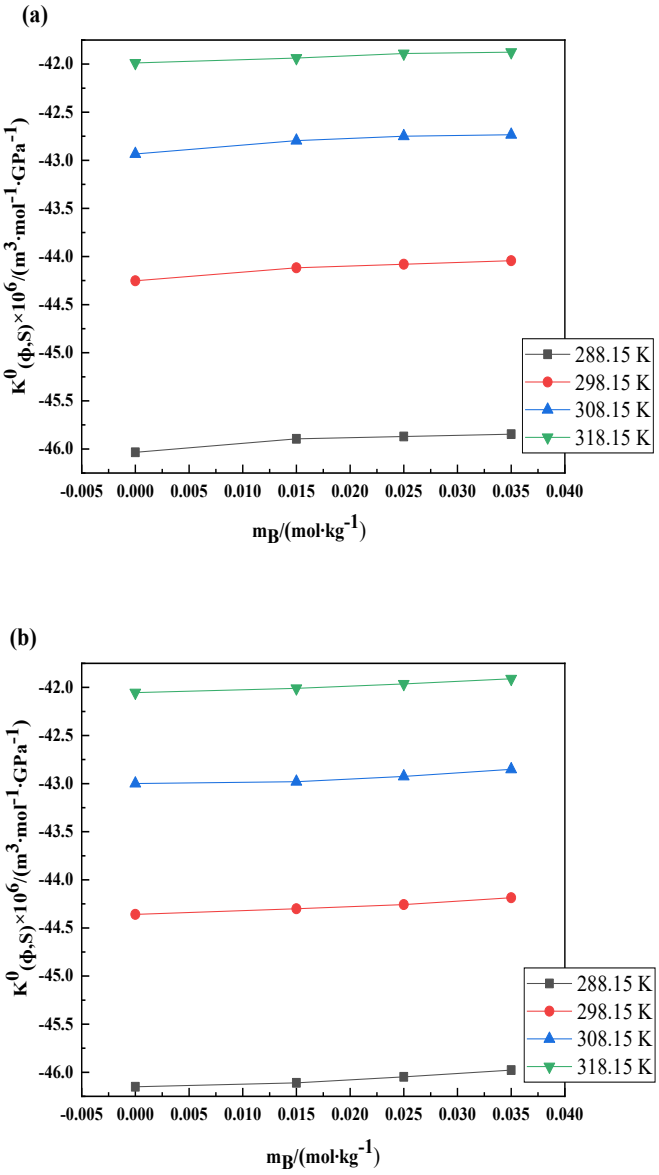

Figure 4.52 Plots of distinctions of $K^0_{\emptyset,S}$ for (a) tartaric acid and (b) lactobionic acid in water-soluble potassium benzoate solution at several temperatures.

4.7.6 Partial molar volume of transfer

In thermodynamic studies, $\Delta_{tr}V_{\emptyset}^{0}$ denotes the volumetric alteration observed during the solute's transition between phases. The expression stated in **equation 4.3** is applied to quantify the volume change as solutes are moved from pure water into the potassium benzoate solution. The data in **Table 4.66** indicate that $\Delta_{tr}V_{\emptyset}^{0}$ for tartaric and lactobionic acids in PB-based aqueous systems remain positive and increase with solvent concentration, although temperature fluctuations affect the consistency of this trend. This thermodynamic parameter serves as a key indicator of the strength of molecular associations between the solvent and solute. This parameter reflects the solute-solvent affinity, offering understanding into the structural interactions that occur in the mixture. The positive $\Delta_{tr}V_{\emptyset}^{0}$ data may result from the solute's tendency to either develop or interrupt the solvent's structural network due to solvophobic effects and interactions occurring within overlapping hydration shells [26-28].

In the ternary liquid systems containing potassium benzoate (PB) and water-soluble organic acids such as tartaric acid (TA) and lactobionic acid (LBA), the stronger molecular interactions arise due to the presence of several charged and polar moieties. The electrolytic nature of PB and TA/LBA is evident from their dissociation patterns in aqueous media. Potassium benzoate dissociates completely in aqueous media to yield potassium (K^{+}) and benzoate ($C_6H_5COO^{-}$) ions, both of which serve as primary charged species. Tartaric acid, being a diprotic acid contains two carboxyl groups that partially ionize into negatively charged carboxylate ($-COO^{-}$) groups and also possesses hydroxyl groups capable of forming strong hydrogen bonds. Lactobionic acid includes one ionizable carboxyl group and multiple hydroxyl groups distributed across its extended polyhydroxy structure which contributes to intense hydrogen bonding and hydration interactions [29,30]. The examined positive values suggest enhanced electrostatic interactions between potassium benzoate and the organic acids studied. According to Pauling's clathrate theory, voids in the water structure may allow the inclusion of other molecules, tartaric and lactobionic acids disrupt the structured hydrogen-bond network of water and form new interaction networks [31,32]. The positive $\Delta_{tr}V_{\emptyset}^{0}$ values recorded in mixtures of potassium benzoate, water, and the acids provide evidence for significant hydrogen bonding, particularly involving hydrophilic and ionic interactions.

Table 4.66 Transfer property of '$\Delta_{tr}V_{\phi}^{0}$' for potassium benzoate (PB) with tartaric acid (TA) and lactobionic acid (LBA) solutions at several temperatures.

m_B/ (mol·kg^{-1})	$\Delta_{tr}V_{\phi}^{0} \times 10^{6}$/(m^3·mol^{-1})			
	288.15K	298.15K	308.15K	318.15K
		Tartaric Acid		
0.015	0.09	0.08	0.18	0.33
0.025	0.29	0.37	0.47	0.56
0.035	0.60	0.63	0.83	0.88
		Lactobionic Acid		
0.015	0.02	0.19	0.90	1.99
0.025	0.48	0.66	1.60	2.90
0.035	0.97	1.15	2.21	3.47

m_B signifies the molalities of the potassium benzoate solution: the calculated standard uncertainties u are $u(m)$ = 0.01, $u(T)$=0.001 K, $u(\Delta_{tr}V_{\phi}^{0})$= ±0.18×10^6/(m^3·mol^{-1}).

4.7.7 Partial molar isentropic compression of transfer

The computation of $\Delta_{tr}K^{0}_{\emptyset,S}$ for solute transfer from water to PB aqueous media was carried out using the mathematical expression from **equation 4.11. Table 4.67** reports the values for tartaric and lactobionic acids transitioning from pure water into infinitely diluted PB solutions. The trend is well supported by the co-sphere overlap principle which proposes that volume modifications arise from overlapping hydration shells causing water to be excluded from polar interaction sites [33].

This concept suggests that the observed positive values are indicative of water molecules being displaced from hydrophilic regions. The increasing trend of $\Delta_{tr}K^{0}_{\emptyset,S}$ with higher potassium benzoate concentrations in this study point toward enhanced solute structuring and more dominant solute-solvent associations. The incorporation of potassium benzoate along with tartaric or lactobionic acids results in positive $\Delta_{tr}K^{0}_{\emptyset,S}$ values suggest enhanced molecular organization and reduced compressibility [34,35]. This indicates that the interactions among these constituents remarkably impact the structural properties of the solution. The strengthening interaction between the acids and PB contributes to improved system integrity.

Table 4.67 Data of transfer parameter $\Delta_{tr}K^0_{\emptyset,S}$, of the ternary system of potassium benzoate (PB) in water-soluble tartaric acid (TA) and lactobionic acid (LBA) at several temperatures.

m_B/ (mol·kg^{-1})	$\Delta_{tr}K^0_{\emptyset,S} \times 10^6$/(m^3·mol^{-1}·GPa^{-1})			
	288.15K	298.15K	308.15K	318.15K
		Tartaric Acid		
0.015	0.14	0.14	0.14	0.05
0.025	0.17	0.17	0.18	0.10
0.035	0.19	0.21	0.20	0.11
		Lactobionic Acid		
0.015	0.04	0.06	0.02	0.04
0.025	0.10	0.10	0.07	0.09
0.035	0.17	0.17	0.15	0.14

m_B signifies the molalities of the potassium benzoate solution: the standard uncertainties u are $u(m)$ = 0.01, $u(T)$=0.001 K, $u(\Delta_{tr}K^0_{\emptyset,S})$ = 0.01×10^6/(m^3·mol^{-1}·GPa^{-1}).

4.7.8 Temperature-dependent partial molar volumes

The **equation 4.4** were fitted to a second order polynomial equation which is used to describe the strong dependence of the V_ϕ^0 on changes in temperature. The fitting was carried out using least squares regression approach and the empirical parameters a^*, b^*, c^* listed in **Table 4.68** correspond to tartaric and lactobionic acids in potassium benzoate aqueous media, where T stands for temperature (K) and the reference temperature (T_{ref}) is 298.15K. These constants are used to evaluate ARD deviations with the help of **equation 4.5** based on the difference between experimental and theoretical values [36]. In the current analysis, the polynomial model is expressed as $Y = V_\phi^0$ exhibits minimal deviations, which suggests a high degree of correlation and excellent agreement with the experimental data. The high values of the correlation coefficient (R^2 = 0.999) and low standard error confirm the excellent agreement between the experimental and fitted values. This statistical treatment highlights the systematic dependence of V_ϕ^0 on temperature for the studied systems. The negative c values reported in the table account for the dispersion observed in the V_ϕ^0 data. A primary aim of this work is to determine the expansibilities using the formula from **equation 4.6** [30 ,37,38]. The sustained positive values of E_ϕ^0 shown in **Table 4.69** reflect persistent solute-solvent associations, often linked with structural compactness or cage-like formations [39,40]. Hepler's thermodynamic principle [41] was utilized with **equation 4.7** to evaluate whether the solute constructs or disturbs the solvent's structural organization. Hepler's thermodynamic model was widely used in this investigation to identify whether TA and LBA act as structure creators or disruptor agents in potassium benzoate mixtures [42,43]. In this study, **Table 4.69** reveals that the expansibility derivatives show negative values for TA and LBA at all concentrations except 0.015 mol·kg^{-1} for TA. These outcomes point to a structure-disrupting effect of these acids in aqueous PB systems.

Table 4.68 Examined empirical parameters of potassium benzoate (PB) in water-soluble tartaric acid (TA) and lactobionic acid (LBA).

m_B/(mol·kg^{-1})	$a \times 10^6$/ (m^3·mol^{-1})	$b \times 10^6$/ (m^3·mol^{-1}·K^{-1})	$c \times 10^6$/ (m^3·mol^{-1}·K^{-2})	R^2	ARD
			Tartaric Acid		
0.015	82.95	0.0288	0.0002	0.9999	0.0000
0.025	83.24	0.0333	-0.0002	0.9999	0.0000
0.035	83.55	0.0348	-0.0002	0.9999	0.0000
			Lactobionic Acid		
0.015	223.41	0.3940	-0.0025	0.9999	0.0000
0.025	223.91	0.4045	-0.0020	0.9999	0.0000
0.035	224.45	0.4093	-0.0021	0.9999	0.0000

m_B signifies the molalities of the potassium benzoate solution: standard uncertainties are *u(m)* = 0.01, *u(T)*=0.001 K, *u(p)* =0.01 MPa.

Table 4.69 Data of partial molar expansibilities 'E_{Φ}^{0}' potassium benzoate (PB) in water-soluble solutions with tartaric acid (TA) and lactobionic acid (LBA) at various temperatures

m_B/ (mol·kg^{-1})	$E_{\Phi}^{0} \times 10^{6}$/(m^3·mol^{-1}·K^{-1})				$\left(\frac{\partial E_{\Phi}^{0}}{\partial T}\right)_P$ /(m^3·mol^{-1}·K^{-2})
	288.15K	298.15K	308.15K	318.15K	
			Tartaric Acid		
0.015	0.025	0.029	0.032	0.036	0.0004
0.025	0.037	0.033	0.030	0.027	-0.0003
0.035	0.038	0.035	0.031	0.027	-0.0004
			Lactobionic Acid		
0.015	0.445	0.394	0.343	0.293	-0.0051
0.025	0.444	0.404	0.364	0.324	-0.0040
0.035	0.452	0.409	0.367	0.324	-0.0043

m_B implies the molalities of potassium benzoate solution: calculated standard uncertainties are *u(m)* = 0.01, *u(T)*=0.001 K, $u(E_{\phi}^{0})$ = 0.04 ×10^6/(m^3·mol^{-1}·K^{-1}), $u(\frac{\partial E_{\phi}^{0}}{\partial T})$ = 0.00098/(m^3·mol^{-1}·K^{-2}), *u(p)* =0.01 MPa.

4.7.9 Interaction coefficients

Interactions involving two and three components, expressed as $V_{AB,}$ V_{ABB}; $K_{AB,}$ K_{ABB} are derived through the set of **equations 4.12** and **4.13**. The variables V_{AB} and V_{ABB} denote volumetric interaction parameters for binary and ternary systems. K_{AB} and K_{ABB} correspond to the respective interactions for isentropic compressibilities as summarized in **Table 4.70**. Tartaric and lactobionic acids serve as the solute (A) while potassium benzoate acts as the solvent (B).

The concept of interaction coefficients originates from the theoretical model proposed by McMillan and Mayer, which was subsequently refined by Krishnan and Friedman to incorporate molecular-level interactions influencing solution properties [44,45]. The overlapping of solvation layers triggers the displacement of H_2O molecules to the bulk medium of the mixture [46]. Throughout the studied temperature range, tartaric and lactobionic acids exhibit consistently positive pairwise coefficients V_{AB} and $K_{AB,}$ except for the volume interaction parameter at 288.15 K and 298.15 K for tartaric acid, which signifies stable and efficient molecular interactions. This behavior illustrates the molecular compatibility of the components. Additionally, the pairwise effects in the PB-based ternary mixtures with water and acids appear to be more significant than the triplet effects.

Table 4.70 Calculated Pair and triplet coefficients of (TA/LBA) with potassium benzoate solutions at numerous temperatures.

T/K	V_{AB} × 10^6/(m^3·mol^{-2}· kg)	V_{ABB} × 10^6/(m^3·mol^{-3}·kg^2)	K_{AB}×10^6 /(m^3·mol^{-2}· kg·GPa^{-1})	K_{ABB}×10^6 /(m^3·mol^{-3}·kg^2·GPa^{-1})
		Tartaric Acid		
288.15	-1.01	182.00	5.69	-57.98
298.15	-0.39	183.95	5.29	-44.77
308.15	2.04	187.77	5.91	-58.38
318.15	9.01	66.59	2.12	-9.10
		Lactobionic Acid		
288.15	-6.35	391.29	0.72	34.12
298.15	0.87	301.21	1.39	20.20
308.15	30.30	27.51	-0.35	47.02
318.15	79.07	-562.39	1.08	18.75

Standard uncertainties are $u(T)$=0.001 K.

Problem 8

4.8 Title: "Exploration of Intermolecular Interactions of Butyric and Tartaric Acids with Sodium Benzoate in Aqueous Medium"

The study examines the behavior of butyric and tartaric acids in water-soluble sodium benzoate solutions by recording density and velocity of sound at 0.00-0.09 mol·kg^{-1} concentrations and at four successive temperatures using a Density and Sound Velocity Analyzer.

4.8.1 Density and sound speed

The densities and sound speeds data were collected for butyric and tartaric acids in sodium benzoate mixtures across various temperature ranges and varying concentrations (0.00, 0.05, 0.07, 0.09) mol·kg^{-1}. **Table 4.71** presents the detailed outcomes which show that at fixed concentration levels of sodium benzoate, an increase in the molality of the acids, butyric and tartaric acids that results in a consistent rise in the density of the solution. Conversely, as the temperature rises, a minor yet noticeable decrease in density is observed, which is likely due to thermal expansion and the weakening of intermolecular forces. This trend is attributed to the stronger solute-solvent bonds and the structural organization in the solution. **Table 4.71** shows that under constant PB concentration, the sound velocity increases with higher molality of tartaric or butyric acids in water-soluble SB solution. This rise in sound speed suggests the creation of intricate hydrogen-bond networks within the components of the system. An elevation in the temperature weakens the hydrogen bonds in water molecules, allowing them to migrate into the voids and become enclosed within cage-like formations created by other water molecules. This phenomenon contributes to the formation of more compact molecular structures [4,10,47]. Simultaneously, the bonds between SB and water are disrupted and new hydrogen bonds emerge among butyric and tartaric acids with SB. Furthermore, the ultrasonic velocity measurements offer significant information regarding interactions amid ions and solvent molecules as well as within solvent molecules themselves [9,48,49].

Table 4.71 Data of 'ρ' and 'c' were investigated for sodium benzoate in aqueous butyric and tartaric acids mixtures at several temperatures.

m_A/ (mol·kg^{-1})	$\rho \times 10^{-3}$/(kg·m^{-3})				c/(m·s^{-1})			
	288.15K	298.15K	308.15K	318.15K	288.15K	298.15K	308.15K	318.15K
0.00 (mol·kg^{-1}) Sodium Benzoate + Tartaric Acid								
0.00000	0.99926	0.99705	0.99404	0.99036	1466.59	1495.85	1519.14	1536.02
0.10542	1.00630	1.00406	1.00103	0.99734	1470.49	1499.64	1522.75	1540.24
0.19266	1.01200	1.00975	1.00671	1.00300	1474.07	1502.82	1525.63	1544.08
0.30748	1.01935	1.01708	1.01402	1.01030	1478.83	1506.93	1529.85	1547.96
0.39615	1.02491	1.02262	1.01955	1.01581	1482.34	1510.28	1532.46	1551.72
0.50027	1.03131	1.02900	1.02590	1.02215	1485.92	1514.06	1536.17	1555.27
0.05 (mol·kg^{-1}) Sodium Benzoate + Tartaric Acid								
0.00000	1.00206	1.00027	0.99709	0.99281	1473.51	1503.56	1525.29	1541.36
0.09456	1.00833	1.00649	1.00327	0.99895	1478.05	1508.27	1529.32	1546.51
0.19384	1.01474	1.01285	1.00959	1.00523	1483.19	1513.42	1533.95	1552.63
0.30295	1.02157	1.01962	1.01633	1.01192	1487.92	1518.38	1538.76	1557.97
0.39961	1.02743	1.02545	1.02210	1.01765	1492.53	1523.71	1542.85	1562.09
0.49129	1.03284	1.03078	1.02742	1.02295	1497.08	1528.69	1548.04	1567.81
0.07 (mol·kg^{-1}) Sodium Benzoate + Tartaric Acid								
0.00000	1.00329	1.00152	0.99829	0.99395	1475.84	1506.09	1528.35	1544.03
0.10267	1.01005	1.00823	1.00495	1.00055	1480.29	1511.46	1533.51	1549.32
0.20113	1.01637	1.01448	1.01114	1.00670	1484.87	1516.18	1537.89	1554.84
0.30386	1.02277	1.02080	1.01740	1.01293	1489.35	1522.03	1542.78	1558.96
0.40335	1.02878	1.02676	1.02327	1.01876	1494.62	1526.91	1547.94	1564.09
0.49584	1.03421	1.03212	1.02858	1.02402	1499.83	1530.79	1552.15	1570.18
0.09 (mol·kg^{-1}) Sodium Benzoate + Tartaric Acid								
0.00000	1.00435	1.00268	0.99928	0.99489	1477.63	1508.62	1529.81	1547.12
0.10693	1.01135	1.00962	1.00617	1.00173	1482.39	1513.56	1534.58	1552.39
0.20489	1.01757	1.01579	1.01229	1.00781	1488.05	1518.95	1539.25	1556.64

0.30574	1.02382	1.02198	1.01843	1.01388	1493.44	1524.11	1543.77	1560.93
0.40841	1.03000	1.02810	1.02450	1.01991	1497.87	1528.86	1547.91	1564.41
0.50403	1.03557	1.03362	1.02994	1.02534	1502.16	1534.02	1551.89	1568.48
0.00 (mol·kg^{-1}) Sodium Benzoate + Butyric Acid								
0.00000	0.99926	0.99705	0.99404	0.99036	1466.59	1495.85	1519.14	1536.02
0.09887	0.99950	0.99729	0.99429	0.99062	1472.07	1501.12	1523.26	1540.22
0.20651	0.99977	0.99757	0.99457	0.99092	1478.23	1506.18	1527.53	1544.88
0.29671	1.00000	0.99780	0.99482	0.99118	1483.32	1510.04	1530.79	1548.51
0.40733	1.00030	0.99810	0.99513	0.99151	1489.16	1514.75	1534.73	1552.76
0.49683	1.00055	0.99836	0.99539	0.99178	1494.11	1518.89	1537.89	1555.61
0.05 (mol·kg^{-1}) Sodium Benzoate + Butyric Acid								
0.00000	1.00206	1.00027	0.99709	0.99281	1473.51	1503.56	1525.29	1541.36
0.09183	1.00225	1.00046	0.99730	0.99304	1476.32	1507.09	1528.48	1544.05
0.20937	1.00250	1.00072	0.99757	0.99334	1479.56	1510.65	1531.77	1547.61
0.29452	1.00269	1.00091	0.99778	0.99356	1482.07	1513.52	1534.68	1550.09
0.40158	1.00294	1.00117	0.99805	0.99386	1485.23	1516.14	1537.51	1553.26
0.50437	1.00319	1.00142	0.99831	0.99414	1487.74	1519.03	1540.42	1556.64
0.07 (mol·kg^{-1}) Sodium Benzoate + Butyric Acid								
0.00000	1.00329	1.00152	0.99829	0.99395	1475.84	1506.09	1528.35	1544.03
0.10874	1.00350	1.00173	0.99852	0.99421	1478.61	1509.73	1531.84	1547.19
0.19567	1.00367	1.00191	0.99871	0.99442	1482.09	1512.82	1534.41	1550.48
0.29843	1.00388	1.00213	0.99895	0.99468	1485.01	1515.54	1537.76	1553.62
0.40195	1.00411	1.00236	0.99920	0.99495	1488.18	1518.00	1540.28	1556.74
0.50448	1.00434	1.00260	0.99946	0.99523	1491.45	1521.36	1543.17	1559.39
0.09 (mol·kg^{-1}) Sodium Benzoate + Butyric Acid								
0.00000	1.00435	1.00268	0.99928	0.99489	1477.63	1508.62	1529.81	1547.12
0.09487	1.00452	1.00285	0.99947	0.99510	1481.04	1511.36	1532.24	1549.85
0.19529	1.00471	1.00305	0.99968	0.99534	1484.62	1514.78	1536.01	1551.56
0.30185	1.00492	1.00326	0.99992	0.99560	1487.93	1517.82	1539.21	1554.06
0.40997	1.00514	1.00349	1.00017	0.99588	1490.23	1520.57	1542.67	1557.73

0.49833	1.00533	1.00369	1.00038	0.99611	1492.75	1522.95	1545.18	1560.19

m_A specifies the molality of organic (TA/BA) acids in sodium benzoate solution: the calculated standard uncertainties u are $u(m)$ = 0.02, $u(T)$=0.001 K, $u(\rho)$= (0.00083) g·cm^{-3}, $u(c)$=1.94 m·s^{-1}.

4.8.2 Apparent molar volume (AMV)

AMV is widely recognized as a fundamental parameter for probing the interactions in BA/TA and SB-based ternary systems. These values were obtained from the observed density data through the use of **equation 4.1**. The term m_A corresponds to the molality of butyric or tartaric acids in a one-kilogram solution of sodium benzoate and water.

Table 4.72 presents the AMV values for butyric and tartaric acid in aqueous sodium benzoate across a range of temperatures. Molecular interactions between these acids and SB are schematically presented in **Figure 4.53**. Positive V_ϕ values from the data confirm that the interaction within solute and solvent becomes stronger. It reduces the compactness of water induced by electrostriction as the concentration of sodium benzoate rises.

Tartaric acid displays a gradual rise in apparent molar volume as illustrated in **Figure 4.54,** as the concentration of SB rises from 0.05 to 0.09 mol·kg^{-1}. This continuous elevation in V_ϕ values indicate more stronger solute-solvent bonds in case of tartaric acid which become more evident with increasing SB levels and temperatures. The pronounced response of tartaric acid to SB concentration is attributed to its multiple hydroxyl and carboxyl functional groups which facilitate significant hydrogen bonding and dipole interactions with the benzoate ions in solution [50,51]. Due to its strong affinity for water, tartaric acid readily establishes stable hydrogen bonds with both water and sodium benzoate which promotes an organized molecular arrangement and results in an increase in solution volume[52]. **Figure 4.55** displays a reduction in apparent molar volume for butyric acid as SB concentration rises which may result from its propensity to form hydrogen bonds and the predominant hydrophobic nature of its carbon chain [33,53]. Enhanced solvation behavior is evident from this trend in the tartaric acid as compared to the butyric acid.

Table 4.72 Apparent molar volumes 'V_ϕ' were determined for sodium benzoate in aqueous butyric and tartaric acids mixtures at several temperatures.

m_A/ (mol·kg^{-1})	$V_\phi \times 10^6$/(m^3·mol^{-1})				m_A/ (mol·kg^{-1})	$V_\phi \times 10^6$/(m^3·mol^{-1})			
	288.15K	298.15K	308.15K	318.15K		288.15K	298.15K	308.15K	318.15K
0.00 (mol·kg^{-1}) Sodium Benzoate + Tartaric Acid					**0.00 (mol·kg^{-1}) Sodium Benzoate + Butyric Acid**				
0.10542	82.75	83.01	83.25	83.44	0.09887	85.72	85.89	86.06	86.22
0.19266	82.91	83.16	83.39	83.57	0.20651	85.66	85.81	85.98	86.13
0.30748	83.08	83.34	83.55	83.76	0.29671	85.61	85.75	85.92	86.07
0.39615	83.21	83.47	83.68	83.89	0.40733	85.54	85.68	85.83	85.99
0.50027	83.37	83.61	83.84	84.06	0.49683	85.47	85.61	85.77	85.93
0.05 (mol·kg^{-1}) Sodium Benzoate + Tartaric Acid					**0.05 (mol·kg^{-1}) Sodium Benzoate + Butyric Acid**				
0.09456	83.19	83.78	84.28	84.81	0.09183	85.88	85.99	86.08	86.24
0.19384	83.57	84.12	84.61	85.12	0.20937	85.81	85.91	86.01	86.15
0.30295	84.01	84.56	85.02	85.53	0.29452	85.75	85.85	85.96	86.09
0.39961	84.42	84.94	85.43	85.95	0.40158	85.68	85.78	85.89	86.01
0.49129	84.78	85.37	85.82	86.32	0.50437	85.61	85.71	85.83	85.95
0.07 (mol·kg^{-1}) Sodium Benzoate + Tartaric Acid					**0.07 (mol·kg^{-1}) Sodium Benzoate + Butyric Acid**				
0.10267	83.58	84.17	84.72	85.34	0.10874	85.91	86.02	86.11	86.25
0.20113	83.91	84.51	85.16	85.71	0.19567	85.86	85.96	86.05	86.18
0.30386	84.28	84.95	85.61	86.14	0.29843	85.80	85.88	85.98	86.10
0.40335	84.67	85.33	86.05	86.59	0.40195	85.73	85.81	85.91	86.03

0.49584	85.03	85.72	86.43	86.98	0.50448	85.67	85.74	85.84	85.96
0.09 (mol·kg^{-1}) Sodium Benzoate + Tartaric Acid					**0.09 (mol·kg^{-1}) Sodium Benzoate + Butyric Acid**				
0.10693	83.99	84.59	85.07	85.64	0.09487	85.94	86.03	86.13	86.26
0.20489	84.36	84.95	85.49	86.01	0.19529	85.88	85.97	86.07	86.19
0.30574	84.68	85.27	85.83	86.45	0.30185	85.82	85.90	85.99	86.11
0.40841	85.01	85.61	86.19	86.79	0.40997	85.75	85.83	85.92	86.04
0.50403	85.37	85.97	86.63	87.16	0.49833	85.69	85.77	85.86	85.98

m_A signifies the molality of the organic acids in sodium benzoate: the calculated standard uncertainties u are $u(m) = 0.02$, $u(T) = 0.001$ K, $u(V_\phi) = 0.08 \times 10^{-6}/(m^3 \cdot mol^{-1})$.

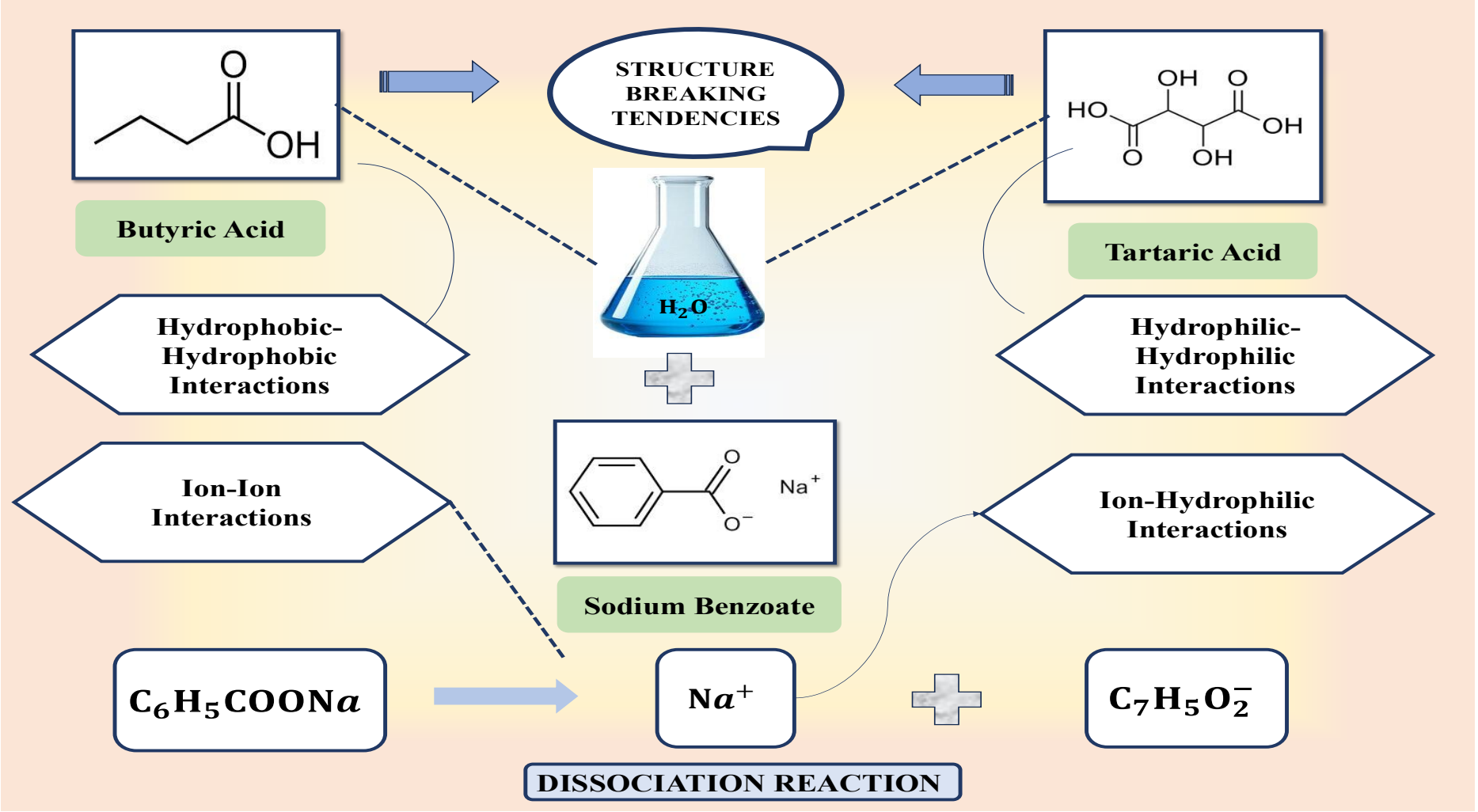

Figure 4.53 Tartaric Acid/ Butyric Acid and Sodium Benzoate interactions.

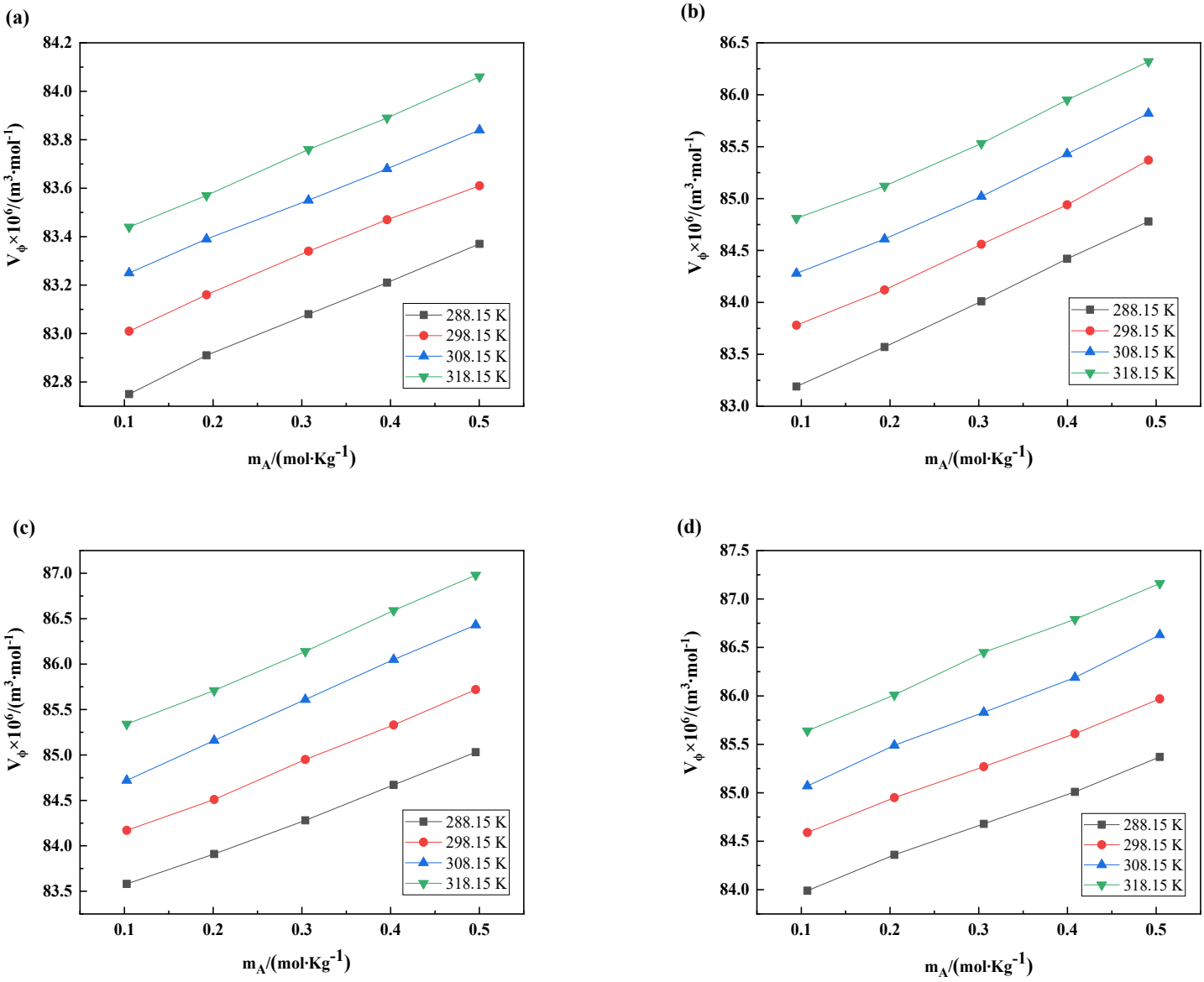

Figure 4.54 Plots demonstrate the variations in $(V_\emptyset)$ of (a) 0.00 SB; (b) 0.05 SB; (c) 0.07 SB; (d) 0.09 SB for molality of tartaric acid at varying temperatures.

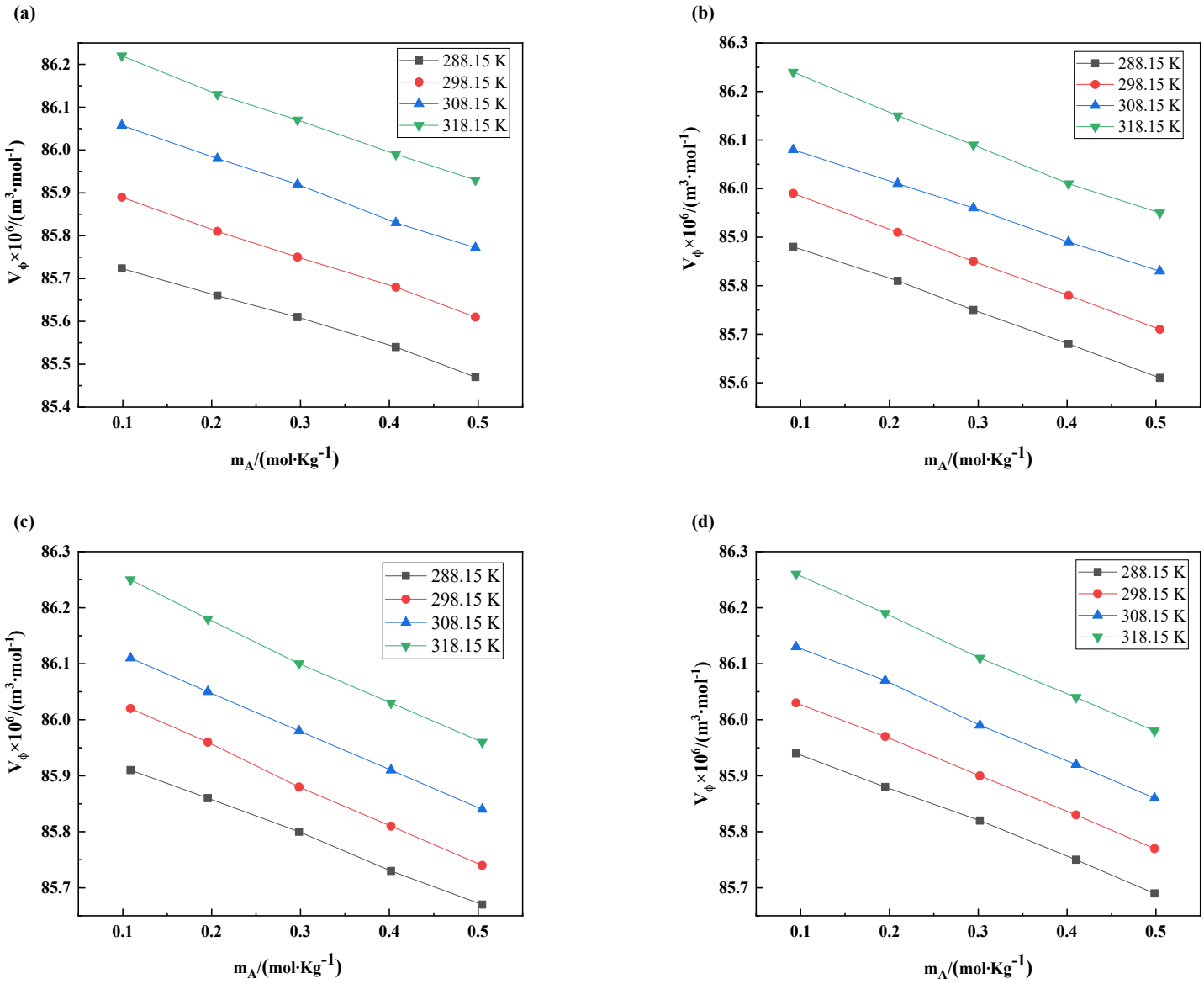

Figure 4.55 Plots demonstrate the variations in ($V_\emptyset$) of (a) 0.00 SB; (b) 0.05 SB; (c) 0.07 SB; (d) 0.09 SB for molality of butyric acid at varying temperatures.

4.8.3 Apparent molar isentropic compressibility

The determination of κ_S was based on the application of Laplace's formula in **equation 4.8** to the ultrasonic velocity values measured at different temperatures [54]. The **equation 4.9** is applied to calculate the values of $K_{\phi,S}$ for butyric acid and tartaric acid in sodium benzoate solutions containing water. **Table 4.73** shows that the compressibility parameter $K_{\phi,S}$ remains negative under all tested conditions which suggests that compression-based interactions are present. These negative values increase with the increased molality of butyric or tartaric acids but tend to reduce as the temperature rises. Higher SB concentration leads to a shift toward smaller negative values as seen in **Figures 4.56** and **4.57**.

The hydroxyl groups of acids form dipole-dipole interactions with nearby water molecules, thereby enhancing solute-solvent association. The compressibility of water close to the acid's ionic sites is lower than that of bulk water, which results in a modified hydration structure around the solute [13,14,55]. This configuration favors stable hydrogen bonding by increasing the affinity between the acids and the surrounding water. The zwitterionic characteristics of butyric and tartaric acids stem from the coexistence of positive and negative groups in one molecule. In sodium benzoate aqueous media, enhanced hydrogen bond formation promotes structural compaction and reduces isentropic compressibility. Consequently, clusters of hydrated molecules develop around the solute, which enhances both ion-solvent and ion-ion interactions due to the high polarity of water [17,56,57].

Table 4.73 Values of '$K_{\phi,s}$' of sodium benzoate in water-soluble solutions with tartaric acid (TA) and butyric acid (BA) at different temperatures.

m_A/ (mol·kg^{-1})	$K_{\phi,s} \times 10^6$/(m^3·mol^{-1}·GPa^{-1})				m_A/ (mol·kg^{-1})	$K_{\phi,s} \times 10^6$/(m^3·mol^{-1}·GPa^{-1})			
	288.15K	298.15K	308.15K	318.15K		288.15K	298.15K	308.15K	318.15K
0.00 (mol·kg^{-1}) Sodium Benzoate + Butyric Acid					**0.00 (mol·kg^{-1}) Sodium Benzoate + Tartaric Acid**				
0.09887	-46.01	-44.22	-42.91	-41.96	0.10542	-46.35	-44.56	-43.23	-42.28
0.20651	-46.27	-44.47	-43.15	-42.20	0.19266	-46.82	-45.01	-43.67	-42.71
0.29671	-46.35	-44.55	-43.23	-42.28	0.30748	-47.25	-45.42	-44.07	-43.11
0.40733	-46.40	-44.61	-43.28	-42.33	0.39615	-47.55	-45.71	-44.35	-43.37
0.49683	-46.43	-44.64	-43.31	-42.36	0.50027	-47.87	-46.02	-44.65	-43.67
0.05 (mol·kg^{-1}) Sodium Benzoate + Butyric Acid					**0.05 (mol·kg^{-1}) Sodium Benzoate + Tartaric Acid**				
0.09183	-45.60	-43.74	-42.51	-41.64	0.09456	-45.90	-44.02	-42.79	-41.91
0.20937	-45.90	-44.02	-42.79	-41.91	0.19384	-46.45	-44.55	-43.30	-42.41
0.29452	-45.97	-44.09	-42.86	-41.98	0.30295	-46.85	-44.93	-43.67	-42.77
0.40158	-46.02	-44.14	-42.91	-42.03	0.39961	-47.15	-45.22	-43.95	-43.05
0.50437	-46.06	-44.18	-42.94	-42.07	0.49129	-47.42	-45.48	-44.20	-43.29
0.07 (mol·kg^{-1}) Sodium Benzoate + Butyric Acid					**0.07 (mol·kg^{-1}) Sodium Benzoate + Tartaric Acid**				
0.10874	-45.44	-43.67	-42.44	-41.57	0.10267	-45.82	-43.94	-42.70	-41.81
0.19567	-45.64	-43.86	-42.63	-41.75	0.20113	-46.33	-44.42	-43.17	-42.28
0.29843	-45.73	-43.95	-42.71	-41.83	0.30386	-46.70	-44.78	-43.51	-42.61
0.40195	-45.78	-44.00	-42.76	-41.88	0.40335	-47.01	-45.08	-43.80	-42.89
0.50448	-45.81	-44.03	-42.79	-41.92	0.49584	-47.28	-45.33	-44.05	-43.13

0.09 (mol·kg^{-1}) Sodium Benzoate + Butyric Acid					**0.09 (mol·kg^{-1}) Sodium Benzoate + Tartaric Acid**				
0.09487	-45.33	-43.46	-42.33	-41.35	0.10693	-45.70	-43.82	-42.67	-41.68
0.19529	-45.58	-43.71	-42.57	-41.59	0.20489	-46.19	-44.28	-43.12	-42.13
0.30185	-45.68	-43.80	-42.66	-41.68	0.30574	-46.54	-44.63	-43.45	-42.45
0.40997	-45.73	-43.85	-42.70	-41.73	0.40841	-46.86	-44.93	-43.75	-42.74
0.49833	-45.75	-43.88	-42.73	-41.75	0.50403	-47.14	-45.19	-44.00	-42.99

m_A infers the molality of the organic acids (TA/BA) in sodium benzoate: the calculated standard uncertainties u are $u(m)$ = 0.02, $u(T)$=0.001 K, $u(K_{\phi,S})$ = 0.13 × 10^{-6}/(m^3·mol^{-1}·GPa^{-1}).

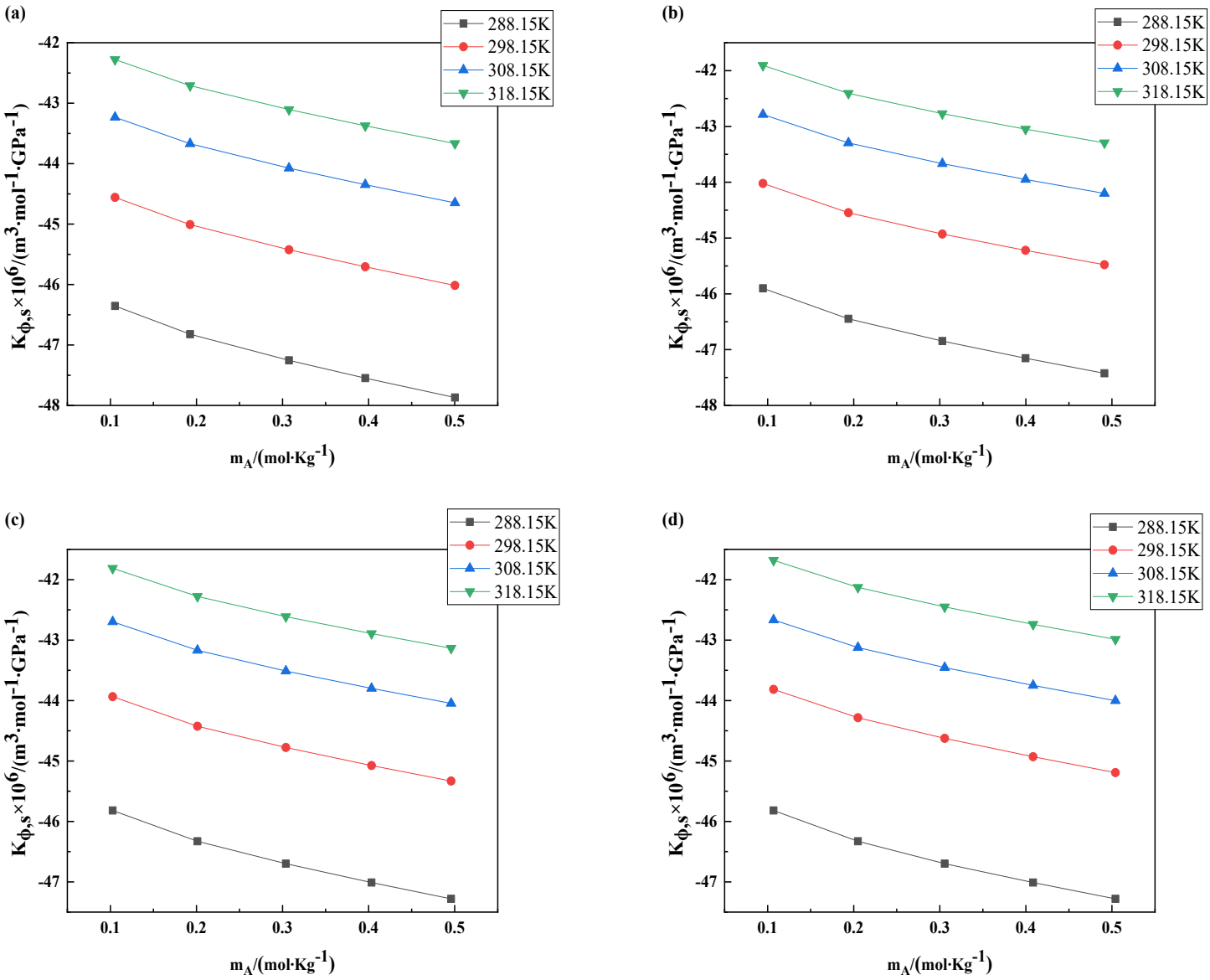

Figure 4.56 Variations of $K_{\phi,s}$, of tartaric acid (TA) in water-soluble sodium benzoate at varying concentrations.

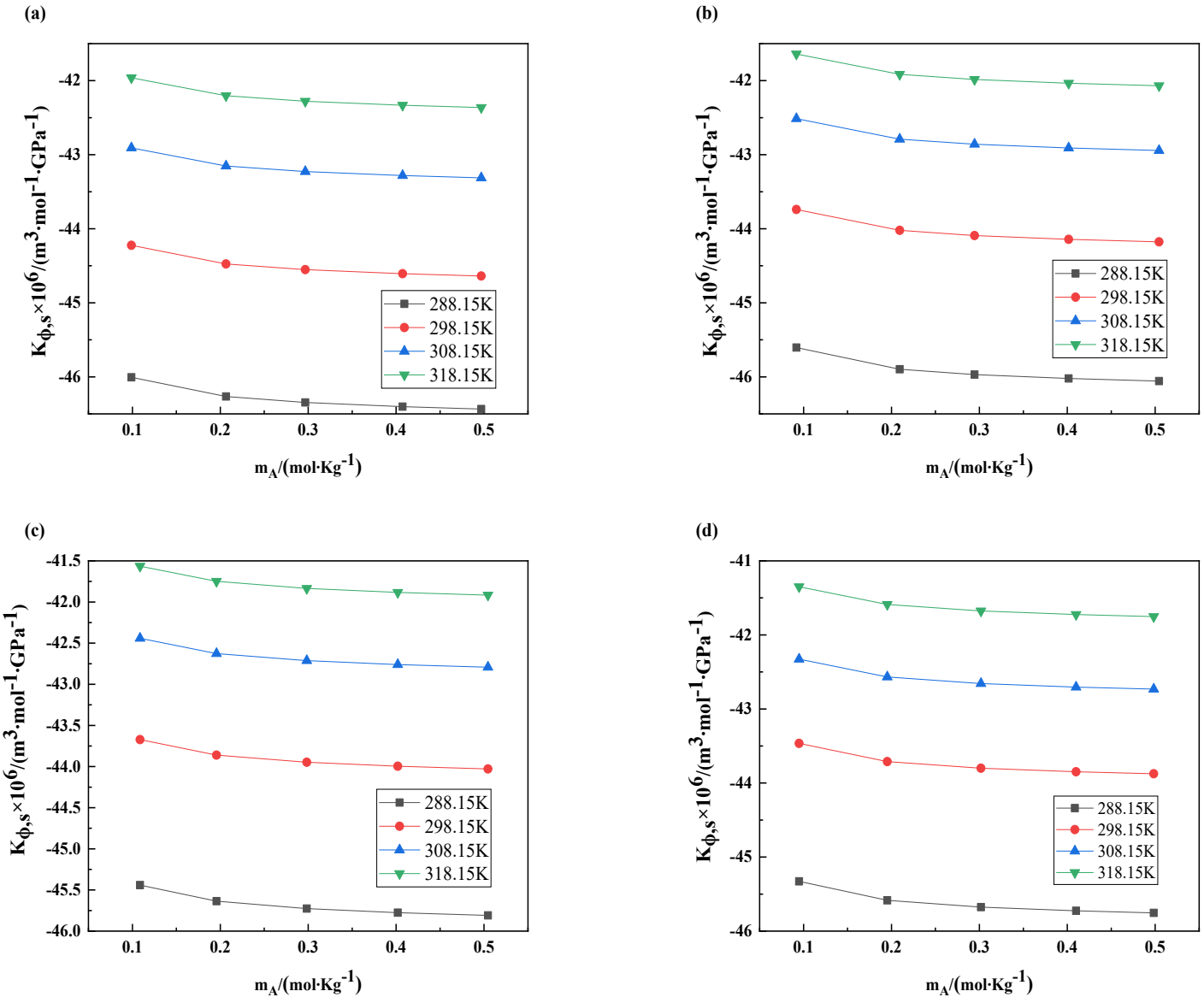

Figure 4.57 Variations of $K_{\phi,s}$, of butyric acid (BA) in water-soluble sodium benzoate at varying concentrations.

4.8.4 Partial molar volume (PMV)

The mathematical expression used in **equation 4.2** given below was applied to assess the V_ϕ^0 for ternary systems composed of SB and organic acids (butyric or tartaric acids). **Table 4.74** reports the V_ϕ^0 and S_V^* values derived via least squares regression. At all evaluated temperatures, V_ϕ^0 for both butyric and tartaric acids showed positive values and exhibited a regular upward trend with increasing sodium benzoate concentrations as visualized in **Figure 4.58.**

The co-sphere overlap concept explains that overlapping hydration zones of ions in solution can expand the overall volume due to the spatial contribution of both ions and their solvation shells. As the molality of butyric acid and tartaric acid rise, a corresponding increase in V_ϕ^0 for SB is observed which suggests that ionic and hydrophilic associations play a more prominent role than hydrophobic effects [38,58]. Sodium benzoate maintained positive S_V^* values throughout the examined temperature span which reflect active solute interactions. However, inconsistencies in this parameter's trend may result from other intermolecular forces or environmental variables in the surrounding conditions. The smaller S_V^* values when compared with V_ϕ^0 highlight the prevalence of solute-solvent interactions. The co-sphere overlap mechanism explains this through the volume increase caused by intersecting hydration layers, suggesting that the solute-solvent bonding is more prominent than solute-solute interactions [34,59].

Table 4.74 Values of $'V_{\phi}^{0}'$ and $'S_{V}^{*}'$ of sodium benzoate (SB) in water-soluble solutions with tartaric acid (TA) and butyric acid (BA) with their standard errors.

m_B/ (mol·kg^{-1})	$V_{\phi}^{0} \times 10^{6}$/(m^3·mol^{-1})				$S_{V}^{*} \times 10^{6}$ /(m^3·kg·mol^{-2})			
	288.15K	298.15K	308.15K	318.15K	288.15K	298.15K	308.15K	318.15 K
Tartaric Acid								
0.00	82.60(±0.01)	82.86(±0.01)	83.10(±0.01)	83.27(±0.01)	1.55(±0.03)	1.52(±0.04)	1.48(±0.02)	1.57(±0.02)
0.05	82.80(±0.01)	83.37(±0.04)	83.88(±0.04)	84.40(±0.04)	4.03(±0.04)	4.00(±0.12)	3.90(±0.11)	3.85(±0.13)
0.07	83.18(±0.02)	83.74(±0.02)	84.28(±0.01)	84.88(±0.03)	3.70(±0.07)	3.96(±0.07)	4.36(±0.04)	4.21(±0.08)
0.09	83.64(±0.02)	84.23(±0.02)	84.67(±0.04)	85.24(±0.03)	3.42(±0.07)	3.43(±0.06)	3.83(±0.12)	3.83(±0.08)
Butyric Acid								
0.00	85.79(±0.01)	85.96(±0.00)	86.13(±0.00)	86.29(±0.01)	-0.63(±0.02)	-0.69(±0.01)	-0.72(±0.01)	-0.72(±0.02)
0.05	85.82(±0.00)	85.98(±0.00)	86.17(±0.00)	86.30(±0.01)	-0.66(±0.01)	-0.68(±0.00)	-0.61(±0.01)	-0.71(±0.02)
0.07	85.84(±0.00)	86.01(±0.00)	86.19(±0.00)	86.31(±0.01)	-0.61(±0.01)	-0.71(±0.01)	-0.68(±0.00)	-0.73(±0.02)
0.09	85.86(±0.00)	86.04(±0.00)	86.21(±0.00)	86.32(±0.00)	-0.62(±0.01)	-0.65(±0.01)	-0.68(±0.01)	-0.70(±0.01)

m_B denotes the concentration of sodium benzoate: calculated standard uncertainties u are $u(m)$ = 0.02, $u(T)$=0.001 K, $u\ (V_{\phi}^{0})$= (0.14-0.23) × 10^{-6}/(m^3·mol^{-1}) and $u\ (S_{V}^{*})$=±0.37 × 10^{-6}/(m^3·kg·mol^{-2}).

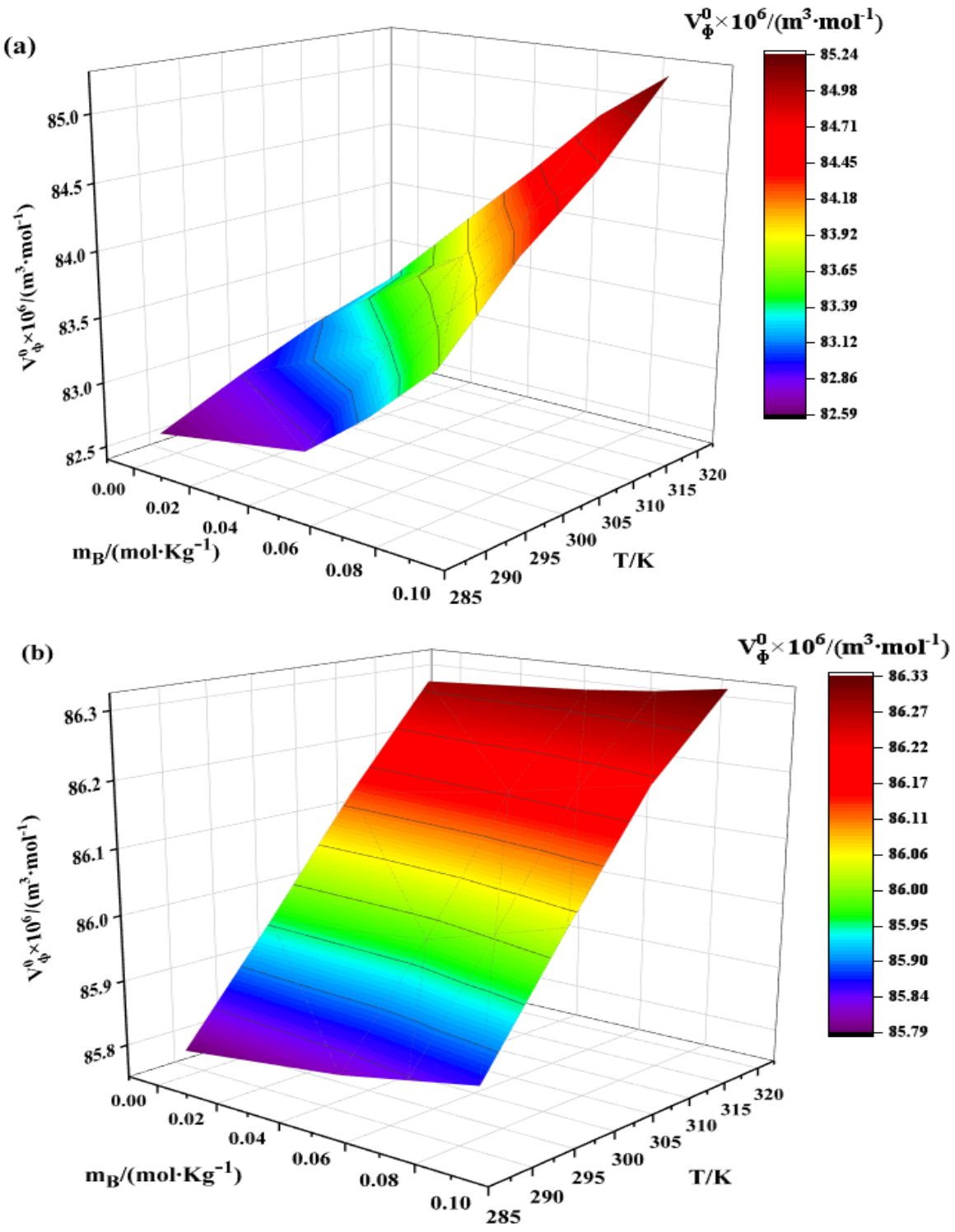

Figure 4.58 The comparative plot presents the changes in $V_\emptyset^0$, for tartaric acid butyric acid within a sodium benzoate aqueous solution at several temperatures.

4.8.5 Partial molar isentropic compression

The variation between the partial molar isentropic compressibility and solute molality is expressed through the mathematical **equation 4.10**. The acoustic virial coefficient is labelled as S_K^* helps determine solute interaction behavior. When the temperature increases, the $K_{\phi,s}^0$ values drop further, indicating interaction intensity as demonstrated in **Table 4.75** and **Figure 4.59**.

It is clear from this table that the lesser value of S_K^* compared to $K_{\phi,s}^0$ highlights weak interactions among solute molecules and emphasizes the prominence of solute-solvent bonding. The observation that $K_{\phi,s}^0$ becomes more negative with rising temperature and higher molalities of BA or TA indicate stronger molecular attraction, which in turn reduces the compressibility and mobility of nearby water molecules [16,18]. The inherent compressibility of the solvent contributes positively to $K_{\phi,s}^0$ as expanded molecular spacing in the solution promotes further compression. On the other hand, a negative effect is observed when solvent molecules interact with solute ions and occupy the empty spaces between them. Kirkwood's model [22] suggests that these interactions diminish electrostriction effects, which cause water molecules to be displaced into the bulk liquid medium. Due to its compact configuration, electrostricted water displays higher compressibility than normal bulk water [60-62].

Table 4.75 Evaluated $K^0_{\phi,S}$, and S^*_K values of the combination of sodium benzoate (SB) in water-soluble solutions with tartaric acid (TA) and butyric acid (BA) at several temperatures.

m_B/ (mol·kg^{-1})	$K^0_{\phi,S} \times 10^6$/(m^3·mol^{-1})				$S^*_K \times 10^6$ /(m^3·kg·mol^{-2})			
	288.15K	298.15K	308.15K	318.15K	288.15K	298.15K	308.15K	318.15 K
				Tartaric Acid				
0.00	-46.04 (±0.08)	-44.25(±0.08)	-42.93(±0.07)	-41.99(±0.07)	-3.78(±0.24)	-3.63(±0.23)	-3.53(±0.22)	-3.46(±0.22)
0.05	-45.64(±0.09)	-43.77(±0.09)	-42.54(±0.09)	-41.67(±0.09)	-3.76(±0.28)	-3.60(±0.27)	-3.49(±0.27)	-3.42(±0.26)
0.07	-45.53(±0.08)	-43.66(±0.08)	-42.43(±0.08)	-41.55(±0.08)	-3.65(±0.25)	-3.48(±0.24)	-3.37(±0.24)	-3.30(±0.23)
0.09	-45.52(±0.09)	-43.53(±0.08)	-42.39(±0.08)	-41.41(±0.07)	-3.62(±0.27)	-3.41(±0.23)	-3.31(±0.22)	-3.23(±0.22)
				Butyric Acid				
0.00	-45.99 (±0.08)	-44.21(±0.08)	-42.89(±0.08)	-41.95(±0.08)	-1.00(±0.24)	-0.97(±0.24)	-0.95(±0.23)	-0.93(±0.23)
0.05	-45.60(±0.09)	-43.74(±0.09)	-42.51(±0.09)	-41.64(±0.08)	-1.02(±0.27)	-0.99(±0.26)	-0.97(±0.26)	-0.97(±0.25)
0.07	-45.42(±0.07)	-43.65(±0.06)	-42.42(±0.06)	-41.54(±0.06)	-0.87(±0.20)	-0.84(±0.19)	-0.83(±0.19)	-0.83(±0.19)
0.09	-45.32(±0.08)	-43.46(±0.08)	-42.32(±0.08)	-41.34(±0.08)	-0.98(±0.25)	-0.94(±0.24)	-0.93(±0.23)	-0.93(±0.23)

m_B denotes the concentration of sodium benzoate: the calculated standard uncertainties u are $u(m) = 0.02$, $u(T) = 0.001$ K, $u(K^0_{\phi,S}) = 0.27 \times 10^{-6}$/(m^3·mol^{-1}·GPa^{-1}), $u(S^*_K) = \pm 0.23 \times 10^{-6}$/(kg·m^3·kg·mol^{-2}·GPa^{-1}).

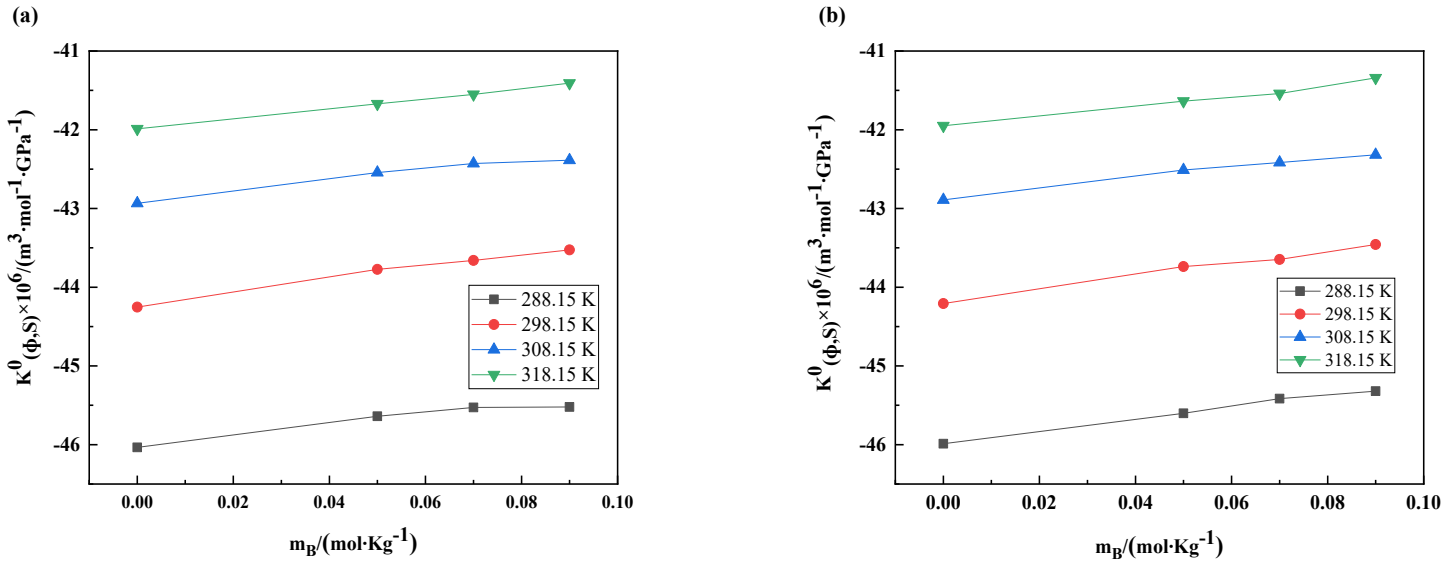

Figure 4.59 Plots of distinctions of $K^0_{\emptyset,S}$ for (a) tartaric acid and (b) butyric acid in water-soluble sodium benzoate solution at several temperatures.

4.8.6 Transfer of partial molar volume

The volumetric transfer parameter $\Delta_{tr}V_{\emptyset}^{0}$ defines the change observed during movement between distinct phases in thermodynamic studies. The expression from **equation 4.3** is applied to compute the volume change as solutes shift from pure water into the sodium benzoate solution. This parameter as a significant thermodynamic property signifies the bonding tendencies between the solute and solvent. It helps in understanding the structural dynamics that arise within the solution. The results summarized in **Table 4.76** show that for PB-based aqueous systems, $\Delta_{tr}V_{\emptyset}^{0}$ values of butyric and tartaric acids are positive and exhibit an upward pattern as solvent concentration increases, despite some irregularities caused by temperature changes. The complete dissociation of SB and the ionizing behavior of butyric and tartaric acids in aqueous media highlight their electrolytic nature. Being a salt formed from a strong base and weak acid, sodium benzoate ionizes completely into Na^{+} and benzoate ions. The observed positive values point to intensified electrostatic interactions with the organic acids [63]. Their ionization promotes both ion-ion and ion-solvent interactions which influence the overall physical and chemical characteristics and molecular associations in the ternary system. Pauling's theory of clathrates suggests that voids in the water's structural network can be occupied by solute molecules [64,65]. The positive data of $\Delta_{tr}V_{\emptyset}^{0}$ can be explained by the solute's influence on the solvent structure which may be enhanced or perturbed owing to solvophobic effects and interactions within intersecting hydration shells. Butyric and tartaric acids modify this organized hydrogen bond system and establish new molecular associations. The observed positive values in the current investigation indicate stronger hydrogen bonding, ion-ion, ion-hydrophilic, and hydrophilic-hydrophilic bonds for the ternary system.

Table 4.76 Transfer property of 'ΔV_{ϕ}^{0}' of sodium benzoate in aqueous butyric and tartaric acids mixtures at several temperatures.

m_B/ (mol·kg^{-1})	$\Delta V_{\phi}^{0} \times 10^{6}$/(m^3·mol^{-1})			
	288.15K	298.15K	308.15K	318.15K
		Tartaric Acid		
0.05	0.20	0.51	0.78	1.13
0.07	0.58	0.88	1.18	1.61
0.09	1.04	1.37	1.57	1.97
		Butyric Acid		
0.05	0.03	0.02	0.04	0.01
0.07	0.05	0.05	0.06	0.02
0.09	0.07	0.08	0.08	0.04

m_B denotes the concentration of sodium benzoate: the calculated standard uncertainties *u* are *u(m)* = 0.02, *u(T)* = 0.001 K, $u(\Delta V_{\phi}^{0}) = \pm 0.13 \times 10^{-6}$/(m^3·mol^{-1}).

4.8.7 Transfer of partial molar isentropic compression

The variation in $\Delta_{tr}K^{0}_{\emptyset,S}$ due to the solute transition from water to the SB aqueous phase was computed through the use of **equation 4.11**. **Table 4.77** shows the examined $\Delta_{tr}K^{0}_{\emptyset,S}$ values corresponding to the migration of butyric and tartaric acids from water into SB aqueous mixtures. This observation is validated by the co-sphere overlap approach which explains volume variation as a consequence of overlapping hydration spheres that displace water from active polar sites [44]. The increase in structural order and the corresponding decline in compressibility, as shown by the positive $\Delta_{tr}K^{0}_{\emptyset,S}$ values obtained after adding sodium benzoate with butyric and tartaric acids illustrate the significant contribution of their mutual interactions in characterizing the solution properties. The association between BA/TA and sodium benzoate contributes to enhanced structural integrity of the system. Consequently, increasing the concentration of sodium benzoate lowers the solution's compressibility, making the mixture more resistant to compression than the pure solvent [66,67]. This shift is also linked to a decrease in electrostriction which influences the solute's molecular configuration at elevated SB levels. The phenomenon is attributed to the strong bonding between the water-soluble sodium benzoate and the zwitterionic sites present in butyric and tartaric acids. The occurrence of positive $\Delta_{tr}K^{0}_{\emptyset,S}$ values demonstrate that butyric and tartaric acids facilitate molecular bonding with water which enhances the extent of intermolecular interaction [27]. This effect brings about solvent inclusion in the solute's hydration layer. Conversely, negative $\Delta_{tr}K^{0}_{\emptyset,S}$ values signify more dominant ion-solvent binding which leads to tighter molecular packing and reduced compressibility [68].

Table 4.77 Values of $\Delta K^0_{\phi,S}$, of the combinations of sodium benzoate (SB) in water-soluble solutions with tartaric acid (TA) and butyric acid (BA) at several temperatures.

m_B/ (mol·kg^{-1})	$\Delta K^0_{\phi,S} \times 10^6$/(m^3·mol^{-1}·GPa^{-1})			
	288.15K	298.15K	308.15K	318.15K
		Tartaric Acid		
0.05	0.40	0.48	0.39	0.32
0.07	0.51	0.59	0.51	0.44
0.09	0.51	0.73	0.55	0.58
		Butyric Acid		
0.05	0.39	0.47	0.38	0.31
0.07	0.57	0.56	0.47	0.41
0.09	0.67	0.75	0.57	0.61

m_B denotes the concentration of sodium benzoate: the calculated standard uncertainties u are $u(m) = 0.02$, $u(T) = 0.001$ K, $u(\Delta K^0_{\phi,S}) = 0.02\times10^{-6}$/(m^3·mol^{-1}·GPa^{-1}).

4.8.8 Temperature effect on partial molar volume

The association among V_ϕ^0 and temperature plays a substantial role in interpreting molecular interactions in ternary systems and is often expressed with a polynomial **equation 4.4**. **Table 4.78** records the empirical coefficients *a, b*, and *c* for butyric and tartaric acids in aqueous sodium benzoate solutions, where T denotes temperature in Kelvin and a reference temperature (T_{ref}) is taken as 298.15 K. These constants are utilized by analyzing the variation between the actual and model-derived values to compute ARD deviations from **equation 4.5** [69]. A low average relative deviation (ARD) signifies excellent consistency among the measured and computed values, validating the effectiveness of the fitted polynomial model. The negative values of parameter c listed in the table represent the variability found in the V_ϕ^0 data. One of the primary objectives of this study is to evaluate the expansibility using **equation 4.6** [25,70]. The $E_\emptyset^0$ values are positive as reported in **Table 4.80**, which is generally caused by the effect of molecular caging or dense structural packing in the medium [40,71]. This phenomenon implies that changes in the (sodium benzoate + water) solvent system lead to an expansion of the volume occupied by the hydration layers around solute molecules. The primary cause of this expansion is the intensified interactions within the solute and sodium benzoate molecules [5].

Table 4.78 Calculated empirical parameters of sodium benzoate (SB) in water-soluble tartaric acid (TA) and butyric acid (BA) at several concentrations.

m_B/(mol·kg^{-1})	$a \times 10^6$/ (m^3·mol^{-1})	$b \times 10^6$/ (m^3·mol^{-1}·K^{-1})	$c \times 10^6$/ (m^3·mol^{-1}·K^{-2})	R^2	ARD
			Tartaric Acid		
0.05	83.36	0.0543	-0.0001	0.9999	0.0000
0.07	83.73	0.0555	0.0001	0.9999	0.0000
0.09	84.19	0.0531	-0.0001	0.9999	0.0000
			Butyric Acid		
0.05	85.99	0.0171	-0.0001	0.9999	0.0000
0.07	86.02	0.0171	-0.0001	0.9999	0.0000
0.09	86.05	0.0173	-0.0002	0.9999	0.0000

m_B denotes the concentration of sodium benzoate: calculated standard uncertainties are *u(m)* = 0.02, *u(T)* = 0.001 K, *u(p)* = 0.01 MPa.

4.8.9 Hepler's constant

Hepler's thermodynamic principle is commonly applied to distinguish between structure-enhancing and structure-disrupting behavior of solutes in binary or ternary solvent systems [41]. The analysis is conducted using **equation 4.7**. The derivative $(\partial E_{\phi}^{0}/\partial T)_{p}$ is employed to assess whether a solute promotes or disrupts the solvent structure. The computed data of this parameter is recorded in **Table 4.79**. A positive value of this parameter suggests the structure-forming behavior of solute molecules in the solvent (water + sodium benzoate), while a negative value indicates the structure-breaking capacity [29,72]. During this investigation, Hepler constants for both butyric and tartaric acids in water yielded negative values except for the 0.07 SB concentration for tartaric acid and 0.05 SB for butyric acid, which reflects their behavior in disrupting water's structure.

Table 4.79 Data of partial molar expansibilities 'E_{Φ}^{0}' sodium benzoate (SB) in water-soluble solutions with tartaric acid (TA) and butyric acid (BA) at various temperatures

m_B/ (mol·kg^{-1})	$E_{\Phi}^{0} \times 10^{6}$/(m^3·mol^{-1}·K^{-1})				$\left(\frac{\partial E_{\Phi}^{0}}{\partial T}\right)_P$/(m^3·mol^{-1}·K^{-2})
	288.15K	298.15K	308.15K	318.15K	
			Tartaric Acid		
0.05	0.056	0.054	0.052	0.050	-0.0002
0.07	0.053	0.056	0.058	0.060	0.0002
0.09	0.054	0.053	0.052	0.051	-0.0001
			Butyric Acid		
0.05	0.025	0.029	0.032	0.036	0.0004
0.07	0.037	0.033	0.030	0.027	-0.0003
0.09	0.038	0.035	0.031	0.027	-0.0004

m_B denotes the concentration of sodium benzoate: calculated standard uncertainties are $u(m)$ = 0.02, $u(T)$ = 0.001 K, $u(E_{\phi}^{0})$ = 0.0024 ×10^{-6}/(m^3·mol^{-1}·K^{-1}), $u(\frac{\partial E_{\phi}^{0}}{\partial T})$ = 0.00012/(m^3·mol^{-1}·K^{-2}), $u(p)$ = 0.01 MPa.

4.8.10 Interaction coefficients

The interaction terms involving both binary and ternary systems, denoted as $V_{AB,}$ $V_{ABB;}$ $K_{AB,}$ $K_{ABB,}$ are evaluated from the mathematical formulations outlined in **equations 4.12** and **4.13**. In these equations, A represents the solute components- namely, butyric and tartaric acids, while B refers to the solvent, sodium benzoate. The term m_B corresponds to the molality of the sodium benzoate-water mixtures. The terms V_{AB} and V_{ABB} denote volume interaction parameters for binary and ternary systems, respectively, while K_{AB} and K_{ABB} reflect isentropic compressibility interactions, as outlined in **Table 4.80**.

The concept of splitting in the solute interactions, originally proposed by McMillan and Mayer, explains how pairwise and triplet molecular associations can independently affect the structure of liquid mixtures [45]. This idea has been further explored and elaborated upon by Franks [73] and by Friedman and Krishnan [33]. A comprehensive analysis of both the nature and scope of such interactions is crucial to predict the solute behavior in liquid systems. Overlap between solute hydration zones result to the expulsion of water into the bulk of the mixture [74]. Positive trends in the pairwise interaction terms VAB and KAB are observed for butyric and tartaric acids, which prevail over the studied temperatures in the current investigation, reflecting molecular interaction patterns.

Table 4.80 Calculated Pair (V_{AB}, K_{AB}) and triplet (V_{ABB}, K_{ABB}) coefficients of (TA/BA) in water-soluble mixtures of sodium benzoate at numerous temperatures.

T/K	V_{AB} × 10^6/(m^3·mol^{-2}· kg)	V_{ABB} × 10^6/(m^3·mol^{-3}·kg^2)	K_{AB}×10^6 /(m^3·mol^{-2}· kg·GPa^{-1})	K_{ABB}×10^6 /(m^3·mol^{-3}·kg^2·GPa^{-1})
		Tartaric Acid		
288.15	-2.42	61.00	5.59	-19.98
298.15	1.85	42.51	5.55	-11.48
308.15	6.79	14.69	5.13	-15.32
318.15	12.27	-9.41	3.04	1.22
		Butyric Acid		
288.15	0.20	1.40	4.39	-4.56
298.15	-0.01	3.59	4.87	-5.81
308.15	0.35	0.70	4.46	-9.58
318.15	0.05	1.18	2.44	6.53

Standard uncertainties are u(T)=0.001 K.

References

1. Ashima, K.C. Juglan and H. Kumar, Results Chem. 2, 100049 (2020).
2. P. Kaur, K.C. Juglan, H. Kumar and M. Singla, Braz. J. Chem. Eng. 40, 1213–1226 (2023).
3. N. Chakraborty, K.C. Juglan and H. Kumar, J. Chem. Thermodyn. 154, 106326 (2021).
4. Ashima, K.C. Juglan and H. Kumar, J. Chem. Thermodyn. 140, 105916 (2020).
5. H. Kaur, N. Chakraborty, K.C. Juglan and A. Upmanyu, J. Mol. Liq. 392, 123403 (2023).
6. M. Lamba, N. Chakraborty, K.C. Juglan, R. Sharma and M. Singla, J. Chem. Eng. Data 69, 171–184 (2024).
7. Y. Marcus, Chem. Rev. 111, 2761–2783 (2011).
8. M.L. Parmar and R.C. Thakur, J. Mol. Liq. 128, 85–89 (2006).
9. D. Chawla, N. Chakraborty, K.C. Juglan and H. Kumar, Chem. Pap. 75, 1497–150 (2021).
10. H. Kitano, M. Imai, K. Sudo and M. Ide, J. Phys. Chem. B 106, 11391–11396 (2002).
11. T.S.D. Oliveira, A. Ghosh and P. Chaudhuri, J. Phys. Chem. A 127, 3551–3559 (2023).
12. S.S. Dhondge, R.L. Paliwal and N.S. Bhave, J. Chem. Thermodyn. 59, 158–165 (2013).
13. I. Bahadur and N. Deenadayalu, Thermochim. Acta 566, 77–83 (2013).
14. M.T. Zafarani-Moattar and H. Shekaari, J. Chem. Thermodyn. 37, 1029–1035 (2005).
15. N. Chakraborty, K.C. Juglan and H. Kumar, Braz. J. Chem. Eng. 39, 869–884 (2022).
16. K. Dhal, S. Singh and M. Talukdar, J. Mol. Liq. 352, 118659 (2022).
17. S. Panda, V. Singh, N. Islam and R.L. Gardas, Fluid Ph. Equilib. 445, 35–44 (2017).
18. I. Gheorghe, C. Stoicescu and F. Sirbu, J. Mol. Liq. 218, 515–524 (2016).
19. R.C. Thakur, R. Sharma, A. Kumar, S. Kumar and M.L. Parmar, Orient. J. Chem. 30, 2037–2041 (2014).
20. S. Li, W. Sang and R. Lin, J. Chem. Thermodyn. 34, 1761–1768 (2002).
21. S.K. Lomesh, M. Bala and V. Nathan, J. Mol. Liq. 283, 133–146 (2019).
22. J.G. Kirkwood, Chem. Rev. 24, 233–251 (1939).
23. N. Chakraborty, K.C. Juglan and H. Kumar, ACS Omega 5, 32357–32365 (2020).
24. R. Sadeghi and F. Ziamajidi, J. Chem. Eng. Data 52, 1037–1044 (2007).
25. M. Lamba, N. Chakraborty and K.C. Juglan, J. Chem. Eng. Data 70, 244–260 (2025).
26. N. Chakraborty, K.C. Juglan and H. Kumar, J. Chem. Thermodyn. 163, 106584 (2021).
27. A. Thakur, K.C. Juglan, H. Kumar and K. Kaur, J. Mol. Liq. 288, 111014 (2019).
28. C.M. Romero and F. Negrete, Phys. Chem. Liq. 42, 261–267 (2004).
29. K. Kaur, K.C. Juglan and H. Kumar, J. Mol. Liq. 268, 700–706 (2018).
30. T. Sharma, H. Singh, R.K. Bamezai and A. Kumar, J. Mol. Liq. 349, 118412 (2022).

31. L. Pauling and R.B. Corey, Proc. Natl. Acad. Sci. U.S.A. 38, 86–93 (1952).
32. L. Pauling and R.E. Marsh, Proc. Natl. Acad. Sci. U.S.A. 38, 112–118 (1952).
33. H.L. Friedman and C.V. Krishnan, J. Solution Chem. 2, 119–140 (1973).
34. Nidhi, R.C. Thakur, A. Kumar, P.K. Sharma, V. Pathania and A. Garg, Phys. Chem. Liq. 63, 162–180 (2025).
35. R.C. Thakur and R. Sharma, Russ. J. Phys. Chem. 91, 1703–1709 (2017).
36. P. Kaur, N. Chakraborty, K.C. Juglan, H. Kumar and M. Singla, J. Mol. Liq. 339, 116810 (2021).
37. K. Bhakri, N. Chakraborty, K.C. Juglan, H. Kumar and R. Sharma, J. Therm. Anal. Calorim. 148, 7185–7205 (2023).
38. A. Beri, P.K. Banipal and T.S. Banipal, Food Chem. 266, 110–118 (2018).
39. A. Ghosh and K.S. Schweizer, Macromolecules 53, 4366–4380 (2020).
40. X. Chen, Z. Huang, W. Hua, H. Castada and H.C. Allen, Langmuir 26, 18902–18908 (2010).
41. L.G. Hepler, Can. J. Chem. 47, 4613–4617 (1969).
42. K. Dhal, S. Singh and M. Talukdar, J. Mol. Liq. 368, 120761 (2022).
43. P. Devi, P. Rani and J. Kataria, J. Taiwan Inst. Chem. Eng. 159, 105468 (2024).
44. C.V. Krishnan and H.L. Friedman, J. Solution Chem. 2, 37–51 (1973).
45. W.G. McMillan and J.E. Mayer, J. Chem. Phys. 13, 276–305 (1945).
46. H. Kaur, N. Chakraborty and K.C. Juglan, J. Chem. Eng. Data 69, 2461–2474 (2024).
47. N. Muñoz-Rujas, J.P. Bazile, F. Aguilar, G. Galliero, E. Montero and J.L. Daridon, Fluid Ph. Equilib. 449, 148–155 (2017).
48. N. Chakraborty, K.C. Juglan and H. Kumar, J. Mol. Liq. 337, 116605 (2021).
49. K. Kaur, K.C. Juglan, H. Kumar and I. Behal, J. Chem. Eng. Data 63, 3237–3251 (2018).
50. S.D. Deosarkar, A.D. Arsule, R.T. Sawale and V.G. Pingle, J. Mol. Liq. 323, 114925 (2021).
51. Ankita and A.K. Nain, J. Mol. Liq. 298, 112006 (2020).
52. A. Thakur, K.C. Juglan, H. Kumar and K. Kaur, Phys. Chem. Liq. 58, 803–819 (2020).
53. W. Blokzijl and J.B.F.N. Engberts, Angew. Chem. Int. Ed. Engl. 32, 1545–1579 (1993).
54. N. Chakraborty, K.C. Juglan, H. Kumar and M. Singla, J. Chem. Thermodyn. 174, 106876 (2022).
55. R. Rani, A. Kumar, T. Sharma, B. Saini and R.,K. Bamezai, ACSi 589–601 (2016).

56. T. Kondo, K. Nomura, M. Gemmei-Ide, H. Kitano, H. Noguchi, K. Uosaki and Y. Saruwatari, Colloid Surf. B. Biointerfaces 113, 361–367 (2014).

57. A.K. Gill, N. Chakraborty and K.C. Juglan, Int. J. Thermophys. 46, 46 (2025).

58. N. Chakraborty, H. Kumar, K. Kaur and K.C. Juglan, J. Chem. Thermodyn. 126, 137–146 (2018).

59. P. Patnaik, N. Chakraborty, P. Kaur, K.C. Juglan and H. Kumar, Adv. Funct. Mater. 403–424 (2023).

60. B. Ghosh, A. Sinha, N. Roy, B. Rajbanshi, M. Mondal, D. Roy, A. Das, N.N. Ghosh, V.K. Dakua and M.N. Roy, Fluid Ph. Equilib. 557, 113415 (2022).

61. H. Kumar and I. Behal, J. Mol. Liq. 219, 756–764 (2016).

62. P. Kaur, N. Chakraborty, K.C. Juglan and H. Kumar, J. Mol. Liq. 315, 113763 (2020).

63. R. Sadeghi and A. Gholamireza, J. Chem. Thermodyn. 43, 200–215 (2011).

64. S. Baluja and S. Oza, Fluid. Ph. Equilib. 178, 233–238 (2001).

65. S. Chauhan and K. Kumar, J. Mol. Liq.194, 212-226 (2014).

66. I. Bahadur and N. Deenadayalu, J. Solution Chem. 40, 1528–1543 (2011).

67. Riyazuddeen and I. Khan, J. Mol. Liq. 152, 57–62 (2010).

68. S.K. Begum, R.J. Clarke, M.S. Ahmed, S. Begum and M.A. Saleh, J. Mol. Liq. 177, 11–18 (2013).

69. T.S. Banipal, H. Singh, P.K. Banipal and V. Singh, Thermochim. Acta 553, 31–39 (2013).

70. A.K. Gill and N. Chakraborty and K.C. Juglan, Phys. Scr. 99, 115009 (2024).

71. R. Gopal, D.K. Aggarwal and R. Kumar, Indian J. Chem. 11, 1061–1062 (1973).

72. K. Kaur, K.C. Juglan and H. Kumar, J. Mol. Liq. 268, 700–706 (2018).

73. F. Franks, M. Pedley and D.S. Reid, J. Chem. Soc., Faraday Trans. 1 72, 359 (1976).

74. E. Ayranci and M. Sahin, J. Chem. Thermodyn. 40, 1200–1207 (2008).

Summary and Conclusions

The thesis entitled "**Study of Thermo-Acoustic Behaviour of Benzoic Acid Derivatives in Aqueous Solutions of Carboxylic Acids**" presents an extensive analysis of the physicochemical characteristics of the ternary mixtures composed of three benzoic acid derivatives-sodium benzoate, potassium benzoate, and sodium methyl parahydroxybenzoate in combination with a wide range of carboxylic acids. The systems were examined at multiple concentrations of the benzoic acid derivatives and at temperatures ranging from 288.15 K to 318.15 K with 10 K intervals under a constant pressure of 0.1 MPa. The research highlights significant structural aspects of these ternary systems. A systematic analysis of the volumetric and acoustic properties of the mixtures (sodium benzoate + water + glycolic acid/lactobionic acid) was performed across the entire concentration range of sodium benzoate (0.1,0.4, and 0.7) mol·kg^{-1} and at varying temperatures. High-precision experimental data for density and ultrasonic velocity were obtained with the Anton Paar DSA 5000 M instrument. The experimental results provided the basis for evaluating molar properties such as apparent and partial molar volume, and transfer properties along with interaction coefficients, including pair and triplet parameters. These properties offered valuable insights into solute-solvent interactions within the mixtures with an observed increase in interaction strength from glycolic acid to lactobionic acid. The study further demonstrated multiple interactions, such as hydrophilic-hydrophilic, dipole-dipole, and ion-hydrophilic interactions. The consistently positive values of the expansibility coefficient confirmed the ability of solute molecules to promote structure within the liquid medium. Pair and triplet coefficients also indicated that pairwise interactions predominated in the ternary (sodium benzoate + water + glycolic acid/lactobionic acid) systems. In the second problem, sodium methyl p-hydroxybenzoate (SMP) was investigated in aqueous solutions of glycolic and lactic acids at concentrations of 0.015, 0.025, 0.035 mol·kg^{-1} within the temperature range 288.15-318.15 K. The apparent molar volume values obtained for these mixtures are positive which reflects significant solute-solvent interactions with stronger interactions observed in the presence of lactic acid compared to glycolic acid. The positive values of limiting apparent molar volume indicate the contribution of hydrogen bonding between the hydroxyl and carboxyl groups of the acids and the polar regions of SMP which arises from the aromatic moiety of the preservative. At all concentrations and temperatures, the slope parameter (S_V^*) remained positive which suggests the predominance of pairwise interactions between solute species. Both the apparent molar expansibility and its temperature derivative were positive which signified that SMP in

combination with hydroxy acids, strengthens the local structure of the solvent medium. The isentropic compressibility values were negative which implies that water molecules in the vicinity of SMP and the acids exhibit reduced compressibility compared to bulk water. A gradual reduction in the magnitude of negative $K_{\phi,s}^{0}$ with increasing temperature further points to attractive solute-solvent associations. Negative values of S_K^* confirmed that such interactions persist even at infinite dilution. In the third problem, ternary mixtures consisting of potassium benzoate with either glycolic acid or malic acid in aqueous medium were examined. The study focused on the evaluation of apparent molar, partial molar, and transfer properties derived from experimentally measured parameters at a constant pressure of 0.1 MPa and within the temperature range of 288.15-318.15 K. Potassium benzoate was investigated at three concentrations: 0.04, 0.05, and 0.06 mol·kg^{-1}. The positive values of apparent molar volume obtained across the studied concentrations and temperatures indicate pronounced solute-solvent interactions in the ternary system. The relatively small S_V^* values compared to V_ϕ^0 further confirm that solute-solvent interactions predominate over solute-solute interactions. The transfer properties provide additional insight into the nature of the interactions. Positive values of ΔV_Φ^0 suggest that ion-hydrophilic and hydrophilic-hydrophilic interactions dominate between potassium benzoate, hydroxy acids and water molecules. Similarly, the positive values of the expansibility coefficient across the investigated temperatures point to significant ion-hydrophilic interactions which enhance the structural organization of the solution. Negative values of the isentropic compression parameter throughout the studied concentration range indicate penetration of solvent molecules into the interionic free spaces of the solute species which reduced the compressibility of the system relative to bulk water. The overall evaluation of pair and triplet coefficients revealed that pairwise interactions dominate under the studied conditions. In the fourth problem, sodium benzoate in aqueous solutions of lactic and malic acids was examined at 0.01 to 0.03 mol·kg^{-1} within the temperature range 288.15-318.15 K. Density and ultrasonic velocity data revealed strong solute-solvent interactions that increased with concentration and molecular size of the acids. Transfer properties confirmed dominance of ion-hydrophilic, hydrophilic-hydrophilic, and ion-ion interactions over hydrophobic effects. The rise in apparent molar volume with concentration indicated hydrogen bond formation between hydroxyl groups of the acids and sodium benzoate, leading to disruption of the water structure. Negative compressibility values reflected reduced electrostriction and solvent rigidity, emphasizing the prevalence of solute-solvent interactions. These findings highlight the role of sodium benzoate-alpha-hydroxy acids-water systems in food preservation,

pharmaceuticals, and cosmetics through solvent stabilization, reduction of free water, improvement of formulation stability and extension of shelf-life. In the fifth problem, the molecular interactions within the ternary liquid systems containing potassium benzoate, L(+)-lactic acid, and butyric acid in aqueous medium were examined through precise density and ultrasonic velocity measurements at concentrations of 0.01,0.02, and 0.03 $mol \cdot kg^{-1}$ over a range of temperatures. From the experimental data, a series of acoustical and volumetric parameters was derived to elucidate the structural and stability features of the mixtures. Positive deviations in the apparent molar quantities coupled with reduced compressibility values reflected a compact solution structure dominated by solute-solvent associations. The results indicated that the introduction of PB, together with LA and BA strengthens the molecular organization of the system by forming hydrogen bonds between PB and the hydroxyl functionalities of the acids, thereby disrupted the bulk water network and decreased the proportion of free water. The interaction coefficients confirmed the existence of specific pairwise associations between potassium benzoate and the acids. Multiple interaction modes- ion-ion, dipole-dipole, ion-hydrophilic, hydrophobic-hydrophobic, and ion-hydrophilic were found to govern the molecular dynamics of these ternary solutions. The outcomes suggest that the inclusion of lactic and butyric acids in PB solutions enhances antimicrobial efficiency, improves structural stability, and contributes to extended shelf life, thereby offered a practical strategy for the design of safer and more effective preservative systems in food, cosmetic, and pharmaceutical applications. In the sixth problem, a comprehensive evaluation of volumetric and acoustic parameters was carried out to explore the solvation dynamics of tartaric or malic acids in aqueous sodium methyl parahydroxybenzoate mixtures. Experimental values of density and ultrasonic velocity were determined and compared with available literature to validate the trends. The transfer parameters reflected a predominance of hydrophilic effects over hydrophobic. Contributions from these effects further reinforced the structural preferences of the solute-solvent system. Analysis of the interaction coefficients highlighted the greater importance of pairwise interactions compared with triplet interactions. The overall findings revealed that the incorporation of α-hydroxy acids into SMP-water mixtures improved the structural stability of the system and enhanced its functional potential. Such characteristics underline the suitability of these formulations in preservative applications across food, cosmetic, and pharmaceutical industries. In the seventh problem, solute-solvent interactions of tartaric or lactobionic acid and in potassium benzoate-water mixtures were examined through physicochemical analysis. Experimental data for density and sound velocity were

compared with previously reported values and subjected to detailed evaluation. The calculated transfer parameters ($\Delta K^0_{\phi,S}$, ΔV^0_ϕ) revealed a predominance of ion-hydrophilic and hydrophilic-hydrophilic interactions, while hydrophobic contributions remained negligible. The addition of potassium benzoate reduced electrostriction effects in the hydration sphere of the solute. The negative values of the temperature derivative of the Jones-Dole coefficient (E^0_ϕ) reflected the solute's capacity to impose structural effects on the surrounding solvent. These findings established the molecular association patterns in potassium benzoate-acid-water systems and provided clarity on their structural and thermodynamic behavior. In the eighth problem, density and ultrasonic velocity were measured with the DSA 5000 M to conduct a detailed volumetric and acoustical analysis of ternary systems composed of butyric acid, lactic acid, sodium benzoate, and water. These measurements offered crucial insight into the molecular forces that determine the structural and dynamic characteristics of the mixtures. The results demonstrated the coexistence of several interaction modes, such as ion-ion, hydrophobic, hydrophilic, and dipole-dipole forces. Among these, hydrogen bonding emerged as the primary factor. The hydroxyl groups of TA and the functional sites of BA formed hydrogen bonds with the carboxylate and benzoate groups of SB, thereby reinforcing solute-solvent bonds. The structural effects of the solutes on the solution were assessed through the application of Hepler's thermodynamic criterion together with the co-sphere overlap concept. This extensive interaction network destabilized the bulk water structure and diminished the proportion of free water molecules, ultimately resulting in greater stability of the ternary mixtures.

The present investigation provides a comprehensive analysis of the thermo-acoustic behaviour of benzoic acid derivatives in aqueous solutions of various carboxylic acids over a wide temperature and concentration range. The experimental measurements of density and ultrasonic velocity enabled the evaluation of several volumetric and acoustical parameters, including apparent and partial molar volumes, transfer properties, isentropic compressibility, and interaction coefficients. The results consistently indicate the predominance of strong solute–solvent interactions in the studied ternary systems. Positive values of apparent molar volumes and expansibility coefficients, along with negative compressibility parameters, reveal the presence of significant hydrogen bonding, ion–hydrophilic, and dipole–dipole interactions. The interaction coefficient analysis further demonstrates that pairwise interactions dominate over triplet interactions in most of the investigated systems.

Overall, the study highlights that the presence of benzoic acid derivatives together with hydroxy acids leads to enhanced structural organization of the solvent medium through specific

molecular associations. These findings contribute to a better understanding of solute–solvent interaction mechanisms in complex liquid systems and provide valuable physicochemical data that may be useful for the design of stable preservative systems in pharmaceutical, cosmetic, and food formulations.

Although the present investigation provides significant insights into the thermo-acoustic behavior and intermolecular interactions of benzoic acid derivatives in aqueous solutions of carboxylic acids, certain limitations should be acknowledged. The experimental measurements were carried out within a specific range of temperatures and concentrations, which may limit the generalization of the results beyond these conditions. In addition, the study mainly relies on volumetric and ultrasonic techniques to interpret solute–solvent interactions, while complementary spectroscopic or computational approaches could provide deeper molecular-level understanding. Furthermore, the investigation focuses on selected benzoic acid derivatives and carboxylic acids; therefore, extending the study to a broader range of related compounds may provide additional insight into the interaction mechanisms. Despite these limitations, the present work offers valuable experimental data and contributes to a better understanding of thermo-acoustic properties and molecular interactions in such solution systems.

Future scope of the work

The investigation of benzoic acid derivatives and organic acids through volumetric and acoustic methods provides a basis for both fundamental and applied advancements in solution chemistry and material sciences. Further studies may extend this work by examining a wider range of temperatures, concentrations, and pH values to gain a clearer understanding of solute-solvent and solute-solute interactions along with structural modifications within multicomponent systems.

The application of additional volumetric and acoustic parameters may refine the interpretation of molecular association and structural reorganization in complex solutions. The industrial implications of these investigations are considerable. The synergy between benzoates and organic acids may be exploited to design preservative systems with higher antimicrobial efficiency, reduced dosage levels, and improved stability for food, cosmetic, and pharmaceutical applications. Formulations developed on the basis of this understanding may result in safer, economically viable, and consumer-acceptable products with prolonged shelf life.

Hydroxy acids serve as important precursors for biopolymers and biodegradable plastics, while benzoic acid derivatives provide structural stability and antimicrobial functionality. Further exploration of these systems may therefore contribute to the advancement of food technology, pharmaceutical sciences, cosmetic formulations, and sustainable materials. Future investigations may integrate experimental volumetric and acoustic data with computational simulations and spectroscopic methods to establish predictive models of solution behavior. This approach can promote the rational design of preservative blends, controlled release systems, and solvent media with well-defined physicochemical properties.

List of Publications

1. **Ashpinder Kaur Gill**, Nabaparna Chakraborty, Kailash Chandra Juglan, "Study of glycolic and lactobionic acids in water-soluble sodium benzoate solutions: an acoustic and thermodynamic approaches" (2025) 46, ***International Journal of Thermophysics*** **(Springer Nature Publications)** with **impact factor 2.9** (Q2) https://doi.org/10.1007/s10765-025-03517-5

2. **Ashpinder Kaur Gill**, Nabaparna Chakraborty, Kailash Chandra Juglan, "Analysis of molecular interactions of an aqueous benzoates with glycolic and lactic acid: spectroscopic, acoustic and volumetric approach" (2024) 115000 published in ***Physica Scripta*** **(IOP Publishing)** with **impact factor 2.6** (Q2) https://doi.org/10.1088/1402-4896/ad81be

3. **Ashpinder Kaur Gill**, Nabaparna Chakraborty, Kailash Chandra Juglan, "Volumetric and ultrasonic investigation of glycolic and malic acids with water-soluble potassium benzoate solutions at different temperatures" (2025) 2260-2276 published in ***Journal of Chemical and Engineering Data*** **(ACS Publications)** with **impact factor 2.1** (Q2) https://doi.org/10.1021/acs.jced.5c00085

4. **Ashpinder Kaur Gill**, Nabaparna Chakraborty, Kailash Chandra Juglan, "Investigating interactions of alpha-hydroxy acids with sodium benzoate for advanced formulation and translational applications: An ultrasonic approach" (2025) 100843, published in ***Chemical Physics Impact*** **(Elsevier Publications)** with **impact factor 4.3** (Q2) https://doi.org/10.1016/j.chphi.2025.100843

5. **Ashpinder Kaur Gill**, Nabaparna Chakraborty, Kailash Chandra Juglan, "Molecular interactions of butyric and L (+)- lactic acids in water-soluble potassium benzoate solutions: An acoustic and thermodynamic study" published in ***The Journal of Chemical Thermodynamics*** **(Elsevier Publications)** with **impact factor-2.2** (Q2) https://doi.org/10.1016/j.jct.2025.107586

6. **Ashpinder Kaur Gill**, Nabaparna Chakraborty, Kailash Chandra Juglan, "Acoustic and volumetric analysis of malic and tartaric acids in aqueous medium of sodium methyl p-hydroxybenzoate from 288.15 K to 318.15" published in ***Journal of the Indian Chemical Society*** **(Elsevier Publications)** with **impact factor-3.4** (Q2)**.**

7. **Ashpinder Kaur Gill**, Nabaparna Chakraborty, Kailash Chandra Juglan, "Thermodynamic analysis of tartaric and lactobionic acids with aqueous potassium benzoate mixtures through volumetric and acoustic methods" (2025) 100216, published in ***Chemical Thermodynamics and Thermal Analysis*** **(Elsevier Publications)** (Q2) https://doi.org/10.1016/j.ctta.2025.100216

8. **Ashpinder Kaur Gill**, Nabaparna Chakraborty, Kailash Chandra Juglan, "Exploration of intermolecular interactions of butyric and tartaric acids with sodium benzoate in aqueous medium" published in ***Journal of Molecular Liquids*** **(Elsevier Publications)** with **impact factor-5.2** (Q1) https://doi.org/10.1016/j.molliq.2025.129024

9. **Ashpinder Kaur Gill**, Nabaparna Chakraborty, Kailash Chandra Juglan, "Thermo-Acoustic Investigations on Benzoate-Based Mixtures Using Ultrasonic Technique" (2024) 450-459, published in ***Cutting-Edge Applications of Nanomaterials in Biomedical Sciences*** **(IGI Global Scientific Publishing)** "**Scopus"** https://doi.org/10.4018/979-8-3693-0448-8.ch019

List of communicated papers

1. Kanika Bhakri, **Ashpinder Kaur Gill**, K.C. Juglan, Nabaparna Chakraborty, "Volumetric and acoustical studies of glycols with water-soluble lactobionic acid solutions at different temperatures" submitted to ***Chemical Physics*** with **impact factor-2.4** (Q2)**.**
2. Sunita Devi, **Ashpinder Kaur Gill**, Nabaparna Chakraborty, Kailash Chandra Juglan, Volumetric and Acoustic Evaluation of Temperature-dependent Interactions between Phenoxyethanol and Sodium Ascorbate/Ascorbic Acid in Aqueous Media" submitted to **International Journal of Thermophysics** with **impact factor-2.9** (Q2).
3. **Ashpinder Kaur Gill**, Nabaparna Chakraborty, Kailash Chandra Juglan, **"**Exploring Thermodynamic Properties of Sodium Benzoate Solutions with Alpha-hydroxy and Poly-hydroxy Acids Using Ultrasonic Methods" submitted to ***Wiley-Scrivener Publishing***.

List of Conferences/ Seminar/ Short term courses attended

Conferences

1. **Recent Advances in Fundamental and Applied Sciences**, Lovely Professional University, Phagwara, Punjab, 19th April 2024 and 20th April 2024, "Thermodynamic and physicochemical investigation of carboxylic acids in aqueous benzoate solutions".
2. **9th National Symposium on Advances in Chemical Sciences**, Guru Nanak Dev University, Amritsar, Punjab, 6th March 2025 and 7th March 2025, "Molecular Interactions of Lactic and Butyric Acids in Aqueous Potassium Benzoate Solutions: An Acoustic and Thermodynamic Study".
3. **Recent Advances in Fundamental and Applied Sciences**, Lovely Professional University, Phagwara, Punjab, 18th April 2025 and 19th April 2025, "Acoustic and Volumetric Analysis of Aqueous Hydroxy Acids with Potassium Benzoate Solutions at Different Temperatures".